THE EARLY EVOLUTIONARY HISTORY OF SHARKS AND SHARK-LIKE FISHES

by

PLAMEN STANISLAVOV ANDREEV

A thesis submitted to the University of Birmingham for the degree of

DOCTOR OF PHILOSOPHY

Geosystems

School of Geography, Earth and Environmental Sciences

University of Birmingham

October 2014

Table of contents

	page
List of Figures	vi
Acknowledgements	x
Thesis Abstract	xi
Chapter 1: Introduction	1
Chapter 2: Methodology and definitions of terms	
2.1. Methods	
2.1.1. Scale structure analysis	6
2.1.2. Phylogenetic analysis	7
2.2. Definitions of terms	9
2.3. Acquisition and accession of specimens	12
2.4. Institutional abbreviations	13
Chapter 3: North American scale taxa from the Upper Ordovician shed light on the early evolution of the chondrichthyan integumentary skeleton	
3.1. Introduction	18
3.2. Systematic palaeontology	20
3.3. Discussion	
3.3.1. The characteristics of chondrichthyan scales	31

3.3.2. The integumentary skeleton of Ordovician chondrichthyans 34

3.4. Conclusions 36

Chapter 4: Ordovician origin of Mongolepidida and the integumentary skeleton of basal chondrichthyans

4.1. Introduction 45

4.2. Systematic palaeontology 47

4.3. Discussion

4.3.1. Crown morphogenesis of mongolepid scales 68

4.3.2. Mongolepid scale crown histology 70

4.3.3. Histology of mongolepid scale bases 71

4.3.4. Canal system of mongolepid scales 73

4.3.5. Systematic position of the Mongolepidida 75

4.4. Conclusions 76

Chapter 5: *Elegestolepis* and its kin, the earliest chondrichthyans to develop mono-odontode scale crowns

5.1. Introduction 86

5.2. Systematic palaeontology 88

5.3. Discussion

5.3.1. Chondrichthyan characteristics of elegestolepid mono-odontode scales 99

5.3.2. Elegestolepida in the context of other Lower Pazaeozoic chondrichthyans 101

5.4. Conclusions 104

Chapter 6: Scale-based phylogeny of Palaeozoic chondrichthyans

6.1. Introduction 116

6.2. Results

6.2.1. Classification schemes of scale morphogenesis in chondrichthyans 117

6.2.2. Scale morphogenetic types in chondrichthyans 120

6.2.3. Chondrichthyes-specific developmental pattern of the integumentary skeleton 124

6.2.4. Remarks on the phylogenetic analyses 125

6.2.5. Populating the stem of the chondrichthyan tree 127

6.2.6. Degree of correlation with existing gnathostome phylogenies 130

6.3. Conclusions 132

Chapter 7: Conclusions 149

References 152

Appendix

Matrix of character states assigned to the 51 taxa included in the phylogenetic analyses 183

Character list 188

Taxa included in the analyses, studied material, literature used in the coding the character-taxon matrix 202

List of figures

page

Figure 1. Principle morphological features of scales depicted by a line drawing of a *Mongolepis* scale. 15

Figure 2. Recognised scale components according to their developmental origin and topology. 16

Figure 3. Odontocomplexes composing the poly-odontocomplex crown of a *Teslepis jucunda* scale. 17

Figure 4 . *Tezakia hardingi* gen. et sp. nov. scales from the Sandbian (Upper Ordovician) Harding Sandstone. 37

Figure 5. Light micrographs of a probable ontogenetically young (mono-odontode) *Tezakia hardingi* gen. et sp. nov. scale. 39

Figure 6. *Canonlepis smithae* gen. et sp. nov. scales from the Sandbian (Upper Ordovician) Harding Sandstone. 40

Figure 7. Hard-tissue structure and canal system architecture of *Tezakia hardingi* gen. et sp. nov. and *Canonlepis smithae* gen. et sp. nov. scales. 42

Figure 8. Diagrammatic representation of scale-morphogenesis patterns and odontocomplex structure of known 44

Ordovician chondrichthyans.

Figure 9. Scale morphology of Upper Llandovery–Lower Wenlock (Silurian) mongolepids. 78

Figure 10. SEM micrographs of *Solinalepis levis* gen. et sp. nov. scales from the Sandbian (Upper Ordovician) Harding Sandstone. 80

Figure 11. Histology of the mongolepid integumentary skeleton. 81

Figure 12. Canal system of mongolepid scales. 83

Figure 13. Highlighted odontocomplex organisation of mongolepid scale crowns. 85

Figure 14. Diagrammatic representation of mono-odontode scale types in the Thelodonti and the Chondrichthyes. 105

Figure 15. Line drawings depicting the range of crown-surface morphologies in elegestolepid scales. 106

Figure 16. Scales of *Elegestolepis grossi* from the Upper Ludlow–Pridoli (Upper Silurian) Baital Formation of Tuva. 107

Figure 17. Hard-tissue structure of *Elegestolepis grossi* scales. 108

Figure 18. Scales of *Deltalepis magnus* gen. et sp. nov. from the Upper Llandovery–Lower Wenlock (Silurian) 109

Chargat Formation of north-western Mongolia.

Figure 19. Scales of *Deltalepis parvus* gen. et sp. nov. from the Upper Llandovery–Lower Wenlock (Silurian) Chargat Formation of north-western Mongolia. 110

Figure 20. Hard-tissue structure of *Deltalepis* gen. nov. 112

Figure 21. Volume renderings of the scale canal system (in red) of examined elegestolepids. 113

Figure 22. Characteristics of mono-odontode scales of recognised Lower Palaeozoic chondrichthyans and their stratigraphic range. 115

Figure 23. Types of morphogenetic patterns of chondrichthyan mono-odontode scales. 134

Figure 24. Morphogenetic pattern of chondrichthyan polyodontode non-odontocomplex scales. 136

Figure 25. Types of morphogenetic patterns of chondrichthyan mono-odontocomplex scales. 137

Figure 26. Types of morphogenetic patters of chondrichthyan polyodontocomplex scales. 139

Figure 27. Majority-rule consensus (tree length 597 steps) of 51 most parsimonious trees from phylogenetic analysis I. 141

Figure 28. Strict consensus (tree length 735 steps) of 51 most parsimonious trees from phylogenetic analysis I. 142

Figure 29. Results of phylogenetic analysis II. 143

Figure 30. Results of phylogenetic analysis III. 144

Figure 31. Results of phylogenetic analysis IV. 145

Figure 32. Stratigraphic ranges and inter-relationships of chondrichthyan taxa (in pink) recovered in MPT of phylogenetic analysis I. 146

Figure 33. Diagrammatic representation of odontode, crown and base shapes of the taxa included in the phylogenetic analyses. 147

Figure 34. Types of dentine tubules in respect to their appearance proximally. 148

ACKNOWLEDGEMENTS

This project was funded by the School of Geography, Earth and Environmental Sciences at the University of Birmingham, with additional financing secured from the Small Grants Scheme of the Palaeontological Association. Dick Shelton, Paul Cooper and Michelle Holder deserve a special mention for their assistance during my research at the School of Dentistry (University of Birmingham) and for providing free access to analytical facilities (micro-CT scanner, SEM), without which the completion of the study in this form would not have been possible.

I am grateful to the following people for granting me the opportunity to examine museum collections and/or obtain study material over the course of the project: Ivan Sansom and Jon Clatworthy (University of Birmingham), Valya Karatajūtė-Talimaa (Vilnius University), Michael Coates and Ian Glasspool (Field Museum), Zerina Johanson (Natural History Museum), Ami Henrici (Carnegie Museum of Natural History), Michal Ginter (University of Warsaw), Gilles Cuny (Natural History Museum of Denmark), Jeff Liston (Hunterian Museum), and Stig Walsh (National Museums Scotland).

Above all, my lead supervisor (Ivan Sansom) was responsible for conceiving this project and has had the greatest influence on the final structure of the thesis, which has gone through several edits provoked largely by his comments on chapter manuscripts and our numerous discussions. Other important feedback has been that of Michael Coates (second supervisor) on phylogenetic aspects of the research, complimented by advice on cladistic-analysis methodology from Martin Ezcurra (University of Birmingham).

Thesis abstract

The Middle Ordovician to Late Silurian represents an interval of approximately 50 million years, which has been recognised as the initial, cryptic, period in the evolutionary history of chondrichthyan fish. The fossil remains attributed to early chondrichthyans are dominated by isolated dermal scales that predate the appearance of undisputed chondrichthyan teeth and articulated skeletons in the Lower Devonian. Investigation of the inter-relationships of these scale taxa and their systematic position relative to high-ranked chondrichthyan clades has been hampered by the lack of developed scale-based classification schemes for jawed gnathostomes, coupled with the limited use of scale characters in phylogenetic studies of Palaeozoic Chondrichthyes. Here, all previously documented scale types of alleged Lower Palaeozoic chondrichthyans were examined using a combination of X-ray microtomography, SEM and Nomarski DIC optics. These were found to exhibit a set of characteristics (symmetrical trunk scales, areal crown growth and lack of hard-tissue resorption, cancellous bone and enamel) recognised as specific to the dermal skeleton of chondrichthyans among derived gnathostomes. The collected data permitted the establishment of a hierarchy of scale characters for separate taxonomic ranks, leading to the recognition of three Orders (Mongolepidida, Elegestolepida ordo nov. and Altholepida ordo nov.) of early chondrichthyans, differentiated by distinct types of scale-crown morphogenesis.

A scale-based cladistic analysis of jawed gnathostomes corroborated these results by recovering a chondrichthyan clade that incorporates all examined taxa and ‘acanthodians’ with non-superpositional crown growth patterns. It is thus proposed that chondrichthyan dermoskeletal characters carry a phylogenetic signal, allowing to

interpret the documented diverse types of scale morphogenesis as evidence for a major radiation of chondrichthyan lineages in the Lower Palaeozoic.

Chapter 1: Introduction

The Class Chondrichthyes (cartilaginous fish) is a well-supported (Brazeau 2009; Davis et al. 2012; Zhu et al. 2013; Dupret et al. 2014) clade of crown gnathostomes with a long evolutionary history that has been suggested to date back to the Ordovician Period (Sansom et al. 2001, 2012; Turner et al. 2004). Dermal scales and teeth are among the elements of the chondrichthyan skeleton most commonly preserved in the fossil record, as the latter lacks extensive endoskeletal mineralization and development of macromeric dermal bones. Accordingly, tooth characters feature prominently in the diagnoses of fossil chondrichthyan taxa of all ranks (Cappetta 1987, 2012; Ginter et al. 2010), whereas attributes of scales have predominantly been used to define the total chondrichthyan group (Zangerl 1979, 1981; Maisey 1984, 1986, 1988; Lund and Grogan 1997). The majority of these studies assert that the integumentary skeleton of the Chondrichthyes is micromeric and consists of mono-odontode scales with neck canal openings. This traditional depiction of the chondrichthyan squamation reflects a historical emphasis on descriptions of the scale cover of euselachian elasmobranchs (e.g. Reif 1985; Thies 1995; Johns et al. 1997; Ivanov 2005; Wang et al. 2009; Fischer et al. 2010; Thies and Leidner 2011; Ivanov et al. 2013), which is composed of simple, single odontode scales. A similar condition has been documented in stem chondrichthyans (in Iniopterygii, Zangerl and Case 1973; Grogan and Lund 2009) as well as in members of the stem elasmobranch Orders Phoebodontiformes (Grogan and Lund 2008), Xenacanthiformes (Hampe 1997; Soler-Gijón 1997) and Symmoriiformes (Lund 1985, 1986; Coates and Sequeira 2001) and in stem Paraselachii (e.g. in Helodontiformes, Moy-Thomas 1936 and Chondrenchelyiformes Lund 1982), but it

does not encompass all structural scale types identified in the Palaeozoic record of the clade.

Scales with compound crowns formed of odontodes arranged in longitudinal rows, termed odontocomplexes and originally identified as sequentially deposited units of the dermoskeleton by Ørvig (1977), have been reported in a number of Devonian to Carboniferous taxa known from body fossils (e.g. *Antarctilamna* [Antarctilamniformes] Young 1982; Forey et al. 1992, *Diplodoselache* [Xenacanthiformes] Dick 1981, *Tamiobatis* [Ctenacanthiformes] Williams 1998 and *Orodus* [Orodontiformes] Zangerl 1968). Scales of a similar appearance were regarded by Reif (1978) to exhibit a ctenacanthid-type of development, distinguished from that interpreted as characteristic for euselachian scales in the first published classification scheme of scale morphogenesis types in the Chondrichthyes. However, a substantial body of work on Silurian and Lower Devonian microvertebrate fossils, undertaken prior to the study of Reif (1978), uncovered assemblages of putative chondrichthyan scale taxa that manifest diverse crown architectures (e.g. *Elegestolepis* Karatajūtė-Talimaa 1973, *Mongolepis* Karatajūtė-Talimaa et al. 1990, *Seretolepis* Karatajūtė-Talimaa 1968; Karatajūtė-Talimaa 1997, *Ellesmereia* Vieth 1980, *Altholepis* Karatajūtė-Talimaa 1997 and *Iberolepis* Mader 1986). These new data were incorporated in a comprehensive examination of scale-morphogenesis patterns in Palaeozoic chondrichthyans by Karatajūtė-Talimaa (1992), who proposed a Cambrian or Ordovician origin of the Chondrichthyes on the basis of recognised diverse scale developmental types. Subsequent research substantiated the idea of a Silurian radiation of basal chondrichthyan fish, by identifying new polyodontode scale genera with *Mongolepis*-type odontocomplex structure (*Teslepis* Karatajūtė-Talimaa and Novitskaya 1992, *Sodolepis* Karatajūtė-Talimaa and Novitskaya 1997,

Xinjiangichthys Wang et al. 1998 and *Shiqianolepis* Sansom et al. 2000) along with other polyodontode (*Tuvalepis* Žigaitė and Karatajūtė-Talimaa 2008) and single odontode scale taxa (*Kannathalepis* Märss and Gagnier 2001 and *Frigorilepis* Märss et al. 2002, 2006). Furthermore, a series of publications from the past twenty years, describing scale species from Laurentian ('scale morphology A' Sansom et al. 1996, 'New Genus F' Sansom et al. 2001, 'mongolepid scales' Sansom et al. 2001) and Gondwanan (*Areyongalepis oervigi* Young 1997 and *Tantalepis gatehousei* Sansom et al. 2012) localities, have provided the first tangible evidence for the presumed origin of the chondrichthyan clade in the Ordovician.

Despite these advances, our knowledge of the early evolutionary history of the Chondrichthyes remains fragmentary. This is largely due to the sparse Lower Palaeozoic fossil record of chondrichthyans, dominated by isolated dermal scales, which have traditionally been disregarded as a source of phylogenetic data. Given the lack of endoskeletal and/or dental skeletal elements associated with the scales of putative basal chondrichthyans, only a few Silurian (*Elegestolepis* and *Kannathalepis*) and Lower Devonian (*Polymerolepis* Karatajūtė-Talimaa 1968; Hanke et al. 2013) genera that possess euselachian-type single odontode crowns with neck canal openings have been assigned with a degree of confidence to the Chondrichthyes. It is therefore suggested that a reappraisal of scale characteristics that takes into account the documented types of polyodontode crown architectures and absence of neck canals (in the mongolepid *Sodolepis* Karatajūtė-Talimaa and Novitskaya 1997 and in the alleged stem chondrichthyans *Lupopsyrus* Hanke and Davis 2012 and *Obtusacanthus* Hanke and Wilson 2004) is a necessary first step towards recognising potential dermoskeletal apomorphies of the total group Chondrichthyes. Dermal scale characters are considered to possibly also carry a phylogenetic signal at lower taxonomic levels and have been used to diagnose

Order- and Family-ranked chondrichthyan taxa (Karatajūtė-Talimaa et al. 1990; Sansom et al. 2000), as well as in existing classification schemes of thelodont (Märss et al. 2007) and ‘acanthodian’ (Denison 1979) vertebrates.

The goal of the present study is to build a systematic framework for the geologically oldest chondrichthyan fish by examining scale-based taxa (refer to Chapter 6 for a full list of taxa included in the study) from the Ordovician–Lower Devonian interval, and characterise the primitive condition of the integumentary skeleton in chondrichthyans and its evolution throughout the Lower Palaeozoic. Also investigated were a number of species that have previously been regarded to demonstrate the types of scale morphogenesis prevalent among Upper Palaeozoic chondrichthyans (the *Heterodontus*, *Ctenacanthus* and *Protacrodus* types of Karatajūtė-Talimaa 1992).

Data collection was performed by examining complete and thin-sectioned scale specimens with X-ray microtomography, scanning electron microscopy (SEM) and Nomarski differential interference contrast (DIC) microscopy, which makes this the first large-scale investigation of fossil microvertebrate remains to employ the three investigative techniques.

The information obtained on scale histological, structural and morphological properties was used to interpret scale developmental patterns of early chondrichthyans and relate these to the morphogenetic categories identified by Karatajūtė-Talimaa (1992).

This study assessed the diagnostic potential of scale characters at different taxonomic ranks and classify the examined taxa accordingly. The chondrichthyan affinities and inferred inter-relationships of these species were tested by a scale-based phylogenetic analysis of Palaeozoic jawed gnathostomes. Another aim of the phylogenetic investigation was to resolve the position of the paraphyletic Acanthodii

(Brazeau 2009; Davis et al. 2012, Zhu et al. 2013) members of which (*Brachyacanthus*, *Brochoadmones*, *Climatius*, *Kathemacanthus*, *Obtusacanthus*, *Parexus*, *Ptomacanthus* and *Vernicomacanthus*) have recently been recognized as stem chondrichthyans (Brazeau 2009; Davis et al. 2012; Zhu et al. 2013).

Chapter 2: Methodology and definitions of terms

2.1. METHODS

2.1.1. Scale structure analysis

Scale specimens were isolated from sediment samples by dissolution of the rock matrix with dilute acetic acid and petroleum ether.

Scale morphology was documented with a Zeiss SteREO Discovery.V8 stereo microscope and using the JEOL JSM-6060 and Zeiss EVO LS scanning electron microscopes at the School of Dentistry of the University of Birmingham, UK. Prior to SEM imaging, specimens were sputter-coated with a 25 nm-thick layer of gold/palladium alloy.

For the purpose of studying scale histology and internal structure, thin-sectioned specimens were examined with Nomarski differential interference contrast microscopy (using a ‘Zeiss Axioskop Pol’ polarization microscope) and scanning electron microscopy (using a JEOL JSM-6060 SEM). This involved embedding individual specimens in epoxy resin (©Robnor Resins RX771C) and subsequent sectioning of the set resin blocks close to the scale surface with a Buehler IsoMet® low speed saw. The desired level of the sections was then reached by manually grinding down specimens with silicon carbide abrasive paper (grit sizes P600, P800 and P2500) using a Buehler MetaServ® 2000 grinder-polisher. Sectioned surfaces were polished and glued to petrographic slides with Buehler EpoThin adhesive resin. The sequence of sectioning, grinding and polishing was repeated in order to produce doubly polished thin sections suitable for light microscopy investigation.

Scale examination with X-ray radiation was performed with the SkyScan 1172 microtomography scanner at the School of Dentistry of the University of Birmingham, UK. The acquired microradiographs (tomographic projections) were taken at 0.3° intervals over a 180° rotation cycle at exposure times of 400 ms, using a 0.5 mm thick X-ray attenuating Al filter. These image data were processed with the SkyScan NRecon reconstruction software for the purpose of generating sets of microtomograms that were converted into volume renderings in Amira 5.4 3D analysis software.

2.1.2. Phylogenetic analysis

Data matrix. A data matrix of 90 scale-based characters and 51 taxa (see Appendix) was used to build a phylogeny of jawed gnathostomes that allowed to establish the position of putative and established Palaeozoic chondrichthyan taxa on the resultant trees. From the total number of characters employed in the analyses, 70 are original with the remaining 20 being revised/adapted from recent phylogenetic studies of Palaeozoic vertebrates (Brazeau 2009; Wilson and Märss 2009; Davis et al. 2012; Zhu et al. 2013). Furthermore, 22 of the examined taxa (*Altholepis, Antarctilamna, Elegestolepis, Frigorilepis, Gladbachus*, *Goodrichthys*, *Solinalepis* gen. nov., *Janassa, Kannathalepis, Mongolepis, Canonlepis* gen. nov., *Protacrodus, Seretolepis, Shiqianolepis, Sodolepis, Tantalepis, Teslepis, Wodnika, Tezakia* gen. nov*., Tchunacanthus, Tuvalepis* and *Xinjiangichthys*) have never previously been incorporated in a cladistic framework.

Following Brazeau (2011), contingent coding was implemented (for the purpose of avoiding the logical conflicts inherent to single multistate or presence/absence characters; see Forey and Kitching 2000) in the composition of a dataset that integrates a combination of unordered binary (53) and multistate (37) characters. The total character set was used in the performed four separate phylogenetic analyses (numbered I–IV), for two of which a

weight value of 2 (compared to the default value of 1) was assigned to two subsets of characters. One subset includes scale morphogenetic features (characters 78–90; analysis II), whilst the other is represented by a mixture of histological and morphogenetic scale attributes (characters 57, 67, 68, 74, 76, 84; analysis III) that are thought to differentiate total-group chondrichthyans within Gnathostomata (see Chapter 6 for details). The preferential weighting in analyses II and III was adopted in order to test how tree topology is affected by the strengthening of characters assumed to be diagnostic at high systematic levels.

For analyses I–III, six taxa belonging to Anaspida (*Rhyncholepis*), Thelodonti (*Thelodus, Lanarkia* and *Archipelepis*), Galeaspida (*Polybranchiaspis*) and Osteostraci (*Hemicyclaspis*) were selected as an outgroup. Analysis IV was performed however by including only *Polybranchiaspis* and *Hemicyclaspis* in the outgroup, in accordance with the consistent assignment of Galeaspida and Osteostraci as outgroup taxa in cladistic studies of early jawed vertebrates (Brazeau 2009; Davis et al. 2012; Zhu et al. 2013; Dupret et al. 2014). The ingroup composition is dominated by genera previously referred to the Chondrichthyes (26 taxa, see Appendix), out of which 12 are recognised to be scale-based taxa (*Elegestolepis, Solinalepis* gen. nov*., Kannathalepis, Mongolepis, Canonlepis* gen. nov*., Shiqianolepis, Sodolepis, Tantalepis, Teslepis, Tezakia* gen. nov*., Tuvalepis* and *Xinjiangichthys*); the ‘acanthodian’ *Tchunacanthus* being the only other ingroup genus described solely from scale remains (Karatajūtė-Talimaa and Smith 2003).

Methodology. The character-taxon dataset was assembled in Mesquite version 2.75 (Maddison and Maddison 2011) and exported to TNT version 1.1 (Goloboff et al. 2008) for the purpose of performing the phylogenetic analyses. In all analyses (I–IV), the TNT New Technology Search (set to 10000 random addition sequences with 10000 trees retained in memory) was implemented to generate a set of optimal and suboptimal trees that were

then used to calculate the most parsimonious trees (MPT) with the TNT tree bisection reconnection heuristic algorithm (Traditional Search).

Standard bootstrap values (for 1000 replicates) for strict consensus and most parsimonious trees were obtained with the resample function of TNT, configured to perform a traditional tree search. Bremer supports were calculated with TNT by tree bisection reconnection resampling of consensus trees, retaining trees suboptimal by up to 9 steps.

2.2. DEFINITIONS OF TERMS

Traditionally (e.g. Sykes 1974; Duffin and Ward 1993; Thies 1995) the two main components (the crown and base) of chondrichthyan scales have been identified on the basis of morphological and/or topological criteria without consideration of their developmental origin. This approach can lead to ambiguity when attempting to establish the extent of these structures and, more importantly, can result in equating scale parts with different tissue composition across taxa. To address the above issues, revised definitions are provided for terms used in literature to describe chondrichthyan scales that have relevance to this study. The rationale behind this is to improve identification of homologous scale structures across taxa by introducing a standardised terminology.

Crown – non-attachment portion of the scale comprised of odontogenetic odontogenic hard tissues (new, histology-dependent, interpretation of the structure, Fig. 1).

Pedicle – odontogenically derived attachment portion of scales that do not develop basal bone or in which bone deposition succeeds odontogenic tissue formation (Fig. 2). The term pedicle is adopted from Johns et al. (1997), where it was used to designate the lower, attachment tissue of elasmobranch scales, regarded by these authors to be synonymous with basal bone. Here however, 'pedicle' and 'base' refer to scale parts of different tissue composition.

Base – the non-odontogenic (osteogenic), attachment, portion of the scale (new, histology-dependent, interpretation of the structure, Figs. 1, 2).

Crown surface – the upper (for recurved crowns) or anterior (for erect crowns) face of the scale crown (Fig. 1). Revised from Johns et al. (1997).

Lower crown surface – the lower (for recurved crowns) or posterior (for erect crowns) face of the scale crown delineated by a sharp transition from the crown surface (Fig. 1). Revised from Johns et al. (1997), originally designated as 'subcrown'.

Lower pedicle surface – the lower face of the scale pedicle delineated by a sharp transition from the overlying pedicle face. Revised from Johns et al. (1997), originally designated as 'subpedicle'.

Basal surface – the upper face of the scale base delineated by a sharp transition from the overlying basal face (Fig. 1).

Lower base surface – the lower face of the scale base delineated by a sharp transition from the overlying basal face (Fig. 1).

Lower – the deepest insertion point of the scale within the integument determined through interpretation or direct observation (Fig. 1); a new term for designating the

attachment end of scales, which is given preference over ‘basal’ *sensu* Thies (1995) and Thies and Leidner (2011).

Upper – the most superficial point of the scale in respect to the tissues of the integument, either observed or inferred (Fig. 1); a new term favoured over ‘apical’ *sensu* Thies (1995) and Thies and Leidner (2011).

Odontode – a mineralised integumentary or oro-pharyngeal skeletal element produced by the mesenchymal and epithelial components of a single odontogenic cell condensation (Fig. 2); invariably composed of dentine but can also consist of one or more of the following odontogenic tissues: enameloid, enamel, elamsodine, cementum and bone of attachment (*sensu* Sire et al 2009). This interpretation is in agreement with the current understanding (Fraser et al. 2010) of the nature of odontode elements, but specifies a larger number of tissues that can potentially be involved in their formation.

Primary odontodes – the earliest formed (primordial) odontode in scales with polyodontode crowns and the odontode generations associated with it that are added subsequently in a particular developmental sequence. This introduces a new term and definition for elements previously referred to as ‘principle odontodes’ by Sansom et al. (2000). The odontodes of mono-odontode scales are equivalent to primordial odontodes and are also recognized as primary.

Secondary odontodes – a developmental series of odontodes in polyodontode scales deposited anterior to primary odontodes and formed following the deposition of the crown’s primordial odontode by a non-primary initiator odontode (adopted with revisions from Karatajūtė-Talimaa et al. (1990).

Odontocomplex – a row or a stack of odontodes unidirectionally deposited in temporal succession away from an initially formed, and incipient for the complex, odontode (Fig. 3).

Mono-odontocomplex – pertaining to scale crowns composed of a single odontocomplex.

Polyodontocomplex – pertaining to scale crowns formed of multiple (more than one) odontocomplexes.

2.3. ACQUISITION AND ACCESSION OF SPECIMENS

Institutional prefixes of accession numbers referenced in the text indicate the scientific collection in which figured specimens are deposited.

Specimens from the Stairway Sandstone, the Harding Sandstone, Shell Pine Unit No. 1, the Xiushan Formation and the Yimugantawu Formation were provided by Dr Ivan Sansom (University of Birmingham, UK).

Specimens from the Chester Bjerg Formation (collected by Dr Henning Blom, Uppsala University), housed at the Geological Museum, Copenhagen (Natural History Museum of Denmark), were received on loan from Dr Gilles Cuny (curator of the vertebrate palaeontology collections at the Natural History Museum of Denmark).

Material from the Chargat, Ivane and Dashtygoi Formations was obtained from the private collection of Dr Valentina Karatajūtė-Talimaa (Vilnius University, Lithuania).

Specimens from the Downtonian of the USA were kindly provided by Prof Moya Meredith Smith (King's College London, UK).

Muhua Formation and Czerna 1 (Czech Republic) material was received on loan from the private collection of Prof Michał Ginter (University of Warsaw, Poland).

The Werra Formation and the Marl Slate (Durham Province) material was loaned from the fossil fish collection of the Natural History Museum, London by Dr Alison Longbottom.

2.4. INSTITUTIONAL ABBREVIATIONS

BU and **BIRUG**, Lapworth Museum of Geology, University of Birmingham, UK

FMNH, Field Museum of Natural History, Chicago, USA

GGU, Geological Survey of Denmark and Greenland, Copenhagen, Denmark

IVPP V, Institute of Vertebrate Paleontology and Paleoanthropology, Chinese Academy of Sciences, Beijing, China

NHM, **BMNH** and **NHMUK PV P.**, Natural History Museum, London, UK

NIGP, Nanjing Institute of Geology and Palaeontology, Chinese Academy

of Sciences, Nanjing, China

NMS, National Museums of Scotland, Edinburgh, UK

NRM-PZ X, Naturhistoriska Riksmuseet, Stockholm, Sweden

PKUM, Geological Museum, Peking University, Beijing, China

UALVP, Laboratory for Vertebrate Paleontology, University of Alberta, Edmonton, Canada

UCMZ, University Museum of Zoology, Cambridge, UK

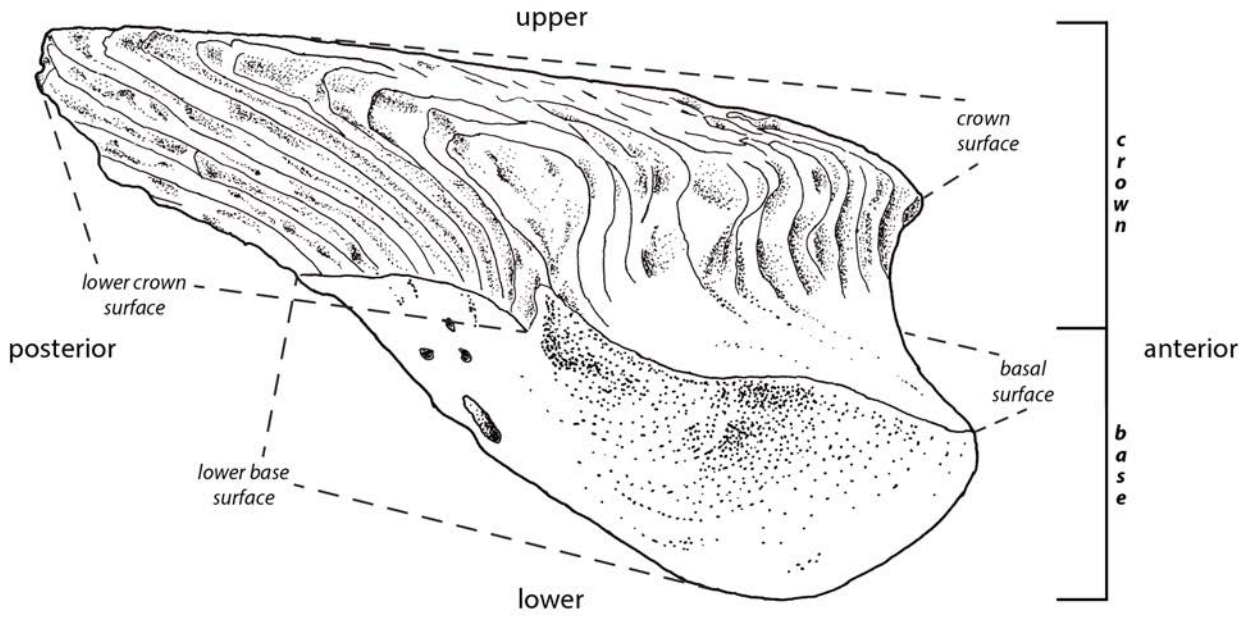

Figure 1. Principle morphological features of scales depicted by a line drawing of a *Mongolepis* scale (BU5296) from the Upper Llandovery–Lower Wenlock (Silurian) Chargat Formation of north-western Mongolia in lateral view.

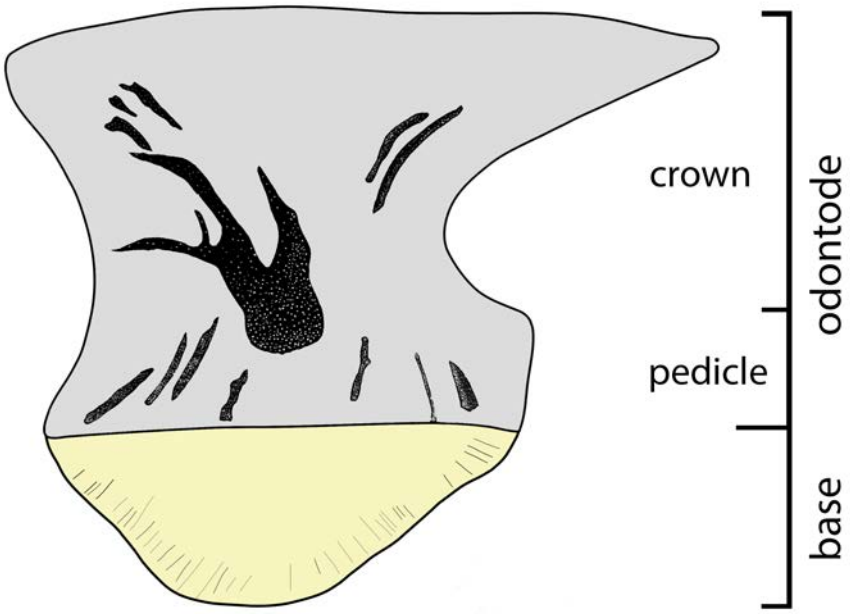

Figure 2. Recognised scale components according to their developmental origin and topology. Line drawing of a longitudinally sectioned *Elegestolepis grossi* scale (BU5283) from the Upper Ludlow of Tuva (Russian Federation). Grey, dentine; yellow, bone.

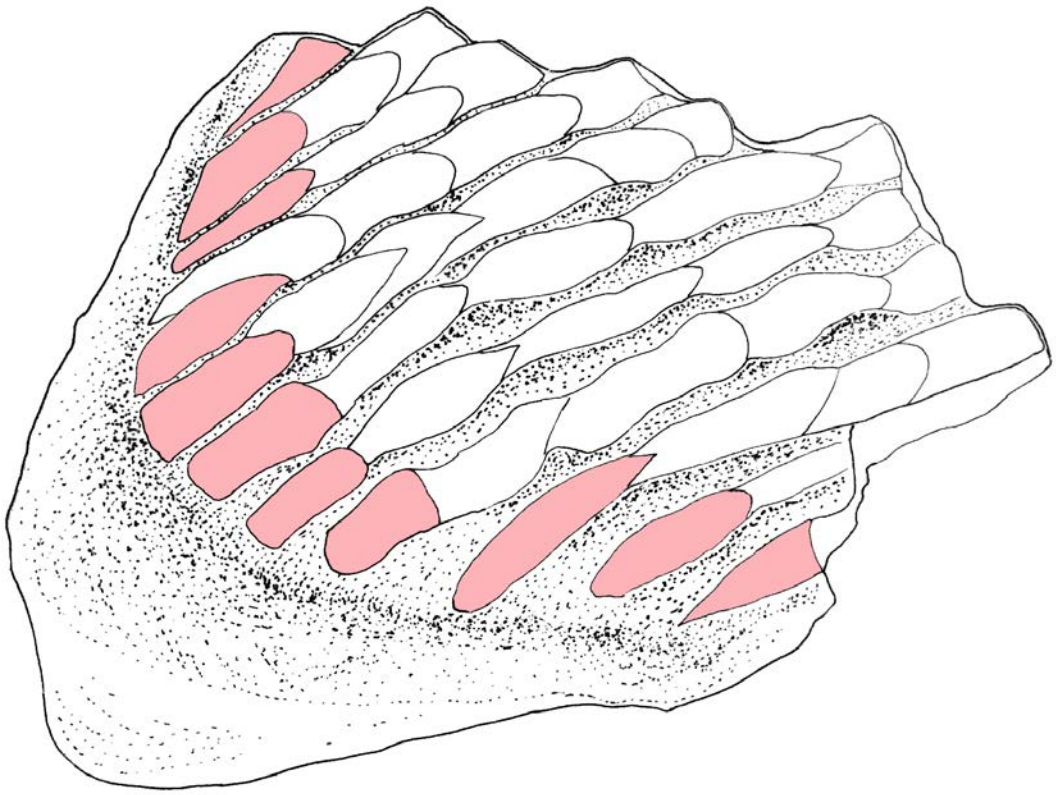

Figure 3. Odontocomplexes composing the polyodontocomplex crown of a *Teslepis jucunda* scale (BU5321) from the Upper Llandovery–Lower Wenlock (Silurian) Chargat Formation of north-western Mongolia. First deposited odontocomplex odontodes highlighted in pink.

Chapter 3: North American scale taxa from the Upper Ordovician shed light on the early evolution of the chondrichthyan integumentary skeleton

3.1. INTRODUCTION

The remains of the phylogenetically diverse Lower to Middle Devonian taxa *Kathemacanthus*, *Seretolepis* (Hanke and Wilson 2010), *Doliodus* (Miller et al. 2003; Maisey et al. 2009) and *Antarctilamna* (Young 1982) comprise the geologically oldest articulated fossils of chondrichthyan fish with preserved integumentary skeleton (represented by scales and spines) and endoskeleton (represented by its neurocranial, splanchnocranial and appendicular components). Coeval to these are the earliest reported examples of oropharyngeal odontodes in Chondrichthyes, manifested by the disarticulated dentitions of the Lochkovian species *Leonodus carlsi* Mader 1986 and *Celtiberina maderi* Wang 1993. This diversity of skeletal systems, however, is not evident in the pre-Devonian record of chondrichthyan fish, as the latter are exclusively known from dermoskeletal elements, predominantly represented by isolated scale remains.

Despite the limited data, a study by Karatajūtė-Talimaa (1992) on the early evolution of the chondrichthyan dermal skeleton identified disparate patterns of morphogenesis in Silurian shark-like scale taxa and interpreted those as indicators of an even earlier, Ordovician, initial radiation of the clade. In subsequent years this suggestion has been given credence by the description of

shallow marine vertebrate assemblages containing putative chondrichthyan scale taxa from Laurentian (Sansom et al. 1996, 2001) and Gondwanan (Young 1997; Sansom et al. 2012) localities; see also reviews by Blieck and Turner (2003) and Turner et al. (2004). *Tantalepis gatehousei* (Sansom et al. 2012) is the geologically oldest of these species, described from the Lower Darriwilian (Middle Ordovician) Stairway Sandstone unit of the Larapinta Group (Northern Territory, Australia), with two more putative chondrichthyan taxa (*Areyongalepis oervigi* and ?Chondrichthyes gen. et sp. indet.) from Gondwana reported by Young (1997) from the Darriwilian beds of the Stokes Formation (Larapinta Group). The other previously recognised Ordovician chondrichthyans are Laurentian scale taxa from the Sandbian (Upper Ordovician) horizons of the Harding Sandstone Formation of Colorado, designated as ‘Scale morphology A’ (Sansom et al. 1996, 2001; Donoghue and Sansom 2002), ‘New Genus F’ (Sansom et al. 2001) and a mongolepid species (Sansom et al. 2001; Donoghue and Sansom 2002) that is formally described in Chapter 4.

‘Scale morphology A’ and ‘New Genus F’ are the subject of the present investigation, which documents the histology, crown architecture and canal system configuration of new ‘Scale morphology A’ scale specimens from the Upper Ordovician of Montana (Shell Pine Unit No. 1 well, Ross 1957), as well as material from the Harding Sandstone referred to ‘Scale morphology A’ and ‘New Genus F’ (Sansom et al. 1996, 2001; Donoghue and Sansom 2002). The collected data contributed towards understanding the phylogenetic relevance of scale characters and allowed the proposed in earlier studies chondrichthyan affinities of the above taxa to be assessed. In more general terms, this work is one of only a few to characterise in detail the histology and patterning of odontodes in Ordovician crown gnathostomes and contributes new information

to the on-going research on the integumentary-skeleton evolution of Palaeozoic vertebrates.

3.2. SYSTEMATIC PALAEONTOLOGY

Class CHONDRICHTHYES Huxley, 1880

Order ALTHOLEPIDA Andreev, Shelton, Cooper, Coates and Sansom ordo nov.

Included Families. Altholepidae fam. nov. and Tezakidae fam. nov.

Diagnosis. Chondrichthyans with growing poly-odontocomplex scale crowns developed through sequential addition of component odontodes in posterior and lateral directions. Primordial scale odontode the largest and most anteriorly positioned crown element. Odontode length varies within odontocomplexes.

Family ALTHOLEPIDAE Andreev, Shelton, Cooper and Sansom fam. nov.

Type and only genus. *Altholepis* Karatajūtė-Talimaa 1997.

Diagnosis. Altholepids with scale attachment composed of bone.

Family TEZAKIDAE Andreev, Shelton, Cooper and Sansom fam. nov.

Type and only genus. *Tezakia* gen. nov.

Diagnosis. Altholepids possessing scales entirely formed of dentine.

Remarks*.* The mono-component (dentine) structure (Fig. 7a–c) of *Tezakia* gen. nov. scales is considered a Family-grade characteristic within the Altholepida, distinguishing Tezakidae from the members of Altholepidae, which possess dermoskeletal bone. This is predicated on the notion that crown morphogenetic pattern is more informative to the ordinal affinities of scale taxa than hard-tissue composition, known to be of variable developmental origin in extant batoid neoselachians (Reif 1979; Miyake et al. 1999). Similarly, in lower vertebrate fossil clades with extensively studied integumentary skeleton histology, such as the Thelodonti, there are documented cases of development in separate taxa of either dermal bone or dentine scale support tissues—e.g. within Phlebolepidiformes (Gross 1967; Karatajūtė-Talimaa 1978).

Genus *Tezakia* gen. nov.

Type and only species. *Tezakia hardingi* gen. et sp. nov.

Derivation of name. Derived from ‘Tezak Heavy Equipment Co.’, owners of the type locality, and the suffix *–ia*.

Diagnosis. As for the type species.

Tezakia hardingi sp. nov.

(Figs. 4, 5, 7a–d, 8)

1996 Scale morphology A; Sansom, Smith and Smith, p. 628, fig. 1, 2.

2001 Scale morphology A; Sansom, Smith and Smith, p. 161, fig. 10.3f.

2002 Unnamed chondrichthyan; Donoghue and Sansom, p. 362, fig. 6.4–6.

2008 Ordovician shark; Johanson, Tanaka, Chaplin and Smith, p. 89. fig. 2k, l.

Derivation of name. From ‘Harding Quarry’, the name of the type locality, and the genitive case-ending –*i*.

Locality and horizon*.* The type locality for *T. hardingi* is the Harding Quarry, situated c. 1 km west of Cañon City (Fremont County, Colorado, USA), with a second locality at the Shell Pine Unit No. 1 well (Wibaux County, Montana, USA). The Harding Quarry specimens come from horizons H94-16, H94-20 and H96-20 of the Sandbian (Upper Ordovician) Harding Sandstone Formation (Sansom et al. 1996). The Shell Pine material is derived from core-samples from the Winnipeg Formation (Ross 1957) that is coeval to the Harding Sandstone.

Holotype. An isolated scale (BU5327; Fig. 4b, c) from the Harding Sandstone Formation.

Referred material. A total of approximately three hundred isolated scales (including material figured here and in Sansom et al. 1996, BU2581–BU2583) from the Harding Sandstone Formation and the Winnipeg Formation. Non-figured specimens stored in the Lapworth Museum of Geology, University of Birmingham, UK and the Naturhistoriska Riksmuseet, Stockholm, Sweden, respectively.

Diagnosis*.* Altholepids possessing scales with predominantly needle-shaped to lanceolate scale odontodes organised into multiple odontocomplex rows (up to 15) not divided by inter-odontocomplex spaces. Primordial odontode the longest and the most anteriorly positioned element of the crown. Tubular dentine forms both crown and pedicle components of scales.

Description.

Morphology. Scale shape is primarily rhomboid to ovate (Fig. 4a–g, k), whilst a minority of the specimens (less than 10 per cent) are strongly elongate in either antero-posterior or lateral aspect (Fig. 4j). Scale length exceeds 1 mm in c. 20 per cent of specimens and can be as much as 1.5 mm, whereas the smallest scales are c. 0.4 mm long. The width of the scales varies between 0.4 and 2.3 mm and equals their length in all specimens with the exception of the oblong morphovariants.

Scale crowns are composite structures formed out of 3 or more (up to c. 25) horizontally oriented odontodes that are in contact along their lower anterior and posterior surfaces. The crown primordium is represented by the most anteriorly positioned odontode (Fig. 4), whose shape varies across specimens from teardrop to lanceolate and is consistently identified as the largest (up to c. 400 μm wide) element of the crown. In some specimens (Fig. 4f), the two odontodes flanking the primordium are also larger than the slender odontodes that are the most numerous crown components. Longitudinal odontocomplex rows are evident in crowns with high odontode counts (10 or more) and these originate at an increasingly posterior position away from the sagittal plane of the crown. The maximal number of principle odontode rows (originating at the anterior crown margin) reaches 15, with additional rows commonly inserted further posteriorly along the sides of the odontocomplex initiated by the primordial odontode (Fig. 4d, h, i). Medial odontocomplexes contain the most odontode elements (up to 3–4), whose number progressively decreases to one in the most lateral odontocomplexes. Odontode surfaces are devoid of ornament

and appear featureless apart from the presence of a pronounced medial crest in less than half of the specimens.

Scale pedicles are rhomboid to oval-shaped structures protruding beyond the anterior and lateral crown margins. The anterior half of the pedicle is accentuated by a thickened rim that commonly extends into a bulbous or spike-shaped projection aligned with the primordial odontode. Less than half (c. 40%) of the scales exhibit marked pedicle asymmetry manifested by disproportionate anterior margins, the longer of which is characterised by a strongly indented surface (Fig. 4h, j). The pedicles range from shallow profile ones (less than 200 µm), with a concave to flat lower surface (Fig. 4e), to ones that have massive (200–300 µm thick), bulbous appearance (Fig. 4g). Only the lower surface of the shallow-profile morphology displays numerous canal foramina represented by a large (up to c. 150 µm in diameter) elliptical opening, located under the anterior portion of the primordial odontode, and a more posterior series of smaller (up to c. 70 µm in diameter) foramina similarly distributed under the lower ends of odontodes.

Histology. The crown and pedicle components of the scales are formed of acellular, tubular dentine (Fig. 7a–d). The tubular network is most dense inside the odontodes where it assumes a tangled, arborescent appearance. These tubules (diameter 2–3 µm; Fig. 7d) have a preferentially vertical orientation and exhibit extensive branching along their course. The tubular system of the odontodes emerges from the termini of short dentine canals (diameter up to c.15 µm) that issue apically from the pulp canal. When preserved, the pulps constitute a narrow cavity that extends the odontode length (Fig. 7a) and continues inside the pedicle portion of the scale as a wide vertical canal

(maximal diameter of over 30 µm) that is open on the lower surface of shallow pedicles (Fig. 7b). Similarly to crown pulps, bundles of tubules emerge from these large-calibre dentine canals (Fig. 7b), whereas the rest of the pedicle tubule system connects to a set of smaller-diameter vertical canals (up to c. 10 µm; Fig. 7b–d).

No optically distinct boundary separates the dentine of the crown from that of the underlying pedicle and the two appear to be composed of a single continuous tissue. The pedicle dentine exhibits an uninterrupted series of growth lamellae that vary in thickness (5–20 µm) across the extent of the tissue. The predominant lamella geometry is basally convex, but locally changes to sinuous (Fig. 7b) in proximity of the large-calibre canal spaces.

Remarks. Cyclomorial growth has been proposed as the mechanism of scale development in *Tezakia hardingi* gen. et sp. nov. by Sansom et al. (1996), and this interpretation is also supported by the present study. The evidence for crown growth comes from the observed disparate odontode counts (from three to twenty five) of *Tezakia* gen. nov. scales, considered to indicate discrete phases of crown formation. Inferring growth means that the ontogenetically youngest scales are the ones possessing the fewest number of odontodes, and in *Tezakia* gen. nov. these contain a primordial odontode and two flanking primary odontodes. Specimens that could possibly represent an even earlier, mono-odontode, developmental stage (primordial odontode supported by a rim of attachment tissue; Fig. 5) are also present in the material and have previously been described by Sansom et al. (1996, fig. 3a–d) as thelodont. Furthermore, the decrease of odontocomplex length in the direction of the lateral crown margins is considered indicative of bidirectional odontode addition—towards the

posterior via odontocomplex elongation and lateral through inception of new odontocomplex rows.

Incremental growth, evidenced by depositional lines, is also characteristic for the pedicle support to the crown. Due to preservational bias, the laminated architecture of pedicle dentine is discernable only in *Tezakia* gen. nov. specimens from the Winnipeg Formation, and these demonstrate stacked arrangement of the pedicle lamellae, each covering the lower surface of the previously deposited one. The latter do not form a continuous growth sequence with the lamellae of crown dentine, which are deposited concentrically around odontode pulp canals (Sansom et al. 1996, fig. 2c, d). Morphological data are also supportive of histological observations by revealing variation in pedicle thickness and surface relief between specimens (from low pedicles with concave, pitted surface to massive, smooth-surfaced, bulbous ones), considered representative of progressive stages of pedicle dentine formation.

The mechanism of ontogenetic development of *Tezakia* gen. nov. scales is interpreted as *Altholepis*-like, in accordance with the conclusions reached by Sansom et al. (1996). The *Altholepis*-type of morphogenesis represents a distinct kind of scale growth pattern characteristic for Altholepida, which in light of the new data is diagnosed somewhat differently here from the original definition of Karatajūtė-Talimaa (1992). *Contra* Karatajūtė-Talimaa (1992), a yet-to-be-described partial, articulated specimen of *Altholepis* (UALVP 41483) from the Lochkovian of Canada (Man on the Hill section, Mackenzie Mountains, Northwest Territories, Canada; Hanke and Wilson 2006) provides evidence for formation of new scales during ontogeny by exhibiting scales in various stages of development (up to twofold difference in size and odontode number between

neighbouring scales). Another set of morpho-developmental features shared by the squamation of *Altholepis* and *Tezakia* nov. gen. is the combination of a large primordial odontode, linear odontocomplex architecture and variable length of odontocomplex odontodes, considered characteristic for Altholepida. In contrast, the scale attachment tissues of the two genera are histologically distinct and exhibit different growth patterns—a succession of convex up depositional lamellae typifying the basal bone of *Altholepis* (Karatajūtė-Talimaa 1997) and predominantly convex dentine lamellae documented in *Tezakia* gen. nov. pedicles. Hence, characterization of the attachment tissue surface curvature is omitted from the definition of the *Altholepis* morphogenetic type, despite being included previously by Karatajūtė-Talimaa (1992), as it is known to vary greatly among scale taxa classified on a basis of their particular pattern of crown development (e.g. mongolepid chondichthyans Sansom et al. 2000; Chapter 4).

Order *incertae sedis*

Family *incertae sedis*

Genus *Canonlepis* gen. nov.

Type and only species. *Canonlepis smithae* gen. et sp. nov.

Derivation of name. After Cañon City, situated in proximity of the type locality, and ‘lepis’, scale in Greek.

Diagnosis. As for the type and only species.

Canonlepis smithae sp. nov.

(Figs. 6, 7e–k, 8)

2001 New Genus F; Sansom, Smith and Smith, p. 164, fig. 10.4h.

Derivation of name. In recognition of Professor Moya Meredith Smith (King's College London) and her contribution to studies on the histology of Palaeozoic fish.

Locality and horizon*.* The Harding Quarry, situated c. 1 km W of Cañon City (Fremont County, Colorado, USA), is the type and only known locality of *C. smithae*. The material comes from a Sandbian (Upper Ordovician) horizon (sample number H94-7) of the Harding Sandstone Formation.

Holotype. An isolated scale with accession number BU5265 (Fig. 6a, b).

Referred material*.* Five isolated scales (figured here), including the holotype.

Diagnosis*.* Chondrichthyans possessing growing polyodontode scales with crowns composed of up to eight ovate odontodes organised into three sutured odontocomplexes. Odontode size changes randomly inside scale crowns. Crown surface of odontodes ornamented by vertical ridges.

Description*.*

Morphology. Small scales (maximal length of 0.6 mm) with rhomboid or lanceolate crowns (Fig. 6) that extend posteriorly beyond the limit of the supporting base. The scale crowns consist of five to eight sutured odontodes that are arranged in a medial odontocomplex row (up to four odontodes long;

Fig. 6a–d, h) flanked by short, incipient odontocomplexes (one or two odontodes each; Fig. 6a–d, h). The odontodes are posteriorly curved, ovate to lanceolate elements ornamented by prominent vertical ridges that bifurcate basally from half way down the crown (Fig. 6b, c, e). The medial odontocomplex is composed of the largest scale odontodes (up to 0.2 mm wide), whose size varies randomly within an individual specimen.

The scale base has an irregular, lobate, outline and when intact protrudes beyond the anterior crown border (Fig. 6a, b). Deep furrows mark the basal surface, whereas the lower-base face demonstrates highly granular texture and multiple foramina of variable diameter (30–90 µm).

Histology. Scale odontodes are composed of acellular dentine tissue (Fig. 7e–g) characterised by proximally wide tubules (diameter of c. 5 µm) that bifurcate as straight and long rami (2–3 µm in diameter and more than half of overall tubule length) branched terminally into fine-calibre tubules (c. 1 µm in diameter). The tubular system of each odontode radiates out of a short (less than half the odontode height) pulp cavity space (Fig. 7f, g). The latter continues inside the scale base as a large-calibre vertical canal (maximal diameter of c. 60 µm; Fig. 4f, h) that opens at the lower-base surface (Fig. 7i). The basal bone exhibits a succession of depositional lamellae (Fig. 7h) of wavy geometry that match the outline of the lower basal surface. Oriented parallel to the boundaries of these growth increments are the intrinsic mineralised fibres (*sensu* Ørvig 1966) of the bone tissue matrix, which are intersected by c. 5 µm wide vertical bundles (Fig. 7h) of extraneous fibres (*sensu* Ørvig 1966).

Remarks. The proposed bidirectional (posterior and lateral) crown growth pattern of *Tezakia* gen. nov. is similarly determined to be a feature of *Canonlepis*

gen. nov. scales, as these too exhibit odontocomplex shortening (decrease in odontode number) lateral of the initial odontocomplex. The two taxa are found to share a common odontocomplex structure (Fig. 8) typified by non-regular size change of constituent odontodes, but, whereas the primordial odontode of *Tezakia* gen. nov. is consistently the longest crown element this does not appear to be the norm for *Canonlepis* gen. nov. scales. Considering that *Canonlepis* gen. nov. scales do not possess a large primordial odontode, characteristic for Altholepida, they are regarded to develop a distinct type of crown structure that is similar to that seen in the Devonian putative chondrichthyan scale taxa *Ohiolepis* sp. (Basden et al. 2000, fig. 11.8), *Ohiolepis newberryi* (Wells 1944, pl. III, fig. 11, 13, 14; Gross 1973, pl. 30, fig. 8–10, 12–21; fig. 21 a, b) and *Hercynolepis meischneri* (Gross 1973, pl. 33, fig. 13–15). This patterning of scale odontodes, however, is also recognised in birkeniid anaspids (Märss 1986, pl. XXVI; Blom et al. 2002; Märss 2002, fig. 2–4) and indicates a phylogenetically more basal origin of the *Canonlepis*-type of scale morphogenesis. Following from this, the proposed placement of *C. smithae* gen. et sp. nov within the Chondrichthyes is dictated by the possession of a combination of scale characters not known to occur outside the clade (see Discussion section for details).

3.3. DISCUSSION

3.3.1. The characteristics of chondrichthyan scales

Previous work on the developmental aspects of the chondrichthyan integumentary skeleton has identified widely diverse patterns of scale morphogenesis in Palaeozoic Chondrichthyes (Reif 1978; Karatajūtė-Talimaa 1992, 1998), whereas much less is known about how these compare with the scale development characteristics of other lower vertebrates. It is argued here that the prevalent type of crown architecture of Palaeozoic chondrichthyans with polyodontode scales (e.g. present in Mongolepidida Karatajūtė-Talimaa 1998, ctenacanth-like scales Derycke et al. 1995; Ivanov 1996; Ginter and Sun 2007 and Orodontiformes Zangerl 1968) is also developed in stem osteichthyans (in the Devonian genus *Ligulalepis* Schultze 1968; Burrow 1994). Likewise, the mode of scale formation of the earliest recorded chondrichthyans with mono-odontode scale cover (*Elegestolepis* Karatajūtė-Talimaa 1973 and *Kannathalepis* Märss and Gagnier 2001) is also recognised in thelodontiform thelodonts (*Turinia* and *Helenolepis* Karatajūtė-Talimaa 1978, fig. 14, 15, 27). This has been acknowledged in earlier work (Märss et al. 2007) and indicates that some of the types of scale odontode patterning and development documented in basal chondrichthyans have evolved independently outside the clade.

Neck canal openings (*sensu* Reif 1978), traditionally considered a characteristic of the total-group Chondrichthyes (Maisey 1984, 1986; Lund and Grogan 1997), have also been documented in the scales of phylogenetically more basal acanthodian-grade gnathostomes (e.g. *Diplacanthus* Valiukevičius 2003a; pers. obs., *Cheiracanthus* Gross 1973, fig. 35 b and *Gladiobranchus*

Hanke and Davis 2008, fig. 13) as well as in sister-group taxa (e.g. the stem osteichthyan *Andreolepis* Gross 1968 and the basal actinopterygian *Cheirolepis* Gross 1973, fig. 33 d, 34 d). Furthermore, the external exposure of odontode pulps in the proximity of the crown's support tissue in certain basal chondrichthyans is now understood to be either a transient feature that becomes evident only at particular stages of scale ontogenesis (Märss et al. 2006; Hanke and Wilson 2010) or not to develop altogether (in the Ordovician species *Tantalepis gatehousei* Sansom et al. 2012). The former condition is exemplified by the identified growth series of *Elegestolepis* (Karatajūtė-Talimaa 1973; this study) and *Kannathalepis* (Märss and Gagnier 2001) scales that exhibit formation of neck canals only late in ontogeny through enclosure of vascular cavities by the growing crown. Neck canals can also be masked by rapid deposition of dentine during early scale development (in the mongolepid *Sodolepis* Karatajūtė-Talimaa 1997; Chapter 4).

The linear odontocomplex architecture of *Tezakia* gen. nov. and *Canonlepis* gen. nov. scales is widely developed among Palaeozoic chondrichthyans (e.g. present in Mongolepidida Karatajūtė-Talimaa 1998, Kathemacanthidae Hanke and Wilson 2010; Martínez-Pérez et al. 2010 and Orodontiformes Zangerl 1968), but also occurs in anaspid agnathans (Märss 1986; Blom et al. 2002). The poly-odontocomplex scales of chondrichthyans, nevertheless, can be recognised by the absence of osteons that otherwise commonly develop in the dermal skeleton of the Anaspida (Märss 1986; Blom et al. 2002) and other stem gnathostome clades (e.g. Pteraspidomorphi Denison 1953, 1967; Ørvig 1989 and Osteostraci Stensiö 1932; Denison 1952).

The primitive state of polyodontode micromeric dermoskeletal elements in jawed gnathostomes is represented by various ‘placoderm’ lineages (e.g. Rhenanida [*Ohioaspis*, Gross 1973; Burrow and Turner 1999], Acanthothoraci [*Romundina*, Giles et al. 2013] and Arthrodira [Buchanosteidae, Burrow and Turner 1998]) and is typified by plesiomorphic characteristics, viz superpositional crown growth and cancellous bone formation, shared with Heterostraci, Astraspida (Denison 1967) and Osteostraci (Denison 1952). These are also a feature of the poly-odontocomplex squamation of the Osteichthyes (present in the stem taxa *Lophosteus* Gross 1969, *Andreolepis* Gross 1968 and *Ligulalepis* Schultze 1968)—a sister group of the Chondrichthyes according to most recent phylogenies (Brazeau 2009; Davis et al. 2012)—an observation that further emphasises the specialised nature of chondrichthyan poly-odontocomplex scales.

The existing way of identifying chondrichthyan scales, based on morphogenetic and/or vascular system features, therefore needs to be substituted for an approach that factors in a wider range of morphological, developmental and histological scale attributes. Accordingly, the proposed systematic placement of *Tezakia* gen. nov. and *Canonlepis* gen. nov. is dictated by a set of shared characters—scale symmetry and poly-odontocomplex crown coupled with the absence of enamel, cancellous bone, hard tissue resorption and superpositional odontode generation—that does not exclude their placement inside Chondrichthyes, but is at odds with the known integumentary skeleton characteristics of other lower vertebrate clades.

3.3.2. The integumentary skeleton of Ordovician chondrichthyans

Ordovician chondrichthyan scale taxa share a poly-odontode crown structure, considered to be produced by two different styles of crown morphogenesis that are distinguished by the presence or absence of odontocomplex organisation of scale odontodes. The latter type is identified in the Darriwilian species *Tantalepis gatehousei* (Sansom et al. 2012), where specimens in a supposedly mono-odontode developmental stage have been described (Sansom et al. 2012, fig. 2 d). Comparison of these mono-odontode scales with the more common three-odontode *Tantalepis* scales implies bidirectional addition of odontodes laterally of the crown primordium (Fig. 8). This type of growth has been termed opposite-side zonal by Stensiö (1961, fig. 2G_1–G_8) and outside of *Tantalepis* is known only to occur in the scales of eugeneodontiform chondrichthyans (e.g. in *Eugeneodus* Zangerl 1981). A more complex kind of crown morphogenesis, that involves both lateral and posterior odontode generation (through odontocomplex formation), appears to be prevalent in Ordovician chondrichthyans (identified in *Tezakia* gen. nov., *Canonlepis* gen. nov. and in the mongolepid *Solinalepis* gen. nov. described in Chapter 4). The irregular pattern of odontode-size change within the odontocomplex units of *Tezakia* gen. nov. and *Canonlepis* gen. nov. (Fig. 8) departs considerably from the gradual posterior increase in odontode length documented in mongolepid scales. These odontocomplex architectures have a rather wide distribution among Palaeozoic Chondrichthyes, as they are also recognised in the squamation of post-Silurian chondrichthyans (see above for details).

The available histological data (this study, Sansom et al. 1996, 2000; Karatajūtė-Talimaa 1998; Donoghue and Sansom 2002) reveal that dentine is

the sole crown component of integumentary odontodes in chondrichthyan lineages originating in the Ordovician. Additional evidence indicates that this scale odontode structure has also been retained in Silurian chondrichthyan taxa (Karatajūtė-Talimaa 1998; Märss et al. 2006; Žigaitė and Karatajūtė-Talimaa 2008), *contra* Sire et al. (2009) who have erroneously claimed enameloid in mongolepid and elegestolepid scales.

Tezakia gen. nov. and *Canonlepis* gen. nov. odontodes demonstrate the geologically oldest tubular dentines recorded in the Chondrichthyes. The dentine structure of *Tezakia* gen. nov. is found to be broadly similar to the thelodont type 2b dentine of Žigaitė et al. (2013)— arborescent tubules confluent with large-calibre dentine canals—described in the Silurian genera *Helenolepis* (Karatajūtė-Talimaa 1978) and *Shielia* (Märss and Karatajūtė-Talimaa 2002). The linear, large-calibre dentine-tubule architecture developed in *Canonlepis* gen. nov. is likewise present in the Thelodonti (the *Turinia* histological type of Märss et al. 2007) and within crown gnathostomes appears in the putative chondrichthyan scale taxon *Kannathalepis milleri* (Märss and Gagnier 2001). Uncharacteristically for chondrichthyan polyodontode scales, the pedicle dentine of *Tezakia* gen. nov. provides the only support for the crown odontodes, as dermal bone is absent in this genus. This is a feature shared with the mono-odontode scales of neoselachians (Johanson et al. 2008). In contrast, *Canonlepis* gen. nov. along with the Ordovician mongolepid *Solinalepis* gen. nov. (Donoghue and Sansom 2002; Chapter 4) possess the earliest known chondrichthyan scales with a two-component (odontogenic and osteogenic) organization that is common among Palaeozoic chondrichthyans.

3.4. CONCLUSIONS

The present study of *Tezakia* gen. nov. and *Canonlepis* gen. nov. establishes a hierarchy of scale characters according to which these taxa are classified at an ordinal (scale-crown odontode patterning), familial (scale support-tissue histology) and generic (scale morphology) level. On the basis of the new data, it is proposed that the general pattern of scale-crown morphogenesis and the hard tissue structure of the two taxa conform to that of basal chondrichthyans and justifies their placement within the Chondrichthyes, in agreement with previous studies (Sansom et al. 1996; Sansom et al. 2001; Donoghue and Sansom 2002; Johanson et al. 2008).

The identification of contrasting crown architecture and hard-tissue composition between *Tezakia* gen. nov. and *Canonlepis* gen. nov. specimens, coupled with evidence from other Ordovician chondrichthyan scale taxa (Donoghue and Sansom 2002; Sansom et al. 2012; Chapters 4, 6), is linked to rapid evolution of the integumentary skeleton within the clade and is interpreted to point to an extensive early diversification of basal chondrichthyan fish.

Figure 4 (on the following page). *Tezakia hardingi* gen. et sp. nov. scales from the Sandbian (Upper Ordovician) Harding Sandstone of central Colorado, USA (**a**–**c**, **f**, **j**, **k**) and the Winnipeg Formation (Shell Pine Unit No. 1) of Montana, USA (**d**, **e**, **g**–**i**). Symmetrical scales with poly-odontocomplex crowns in (**a**) anterior crown (BU5326), **(b**) crown (BU5327 holotype), (**c**) postero-lateral (BU5327 holotype), (**d**) crown (NRM-PZ X1), (**e**) basal (NRM-PZ X2), (**f**) crown (BU5330), (**g**) basal (NRM-PZ X3) and (**j**) crown (BU5332) views. Poly-odontocomplex asymmetrical scales (**h**) NRM-PZ X3 and (**i**) NRM-PZ X4 in crown view. (**k**) Symmetrical scale (BU5335) in crown view displaying incipient odontocomplexes. Anterior towards the bottom in (b, d–k). (a, b, d–k) SEM micrographs; (c) volume rendering. Scale bar represents 200 µm in (a–g, j, k) and 300 µm in (h, i).

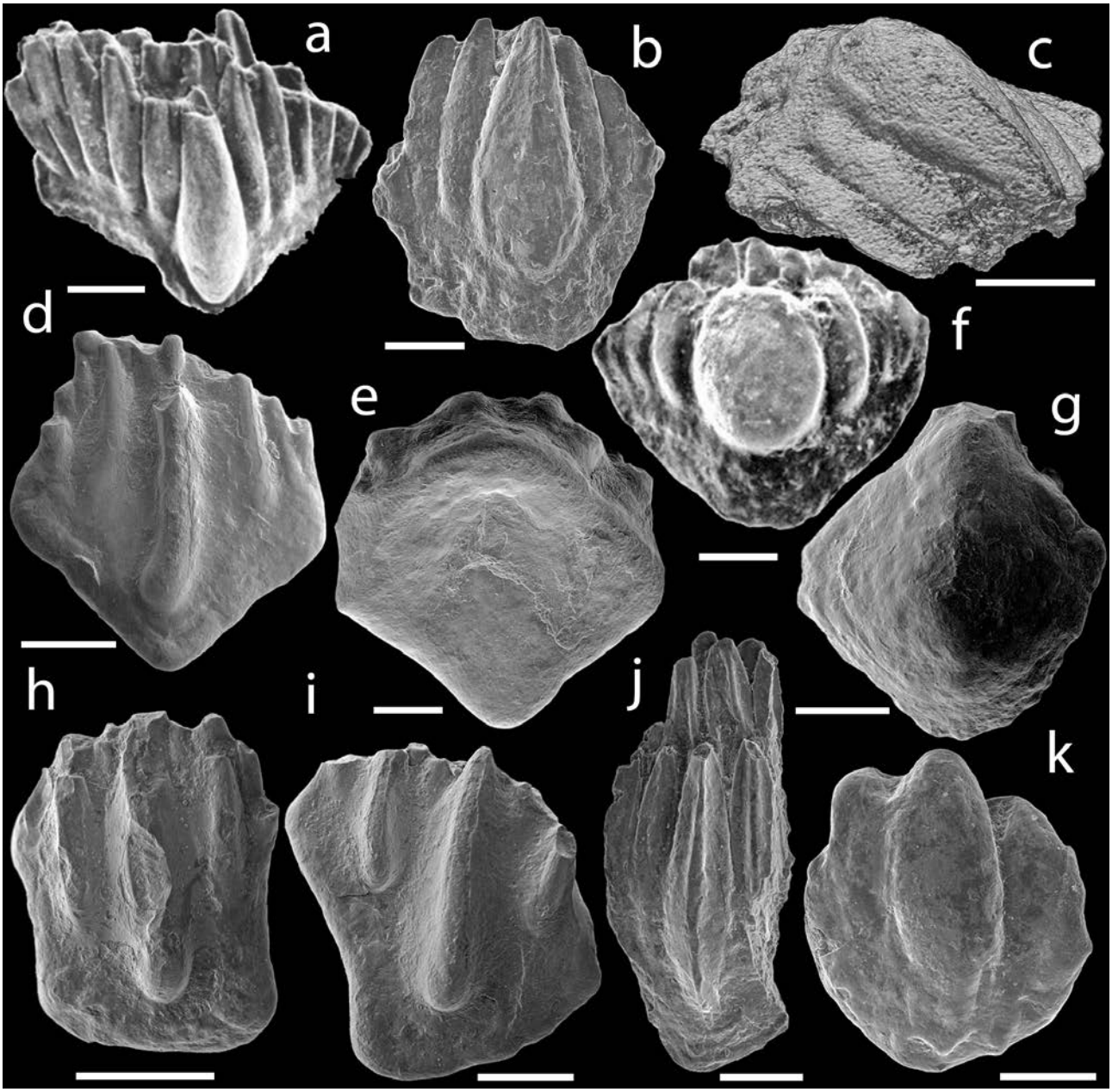
a
b
c
d
e
f
g
h
i
j
k

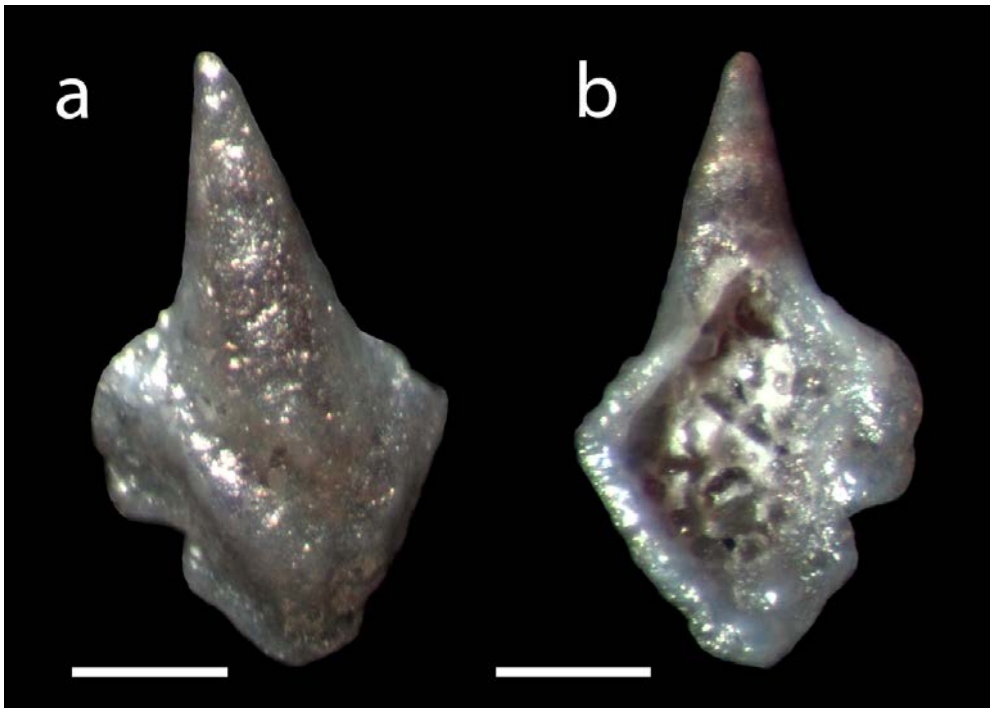

Figure 5. Light micrographs of a probable ontogenetically young (mono-odontode) *Tezakia hardingi* gen. et sp. nov. scale (BU5336) from the Sandbian (Upper Ordovician) Harding Sandstone of central Colorado (USA), depicted in (**a**) crown and (**b**) basal view. Scale bar represents 200 µm.

Figure 6 (on the following page). *Canonlepis smithae* gen. et sp. nov. scales from the Sandbian (Upper Ordovician) Harding Sandstone of central Colorado, USA. (**a**) Crown and (**b**) lateral crown views of BU5265 (holotype). (**c**, **d**) Crown views of BU5266 and BU5267. (**e**–**g**) BU5268 in (**e**) anterior, (**f**) basal and (**g**) posterior views. (**h**) Specimen BU5346 in lateral crown view. (a–d, h) SEM micrographs; (e–g) volume renderings. Anterior towards the bottom in (a, c, d, f) and towards the left in (b, h). Scale bar represents 200 µm.

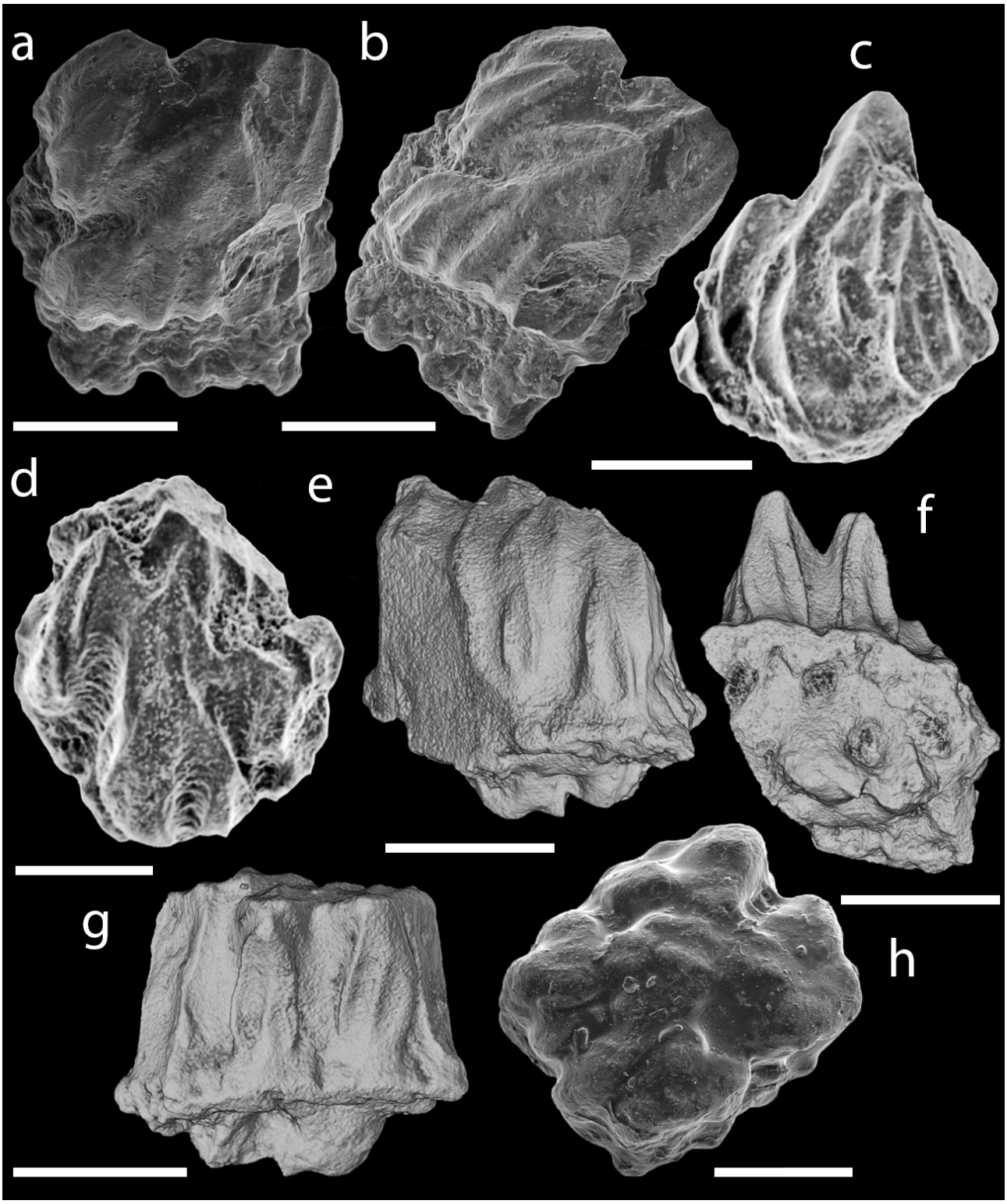
a
b
c
d
e
f
g
h

Figure 7 (on the following page). Hard-tissue structure and canal system architecture of (**a**–**d, i**) *Tezakia hardingi* gen. et sp. nov. and (**e**–**h**, **j**, **k**) *Canonlepis smithae* gen. et sp. nov. scales from (**a**, **g**–**k**) the Sandbian (Upper Ordovician) Harding Sandstone of central Colorado, USA and (**b**–**d**) the Winnipeg Formation (Shell Pine Unit No. 1) of Montana, USA. (**a**) Longitudinal sagittal section of BU2582. (**b**, **c**) Transverse vertical sections of NRM-PZ X5 and NRM-PZ X6. (**d**) Detail of (**c**). (**e**) Longitudinal and (**f**) transverse tomographic slices of42 BU5268. (**g**) Scale odontode in longitudinal section (BU5267). (**h**) Portion of the basal bone tissue of a transversely sectioned scale (BU5268). (**i**) Detail of odontodes (top) and scale attachment tissue of BU5337 in basal view. Canals (red) inside a translucent specimen (BU5268) in (**j**) posterior and (**k**) crown views. (a–d, g, h) Nomarski DIC optics micrographs; (e, f, j, k) volume renderings; (i) SEM micrograph. Anterior towards left in (a, g) towards right in (e) and towards the bottom in (i, k). bbc, basal bone canal; pc, pulp canal; pdc, pedicle dentine canal; pdco, pedicle dentine canal opening; arrowheads point at dentine tubules in (e–g). Scale bar represents 200 µm in (a–c, f, i, k), 100 µm in (d, e, j) and 25 µm in (h).

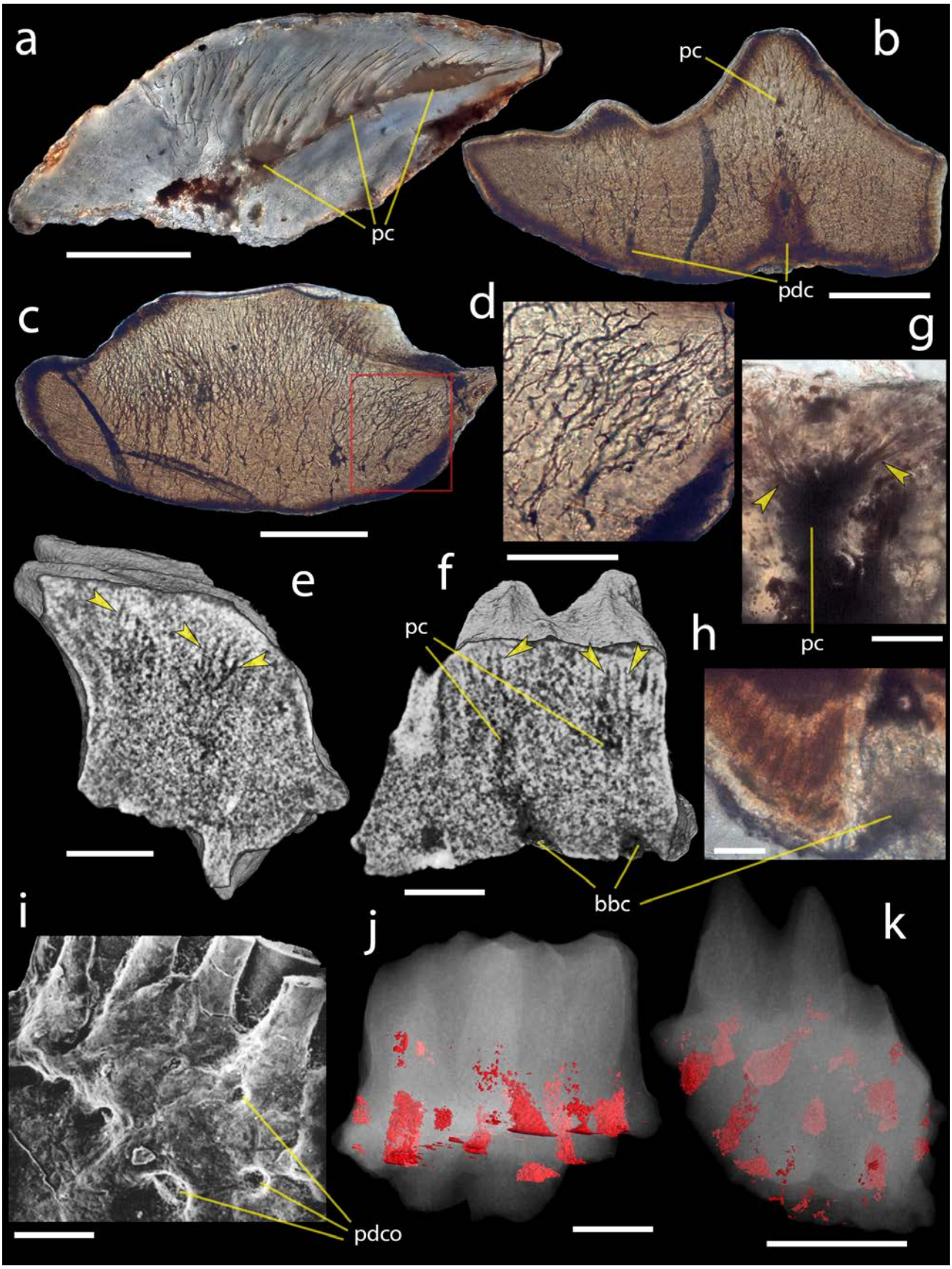
a
pc
b
pc
pdc
c
d
g
e
f
pc
h
pc
bbc
i
j
k
pdco

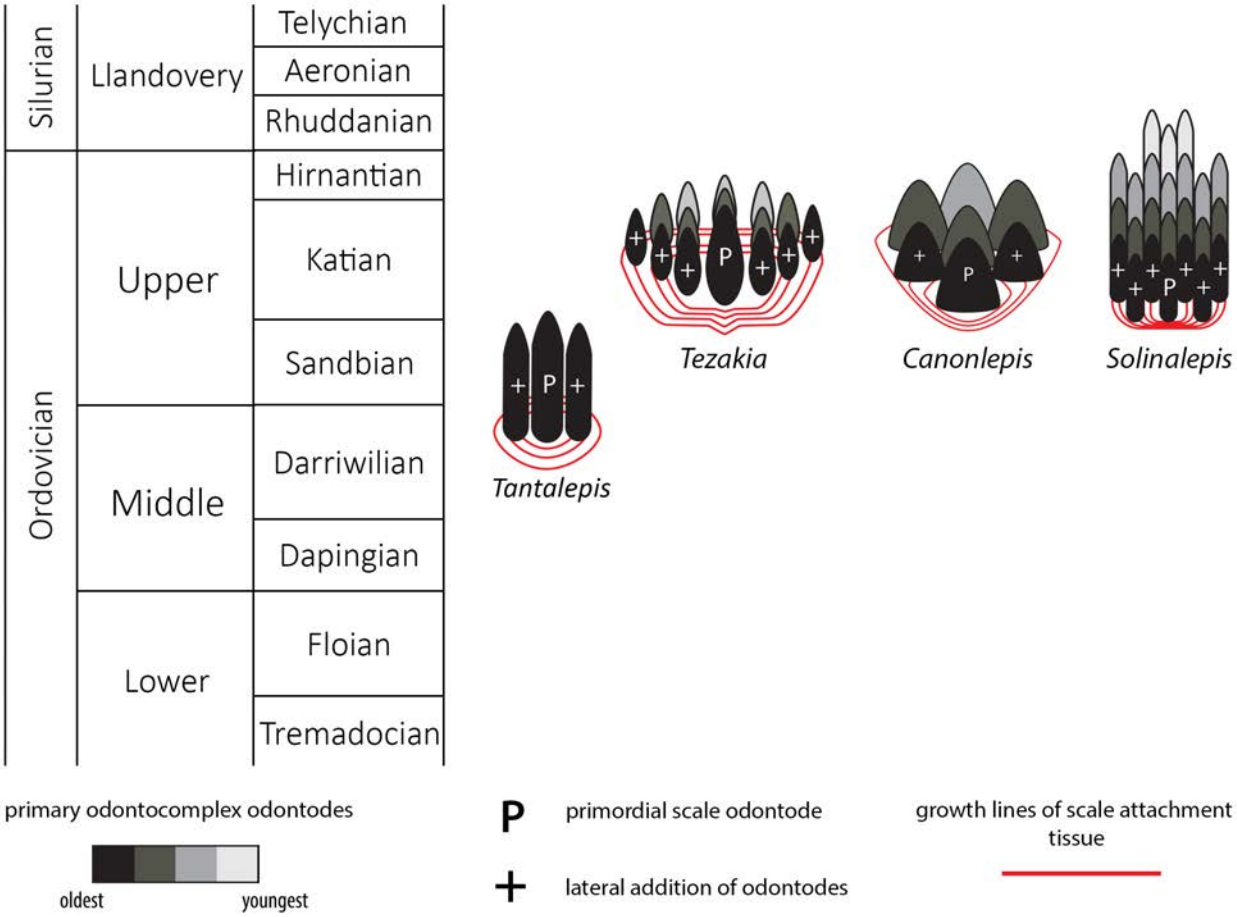

Figure 8. Diagrammatic representation of scale-morphogenesis patterns and odontocomplex structure of known Ordovician chondrichthyans. Recognised morphogenetic types: *Eugeneodus*-type (*sensu* this study, see Chapter 6) in *Tantalepis*, *Altholepis*-type (*sensu* this study, see Chapter 6) in *Tezakia* gen. nov., *Ohiolepis*-type (*sensu* this study, see Chapter 6) in *Canonlepis* gen. nov. and *Mongolepis*-type (*sensu* this study, see Chapter 6) in *Solinalepis* gen. nov.

Chapter 4: Ordovician origin of Mongolepidida and the integumentary skeleton of basal chondrichthyans

4.1. INTRODUCTION

Middle Ordovician to Upper Silurian strata have yielded a number of disarticulated remains that have been assigned to the chondrichthyans with varying degrees of confidence; a 50 million year record pre-dating the first appearance in the Devonian of clear chondrichthyan teeth (*Leonodus* and *Celtiberina* Botella et al. 2009) and the earliest articulated specimens (*Doliodus* Miller et al. 2003; Maisey et al. 2009 and *Antarctilamna* Young, 1982). These, largely microscopic, remains include the elegestolepids (Karatajūtė-Talimaa 1973), sinacanthids (Zhu 1998; Sansom et al. 2005b), taxa such as an as-yet-unnamed scale-based form from the Harding Sandstone (Sansom et al. 1996), *Tantalepis* (Sansom et al. 2012), *Kannathalepis* (Märss and Gagnier 2001) and *Pilolepis* (Thorsteinsson 1973), and, perhaps the most widely distributed and diverse collection of what Ørvig and Bendix-Almgreen, quoted in Karatajūtė-Talimaa (1995), referred to as ‘praechondrichthyes’, the mongolepids (Karatajūtė-Talimaa et al. 1990; Karatajūtė-Talimaa and Predtechneskyj 1995; Sansom et al. 2000). It is the latter which this work concentrates on, re-assessing and re-defining previously described members of the Mongolepidida, and describing a new taxon that extends the range of the order into the Ordovician, adding further evidence for a diversification of early chondrichthyans as part of the Great Ordovician Biodiversification Event that encompasses a wide variety of taxa, both invertebrate (e.g. Webby et al.

2004; Servais et al. 2010) and vertebrate (Sansom et al. 2001; Turner et al. 2004 in Webby et al. 2004 etc).

Previous work on mongolepids.

Mongolepids were first described by Karatajūtė-Talimaa et al. (1990) from the Chargat Formation (Upper Llandovery–Lower Wenlock) in north-western Mongolia, together with a diverse assemblage of early vertebrates including pteraspidomorphs (Karatajūtė-Talimaa et al. in prep.), thelodonts (Žigaitė et al. 2011), acanthodians and elegestolepids. The type species *Mongolepis rozmanae* was subsequently added to with the description of *Teslepis jucunda* Karatajūtė-Talimaa and Novitskaya (1992) and *Sodolepis lucens* Karatajūtė-Talimaa and Novitskaya (1997), also from the Chargat Formation. *Shiqianolepis hollandi* from the Xiushan Formation (Telychian) of south China was also placed within the order by Sansom et al. (2000), although a new family, the Shiqianolepidae, was erected based upon an interpretation of the scale growth patterns within mongolepids. Additional material from the upper Llandovery of the Tarim Basin (Xinjiang Uygyr Autonomous Region, north-west China), due to be described by Wang et al. (in prep.), is also referable to the group. Thus, to date, the distribution of mongolepids has been limited to a very narrow time frame (Llandovery–Wenlock) and is also concentrated within the Mongol-Tuva, South China and Tarim tectonic blocks.

The taxonomic placement of the group has been greatly hampered by the absence of any articulated specimens that exhibit any anatomical detail of the mongolepid bauplan (Karatajūtė-Talimaa et al. 1990; Karatajūtė-Talimaa 1995).

4.2. SYSTEMATIC PALAEONTOLOGY

Class CHONDRICHTHYES Huxley, 1880

Order MONGOLEPIDIDA Karatajūtė-Talimaa, Novitskaya, Rozman and Sodov, 1990

Included families. Mongolepididae Karatajūtė-Talimaa et al. 1990 and Shiqianolepidae Sansom et al. 2000.

Emended diagnosis. Chondrichthyans with polyodontode growing scale crowns formed by multiple antero-posteriorly oriented primary odontocomplex rows. Odontode size within each row increases gradually towards the posterior of the scale. Individual odontodes formed exclusively of inotropically and spheritically mineralised atubular, acellular dentine (lamellin).

Remarks. The current study has determined scale crown growth (*sensu* Reif 1978) to be a characteristic shared by all mongolepid taxa (see Discussion for details), contrary to previous interpretations of synchronomorial development of scale odontodes in Mongolian mongolepid species (Karatajūtė-Talimaa et al. 1990; Karatajūtė-Talimaa and Novitskaya 1992, 1997). Under the revised definition of the order, the Mongolepidida retains the families Mongolepididae (Karatajūtė-Talimaa et al. 1990) and Shiqianolepidae (Sansom et al. 2000), yet *contra* Sansom et al. (2000) these are diagnosed on the basis of base histology (see below) and are expanded to also include the genera *Rongolepis* and *Xinjiangichthys* respectively. A third newly identified mongolepid species, *Solinalepis levis* gen. et sp. nov., is placed as *incertae sedis* due to it not exhibiting the family-grade characteristics of the other members of the clade.

Family MONGOLEPIDIDAE Karatajūtė-Talimaa, Novitskaya, Rozman and Sodov, 1990

Included genera. *Mongolepis* Karatajūtė-Talimaa et al. 1990*, Teslepis* Karatajūtė-Talimaa and Novitskaya 1992, *Sodolepis* Talimaa and Novitskaya 1997 and *Rongolepis* Sansom et al. 2000.

Emended diagnosis. Mongolepids possessing scale bases composed of acellular bone tissue with plywood-like layering.

Remarks. Scale-derived phylogenetic data (see Chapter 6) identify two monophyletic groups inside Mongolepidida distinguished by differences in the bone histology of the scale base. These substitute the scale-crown developmental characteristics used previously by Sansom et al. (2000) to establish the family structure of the Mongolepidida.

Genus *Mongolepis* Karatajūtė-Talimaa, Novitskaya, Rozman and Sodov, 1990

Type and only species. *Mongolepis rozmanae* Karatajūtė-Talimaa et al. 1990, from the Chargat Formation, Salhit regional Stage (Upper Llandovery–Lower Wenlock) of north-western Mongolia.

Emended diagnosis. As for the type species.

Mongolepis rozmanae Karatajūtė-Talimaa, Novitskaya, Rozman and Sodov, 1990

(Figs. 9a–c, 11a–c, 12a–c, 13d)

Emended diagnosis. Mongolepidids (pertaining to Mongolepididae) possessing scale crowns that attain lengths of up to 3 mm. Crowns containing a maximum of 40 primary odontocomplex rows separated by inter-odontocomplex spaces. Primary odontode pulps

opened on the crown surface via a pair of horizontal canals. Bulbous base with prominent crescent-shaped anterior platform that extends beyond the limit of the crown.

Holotype. An ontogenetically mature scale (M-1-031) deposited in collection M-1 of the Lithuanian Geological Survey, Vilnius (Karatajūtė-Talimaa et al. 1990).

Referred material. Hundreds of isolated scales (including material figured here and in Karatajūtė-Talimaa et al. 1990 and Karatajūtė-Talimaa and Novitskaya 1992, M-1-023) from the type locality; samples 16/3 and ЦГЭ N1009. Non-figured specimens stored in the Lapworth Museum of Geology, University of Birmingham, UK.

Description.

Morphology. Primary odontodes of the same generation are of equal size irrespective of scale dimensions. The number of odontocomplex rows changes with the proportions of the crown and its size, with scales of up to 2 mm in length usually possessing less than 20 odontocomplexes, whereas in larger specimens their number varies from 20 to c. 35.

Primary odontodes exhibit posteriorly curved profiles and an incremental increase in length towards the posterior of the scale (Figs. 11a–b, 13d). This creates a significant height difference (over five fold in medial odontocomplexes) between the anterior- and the posterior-most primary odontodes, whilst odontode thickness remains relatively constant at c. 50 µm (Figs. 11a–b, 13d). The crown surface profile is planar (Fig. 9a, b) due to a gradual decrease in the angle of odontode curvature towards the posterior of the scale, accompanied by sloping of the crown/base contact surface (Figs. 11a, 13d).

In scales larger than 1 mm, secondary odontodes are developed to a varying extent along the anterior margin of the crown (Fig. 9a, b). These are arranged into rows and are undivided by inter-odontode spaces (Fig. 9a, b). Similarly to the main crown odontodes, the secondary odontodes are posteriorly arched elements that demonstrate

an unidirectional increase in length (Figs. 11a–b, 13d); the latter being expressed towards the anterior end of the scale.

The scale bases are bulbous structures (Fig. 9a–c) that reach their maximum thickness directly under the anterior apex of the crown. To the posterior, the majority of scale bases display a pitted lower-base surface produced by series of canal openings (Fig. 9b, c).

Histology. Scale odontodes are composed of atubular dentine (Fig. 11a–c); lamellin in Karatajūtė-Talimaa et al. (1990). Within individual odontodes, the lamellin displays two histologically distinct regions—a peripheral (10–20 μm thick) lamellar zone and an inner region dominated by spherites united within *Liesegang* waves (Fig. 11c). The diameter of the calcospherites changes randomly and rarely exceeds 15 μm.

Primary odontode pulps are mostly closed off or greatly constricted by dentine infill, but remain open at their lower end, from which emerges a pair of short (c. 15 μm) horizontal canals that connect the pulp cavity to the odontode surface (Fig. 12c, c1). The foramina of these canals face either the inter-odontocomplex spaces or, in marginal odontodes, are exposed at the periphery of the crown (Fig. 9a).

In a similar manner to primary odontocomplexes, the pulps of secondary odontodes are substantially constricted by dentine deposition, but lack the network of horizontal canals (Figs. 9a–b, 12c) developed inside the rest of the crown.

The scale base consists of acellular bone characterised by a succession of convex-down growth lamellae (up to 150 μm thick; Fig. 11a) that increase in areal extent towards the lower portion of the tissue. Secondary lamination is evident within these primary depositional structures and is produced by intrinsic mineralised fibres (*sensu* Ørvig 1966) of c. 2 μm diameter, which are likewise present at the contact surfaces of

primary lamellae (Fig. 11a). The basal bone tissue also harbors elaborately organised extraneous crystalline fibres (*sensu* Ørvig 1966) of c. 2 µm diameter (Fig. 11a), which have the appearance of hollow cylindrical rods. These are grouped into layers oriented obliquely in respect to one another (Fig. 11a), that propagate through the entire tissue. The layers exhibit upwardly arching profiles and thickness of c. 50-70 µm. A second extraneous component of the mineralised bone matrix consists of vertically directed attachment fibres (Fig. 11a) crosscutting the lamellae of the base. The former are mutually parallel and evenly spaced at approximately 10 µm intervals; never observed to group into higher order structures such as bundles or lamellae.

The base houses a vascular system represented by curved (both anteriorly and posteriorly) large-calibre vertical canals (c. 100 µm; Fig. 12a, b) that are split at their upper end into two or more rami, each merging with one of the primary odontode pulps. Conversely, the secondary odontode pulps are not connected to the canal system of the base.

Remarks. In comparison to earlier work on *Mongolepis* (Karatajūtė-Talimaa et al. 1990; Karatajūtė-Talimaa 1998), the present study interprets in a new way the mechanism of scale ontogenesis of the genus. Recorded size differences between *Mongolepis* scales have been used by previous authors to identify four distinct ontogenetic stages in the development of the scale cover. They have suggested synchronomorial crown growth succeeded by incremental deposition of basal bone to typify the scale morphogenesis of *Mongolepis*, with scales of ever-increasing crown size and base thickness assumed to be added at each stage of scale cover ontogeny.

The conducted re-examination of *Mongolepis* material revealed the presence of bases across the spectrum of documented scale sizes. More to the point, specimens of the sub-millimetre category, corresponding to the papillary and juvenile scales of

Karatajūtė-Talimaa et al. (1990), possess bases that are proportionally as thick as those of larger scales. This questions the validity of reconstructions depicting these scales as composed exclusively of odontodes (Karatajūtė-Talimaa 1998, fig. 11A2, E), perhaps founded upon descriptions of specimens with fully abraded bases. The morphological evidence is thus in favor of a hypothesis proposing incremental and mutually synchronous deposition of *Mongolepis* crown and base scale components. The odontocomplex structure and base depositional lamellae of *Mongolepis* scales are similarly identified in all recognised mongolepid genera and indicate that cyclomorial scale growth is a characteristic of the Mongolepidida (refer to Discussion for details).

Genus *Teslepis* Karatajūtė-Talimaa and Novitskaya, 1992

Type and only species. *Teslepis jucunda* Karatajūtė-Talimaa and Novitskaya, 1992, from the Chargat Formation (Salhit regional Stage, Upper Llandovery–Lower Wenlock) of north-western Mongolia.

Emended diagnosis. As for the type species.

Teslepis jucunda Karatajūtė-Talimaa and Novitskaya, 1992

(Figs. 9d–e, 4d, 12d, 13a)

Emended diagnosis. Mongolepidids with scale crowns that reach length of 1 mm. Crowns possess up to 13 odontocomplex rows divided by linear spaces. Anterior and lateral crown margins composed of a crescent-shaped mass of atubular globular dentine. Lower portions of crown pulps opened at the odontode surface via a pair of horizontal canals. Scale base always thicker than the crown at an antero-basally directed conical projection.

Holotype. An ontogenetically mature scale (M-1-077) deposited in collection M-1 of the Lithuanian Geological Survey, Vilnius (Karatajūtė-Talimaa and Novitskaya 1992).

Referred material. Hundreds of isolated scales (including specimens figured here and in Karatajūtė-Talimaa and Novitskaya 1992) from the type locality; samples 16/3 and ЦГЭ N1009). Non-figured specimens stored in the Lapworth Museum of Geology, University of Birmingham, UK.

Description.

Morphology. The number of the scale odontocomplex rows is related to crown size and its proportions. In small specimens (less than 0.5 mm long) their number varies from 4 to 6, whilst it reaches 13 in scales larger than 1 mm. Within individual odontocomplexes the odontode length gradually increases in a posterior direction (Fig. 11d), whereas odontode thickness remains relatively constant at c. 50 µm.

In the majority of specimens a crescent-shaped platform (Fig. 9d) is formed anterior to the odontocomplexes, and the former can be elevated slightly above the level of the odontodes. The absence of this thickening does not correlate with a particular scale size.

The base is not constricted at the contact with the crown (Fig. 9d, e) and extends away from this junction into an anteriorly-directed conical projection that protrudes beyond the crown margin. The posterior third of the base is shallower in comparison to its thickened anterior (Fig. 11d), and is marked by rows of canal openings (30–60 µm in diameter; Fig. 9e) aligned with the odontocomplexes of the crown.

Histology. The crown odontodes consist of atubular dentine (lamellin; Fig. 11d) exhibiting a predominately lamellar periphery and an inner spheritically mineralised region. The calcospherites of the globular lamellin attain a diameter of approximately 10 µm and

comprise of concentric *Liesegang* rings closed around a central cavity. These exhibit linear or concave arrested growth contact surfaces with other spherites and adjacent *Liesegang* waves. The scale odontodes possess vascular spaces in the form of vestiges of pulp canals that are mostly filled in by lamellin. The pulps branch out laterally as paired short horizontal canals (diameter 10–15 µm) that open on the odontode surface (Fig 12d, d1).

A structural variety of atubular dentine different from lamelline composes the crown platform that surmounts the thickest part of the base (Fig. 11d). This tissue exhibits exclusively spheritic mineralization manifested by tightly packed globules (up to 10 µm in diameter), and lacks a canal system.

The basal bone is acellular and demonstrates a series of depositional lamellae demarcated by basally arched intrinsic fibres (Fig. 11d). The smallest lamellae reside at the level of the anterior-most odontodes, with lamella thickness varying from 15 µm to 20 µm across the extent of the tissue.

The basal bone contains extraneous mineralised fibres grouped into 20–40 µm thick layers with upwardly curved profiles. The fibres within each layer are mutually parallel but also oriented obliquely to those of adjacent lamellae, giving the bone a plywood-like texture. In addition to the abundant fibres with layered organization, the tissue contains a set of extraneous, vertically oriented fibres (Fig. 11d) that are evenly spaced at about 5 µm intervals and propagate up to the level of the crown-base junction.

The base is penetrated by a number of large-calibre vertical vascular canals (Fig. 12d, d1), which connect with the pulp cavities of crown odontodes. The former are predominantly preserved in the posterior (thinnest) third of the base as anteriorly arching canals that gradually widen to c. 40 µm at the lower base surface (Fig. 12d, d1).

Remarks. The anterior crown platform of *Teslepis* scales (developed also in *Sodolepis*) has received little attention in the descriptions of Karatajūtė-Talimaa and Novitskaya (1992) and Karatajūtė-Talimaa (1998), apart from being identified as composed of an undetermined type of globular basal tissue. The platform always forms at the level of the primary odontodes and sutures to the anterior most of them, developing at the place typically occupied by secondary odontodes in *Mongolepis*, *Rongolepis*, *Xinjiangichthys* and *Shiqianolepis* scales. From a histological perspective, the lack of lamellar matrix and the predominantly arrested-growth contact surfaces of spherites resemble the microstructure of certain types of spheritically mineralised dentine (Schmidt and Keil 1971, fig. 46, 47). Consequently, this tissue is regarded to be globular atubular dentine as opposed to globular dermal bone that is commonly formed only in the cavity-rich cancellous zone of the exoskeleton of lower vertebrates (Ørvig 1968; Donoghue et al. 2006; Downs and Donoghue 2009). Contrasting with the well-defined and consistent shape of the odontodes, the anterior platform is a structure with irregular surface and poorly defined boundaries, whose shape is determined by the contours of the underlying base. Following from the above, it could be suggested that this mass of globular dentine is not the product of a well-differentiated dermal papilla, which typifies early odontode development and determines the morphology of odontodes independently of that of the basal bone (Sire 1994; Sire and Huysseune 1996; Sire and Huysseune 2003). Outside *Teslepis* and *Sodolepis*, dentine structures with similar characteristics have not been documented in the integumentary skeleton of gnathostomes.

Cellular basal bone was considered by Karatajūtė-Talimaa and Novitskaya (1992) to be a diagnostic character of *Teslepis* in the original description of the genus. The fusiform odontocyte lacunae identified in that study are demonstrated here to actually represent the hollow interiors of the mineralised fibres of the bone matrix. This would

make the basal bone of *Teslepis* scales homologous to the galeaspidin-like (*sensu* Wang et al. 2005 and Sire et al. 2009) support tissue of most mongolepids.

Genus *Sodolepis* Karatajūtė-Talimaa and Novitskaya, 1997

Type and only species. *Sodolepis lucens* Karatajūtė-Talimaa and Novitskaya, 1997, from the Chargat Formation (Salhit regional Stage, Upper Llandovery–Lower Wenlock) of north-western Mongolia.

Emended diagnosis. As for the type species.

Sodolepis lucens Karatajūtė-Talimaa and Novitskaya, 1997

(Figs. 9f–g, 11e–h, 12e)

Emended diagnosis. Mongolepidids with scales reaching lengths of up to 2.5 mm that possess crowns composed of 4 to 8 odontocomplex rows sutured along their length. Crescent-shaped anterior crown platform formed of globular dentine. Base thicker than the crown and extended into an anteriorly directed conical projection.

Holotype. An isolated scale (M-1-091) deposited in collection M-1 of the Lithuanian Geological Survey, Vilnius (Karatajūtė-Talimaa and Novitskaya 1997).

Referred material. More than a hundred isolated scales (including material figured here and in Karatajūtė-Talimaa and Novitskaya 1997) from the type locality; samples 16/3 and ЦГЭ N1009. Non-figured specimens stored in the Lapworth Museum of Geology, University of Birmingham, UK.

Remarks. The gross morphology of *Sodolepis* scales (Fig. 9f, g) closely resembles that of *Teslepis*, with the two genera demonstrating comparable histology. The latter, however, are distinguished on the basis of differences in scale size and odontocomplex number. *Sodolepis* crowns can have up to 8 odontocomplexes, which is c. 40% less than their maximal number in *Teslepis*, whilst at the same time *Sodolepis* scales are on average twice as large as those of *Teslepis*. This is due to a corresponding increase of odontode and scale size in *Sodolepis*, leading to the formation of a relatively constant number of odontocomplexes irrespective of crown dimensions. In *Teslepis* specimens, on the other hand, odontode size remains consistent across all documented scale lengths.

As noted by Karatajūtė-Talimaa and Novitskaya (1997), a system of horizontal canals cannot be identified inside *Sodolepis* scale crowns (Fig. 12e)—an atypical condition considering that the majority of mongolepid genera develop some type of pulp canal openings on the lower crown surface.

Genus *Rongolepis* Sansom, Aldridge and Smith, 2000

Type and only species. *Rongolepis cosmetica* from the Telychian (Upper Llandovery) of south China, Lower Member of the Xiushan Formation (Sansom et al. 2000).

Emended diagnosis. As for the type species.

Rongolepis cosmetica Sansom, Aldridge and Smith, 2000

(Figs. 9k–m, 11i–j)

Emended diagnosis. Mongolepidid species with up to 2 mm long scale crowns that are widest at their posterior third. Crowns formed of 10 to 20 crown odontocomplex rows ornamented by narrow median ridges, flanked anteriorly and laterally by conical secondary odontodes. Lower crown face pitted by rows of foramina. Base tetragonal or oblong, displaced towards the scale anterior. Lower base surface concave to flat with a central conical projection.

Holotype. An isolated scale (NIGP 130326) from the Xiushan Formation of south China (Sansom et al. 2000).

Referred material. Hundreds of specimens (including material figured here and in Sansom et al. 2000, NIGP 130319–NIGP 130330) from the Telychian (Upper Llandovery, Silurian) Xiushan Formation (sample Shiqian 14B) of Leijiatun (Shiqian county, south China). Non-figured specimens stored in the Nanjing Institute of Geology and Palaeontology, Chinese Academy of Sciences, Nanjing, China.

Remarks. The uncertainty regarding the systematic position of *Rongolepis* in the original description of the genus (Sansom et al. 2000) has been attributed to a suite of characteristics (scale morphology, posterior of the crown composed of acellular lamellar bone and presence of crown odontodes) not known in the scales of other vertebrates. The re-examination of *Rongolepis cosmetica* has enabled the identification of a combination of features diagnostic for Mongolepidida. Of particular importance in this regard is the nature of the tissue composing the flared posterior extension of *Rongolepis* scales. Suggested to be formed of lamellar bone (Sansom et al. 2000), this portion of the scale in fact demonstrates the lamellin-type architecture of an ionotropically and spheritically mineralised atubular tissue devoid of attachment fibres (Fig. 11i, j). Moreover, the segmentation of the crown's posterior part observed in thin sections (Fig. 11i, j; Sansom et al. 2000, fig. 12e) is interpreted to be produced by the contact surfaces of sutured

odontodes. Both the anterior to posterior increase in length of these elements and their arrangement in longitudinal rows over the posterior half of the base are known features of mongolepid primary odontocomplexes. The assignment of *Rongolepis* to Mongolepidida is thus dictated by the possession of its scales of lamellin and poly-odontocomplex growing crowns.

Family SHIQIANOLEPIDAE Sansom, Aldridge and Smith 2000

Included genera. *Xinjiangichthys* Wang et al. 1998 and *Shiqianolepis* Sansom et al. 2000.

Emended diagnosis. Mongolepids with scale bases composed of avascular, cellular bone tissue.

Genus *Xinjiangichthys* Wang, Zhang, Wang and Zhu, 1998

Type and only species. *Xinjiangichthys pluridentatus* Wang, Zhang, Wang and Zhu, 1998, from the Telychian (Upper Llandovery, Silurian) Yimugantawu Formation (north-western margin of the Tarim Basin, Xinjiang, PR China).

Emended diagnosis. As for the type species.

Remarks. The placement of *Xinjiangichthys* inside Mongolepidida by Wang et al. (1998) was justified on the grounds of similarities in crown morphology and odontode patterning with Mongolian mongolepids (the only known mongolepid taxa at the time of its description), and this study advances further on that claim by identifying a poly-odontocomplex crown structure in *Xinjiangichthys* scales.

The presence of atubular dentine in *Xinjiangichthys* scales, another of the diagnostic characteristics of mongolepids (this study; Karatajūtė-Talimaa et al. 1990; Sansom et al. 2000), can be determined in thin-section (Fig. 11k) and through X-ray microtomography (Fig. 12g, h).

Furthermore, Wang et al.'s (1998) interpretation of *Xinjiangichthys* scale bases as non-growing (not supported by evidence) is rejected by demonstrating a conical basal tissue that supports at its apex the primordial odontode and further posteriorly the rest of the scale's primary odontodes (Figs. 11k, 12h), similarly to the growing bases of *Shiqianolepis* and those of mongolepids in large.

Xinjiangichthys pluridentatus Wang, Zhang, Wang and Zhu, 1998

(Figs. 9n–o, 11k, 12g–h)

1998 *Xinjiangichthys tarimensis* Wang, Zhang, Wang and Zhu: pl. 1, fig. e-i.

2000 *Xinjiangichthys* sp. Sansom, Aldridge and Smith: 236, fig. 8.

Emended diagnosis. Shiqianolepids having wider than long scale crows that reach maximal length of 1 mm. Crowns composed of up to 30 sutured odontocomplexes bordered anteriorly by an aggregation of sutured secondary odontodes. Lower crown surface marked by multiple vertical rows of foramina. Pronounced constriction of the crown at the junction with the base. Base low, gracile with concave lower base surface.

Holotype. An isolated scale (IVPP V11663.1) from the Yimugantawu Formation of Xinjiang (Bachu county), China (Wang et al. 1998).

Referred material. Two specimens from the Telychian Xiushan Formation (Leijiatun, Shiqian county, south China; sample Shiqian 14B), in addition to material (NIGP 130291 and NIGP 130292) figured in Sansom et al. (2000), and five specimens (including IVPP V X1, IVPP V X2 and specimens figured in Wang et al. 1998, IVPP V11663.1, IVPP V11663.2, IVPP V11664.1, IVPP V11664.2) from the Telychian Yimugantawu Formation (Bachu County, Xinjiang, China). Non-figured Xiushan Formation specimens are stored in the Nanjing Institute of Geology and Palaeontology, Chinese Academy of Sciences, Nanjing, China, whilst those from the Yimugantawu Formation are stored in the Institute of Vertebrate Paleontology and Paleoanthropology, Chinese Academy of Sciences, Beijing, China.

Remarks. *X*. *tarimensis* and *X*. sp. are synonymised with *X*. *pluridentatus* based upon the absence of differentiating characteristics between the specimens attributed to the two species. The arguments (equal-sized crown odontodes, scale neck and pitted sub-crown surface) of Wang et al. (1998) for erecting *X*. *tarimensis* are considered not valid for the following reasons. The large-diameter anterior odontodes of *X*. *pluridentatus* specimens figured by Wang et al. (1998, pl. Ia, c) represent secondary odontodes not developed in all scale types of the species (specimens identified as *X*. *tarimensis* by Wang et al. 1998, pl. Ie-i), which is consistent with the condition documented in *Mongolepis* (this study and Karatajūtė-Talimaa et al. 1990). The presence of secondary odontodes also accounts for the lack of a distinct neck in the *Xinjiangichthys* scales they form in, by occupying the sloped anterior surface of the base. Addressing the third point of Wang et al. (1998), the numerous foramina present on the lower crown surface of scales attributed to *X*. *tarimensis* (Wang et al. 1998) are also detected (Fig. 9n–o, 12g–h) in *Xinjiangichthys* specimens with secondary odontodes.

Genus *Shiqianolepis* Sansom, Aldridge and Smith, 2000

Type and only species*. Shiqianolepis hollandi* Sansom et al. 2000, from the Telychian (Upper Llandovery) of southern China, Lower Member of the Xiushan Formation.

Emended diagnosis. As for the type species.

Shiqianolepis hollandi Sansom, Aldridge and Smith, 2000

(Figs. 9h–j, 11l, 12f, 13b, e)

Emended diagnosis. Shiqianolepids with trunk scale crowns reaching lengths of c. 1.5 mm. Crowns composed of 5 to 9 primary odontocomplexes, separated posteriorly by deep inter-odontocomplex spaces, and a cluster of tightly sutured secondary odontodes formed anteriorly of crown odontocomplexes. Crown surface ornamented by tuberculate ridges. Multiple canal openings formed on the lower crown surface. Anteriorly displaced scale base with concave lower base surface. Oblong asymmetrical head scales (up to 1 mm long) with irregularly-shaped odontodes distributed peripherally around a medial ridge.

Holotype. An isolated trunk scale (NIGP 130294) from the Xiushan Formation of Leijiatun (Shiqian county) south China (Sansom et al. 2000).

Referred material. Hundreds of isolated scales (including figured here material) and type series specimens (NIGP 130293–NIGP 130318) from the Telychian Xiushan Formation (sample Shiqian 14B) of Leijiatun (Shiqian county, south China). Non-figured specimens stored in the Nanjing Institute of Geology and Palaeontology, Chinese Academy of Sciences, Nanjing, China.

Remarks. Characteristic of *Shiqianolepis* scales is a distinct primordial odontode located at the apex of the conical base. This odontode has been termed ‘proto-scale’ by Sansom et al. (2000) and identified as a diminutive element overlain by the much larger odontodes deposited at later stages of crown ontogeny. Superpositional growth, which results in odontodes not being exposed on the crown surface, is a condition atypical for other mongolepids, also demonstrated not to be a feature of *Shiqianolepis* scales. Upon examination of figured material and newly sectioned specimens, the primordial odontode borders recognised in Sansom et al. (2000, figs. 6b, 7) are considered here to in fact constitute the margins of dentine depositional lamellae (Fig. 11l), as these are occasionally observed to be indented by more peripherally formed calcospherites—evidencing a centripetal mode of dentine histogenesis as opposed to stacking of primary odontodes. As identified here, the primordial odontode in *Shiqianolepis* scales is overlapped only at its anterior end by secondary odontodes, whilst most of its upper margin remains exposed on the crown surface. Similarly to the rest of the crown odontocomplexes of *Shiqianolepis*, the one incepted by the ‘proto-scale’ displays a gradual posterior increase of odontode size.

Family *incertae sedis*

Genus *Solinalepis* gen. nov.

Type and only species*. Solinalepis levis* gen. et sp. nov.

Derivation of name*.* From ‘solinas’ (tube, pipe in Greek), pertaining to the shape of the scale odontodes of the species, and ‘lepis’, scale in Greek.

Diagnosis*.* As for the type species.

Remarks. Characters relating to the dimensions of the scale base (its length and thickness in relation to those of the crown) unite *Solinalepis* gen. nov. (data from the conducted phylogenetic analysis, see Chapter 6) in a clade with members of Shiqianolepidae. Nevertheless, this type of morphological data is not regarded informative at a supra-generic level and the genus is classified outside the two recognised mongolepid families due to differences in scale base histology (acellular bone lacking plywood-like organization of its mineralised matrix). Presently, *Solinalepis* gen. nov. is treated as Mongolepidida *incertae sedis* for the reluctance on part of the author to erect a new mono-generic family.

Solinalepis levis sp. nov

(Figs. 10, 11m–n, 12i–j, 13c)

2001 '?Mongolepid scales'; Sansom, Smith and Smith, p. 161, fig. 10.3g, h.

2002 Unnamed chondrichthyan; Donoghue and Sansom, p. 362, fig. 6.3.

2009 Stem-chondrichthyan; Sire, Donoghue and Vickaryous, p. 424. fig. 10c.

Derivation of name. From the Latin 'levis' (smooth), referring to the unornamented scale crown surface of the species.

Locality and horizon. The type locality is the vicinity of the Harding Quarry, situated c. 1 km west of Cañon City (Fremont County, Colorado, USA). All *Solinalepis* specimens come from Sandbian strata (samples H94-26 and H96-20) of the Harding Sandstone.

Holotype. An isolated trunk scale (BU5310; Fig. 10e).

Referred material. Hundreds of isolated scales, including material figured here. Non-figured specimens stored in the Lapworth Museum of Geology, University of Birmingham, UK.

Diagnosis. Mongolepid species with trunk scales reaching less than a millimeter in width. Trunk scale crowns composed of sutured tubular odontodes organised in longitudinal odontocomplex rows (up to 30 in number). Acellular basal bone housing an elaborate canal system that opens via foramina on the basal surface. Tessera-like or bulbous head scales possessing radially arranged odontode rows.

Description.

Morphology of trunk scales. The scales vary in length between 100–400 µm, which is always less (up to three quarters) than their width. The crowns of specimens with lengths exceeding 200 µm demonstrate polygonal (Fig. 10e–g), often asymmetrical (Fig. 10f, g), outlines. The anterior crown margin of these scales is predominantly wedge-shaped whilst their posterior face is straight (Fig. 10i). In contrast, the crowns of antero-posteriorly short (100–200 µm long) scales tend to be symmetrical, leaf-shaped structures (Fig. 10j–l), rarely demonstrating simple geometrical profiles in crown view.

Irrespective of crown morphology, the odontodes of all trunk scales are organised into closely packed antero-posteriorly aligned rows (Figs. 10f–g, j, 13c). Adjacent rows are displaced by approximately half an odontode diameter (c. 15 µm), resulting in offsetting between odontodes of neighbouring odontocomplexes (Fig. 13c). The odontodes themselves are cylindrical, tube-like elements with sigmoidal profiles that taper to a point apically (Fig. 13j). Odontode length increases gradually towards the scale's posterior end, where the crown can reach a height of c. 400 µm.

The crown/base transition is not marked by a neck-like constriction (Fig. 10e–l), with the base never attaining more than a third of the overall scale height. The basal surface is marked by deeply incised grooves (Fig. 10e–i) that give it a dimpled appearance, characteristic also for the lower base surface. The latter has a predominantly flat profile but can exhibit a central conical projection that is particularly well developed in leaf-shaped specimens (Fig. 10l).

Morphology of head scales. Polyodontode symmetrical or asymmetrical scales with recorded height between 0.5 and 1.3 mm. These are represented by two main morphological variants, a compact, bulbous type (Fig. 10d) and tessera-like scales (Fig. 10a–c) of larger diameter. Both morphotypes possess irregular crowns composed of radially ordered odontodes, and do not exhibit distinct anterior and posterior scale faces. The radiating odontodes form rows (five to nine odontodes long), offset in a manner in which the odontodes of each row oppose the inter-odontode contacts of neighbouring odontocomplexes. Odontode height diminishes gradually towards the crown centre, accompanied by an increase of coalescence between odontodes.

The scales exhibit a prominent central bulge, away from which the crown surface slopes down to the scale margin. The latter has a corrugated outline that in certain specimens is accentuated by deep, peripherally expanding grooves (Fig. 10a, b).

The scale base displays a granular, grooved surface and follows the outline of the crown. At its centre the base attains maximal thickness (Fig. 11m), and gradually decreases in height away from this point. The lower-base surface is predominantly planar or can have a moderate central concavity, but never exhibits the convex topology documented in trunk scale specimens.

Histology of trunk scales. Crown odontodes are structured out of atubular dentine (lamellin; Fig. 11n) that is spherically mineralised in proximity of the pulp (spherite diameter 10–15 µm).

Cylindrical, non-branching pulp cavities occupy the centre of odontodes and are connected at their lower ends with the canal system of the base (Fig. 12i, j). The latter is represented by vertical canals that bifurcate close to the crown-base junction, with each pair of rami re-connecting deeper inside the base, resulting in the formation of a series of vascular loops (Fig. 12i, j). Vertically oriented canals emerge from the looped canal system and open on the lower base surface. The basal surface is similarly marked by numerous foramina that are the exit points for the peripheral canals of the base (Fig. 10h).

The base is composed of acellular bone demonstrating the presence of c. 2 µm thick extraneous mineralised fibres that propagate vertically through the tissue (Fig. 11n).

Histology of head scales. Due to diagenetic alteration, the histology of the crown odontodes is largely obscured. Nevertheless, wide odontode pulp canals are evident in sectioned specimens (Fig. 11m), and these appear to end blindly inside the crown. The upper base surface is perforated by a row of foramina (Fig. 10c, d) similar to the ones documented in trunk scales.

The main structural components of the basal bone matrix are tightly packed, parallel mineralised fibres with horizontal orientation (Fig. 11m). These are crosscut by apically converging fibre bundles (up to 15 µm in diameter), which follow undulating paths across the tissue.

Remarks. The development of lamellin-composed poly-odontocomplex scale crowns identify *Solinalepis levis* gen. et sp. nov. as a mongolepid species. Moreover, the trunk

scale odontocomplexes of *Solinalepis* gen. nov. exhibit the same progressive posterior increase in odontode length documented in members of the order.

Within Mongolepidida, the combination of a large odontocomplex number (>20) and sutured odontodes is present only in the Telychian genus *Xinjiangichthys*. Nevertheless, the two taxa are readily distinguished on the basis of scale dimensions, crown and base morphology and canal-opening distribution on the scale surface. *Solinalepis* gen. nov. is one of only two described mongolepid genera (the other being *Shiqianolepis*) with squamation clearly differentiated into distinct trunk (exhibiting recognisable anterior and posterior faces) and head morphotypes (irregular-shaped elements)—a condition that is consistent with that recorded in a number of heterosquamous Lower Palaeozoic gnathostomes known from articulated specimens (e.g. *Climatius reticulatus* Miles 1973, *Obtusacanthus corroconius* Hanke and Wilson 2004, *Gladiobranchus probaton* Hanke and Davis 2008 and *Ptomacanthus anglicus* Miles 1973; Brazeau 2012).

4.3. DISCUSSION

4.3.1. Crown morphogenesis of mongolepid scales

Shiqianolepis hollandi is recognised as a key taxon for determining the mode of scale crown development in mongolepids, following the identification by Sansom et al. (2000) of ‘proto-scale’ (early-development phase) specimens of the species (Sansom et al. 2000, fig. 4u, w). The size (half of that of ‘mature’ trunk scales) and the small number of crown odontodes (exhibiting only the earliest formed odontodes of incipient primary odontocomplexes) of these scales implies that in *Shiqianolepis* scale ontogenesis

involves crown enlargement through sequential addition of odontodes. Significantly, the *Shiqianolepis*-type of crown architecture (primary odontocomplex rows originating at the most elevated point of the base and characterised by a posterior increase in size of their constituent odontodes) is developed in all members of the Mongolepidida (Figs. 11a, d, h–i, k–l, 13) and this evidence is used to propose that the mongolepids share a cyclomorial pattern of scale ontogenesis.

Data from developmental studies on extant neoselachians indicate that their scales cannot serve as model systems for determining the mechanism of morphogenesis of the compound mongolepid scale crowns, as the former have been shown to be simple mono-odontode elements produced by a single epithelio-ectomesenchymal primordium (Schmidt and Keil 1971; Reif 1980b, Miyake et al. 1999; Sire and Huysseune 2003; Johanson et al. 2007, 2008). Examinations of multiple odontode generation in osteichthyan scales (Kerr 1952; Smith et al. 1972; Smith 1979; Sire and Huysseune 1996), though, provide insight into the timing of deposition of odontode aggregations associated with a dermal bone support tissue. These studies reveal phases of odontode generation that result in an increase of odontode number throughout scale ontogeny.

The hypothesis of scale crown growth in Mongolepidida is further substantiated by evidence from the Palaeozoic record of the Chondrichthyes. The scale crown structure of certain chondrichthyan taxa described from articulated specimens (e.g. *Diplodoselache woodi* Dick 1981, *Tamiobatis vetustus* Williams 1998 and *Orodus greggi* Zangerl 1968), conform closely to the recorded odontode patterning of mongolepid scales. *Diplodeselache* trunk scales were noted by Dick (1981) to closely resemble those of *Orodus* and to be similarly characterised by cyclomorial growth. Previous work (Reif 1978) on the morphogenesis of the chondrichthyan integumentary skeleton also recognised sequential crown elongation through regular addition of odontodes as the

mechanism of scale development in *Orodus*. This pattern of crown formation is also typical for scales with *Ctenacanthus costellatus* type of morphogenesis (defined by Reif 1978 and equivalent to the *Ctenacanthus* B3 morphogenetic type of Karatajūtė-Talimaa 1992) to which *Tamiobatis* scales have been attributed (Williams 1998).

4.3.2. Mongolepid scale crown histology

The origin of dentine is coincident with the emergence of skeletal mineralisation in vertebrates (Donoghue and Sansom 2002; Donoghue et al. 2006), with the phylogenetically most primitive atubular varieties of the tissue being considered to compose the basal bodies of certain conodont genera (Sansom 1996; Smith et al. 1996; Donoghue 1998; Dong et al. 2005). Conodont atubular ‘dentines’ frequently exhibit (Sansom 1996, fig. 2e–h; Donoghue 1998, fig. 5a–c; Dong et al. 2005, pl. 1, figs 3–9) peripheral lamellar fabric, substituted internally by spheritically mineralised matrix, making them comparable to the architecture of mongolepid lamellin (Fig. 11c, e). Apart from their presence in the oro-pharyngeal skeleton of conodonts and mongolepid scale crowns, atubular dentines have been identified with certainty only in the scale odontodes of the pteraspidomorph *Tesakoviaspis concentrica* (Karatajūtė-Talimaa and Smith 2004) and the fin spine ornament of sinacanthid gnathostomes (Sansom et al. 2000, 2005b).

An important aspect of the atubular nature of lamellin is that it provides circumstantial evidence for the involvement of atypical odontoblasts in the generation of the tissue. Commonly, during dentinogenesis mature odontoblasts extend long cellular processes into the mineralised phase, which remain contained inside tubular spaces after formation of the tissue is complete (Linde 1989; Linde and Lundgren 1995; Yoshiba et al. 2002; Magloire et al. 2004, 2009). Consequently, the inability of secretory

odontoblasts to form dentinal tubules is taken to suggest that such cells either did not penetrate at any depth the dentine matrix with their processes or lacked such altogether. Atypical odontoblasts devoid of large cytoplasmic projections have been reported in the tooth germs of the Recent sting ray *Dasyatis akajei* (Sasagawa 1995), but these are found to co-exist with unipolar odontoblasts, characterised by well-developed processes. The apical portions of odontoblasts and their processes have been implicated as ion channel-rich sites capable of being activated by environmental stimuli via tubular fluid movement, and are presumably involved in transmitting sensory input to pulp nerve endings (Okumura et al. 2005; Allard et al. 2006; Magloire et al. 2009). This raises the possibility that mongolepid scale pulps had limited ability to transduce sensory input compared to an odontoblast population that forms tubular network inside a mineralised dentine matrix.

4.3.3. Histology of mongolepid scale bases

This and previous studies (Karatajūtė-Talimaa et al. 1990; Karatajūtė-Talimaa and Novitskaya 1992, 1997; Sansom et al. 2000) identify mongolepid scale odontodes to be supported by a common base composed of lamellar bone (Fig. 11a, d, g–i, k–n). The basal tissue of *Mongolepis* and *Sodolepis* scales has been interpreted as acellular bone (Karatajūtė-Talimaa et al. 1990; Karatajūtė-Talimaa and Novitskaya 1997), with this study also recognizing the absence of osteocyte lacunae in the bases of *Teslepis* (*contra* Karatajūtė-Talimaa and Novitskaya 1992), *Rongolepis* (concordant with Sansom et al. 2000) and *Solinalepis* gen. nov.—restricting the occurrence of cellular bone inside Mongolepidida to the genera *Xinjiangichthys* and *Shiqianolepis* (this study and Sansom et al. 2000).

A plywood-like layering of crystalline fibres is recognised as the predominant type of basal bone texture of mongolepid scales, being documented in the four genera of the family Mongolepididae. This architecture of the mineralised matrix matches closely the organization of the collagen fibres in the deep dermis (stratum compactum) of extant neoselachians (Motta 1977; Miyake et al. 1999; Sire and Huysseune 2003) and osteichthyans (Kerr 1952, 1955; Sire 1993; Gemballa and Bartsch 2002) and is suggested to be indicative of dermal bone histogenesis achieved through mineralisation of a largely unmodified fibrous scaffold of the stratum compactum—a process referred to as metaplastic ossification (Sire 1993; Sire et al. 2009). Consequently, the observed absence of plywood-like layering in the cellular bone of mongolepid scale bases (in *Xinjiangichthys*, *Shiqianolepis* and *Solinalepis* gen. nov.) could be interpreted to result from remodelling of the original fibrous framework of stratum compactum prior to tissue mineralisation (a process described by Sire 1993 in the scales of the armoured catfish *Corydoras arcuatus*).

The data above allow the identification of the site of basal bone formation of mongolepid scales within the deep tiers of the corium, with the tissue being considered to periodically increase in size due to the growth increments documented in sectioned specimens. These depositional phases reveal a common pattern of generation of mongolepid scale bases, wherein each newly laid down lamella covers the lower surface of the previously deposited one. The geometry of the lamellae shows little change, implying retention of a fairly consistent base shape throughout scale ontogeny. Such a pattern of base morphogenesis is not unique to the Mongolepidida, but appears to be the prevalent mode of bone tissue growth in the scales of jawed gnathostomes, being demonstrated in ‘placoderms’ (Burrow and Turner 1998, 1999), ‘acanthodians’ (Denison 1979), basal osteichthyans (Gross 1968; Schultze 1968) and basal chondrichthyans (Karatajūtė-Talimaa 1973; Mader 1986; Wang 1993).

4.3.4. Canal system of mongolepid scales

Previously, the internal canal system architecture of mongolepid scales had been investigated in detail only in *Mongolepis*, *Teslepis* and *Sodolepis* through oil immersion studies of whole specimens and thin section work (Karatajūtė-Talimaa et al. 1990; Karatajūtė-Talimaa and Novitskaya 1992, 1997). The employment of X-ray microtomography allowed these data to be supplemented by visualizing with greater accuracy the three-dimensional structure of scale cavity spaces in the examined genera.

In *Mongolepis*, *Teslepis*, *Sodolepis* and *Solinalepis* gen. nov. the lower ends of odontode pulp cavities are continuous with the canal system of the base. Comparable type of vascularisation is developed in the Upper Ordovician chondrichthyan scales from the Harding Sandstone referred to *Tezakia* in Chapter 3 ('scale morphology A' in Sansom et al. 1996, 2001). The lower base surface of this taxon has been demonstrated to exhibit rows of foramina (Sansom et al. 1996, fig. 2a) that are similar to the basal canal openings of mongolepids. Likewise, the central canal of the basal bone tissue is continuous with the odontode pulp in the Silurian scale genera *Elegestolepis* (Karatajūtė-Talimaa 1973) and *Kannathalepis* (Märss and Gagnier 2001), which are the earliest recorded mono-odontode scale taxa attributed to the Chondrichthyes (see Chapter 5). This condition is also identified in the mono-odontode scales of various Upper Palaeozoic chondrichthyans (e.g. *Janassa* Ørvig 1966; Malzahn 1968, *Ornithoprion* Zangerl 1966 and *Hopleacanthus* Schaumberg 1982), Mesozoic hybodonts (Reif 1978) and extant neoselachians (Reif 1980b; Miyake et al. 1999; Johanson et al. 2008).

Xinjiangichthys, *Shiqianolepis* and *Rongolepis* differ from the other mongolepid genera in having their entire scale canal system confined to the crown, with the lower ends of odontode pulps opening at the crown surface in proximity of the base. The posterior peripheral odontodes of these three genera display additional cavities that are

detected as foramina on the lower crown face. A similarly pitted lower crown surface has also been identified in poracanthodid ‘acanthodians’ (Gross 1956; Valiukevičius 1992; Burrow 2003c), the putative stem chondrichthyan *Seretolepis* (Hanke and Wilson 2010; Martinez-Perez et al. 2010), and in ctenacanthiform scales (e.g. *Tamiobatis vetustus* Williams 1998 and *Ctenacanthus costellatus* Reif 1978). In the scales of *Poracanthodes* these openings represent the posterior exit points of a complex canal network that is absent from mongolepid scale crowns.

Studies on the squamation of jawed gnathostomes reveal the lack of basal tissue vascularisation to be a common feature of many ‘acanthodians’ (Denison 1979; Karatajūtė-Talimaa and Smith 2003; Valiukevičius 2003a; Valiukevičius and Burrow 2005) and chondrichthyans such as *Protacrodus* (Gross 1973), *Orodus* (Zangerl 1968) and *Holmesella* (Ørvig 1966), including some of the earliest known post-Silurian putative chondrichthyan scale taxa (*Iberolepis*, *Lunalepis* Mader 1986 and *Nogueralepis* Wang 1993).

Despite the observed differences in canal architecture, all mongolepid genera with the exception of *Sodolepis* develop canal openings exposed on the scale surface in the region the crown-base interface. These foramina represent the termini of canals homologous to the neck canals of euselachians (*sensu* Reif 1978), as they link the main pulp canal to the odontode surface. In *Mongolepis* and *Teslepis* this connection is established via one pair of short canals (the ‘horizontal canals’ of Karatajūtė-Talimaa et al. 1990, Karatajūtė-Talimaa and Novitskaya 1992 and Karatajūtė-Talimaa 1998) that issue from the lower end of each pulp. The new data presented here indicate that the horizontal canal system of these two genera is housed inside the scale crown, contrary to previous depictions of the feature at the crown-base junction (Karatajūtė-Talimaa 1995, 1998). In contrast, the lower ends of odontode pulp canals of North American and

Chinese mongolepids do not branch out, and either open directly onto the scale surface (*Shiqianolepis* and *Rongolepis*) or continue inside the base (*Solinalepis* gen. nov.).

4.3.5 Systematic position of the Mongolepidida

Scale-based cladistic analyses have never previously been employed (but see Chapter 6) to resolve the inter-relationships of basal gnathostomes, whilst recent phylogenies of Palaeozoic gnathostomes incorporate only a limited set of scale characters (Brazeau 2009; Davis et al. 2012; Zhu et al. 201375). This is also true for phylogenetic investigations of the total group Chondrichthyes (Lund and Grogan 1997; Grogan and Lund 2008; Grogan et al. 2012)—to which mongolepids have been tentatively suggested to belong (Karatajūtė-Talimaa and Novitskaya 1997; Sansom et al. 2000)—that give preference to dental over scale characteristics. Accordingly, high-ranked chondrichthyan clades are largely diagnosed on tooth characters (Zangerl 1981; Stahl 1999; Ginter et al. 2010), whereas Lower Palaeozoic shark-like scale taxa are yet to be included in formal classification schemes of the Chondrichthyes.

The validity of Mongolepidida is reaffirmed here on the basis of an amended character set, which diagnoses the order by the unique combination of scale growth, poly-odontocomplex scale crowns and development of lamellin (the monophyly of Mongolepidida is also supported by scale-based phylogenetic data—see Chapter 6). The placement of mongolepids within Chondrichthyes, on the other hand, has been questioned in the past on the basis of their atubular dentine (lamellin) crowns and the presence of a horizontal canal system (Karatajūtė-Talimaa and Novitskaya 1992). This study demonstrates that the horizontal canals of *Mongolepis* and *Teslepis* are equivalent to euselachian neck canals, whilst revealing similar canal spaces in the crown odontodes of Chinese mongolepids. However, neck-like canals are also known in the scales of

‘placoderms’ (Burrow and Turner 1998) and basal Palaeozoic osteichthyans (Gross 1953, 1968), and are thus not a chondrichthyan apomorphy. Addressing the other argument of Karatajūtė-Talimaa and Novitskaya (1992), scale dentine histology appears to vary greatly within the total group Chondrichthyes (e.g. distinct dentine types are developed in *Elegestolepis* Karatajūtė-Talimaa 1973, *Seretolepis* Hanke and Wilson 2010, *Orodus* Zangerl 1968 and *Hybodus* Reif 1978), which makes it a poor diagnostic character at a supra-ordinal level. By the same token, although atubular dentine occurs in the Mongolepidida, it is also formed in the dermal skeleton of pteraspidomorph agnathans (Karatajūtė-Talimaa and Smith 2004) and therefore is uninformative in respect to the relationships of the order. The systematic affinities of Mongolepidida are determined instead by a unique combination of scale attributes that are shared with particular Palaeozoic chondrichthyan lineages. Reference is made here to the development of predominantly symmetrical trunk scales with multiple crown odontocomplexes that lack cancellous bone, enamel and hard tissue resorption—a type of squamation known also to have evolved in xenacanthiform (*Diplodoselache*, Dick 1981), orodontiform (*Orodus*, Zangerl 1968) and cladodontomorph (e.g. *Cladolepis* Burrow et al. 2000 and *Cladoselache*, Dean 1909) chondrichthyans.

4.4. CONCLUSIONS

The present revision of Mongolepidida established the order as a natural group of early chondrichthyans characterised by poly-odontocomplex growing scales with *Ctenacanthus*-like crown architecture. However, in agreement with Karatajūtė-Talimaa

(1992), the scales of mongolepids are recognised to exhibit a distinct, *Mongolepis*, type of morphogenesis, on account of their lamellin composed crowns.

The description of the mongolepid genus *Solinalepis* gen. nov. from the Sandbian of North America, pushes back the first appearance of the Mongolepidida by 20 My and firmly places the origin of the Chondrichthyes in the Ordovician. Together with reports of other shark-like scale taxa from Ordovician (Sansom et al. 1996, 2001, 2012), this further supports the proposed by Karatajūtė-Talimaa (1992) early chondrichthyan diversification event, that preceded the first known appearance of chondrichthyan teeth and articulated skeletal remains in the Lower Devonian.

Figure 9 (on the following page). Scale morphology of Upper Llandovery–Lower Wenlock (Silurian) mongolepids. (**a**–**c**) *Mongolepis rozmanae* scale BU5296 (Chargat Formation, north-western Mongolia) in (**a**) anterior, (**b**) lateral and (**c**) basal view. (**d**, **e**) *Teslepis jucunda* BU5322 (Chargat Formation, north-western Mongolia) in (**d**) crown and (**e**) basal view. (**f**, **g**) *Sodolepis lucens* scales (Chargat Formation, north-western Mongolia) in (**f**) crown (BU5304) and (**g**) lateral (BU5305) views. (**h**–**j**) *Shiqianolepis hollandi* scales (Xiushan Formation, south China) in (**h**) crown (NIGP 130309), (**i**) postero-basal (NIGP 130307) and (**j**) lateral (NIGP 130307) views. (**k**–**m**) *Rongolepis cosmetica* scale NIGP X1 (Xiushan Formation, south China) in (**k**) crown, (**l**) basal and (**m**) lateral views. (**n**, **o**) *Xinjiangichthys pluridentatus* scale IVPP V X2 (Yimugantawu Formation, north-western China) in (**n**) anterior and (**o**) posterior views. Volume renderings, (a–c), (g) and (i–o). SEM micrographs, (d–f) and (h). Crown and base foramina indicated by arrows and arrowheads respectively. Anterior to the left in (b), (g), (j), (m) and bottom in (c–f), (h), (k). Scale bar equals 400 µm in (a–c), 200 µm in (d, e, i, l–o), 500 µm in (f), and 300 µm in (g, h, j, k).

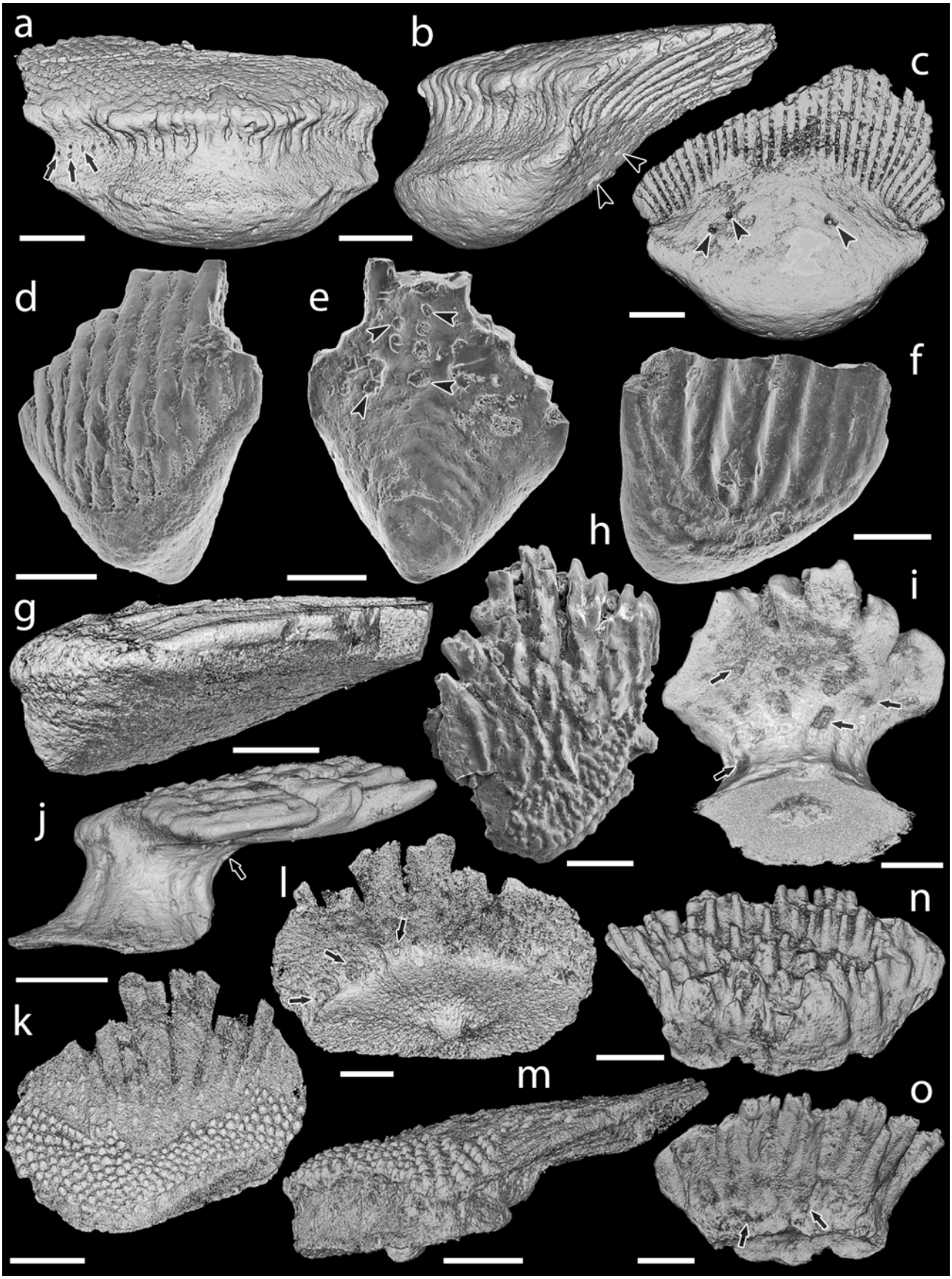
a
b
c
d
e
f
g
h
i
j
k
l
m
n
o

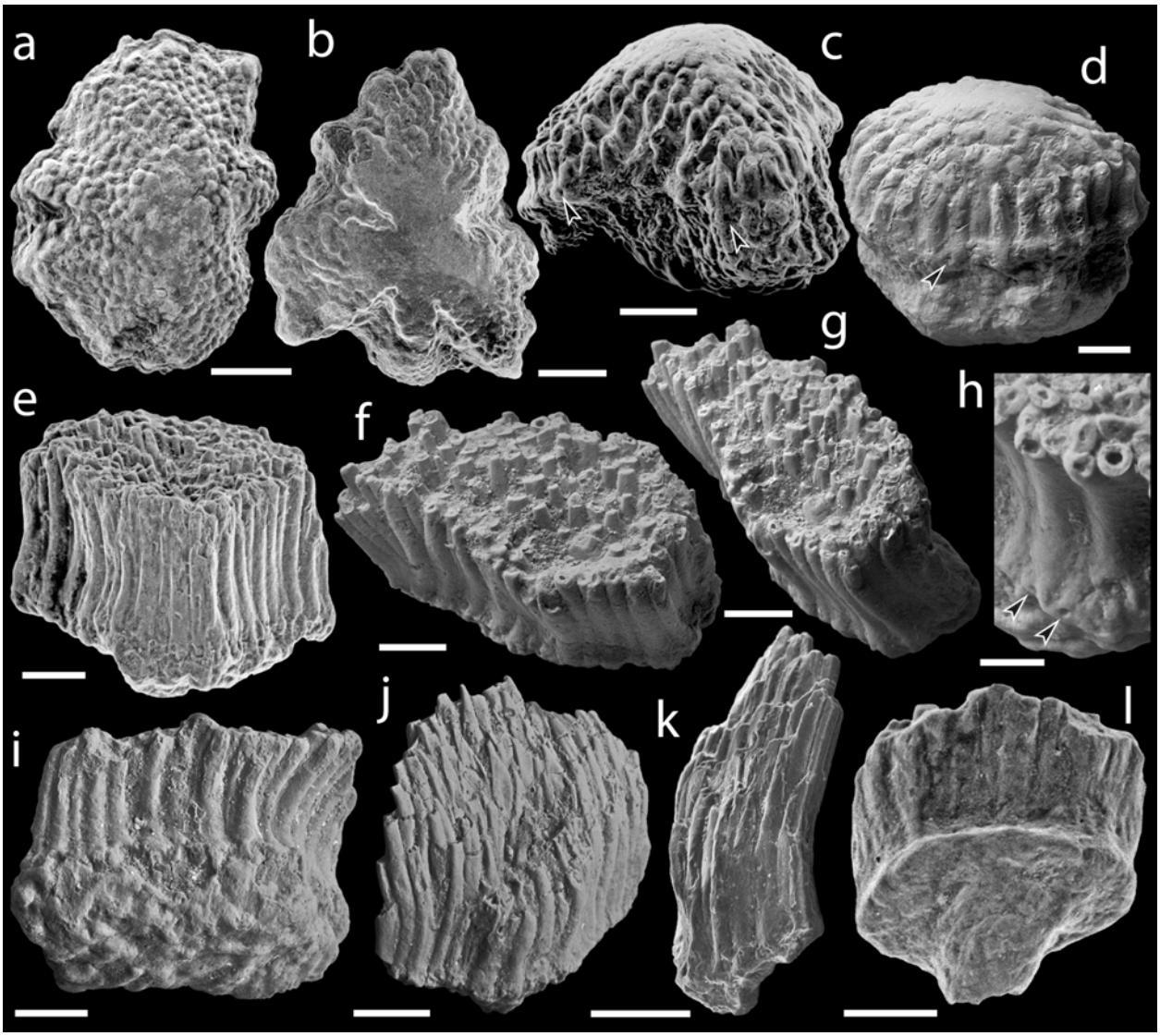

Figure 10. SEM micrographs of *Solinalepis levis* gen. et sp. nov. scales from the Sandbian (Upper Ordovician) Harding Sandstone of Colorado, USA. (**a**–**c**) Tessera-like head scales in (**a**, **b**) crown (BU5307, BU5308) and (**c**) lateral (BU5309) views. (**d**) Bulbous head scale (BU5312) in lateral view. (**e**–**i**) Polygonal trunk scales, (**e**) holotype (BU5310) in anterior view, (**f**) BU5345 in crown, (**g**) corono-lateral and (**h**) partial posterior views, (**i**) BU5313 in basal view. (**j**–**l**) Lanceolate trunk scales in (**j**) anterior (BU5314), (**k**) lateral (BU5315) and (**l**) posterior (BU5311) views. Base foramina indicated by arrowheads. Anterior to the left in (g) and (k). Scale bar equals 300 µm in (a, b), 200 µm in (c), 100 µm in (d–g, i–l), and 50 µm in (h).

Figure 11 (on the following page). Histology of the mongolepid integumentary skeleton. (**a**) Medial longitudinal section of a *Mongolepis rozmanae* scale (BU5297; Chargat Formation, north-western Mongolia). (**b**) Detail of (**a**) depicting primary and secondary odontodes at the anterior crown margin; (**c**) primary odontode lamellin microstructure in a longitudinally sectioned *Mongolepis rozmanae* scale (BU5298; Chargat Formation, north-western Mongolia), etched for 10 min in 0.5% orthophosphoric acid. (**d**) Medial longitudinal section of a *Teslepis jucunda* scale (BU5324; Chargat Formation, north-western Mongolia). (**e**) Lamellin architecture of two odontodes in a longitudinally sectioned *Sodolepis lucens* scale (BU5306; Chargat Formation, north-western Mongolia) etched for 10 min in 0.5% orthophosphoric acid. (**f**) Anterior third of BU5306 showing the contact between the globular crown dentine and the underlying basal bone. (**g**) Basal bone microstructure in BU5306 at the anterior projection of the base. (**h**) Sagittal longitudinal section of a *Sodolepis lucens* scale (BU5344; Chargat Formation, north-western Mongolia). (**i**) Sagittal longitudinal section of a *Rongolepis cosmetica* scale (NIGP 130328; Xiushan Formation, south China). (**j**) Detail of NIGP 130328 showing the mid third of the scale crown. (**k**) *Xinjiangichthys pluridentatus* scale (IVPP V X1; Yimugantawu Formation, north-western China) in longitudinal section. (**l**) Sagittal longitudinal section of a *Shiqianolepis hollandi* trunk scale (NIGP 130312; Xiushan Formation, south China). (**m**) Sectioned *Solinalepis levis* gen. et sp. nov head scale (BU5317; Harding Sandstone, Colorado, USA) (**n**) transverse section of a *Solinalepis levis* gen. et sp. nov trunk scale (BU5316; Harding Sandstone, Colorado, USA). Nomarski differential interference contrast optics micrographs, (a), (b), (d), (e), (h) and (i–n); SEM micrographs, (c), (f) and (g). Anterior towards the left in (a)–(j), (l) and towards the right in (k). **GB**, globular dentine; **LB**, lamellar bone; **red dotted lines**, contact surfaces between primary and secondary odontodes; **white dotted lines**, border between globular dentine and basal bone; **white dashed line**, contact surfaces between primary odontodes in *Rongolepis*. Asterisks mark bone layers with fibre orientation parallel to the section axis. Scale bar equals 400 µm in (a), 100 µm in (b, g, j,m), 20 µm in (c), 200 µm in (d, i, k, n), 50 µm in (e, f, l), and 300 µm in (h).

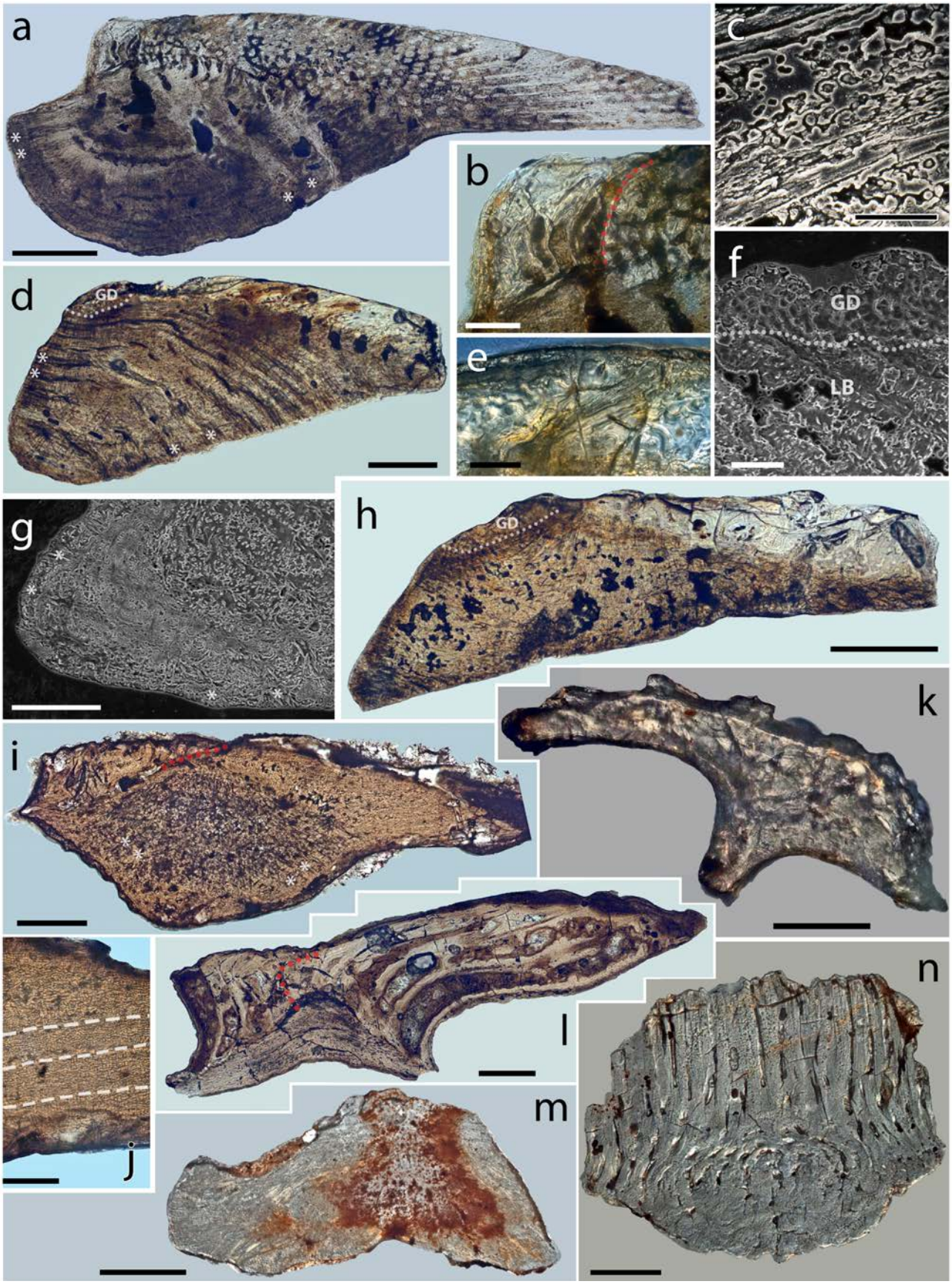
a
b
c
d
GD
e
f
GD
LB
g
h
GD
i
k
j
l
m
n

Figure 12 (on the following page). Canal system of mongolepid scales. Volume renderings. (**a**–**c**) Canals (red) inside a translucent *Mongolepis rozmanae* scale (BU5296) in (**a**) lateral view, in (**b**) posterior view sliced along the plane **1** and in (**c**, **c1**) crown view sliced along plane **2**. (**d**, **d1**) Canals in a transversely sliced *Teslepis jucunda* scale (BU5325) shown in posterior view. (**e**) Pulp cavities (red) in a transversely sliced *Sodolepis lucens* scale (BU5305) shown in postero-lateral view (**f**) Longitudinally sliced *Shiqianolepis hollandi* scale (NIGP 130307) in baso-lateral view. (**g**, **h**) Longitudinally sliced *Xinjiangichthys pluridentatus* scale IVPP V X2 in (**g**) posterior and (**h**) lateral views. (**i**, **j**) Canals system (red) inside a transversely sliced *Solinalepis levis* gen. et sp. nov scale (BU5318) shown in posterior view, (**j**) detail of (**i**). Horizontal canals depicted in purple in c1 and d1. Yellow arrowheads point at canal openings on the sub-crown surface. **Red dotted line**, contact surfaces between primary and secondary odontodes; **grey dotted line**, crown/base border. Scale bar equals 400 µm in (a–c), 100 µm in (d, h, i), 200 µm in (e), 300 µm (f, g) and 50 µm in (j).

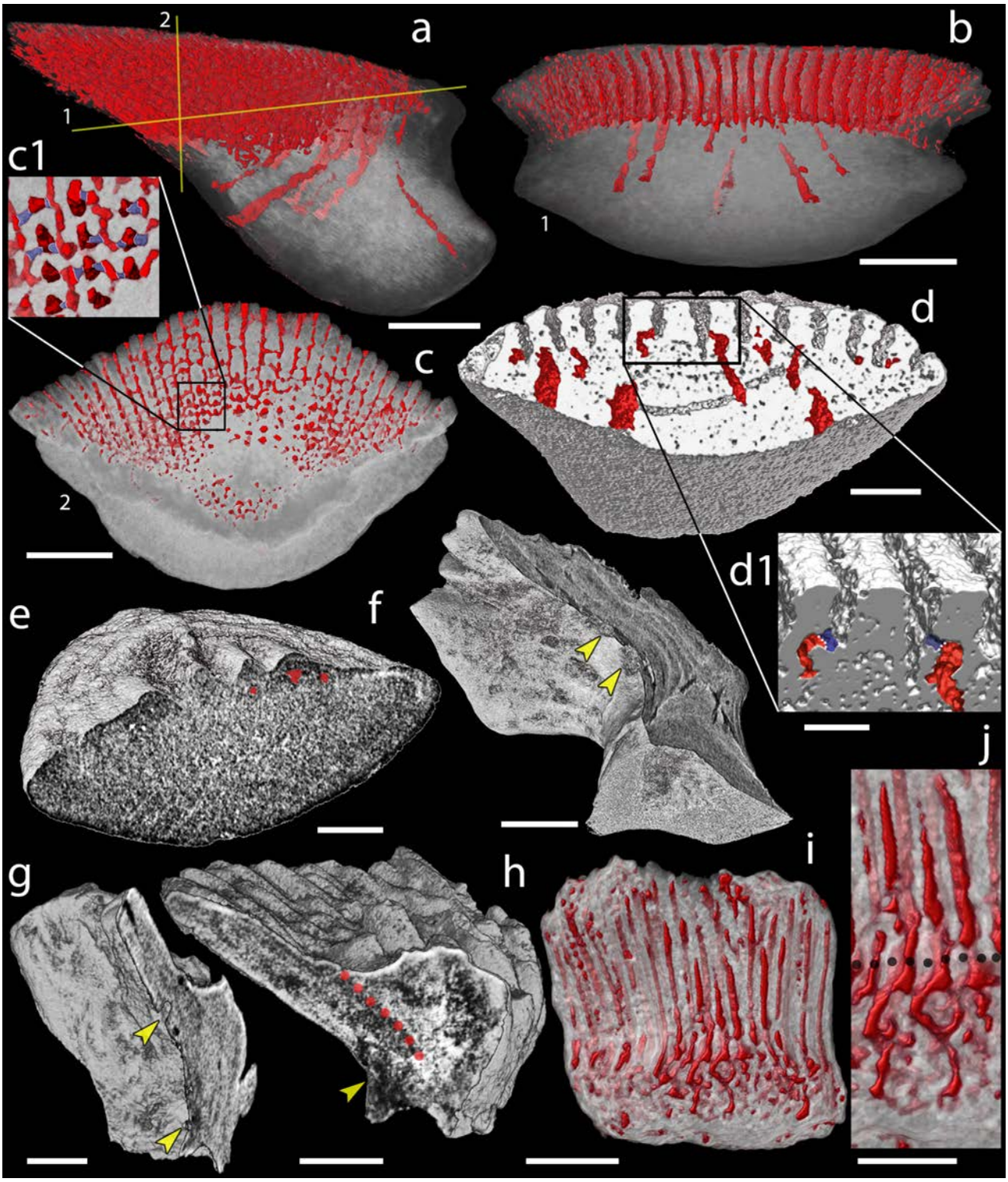
a
b
c1
c
d
d1
e
f
g
h
i
j
1
2

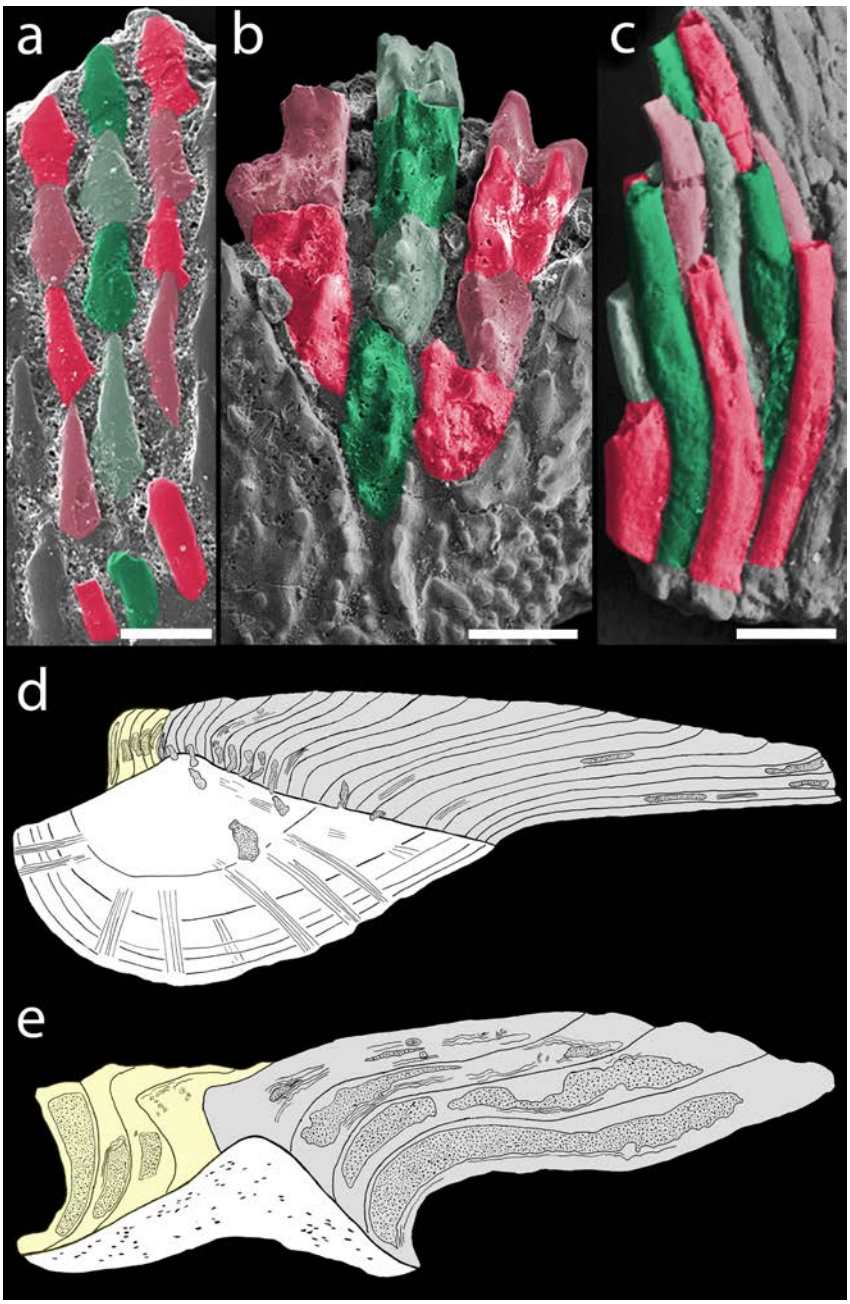

Figure 13. Highlighted odontocomplex organisation of mongolepid scale crowns. (**a**) *Teslepis jucunda* (BU5323) scale, medial portion of the crown. (**b**) *Shiqianolepis hollandi* (NIGP 130309) scale, medial portion of the crown. (**c**) *Solinalepis levis* gen. et sp. nov. trunk scale (BU5314), lateral portion of the crown. Primary odontocomplex structure in Mongolepidida demonstrated by line drawings of longitudinally sectioned (**d**) *Mongolepis rozmanae* (BU5297) and (**e**) *Shiqianolepis hollandi* (NIGP 130312) scales. In (a)–(c) some of the odontocomplexes are highlighted in red and green. **Dark green** and **dark red**, odd numbered odontodes; **light green** and **light red**, even numbered odontodes. In (d), (e)—**light grey,** primary odontodes; **light yellow**, secondary odontodes. Anterior towards the bottom in (a)–(c) and towards the left in (d), (e). Scale bar equals 100 µm in (a), 200 µm in (b) and 50 µm in (c).

Chapter 5: *Elegestolepis* and its kin, the earliest chondrichthyans to develop mono-odontode scale crowns

5.1. INTRODUCTION

The type species of the genus *Elegestolepis* (*E. grossi*) was described (Karatajūtė-Talimaa 1973) from isolated scale remains from Upper Ludlow–Pridoli strata (Elegest and Kadvoj outcrops, Tuva, Russian Federation) of the Tuva-Mongol terrane (Žigaitė et al. 2011)— at the time of publication being the earliest known taxon referred to the Chondrichthyes. Subsequent studies on microvertebrate fossils from the Lower Palaeozoic have led to the identification of stratigraphically older species attributed to *Elegestolepis*, represented by the Upper Llandovery–Lower Wenlock *E.* sp. (Chargat outcrop, north western Mongolia; Karatajūtė-Talimaa et al. 1990) from the Tuva-Mongol terrane and the Middle Llandovery *E. conica* (Nyuya River outcrop, Sakha (Yakutia) Republic, Russian Federation; Karatajūtė-Talimaa and Predtechenskyj 1995) from the adjacent Siberian craton. The palaeogeographical and stratigraphical range of taxa exhibiting *Elegestolepis*-like characteristics was further expanded with the description (Vieth 1980) of the Laurussian chondrichthyan scale species *Ellesmereia schultzei* (from Lochkovian of Ellesmere Island, Nunavut Territory, Canada).

According to the established by Karatajūtė-Talimaa (1992) categories of scale morphogenesis in Palaeozoic chondrichthyans, *Elegestolepis* and *Ellesmereia* belong to the *Elegestolepis* developmental type as a result of possessing scales with a mono-odontode, non-growing crown enclosing a pulp canal that opens at the crown neck via a single foramen. Influenced by the lepidomorial theory put forward by Stensiö and Ørvig

(see 1951–1957 and Stensiö 1961), Karatajūtė-Talimaa (1992, 1998) proposed that elegestolepid scale crowns represent the simplest mono-odontode dermatoskeletal elements, exhibiting many of the characteristics of what were assumed by the theory to be the most elementary skeletal units of the integument (lepidomoria). Thus, the odontode development in elegestolepids was differentiated from that of other chondrichthyans with ‘placoid’ (mono-odontode) scales, whose crowns allegedly form through coalescence of lepidomoria. Karatajūtė-Talimaa (1992, 1998; see also Stensiö 1961 and Zangerl 1981) attributed this complex morphogenetic pattern to the *Polymerolepis* and *Heterodontus* (euselachian; Fig. 14c) scale types identified by her. A hypothesis of odontode evolution in stem chondrichthyans was founded upon these assumptions, and implicates lepidomorium-like elements as the phylogenetic precursors of all chondrichthyan scales (Karatajūtė-Talimaa 1992).

In the years following the conceptualization of the lepidomorial theory, increasing evidence from studies on the development of the integumentary skeleton of Recent neoselachians (Reif 1980b; Miyake et al. 1999; Johanson et al. 2008) has discredited the concrescence model of odontode morphogenesis predicted by the theory, and this is now refuted by most authors (Smith and Coates 1998; Donoghue 2002 and references therein). Considering the above, a re-examination of *Elegestolepis* and *Elegestolepis*-like Silurian scale taxa (e.g. *Ellesmereia*, *Kannathalepis*) identified in the literature is important in developing a better understanding of the early evolution of single odontode integumentary skeletal elements in the Chondrichthyes. For that purpose, the present study investigates the development pattern, histology and canal system of *Elegestolepis grossi* scales and that of previously undescribed scales from the Lower Silurian of Mongolia referred to *Elegestolepis* (Karatajūtė-Talimaa et al. 1990). The new data allowed to establish a systematic framework for *Elegestolepis*-like taxa and test their chondrichthyan affinities, as proposed in the literature.

5.2. SYSTEMATIC PALAEONTOLOGY

Class CHONDRICHTHYES Huxley, 1880

Order ELEGESTOLEPIDA ordo nov.

Included families. Kannathalepididae Märss and Gagnier 2001 and Elegestolepidae fam. nov.

Diagnosis. Chondrichthyan fish possessing mono-odontode scales with growing odontodes that enclose neck-canal branches of the pulp cavity (Fig. 14b). Scale supported by a basal bone tissue whose deposition succeeds the formation of the scale odontode.

Remarks. The recent literature on putative basal chondrichthyan taxa (e.g. mongolepids, elegestolepids, kathemacanthids and polymerolepidiforms) from the Lower Palaeozoic expresses uncertainty regarding their systematic position relative to the major clades (Subclasses) of the Chondrichthyes (Karatajūtė-Talimaa and Novitskaya 1997; Sansom et al. 2000; Märss et al. 2006; Hanke and Wilson 2010; Hanke et al. 2013). This reflects an inadequate understanding of the phylogenetic significance of scale-derived characters, which have been employed to diagnose these taxa given the general absence of chondrichthyan endoskeletal and dental remains in the Lower Palaeozoic.

The odontode growth that typifies the ontogenesis of *Elegestolepis*-like scales does not occur in members of established Subclasses of chondrichthyan fish (Grogan et al. 2012) and requires Elegestolepida to be considered at present Chondrichthyes *incertae sedis*. The rationale behind erecting the order is to unite chondrichthyan species that possess scales with growing single-odontode crowns whose morphogenesis departs from that of elasmobranch ‘placoid’ scales (the *Heterodontus* morphogenetic type of Karatajūtė-Talimaa 1992, 1998; Fig. 14c). This recognition of the *Elegestolepis*-type of scale development as an apomorphy of the Elegestolepida represents a conceptual change from

what was originally identified to be a purely morphogenic category (Karatajūtė-Talimaa 1992, 1998).

KANNATHALEPIDIDAE Märss and Gagnier 2001

Included genera. *Kannathalepis* Märss and Gagnier 2001.

Revised diagnosis. Elegestolepids possessing dermal scales with vertically undivided pulp cavities from which multiple (up to five) horizontal neck canals emerge basally.

Remarks. The monogeneric family Kannathalepididae was introduced by Märss and Gagnier (2001) to distinguish *Kannathalepis*, identified to exhibit a specialised type of scale morphogenesis, from other known Silurian chondrichthyan scale taxa (mongolepid and elegestolepid). It was reported that the squamation of *Kannathalepis* consists of single-odontode scales along with more complex aggregates of fused ‘placoid’ scales that allegedly provide evidence for two separate modes of scale development within the genus (Märss and Gagnier 2001). The current study regards the compound scales of *Kannathalepis* as aberrant, formed by anomalous patterning that is thought to result from suppression of inter-scale domains in accordance with the inhibitory field model outlined by Reif (1980a, 1982). Localised suturing of scales has been documented in stem (*Hydodus delabechei*, Reif 1978 and *Lissodus sardiniensi*, Fischer et al. 2010) and crown (*Echinorhinus brucus*, Reif 1985 and *Asterodermus platypterus*, Thies and Leidner 2011) euselachians with developed mono-odontode trunk scale cover that is known to be prevalent within the order (Dick 1978; Dick and Maisey 1980; Reif 1985; Maisey 1989; Wang et al. 2009; Thies and Leidner 2011).

Complexes of randomly sutured mono-odontode scales consequently cannot be considered equivalent to polyodontode scales (e.g. those of Mongolepidida, Karatajūtė-

Talimaa 1998), since the odontodes of the latter are patterned as a unit in a particular manner and are given support by a common base/pedicle tissue. The scale development in *Kannathalepis* can thus be identified as that of ‘placoid’ scales with a growing odontode and base, corresponding to the *Elegestolepis* morphogenetic type (Fig. 14b) of Karatajūtė-Talimaa (1992). On that basis, Kannathalepididae is placed inside the new order Elegestolepida, and its validity is maintained by acknowledging the diagnostic for the family canal system characteristics (vertically undivided pulp cavity and multiple neck canals) recognised in the original description of the taxon.

Kannathalepididae was expanded subsequent to its erection to include the Wenlockian genus *Frigorilepis*, which was described from articulated body fossils (Märss et al. 2002, 2006). Nevertheless, crown morphogenesis in *Frigorilepis* has not been demonstrated to proceed in discrete growth phases as in elegestolepid taxa, which are further distinguished by the presence of scale-neck canal openings. This absence of diagnostic for Elegstolepida characters requires to treat *Frigorilepis* as family and order *incertae sedis* for the time being.

Family ELEGESTOLEPIDAE Andreev, Karatajūtė-Talimaa, Shelton, Cooper, and Sansom fam. nov.

Included genera*.* The type genus *Elegestolepis* Karatajūtė-Talimaa 1973, *Ellesmereia* Vieth 1980 and *Deltalepis* gen. nov.

Diagnosis. Elegestolepids with scales that develop a vertically branched pulp cavity that gives off a single horizontal neck canal and dentine canals that originate at the lower neck/ pedicle surface independently of the pulp (Fig. 21).

Genus *Elegestolepis* Karatajūtė-Talimaa, 1973

Included species. The type species *E. grossi* Karatajūtė-Talimaa 1973 and *E. conica* Novitskaya and Karatajūtė-Talimaa 1986.

Revised diagnosis. Elegestolepidids (pertaining to the family Elegestolepidae) possessing up to three unornamented scale crown lobes (Fig. 15a; Fig. 16a, b, d, e) incised by deep, linear grooves.

Elegestolepis grossi Karatajūtė-Talimaa, 1973

(Figs. 14b, 15a, 16, 17, 21a–c)

Locality and horizon. Examined specimens come from beds 236, 291, 293 and 295 of the Baital Formation (Upper Ludlow–Pridoli, Vladimirskaya 1978) at the type locality on the Elegest River, Tuva, Russian Federation (Karatajūtė-Talimaa 1973).

Holotype. An ontogenetically mature scale (T-003) from the Baital Formation of Tuva, Russian Federation (Karatajūtė-Talimaa 1973).

Referred material. More than 200 isolated scales (including specimens figured here) and material figured in Karatajūtė-Talimaa (1973). Non-figured specimens stored in the Lapworth Museum of Geology, University of Birmingham, UK.

Revised diagnosis. *Elegestolepis* species possessing 0.3–1 mm long scales that have deltoid to lanceolate, trilobate crowns and develop moderately to strongly constricted necks and bulbous bases during their ontogenesis (Fig. 16). Scale odontode composed of dentine tissue with multipolar odontocyte lacunae from which emerge canaliculi with dendroid branching (Fig. 17f). Cellular basal bone with layered mineralised-fibre organization (Fig. 17c, f, g).

Remarks. Certain differences were noted between the interpreted here scale histology of *E*. *grossi* scales and the original descriptions of Karatajūtė-Talimaa 1973. The chief of these concerns the nature of the most superficial portion of the scale crown and neck, understood by Karatajūtė-Talimaa (1973) to consist of durodentine tissue (one of the less widely used synonyms of enameloid, Ørvig 1967; Smith and Miles 1971; Sire et al. 2009).

This ‘enameloid’ layer is found not to be a persistent feature of *E*. *grossi* scales, and even when present it appears discontinuous and/or absent from most of the upper crown surface (Fig. 17a–e), contrary to previous depictions (Karatajūtė-Talimaa 1973, fig. 2a, b; Sire et al. 2009, fig. 10b). This distribution is also contrary to that of enameloid tissue in neoselachian scales, where it is confined mainly to the upper crown region (Johns et al. 1997; Manzanares et al. in prep.; pers. obs.). Furthermore, the architecture of the superficial crown region cannot be recognised in any of the known enameloid structural types (Johns et al. 1997; Sansom et al. 2005a; Gillis and Donoghue 2007; Guinot and Cappetta 2011; Andreev and Cuny 2012), but instead resembles that of the crown dentine and is regarded as such. The documented more porous appearance of the surface dentine is likely to be diagenetically induced and/or due to alteration of the original tissue microstructure by preparation of the specimens with unbuffered acetic acid (even in low concentration, the latter has been shown to damage the phosphatic tissues of conodont elements, Jeppsson et al. 1985; Jeppsson and Anehus 1995).

This study also demonstrates the presence of previously unidentified depositional lines (Fig. 17g) in the basal bone of *E*. *grossi* scales, although growth of the bone tissue has been inferred from specimens in different stages of development (Karatajūtė-Talimaa 1973, 1998). The lamellae, demarcated by the depositional lines, have concave down profiles that follow the outline of the base, which is a common feature of growing scale

bases in lower vertebrates (e.g. Ørvig 1966; Zangerl 1968; Denison 1979; Burrow and Turner 1998, 1999; Qu et al. 2013b).

Genus *Ellesmereia* Vieth 1980

Included species. *Ellesmereia schultzei* Vieth 1980.

Remarks. *Ellesmereia* (Fig. 15b) was assigned to the Elasmobranchii by Vieth (1980) despite being recognised to possess an *Elegestolepis* type of scale morphogenesis that is not an elasmobranch characteristic (Reif 1978; Karatajūtė-Talimaa 1992), and therefore is transferred to the Elegestolepida. Mature *Ellesmereia* scales also possess a canal system structure (Vieth 1980) that closely resembles the vascularization of *Elegestolepis* and *Deltalepis* gen. nov., and for that reason the three taxa are united at a familial level.

Genus *Deltalepis* gen. nov.

Included species*. Deltalepis magnus* gen. et sp. nov. (type species) and *Deltalepis parvus* gen. et sp. nov.

Derivation of name*.* From ‘delta’ (alluding to the resemblance of the scale crown to the Greek letter Δ) and ‘lepis’, scale in Greek.

Diagnosis*.* Elegestolepidids whose scales possess crowns with three and more lobes ornamented by tuberculate ridges (Fig. 15c, d).

Remarks. The material referred here to *Deltalepis* gen. nov. has never been formally described and/or figured, and was considered to belong to the genus *Elegestolepis* by Karatajūtė-Talimaa et al. (1990) and Karatajūtė-Talimaa and Novitskaya (1997) in their work on the mongolepid taxa from the Chargat Formation. *Deltalepis* gen. nov. scales

possess uncharacteristic for *Elegestolepis* and *Ellesmereia* crown morphology, ornamentation and pulp cavity branching pattern that taken together are suggested to support the erection of the new taxon. This distinction is largely based on the extent of documented intra- and inter-generic variation of trunk-scale morphology (e.g. crown shape, number of crown ridges/lobes and ornamentation) in Recent neoselachian families (Reif 1985; Compagno 1988; Voigt and Weber 2011). The rare among the elegestolepids tuberculate ornament of *Deltalepis* gen. nov. is consequently viewed to be a genus level character, with evidence for its independent occurrence in thelodonts (e.g. *Erepsilepis* Märss et al. 2006 and ?*Thelodus* Märss et al. 2007) and mongolepid chondrichthyans (*Shiqianolepis* and *Rongolepis* Sansom et al. 2000; Chapter 4) further substantiating the claim. The ridged lobes of *Deltalepis* gen. nov. are also a feature of micro-remains from Darriwilian (Middle Ordovician) strata of the Stokes Siltstone (central Australia), attributed to the putative chondrichthyan taxon *Areyongalepis oervigi* (Young 1997). The crown necks and bases of elegestolepid scales, however, are not developed in *Areyongalepis* elements, and the latter do not demonstrate identifiable vertebrate mineralised tissues (Young 1997 and personal observations), making their systematic position for the time being uncertain.

Deltalepis magnus sp. nov.

(Figs. 15c, 18, 20a–b, 21d–f)

Derivation of name. From the Latin word for large, referring to the scale size of the species relative to that of *D. parvus* gen. et sp. nov.

Locality and horizon*.* The type and only known locality for *D. magnus* is 80 km north of Lake Khar-Us, north-western Mongolia (Karatajūtė-Talimaa et al. 1990). All specimens come from sample 16/3 collected from the Upper Llandovery–Lower Wenlock (Salhit

regional Stage) horizons of the Chargat Formation (Karatajūtė-Talimaa et al. 1990; Žigaitė et al. 2011).

Holotype. An isolated, presumably trunk, scale BU5269 (Figs. 15c, 18a–c).

Referred material. Six isolated scales (figured here), including the holotype specimen.

Diagnosis. *Deltalepis* species possessing scales with 0.5–0.7 mm long, deltoid to elliptic, crowns divided into three to five discrete lobes. Parallel tuberculated ridges developed on the lower crown surface. The rami of the pulp cavity formed inside the scale crown connect directly to the main pulp canal.

Description.

Morphology. Scales possess mono-odontode crowns with ovate to acuminate outlines (Fig. 18) that are 500–700 µm long and 400–700 µm wide. The crown surface displays a complex topography that is produced by three to five lobes separated by deeply recessed inter-lobe regions (Fig. 18a–c, e, g, h). The lobes are lanceolate-shaped and can exhibit slight divergence towards the posterior of the scale. Their surface is ornamented by sub-parallel tuberculate ridges (up to 8 per lobe) that are absent from the smooth-faced inter-lobe segments of the crown. Longitudinally directed ridges are similarly developed on the lower crown surface (Fig. 18f, i, j), and these demonstrate regular spacing across its width.

The crown transitions into an unornamented narrow neck (down to a third of the maximal crown width) that is located at the anterior of the scale, overhung on all sides by the crown. The lower portion of the neck is either gently curved outwards or flares out to form an ellipse-shaped pedicle. In specimens with a developed pedicle support (Fig. 18e–g, I, j) the posterior face of the neck is pierced by a single centrally positioned foramen (Fig. 18f) with a diameter of c. 30–40 µm. The lower pedicle surface of some specimens is

deeply indented (Fig. 18i), and penetrated by the scale's canal system, whereas in others it is nearly flat (Fig. 18j), exhibiting only a greatly constricted opening of the pulp.

Histology. The scale odontodes are composed solely from a highly vascular tubular dentine (Fig. 20a, b). The canaliculi of the dentine have a coiled appearance and display a tangled organization as well as extensive ramification along their length (up to c. 20 µm). In the upper portion of the crown, the canalicular network emerges from a complex of horizontally and vertically branched, interconnected, small-calibre dentine canals (diameter of c. 5–25 µm; Fig. 21d). The latter are most prominent inside the crown lobes where they associate with and connect to branches (c. 30–60 µm in diameter) of the pulp canal. For most of their length the pulp branches extend parallel the crown surface, before curving basally to merge (Fig. 21f) into a single pulp canal (c. 60–90 µm wide) inside the scale neck. From the posterior of the pulp issues an unbranched horizontal canal (c. 70 µm long; Fig. 21f) that opens on the scale neck surface. Separate from the pulp cavity system, the posterior half of the scales houses numerous closely spaced (up to c. 10 µm apart) dentine canals (10–20 µm in diameter) whose paths parallel that of the lower crown surface (Fig. 21e). The lower ends of these canals ramify inside the scale neck before either exiting the scale basally (Fig. 21e) or ending blindly inside it.

The tissue (c. 40 µm thick) closing off the lower pedicle opening displays an optically discernable boundary with the overlying dentine (Fig. 20a), but it could not be ascertained whether it constitutes a distinct tissue type.

Deltalepis parvus sp. nov.

(Figs. 15d, 19, 20c–d, 21g–j)

Derivation of name. From the Latin word for small, referring to the scale size of the species relative to that of *D. magnus* gen. et sp. nov.

Locality and horizon. The type and only known locality situated 80 km north of Lake Khar-Us, north western Mongolia (Karatajūtė-Talimaa et al. 1990). All specimens come from the Upper Llandovery–Lower Wenlock (Salhit regional Stage) horizons (sample 16/3) of the Chargat Formation (Karatajūtė-Talimaa et al. 1990; Žigaitė et al. 2011).

Holotype. An isolated, presumed trunk, scale BU5275 (Figs. 15d, 19a, b).

Referred material. Six isolated scales (figured here), including the holotype specimen.

Diagnosis. *Deltalepis* species with ovoid, 0.2–0.5 mm long, scale crowns that are compartmentalised into seven to ten lobes. The lateral crown branches of the pulp cavity do not connect directly to the main pulp canal.

Description.

Morphology. The scale crowns are single odontode structures with ovoid outlines (Fig. 19) that are 200–500 µm long and 200–400 µm wide. Upper crown surface is divided into seven to ten antero-posteriorly aligned lobes (40–60 µm wide; Fig. 19a–f) separated by much narrower, deeply incised grooves that expand towards the posterior (up to c. 20 µm wide). Tubercles organised into parallel rows ornament the upper surface of the crown lobes (up to three rows per lobe), whereas all other scale surfaces are smooth.

The anterior of the crown is constricted into a vertically orientated neck that reaches a third to three-quarters of the maximal crown width, and which in some specimens expands basally to form a pedicle support (Fig. 19c–f, h, i). The posterior lower-neck/pedicle face of these scales is pierced by a single foramen (Fig. 19d, h, i) with a diameter of 20–35 µm. A canal opening is also present on the lower pedicle surface (Fig. 19h), while

a row of elliptical foramina of laterally decreasing diameter (from 70 µm to 40 µm in Fig. 19g) mark the lower face of scales lacking a pedicle attachment.

Histology. Tubular dentine tissue (Fig. 20c, d) is the only component of the scale crown. The dentine canaliculi are less than 2 µm in diameter and up to c. 20 µm long, with arborescent branching (Fig. 20d) that gives the tubular system a tangled appearance. Inside the lobed regions of the crown, the tubules connect to a network or vertically (c. 5–10 µm wide and 25–40 µm long) and horizontally (c. 5 µm wide) oriented dentine canals (Fig. 20c; Fig. 21j) that are confluent with branches of the pulp cavity. These pulp branches (from c. 20 µm to c. 45 µm in diameter; Fig. 21g–j) occupy the crown lobes (one canal per lobe) before curving basally to merge with one another inside the scale neck. The three medial branches emerge from the main pulp canal—confined to the scale neck/pedicle—whereas the more lateral ones are only indirectly connected to it through the medial rami (Fig. 21i). Near its lower end the main pulp canal gives off a short neck canal (Fig. 21i, j) that opens at the scale surface.

Posterior of the pulp-cavity canal system the scale houses a number (c. 15) of mutually parallel, ascending dentine canals (Fig. 21g) with diameters between c. 10 µm and 15 µm. These canals follow the posterior scale profile without establishing connections at any point with the pulp cavity and terminate basally at the lower pedicle surface.

5.3. DISCUSSION

5.3.1. Chondrichthyan characteristics of elegestolepid mono-odontode scales

The odontogenic component of the vertebrate skeleton develops primarily as discrete elements (odontodes), each of which being the product of a single epithelia-mesenchymal cell condensation (Ørvig 1977; Reif 1982; Fraser et al. 2010). Odontodes are the main structural units of scales and in certain groups (e.g. in neoselachian chondrichthyans, Sire and Huysseune 2003; Eames et al. 2007; Sire et al. 2009; Fig. 14c) can form the entire squamation in the absence of osteogenic contribution to the integumentary skeleton. In Lower Palaeozoic vertebrates, dermal odontodes are typically patterned in clusters (polyodontodia in Ørvig 1977) that form compound scale crowns; these have been documented in pteraspidomorphs (Gross 1961; Denison 1967; Sansom et al. 2009), anaspids (Märss 1986; Blom et al. 2002; Märss 2002), galeaspids (Wang et al. 2005), osteostracans (Stensiö 1932) and derived gnathostomes (Schultze 1968; Gross 1969; Schultze 1977; Denison 1979; Karatajūtė-Talimaa 1995; Sansom et al. 1996; Burrow and Turner 1998, 1999; Sansom et al. 2012). The Thelodonti (Märss et al. 2007) and certain chondrichthyan clades (Elegestolepida Karatajūtė-Talimaa 1973, 1998; this study, Iniopterygii Zangerl and Case 1973; Grogan and Lund 2009 and Paleoselachii Lund 1985, 1986; Coates and Sequeira 2001) are the exception, as their scale crowns form only from a single-odontode element.

The integumentary skeleton of thelodonts demonstrates the most phylogenetically primitive type of morphogenesis of mono-odontode scales (Smith and Hall 1990, 1993; Sire et al. 2009; Fig. 14a). In contrast to polyodontode scale development, where each of the component odontodes mineralises in a single step, the scales of thelodonts go through several ontogenetic phases that result in gradual elongation of the crown in basal direction (Gross 1967; Karatajūtė-Talimaa 1978). The latter can also possess basal bone tissue

(Fig. 14a) whose deposition commences only after cessation of odontode growth (Karatajūtė-Talimaa 1978; Märss et al. 2007). The thelodont type of scale development has convergently evolved in what are considered here to be basal chondrichthyans, with the appearance of Elegestolepida in the Llandovery. Nevertheless, during ontogenesis elegestolepid scales develop a more derived canal system architecture that features neck canal opening(s) of the odontode pulp (documented outside the Chondrichthyes in ‘placoderms’ Burrow and Turner 1998, ‘acanthodians’ Denison 1979 and stem osteichthyans Gross 1953, 1968; Qu et al. 2013b) absent from the dermal skeleton of the Thelodonti (Gross 1967; Karatajūtė-Talimaa 1978; Märss et al. 2007). The depth of insertion of the scale into the integument has been suggested to have influence on the formation of neck canals (Hanke and Wilson 2010) and is supported by the position of scale necks inside the upper vascular layer (stratum spongiosum) of the dermis, documented in Recent neoselachians (Reif 1980b; Miyake et al. 1999). The same topological relationship between scales and surrounding integumentary tissues is attributed here to the elegestolepids, whereas the dermal odontode papillae of thelodonts have been interpreted to form superficially at the epithelium-mesenchyme boundary (Karatajūtė-Talimaa 1978; Märss et al. 2007).

Outside the Chondrichthyes, other derived gnathostomes regarded to possess mono-odontode body scales belong to the basal ‘placoderm’ orders Stensioellida and Antiarcha (see above; also refer to Johanson 2002, Brazeau 2009 and Davis et al. 2012 for recent vertebrate phylogenies) whose scale structure is still insufficiently investigated. The available data on the squamation of these taxa (e.g. *Stensioella* Gross 1962, *Pterichthyodes* Hemmings 1978, *Asterolepis* Ivanov et al. 1995, Upeniece 2011 and *Parayunnanolepis* Upeniece 2011; Zhu et al. 2012) provides evidence for non-growing odontodes, implying this to be a plesiomorphic characteristic of the single-odontode scales of jawed gnathostomes. *Asterolepis* is the only histologically described genus from those

identified above, known to exhibit a multi-layered (lamellar and cancellous layers) scale-base bone tissue of the type composing the ‘placoderm’ dermal skeleton (Ivanov et al. 1995; Giles et al. 2013). Within derived gnathostomes the elegestolepid scale hard tissue histogenesis and composition conform to those common for the polyodontode scales of chondrichthyans, which likewise are two-component skeletal elements formed out of lamellar basal bone and crown dentine (Karatajūtė-Talimaa 1992). Another characteristic uniting Elegestolepida with the Chondrichthyes among jawed gnathostomes is the absence of dermoskeletal resorption and remodeling that are prevalent in placoderm-grade gnathostomes (Downs and Donoghue 2009; Giles et al. 2013) and basal osteichthyans (Zhu et al. 2006).

5.3.2. Elegestolepida in the context of other Lower Palaeozoic chondrichthyans

Elegestolepids are recognised as an important component of pre-Devonian chondrichthyan faunas with five currently identified species grouped into two families (Fig. 22), being second only in diversity to the order Mongolepidida (Karatajūtė-Talimaa et al. 1990; Karatajūtė-Talimaa and Novitskaya 1992, 1997; Sansom et al. 2000, 2001; Wang et al. in prep.). Whilst the mongolepids (Sansom et al. 2001; Chapter 4) and several other chondrichthyan lineages (represented by *Areyongalepis* Young 1997, *Tantalepis* Sansom et al. 2012, *Tezakia* Sansom et al. 1996; Chapter 3 and *Canonlepis* Sansom et al. 2001; Chapter 3) have been documented to originate in the Ordovician, no remains attributable to Elegestolepida have been reported from this interval (Sansom et al. 2001; Turner et al. 2004). These Ordovician taxa possess compound (polyodontode) scale crowns and lack neck canal openings, the former of which are now understood to not develop in all basal chondrichthyans (Märss et al. 2007; Hanke and Wilson 2010).

Chondrichthyan scales with neck pulp-canal openings are known to first appear in the stratigraphically oldest elegestolepid species (*E. conica* Novitskaya and Karatajūtė-Talimaa 1986; Karatajūtė-Talimaa and Predtechenskyj 1995), in the Middle Llandovery, and can be recognised as a persistent feature of the canal system of mature elegestolepid scales (Karatajūtė-Talimaa 1973; Vieth 1980; Märss and Gagnier 2001; Fig. 22). This condition is similarly developed in Silurian polyodontode chondrichthyan species (e.g. *Tuvalepis* Žigaitė and Karatajūtė-Talimaa 2008 and the monogolepids *Mongolepis*, *Teslepis* Karatajūtė-Talimaa 1998, *Shiqianolepis* and *Rongolepis* Sansom et al. 2000). In monogolepids pulps exit the lower part of crown either by giving off short rami (termed 'horizontal canals' by Karatajūtė-Talimaa 1995 and considered here equivalent to the neck canals of elegestolepid scales) or opening directly to the crown surface (in *Shiqianolepis* and *Rongolepis* Sansom et al. 2000; Chapter 4).

Elegestolepida and Mongolepidida represent two distinct lineages of early chondrichthyans that provide an insight into the variability of scale characteristics within what are considered to be monophyletic groups. Across both taxa the only features shared by species of the same order are those relating to the pattern of crown morphogenesis, whilst aspects of the vascular system architecture and hard tissue structure of scales can show inter-species differences. Moreover, characters with a sporadic appearance in one of the orders can have a constant presence in the other, as is the case with the neck canal openings of the elegestolepids. The identification of elegestolepid taxa is thus regarded to require the unique character combination of a growing mono-odontode scale crown (order-grade character) and neck canal openings (plesiomorphy of crown-group gnathostomes).

Under the formulated above diagnosis, the Wenlockian species *Frigorilepis caldwelli*, placed inside Kannathalepididae by Märss et al. (2002, 2006), is excluded from Elegestolepida for not demonstrating recognisable stages of scale crown growth. As

Frigorilepis does not develop neck canals (Fig. 22), the polygonal ultrasculptural pattern of the crown surface it shares with *Kannathalepis* has been used instead as a character to support its chondrichthyan affinity (Märss 2006; Märss et al. 2006). Crown ornamentation is regarded non-diagnostic at higher taxonomic levels (see above) and at present no further evidence is available to unite *Frigorilepis* with basal chondrichthyans. As a consequence, the *Elegestolepis*-type of morphogenesis is the only mechanism of development recognised in mono-odontode chondrichthyan scales from the Silurian Period. The inclusion of *Ellesmereia* into Elegestolepida demonstrates that odontode growth has persisted as a feature of the integumentary skeleton of chondrichthyans at least until the Early Devonian (Fig. 22). This last known appearance of an elegestolepid species coincides with a major diversification of chondrichthyans at the base of the Devonian (Ginter 2004; Turner 2004; Grogan et al. 2012) that sees the emergence of taxa with body cover of non-growing ‘placoid’ scales. Some of these species are known from body fossils and represent examples of the earliest recorded articulated chondrichthyan remains (*Polymerolepis whitei* Karatajūtė-Talimaa 1968, 1998; Hanke et al. 2013, *Lupopsyrus pygmaeus* Bernacsek and Dineley 1977; Hanke and Davis 2012 and *Obtusacanthus corroconis* Hanke and Wilson 2004; Fig. 22). Their scales lack the bony base component of the elegestolepid squamation that in Chondrichthyes has only been documented in scales with growing crowns (either mono- or poly-odontode). Moreover, *Lupopsyrus* and *Obtusacanthus*, resolved as stem chondrichthyan fish in recent phylogenies of early vertebrates (Brazeau 2009; Davis et al. 2012; Zhu et al. 2013), do not possess scale-neck openings of the pulp canal. This type of vascularization, where the pulp opens only towards the lower surface of scales, is however also a feature of the earliest recorded chondrichthyan polyodontode scales (Sansom 1996; Sansom et al. 2001; Donoghue and Sansom 2002; Chapter 3).

5.4. CONCLUSIONS

The original concept of *Elegestolepis*-type scale morphogenesis (Karatajūtė-Talimaa 1992) is re-interpreted to feature stepwise crown growth and neck canal formation as its diagnostic characteristics. The presence of neck canal openings in *Elegestolepis*-like scales is considered to distinguish them from the growing mono-odontode scales of the Thelodonti (Märss et al. 2007), whereas the absence of cancellous bone and hard tissue resorption in these taxa are chondrichthyan apomorphies within crown gnathostomes. This implies that total-group Chondrichthyes have evolved two distinct morphogenetic processes for generation of single odontode scales, one characteristic for the elegestolepids and the other producing the non-growing *Heterodontus*-type scales (*sensu* Karatajūtė-Talimaa 1992), known in detail in euselachians. Consequently, the elegestolepid integumentary skeleton is seen to demonstrate one of the early forms of chondrichthyan scale development that are absent from more derived taxa of the clade. It is further speculated that the contribution of osteogenic tissues to elegestolepid scale units represents a phylogenetically basal state in relation to that of taxa with solely odontogenically derived squamation.

Shared morphogenetic patterning unites *Elegestolepis* Karatajūtė-Talimaa 1973 with *Ellesmereia* Vieth 1980*, Kannathalepis* Märss and Gagnier 2001 and *Deltalepis* gen. nov into the newly erected order Elegestolepida, and this extends the known stratigraphic range of elegestolepid taxa from the Lower Silurian (Upper Llandovery–Lower Wenlock) to the Lower Devonian (Lochkovian). Furthermore, a division of the order into two families is established upon differences in pulp cavity architecture between *Kannathalepis* and all the other recognised elegestolepid genera.

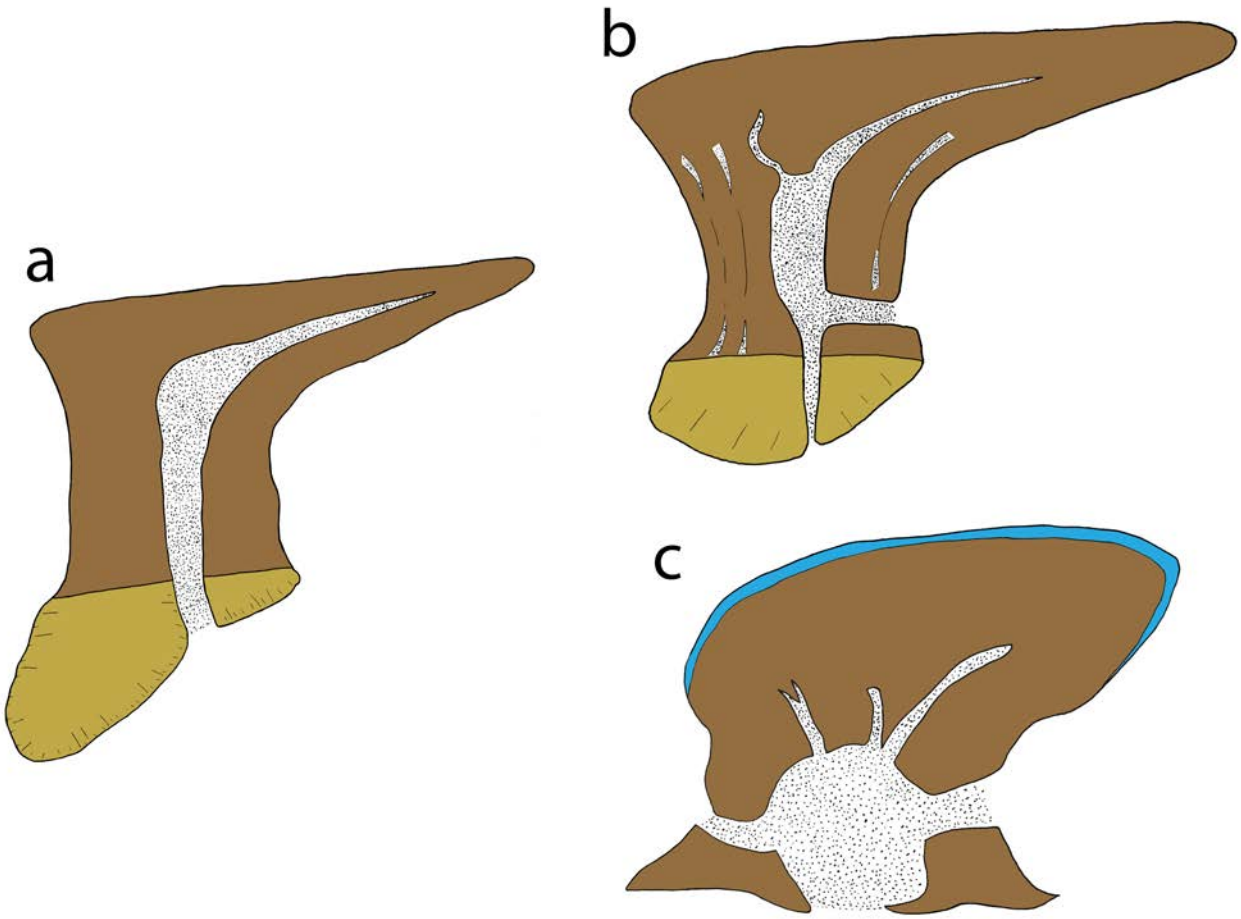

Figure 14. Diagrammatic representation of mono-odontode scale types in (**a**) the Thelodonti and (**b**, **c**) the Chondrichthyes. (**a**) A *Thelodus calvus* scale (adapted from Märss and Karatajūtė-Talimaa 2002, fig. 15F) exemplifying the thelodont morphogenetic type. (**b**) The *Elegestolepis* morphogenetic type represented by an *Elegestolepis grossi* scale (BU5284). (**c**) The *Heterodontus* morphogenetic type represented by a *Triakis semifasciata* scale (BU5341). blue, enameloid; brown, dentine; gold, bone.

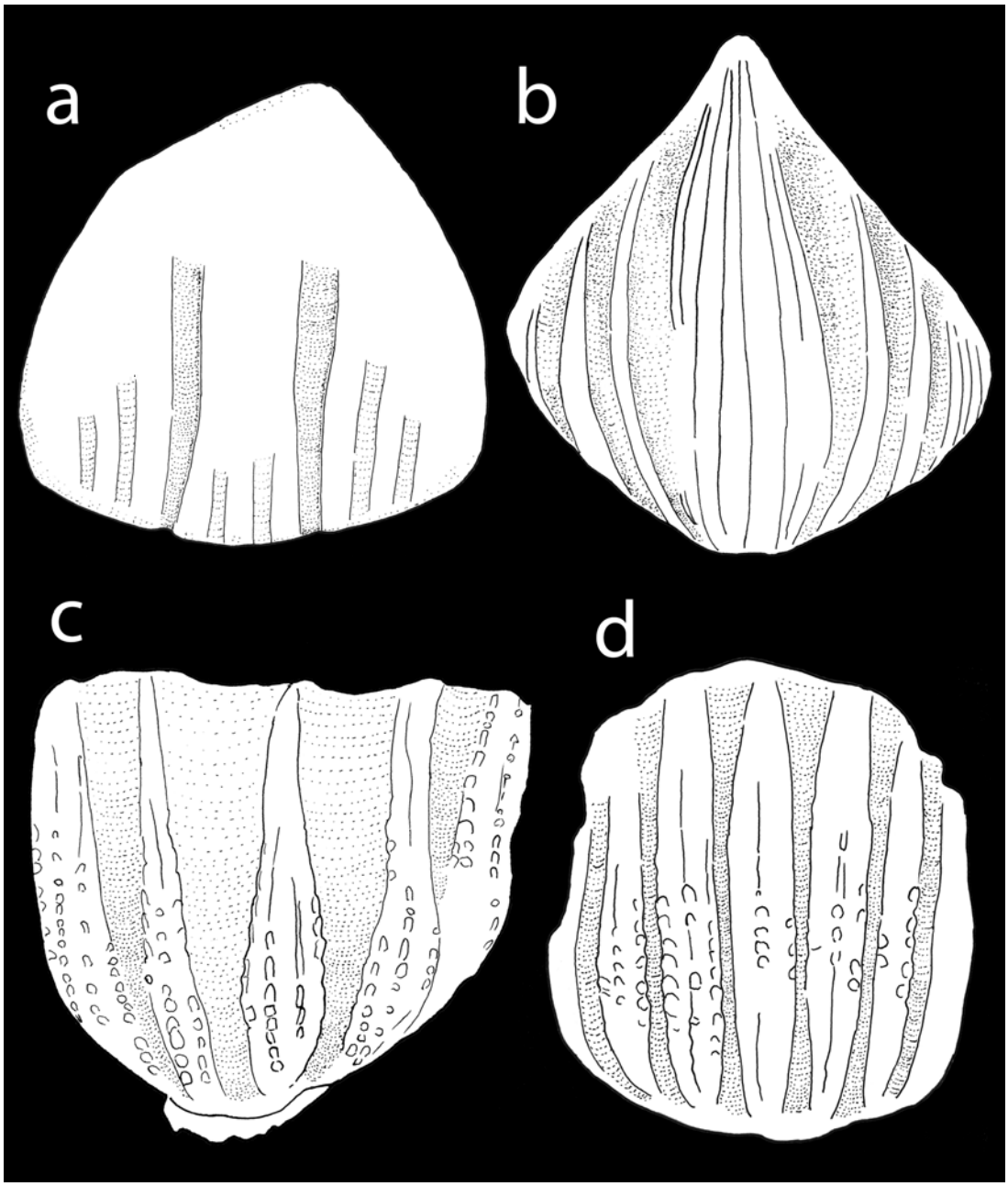

Figure 15. Line drawings depicting the range of crown-surface morphologies in elegestolepid scales. (**a**) *Elegestolepis grossi* (BU5284). (**b**) *Ellesmereia schultzei* (adapted from Vieth 1980, pl. 9.2). (**c**) *Deltalepis magnus* gen. et sp. nov. (holotype BU5269). (**d**) *Deltalepis parvus* gen. et sp. nov. (holotype BU5275). Anterior towards the bottom.

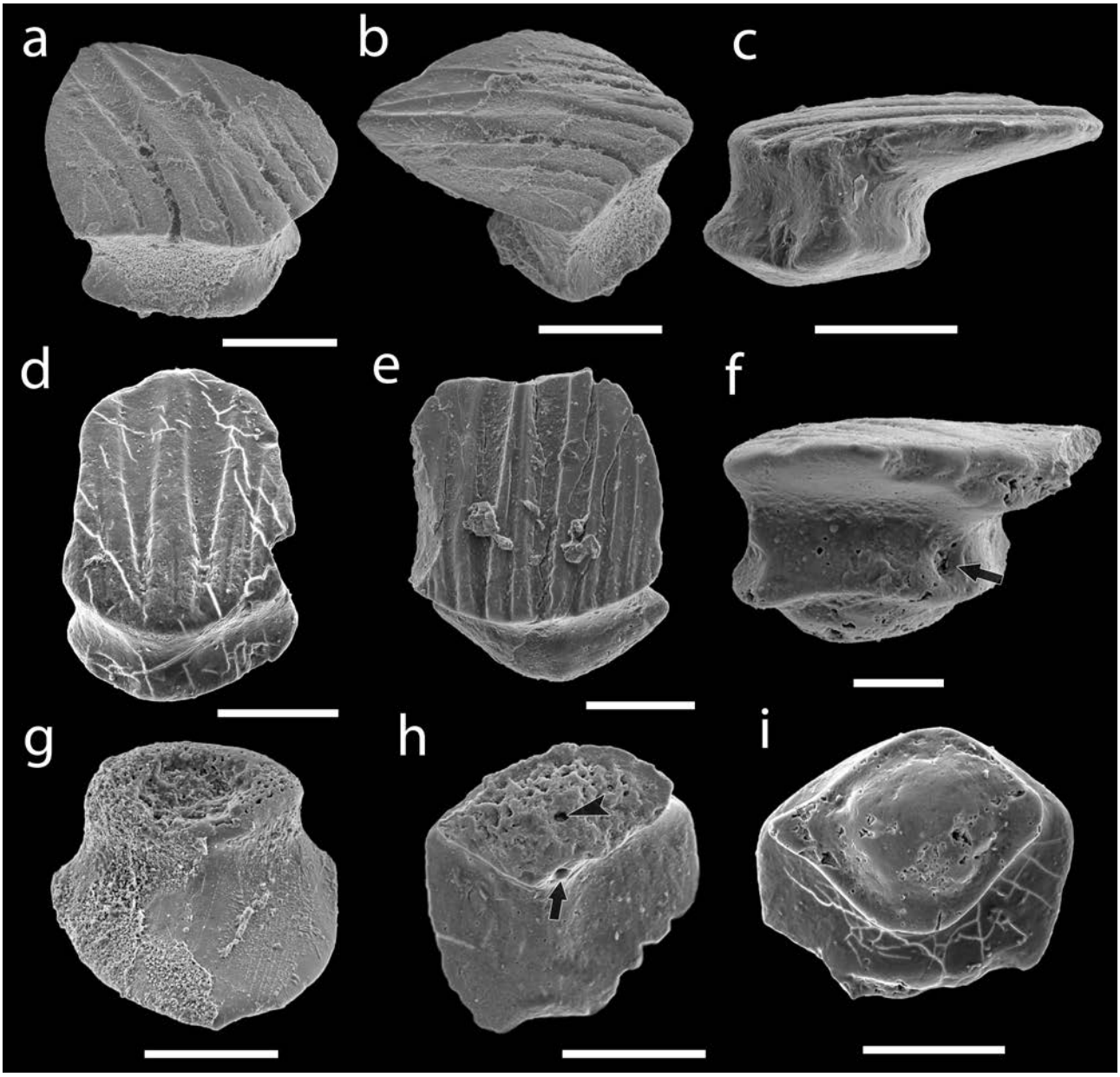

Figure 16. Scales of *Elegestolepis grossi* from the Upper Ludlow–Pridoli (Upper Silurian) Baital Formation of Tuva, Russian Federation. Ontogenetically mature scales shown in (**a**) antero-lateral (BU5285), (**b**) lateral-crown (BU5285), (**c**) lateral (BU5286) and (**d**) (BU5286), (**e**) (BU5287) crown views. (**f**) Postero-lateral view of BU5289 showing the single neck canal opening of the scale crown. (**g**) Postero-basal view of an ontogenetically young scale (BU5343) with not fully formed pedicle support. (**h**) Basal view of a scale (BU5288) with pedicle support at an advanced stage of formation. (**i**) Mature scale (BU5289) in basal view exhibiting bulbous basal bone. SEM micrographs. Anterior towards right in (b), towards left in (c), towards the bottom in (d, e) and towards the top in (h, i); arrows indicate neck canal openings, arrowhead indicates the basal opening of the main pulp canal. Scale bar represents 200 µm in (a–e, g, h) and 100 µm in (f, i).

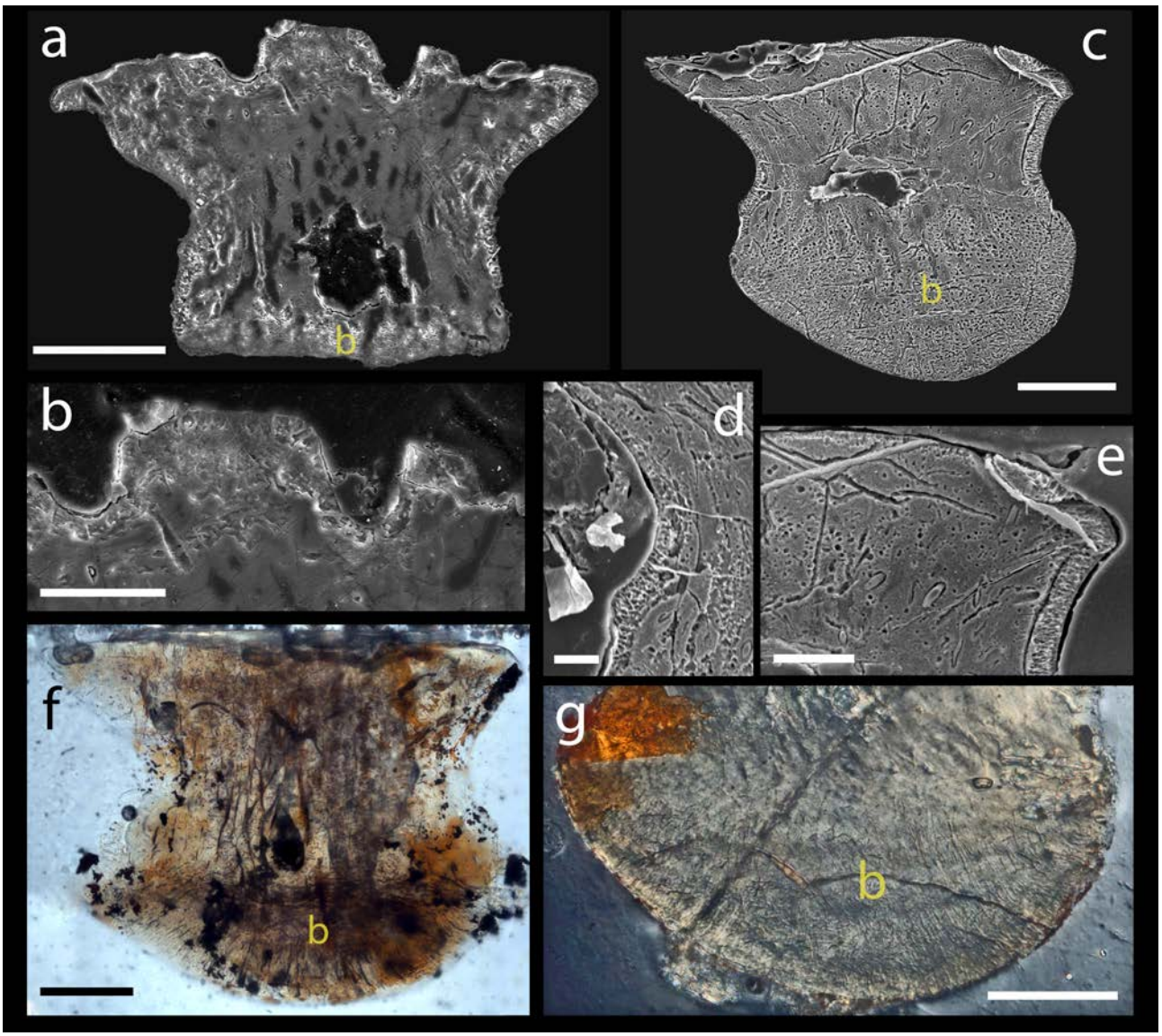

Figure 17. Hard-tissue structure of *Elegestolepis grossi* scales from the Upper Ludlow–Pridoli (Upper Silurian) Baital Formation of Tuva, Russian Federation. (**a**) Vertical cross section of a scale (BU5290) in early stage of bony base formation, etched in 0.5% chromium sulphate solution for 2 hours. (**b**) Detail of (**a**) showing the upper medial portion of the crown. (**c**) Vertical longitudinal section of a scale (BU5291) in advanced stage of basal bone developed (ontogenetically old), etched in 0.5% orthophosphoric acid for 10 minutes. (**d**) Detail of BU5291 depicting the lower posterior margin of the crown. (**e**) Detail of the anterior portion of the crown of BU5291. (**f**) Vertical transverse section of an ontogenetically old scale (BU5292). (**g**) Basal bone of ontogenetically old scale (BU5293) in vertical longitudinal section. (a–e) SEM micrographs; (f, g) Nomarski interference contrast micrographs. Anterior towards the right in (c–e, g); (b), base. Scale bar represents 100 µm in (a, c, f, g) 50 µm in (b, e) and 20 µm in (d).

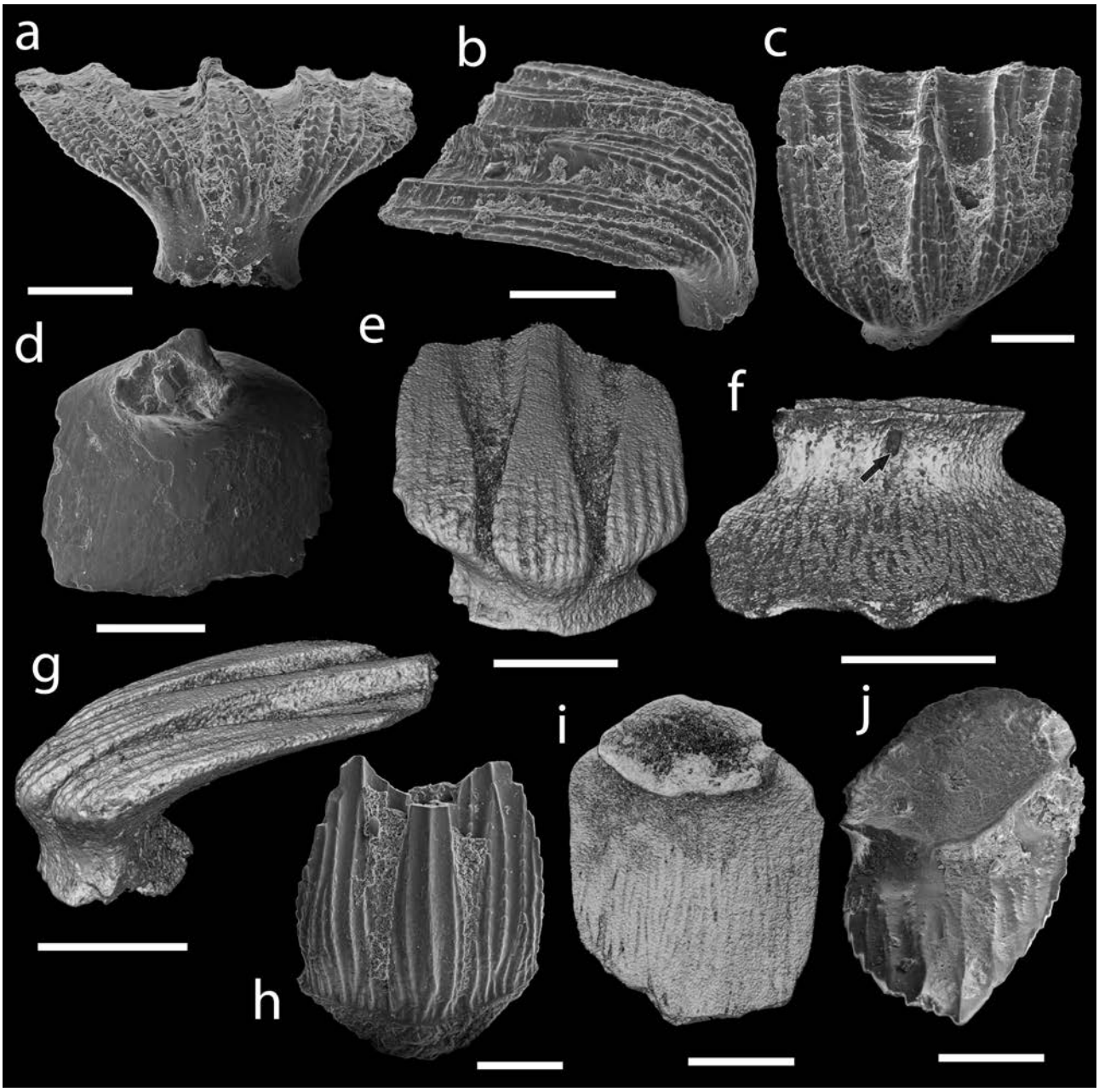

Figure 18. Scales of *Deltalepis magnus* gen. et sp. nov. from the Upper Llandovery–Lower Wenlock (Silurian) Chargat Formation of north-western Mongolia. Holotype specimen (BU5269, scale with a five-lobed crown and a gracile neck) in (**a**) anterior, (**b**) antero-lateral and (**c**) crown view. (**d**) Scale (BU5270) with gracile neck in basal view. Scales with three-lobe crowns in (**e**) anterior, (**f**) posterior, (**g**) lateral (**e**–**g**, BU5273) and (**h**), crown (BU5271) views. (**i**) BU5273 in basal view revealing the lower pedicle surface. (**j**) Basal view of a scale (BU5272) with fully formed pedicle support. (a–c, h–j) SEM micrographs; (d–g) volume renderings. Anterior towards the right in (b), towards the bottom in (c, h) towards the top in (d, i, j); arrow indicates a neck canal opening. Scale bars represent 200 µm.

Figure 19 (on the following page). Scales of *Deltalepis parvus* gen. et sp. nov. from the Upper Llandovery–Lower Wenlock (Silurian) Chargat Formation of north-western Mongolia. Holotype (BU5275) in (**a**) crown and (**b**) anterior-crown view. Scale (BU5280) with a gracile neck in (**c**) anterior and (**d**) posterior view. Scale (BU5277) in (**e**) anterior and (**f**) crown view. (**g**) Scale (BU5278) with a gracile neck in basal view, exposing the rami of the pulp canal system. Scale (BU5279) with formed pedicle support in (**h**) basal and (**i**) postero-basal view. (a, b, e–i) SEM micrographs; (c, d) volume renderings. Anterior towards the bottom in (a, f) towards the top in (g–i); arrows indicate neck canal openings, arrowhead indicates the basal opening of the main pulp canal. Scale bar represents 200 µm in (a–d, g) and 100 µm in (e, f, h, i).

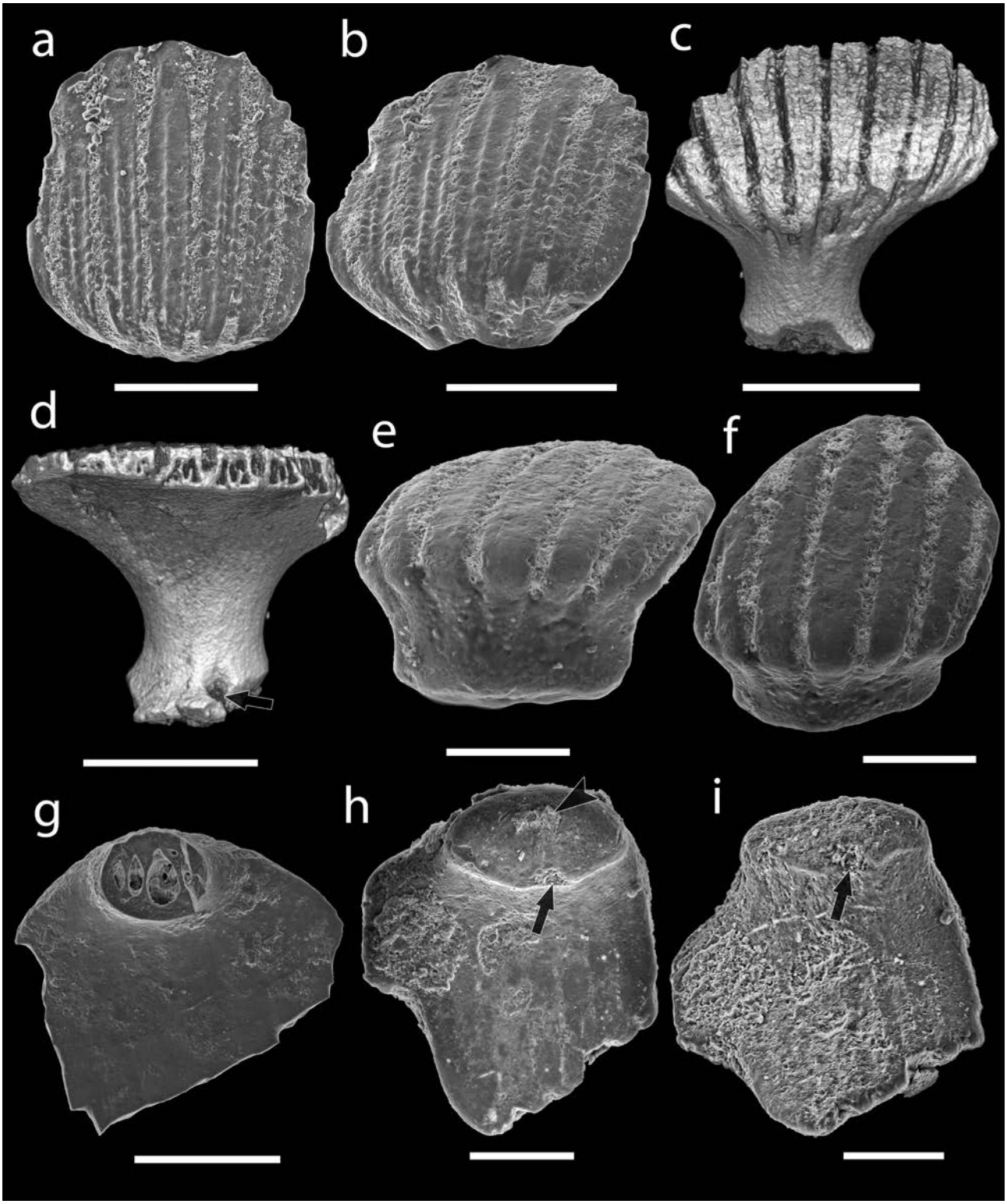
a
b
c
d
e
f
g
h
i

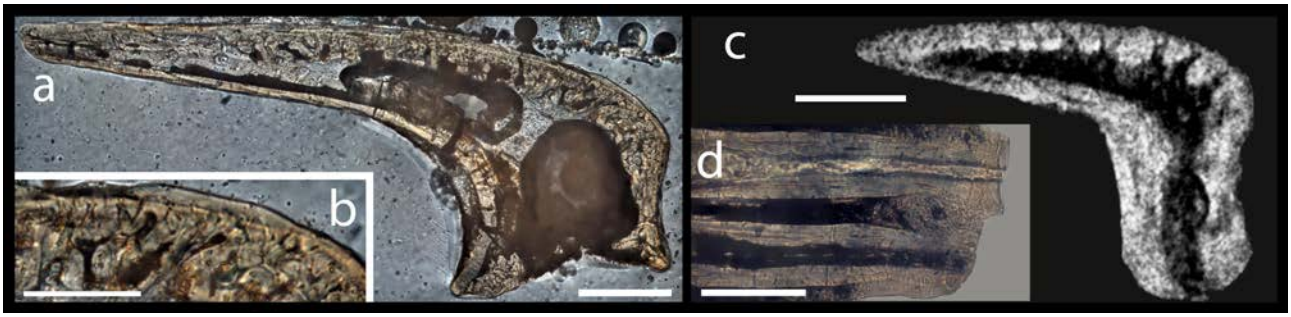

Figure 20. Hard-tissue structure of *Deltalepis* gen. nov. (**a**) Longitudinal vertical section of *Deltalepis magnus* gen. et sp. nov. scale (BU5274). (**b**) Detail of (**a**) showing the upper anterior margin of the crown. (**c**) Longitudinal tomographic 112slice of a *Deltalepis parvus* gen. et sp. nov. scale (BU5280). (**d**) View of the posterior portion of a *Deltalepis parvus* gen. et sp. nov. scale (BU5282) crown immersed in clove oil. (a, b, d) Nomarski interference contrast micrographs; (c) volume rendering. Anterior towards the left. Scale bar represents 100 µm in (a, c, d) and 50 µm in (b).

Figure 21 (on the following page). Volume renderings of the scale canal system (in red) of examined elegestolepids. The scales are made translucent in all renderings, with the exception of (**g**). (**a**–**c**) *Elegestolepis grossi* scale (BU5284) from the Ludlow–Pridoli (Upper Silurian) Baital Formation of Tuva (Russian Federation) in (**a**) anterior, (**b**) postero-lateral and (**c**) crown (depicting the lower portion of the specimen that is transversely sliced through the neck region) view. (**d**–**f**) *Deltalepis magnus* gen. et sp. nov. scale (BU5273) from the Upper Llandovery–Lower Wenlock (Lower–Middle Silurian) Chargat Formation of north-western Mongolia in (**d**) crown and (**e**) posterior view and a (**f**) crown view of the lower portion of the same specimen sliced through the neck region. (**g**–**j**) *Deltalepis parvus* gen. et sp. nov. specimens (BU5280 and BU5281) from the Upper Llandovery–Lower Wenlock (Lower–Middle Silurian) Chargat Formation of north-western Mongolia. (**g**) BU5280 sliced transversely through the crown in crown view. (**h**) BU5280 in anterior view. (**i**, **j**) BU5281 in (**i**) posterior and (**j**) postero-lateral view. Anterior towards the left in (b), towards the top in (c, f, g) and towards the bottom in (d); arrows indicate neck canal openings, arrowheads point at the basal opening of the main pulp canal. Scale bars represent 100 µm.

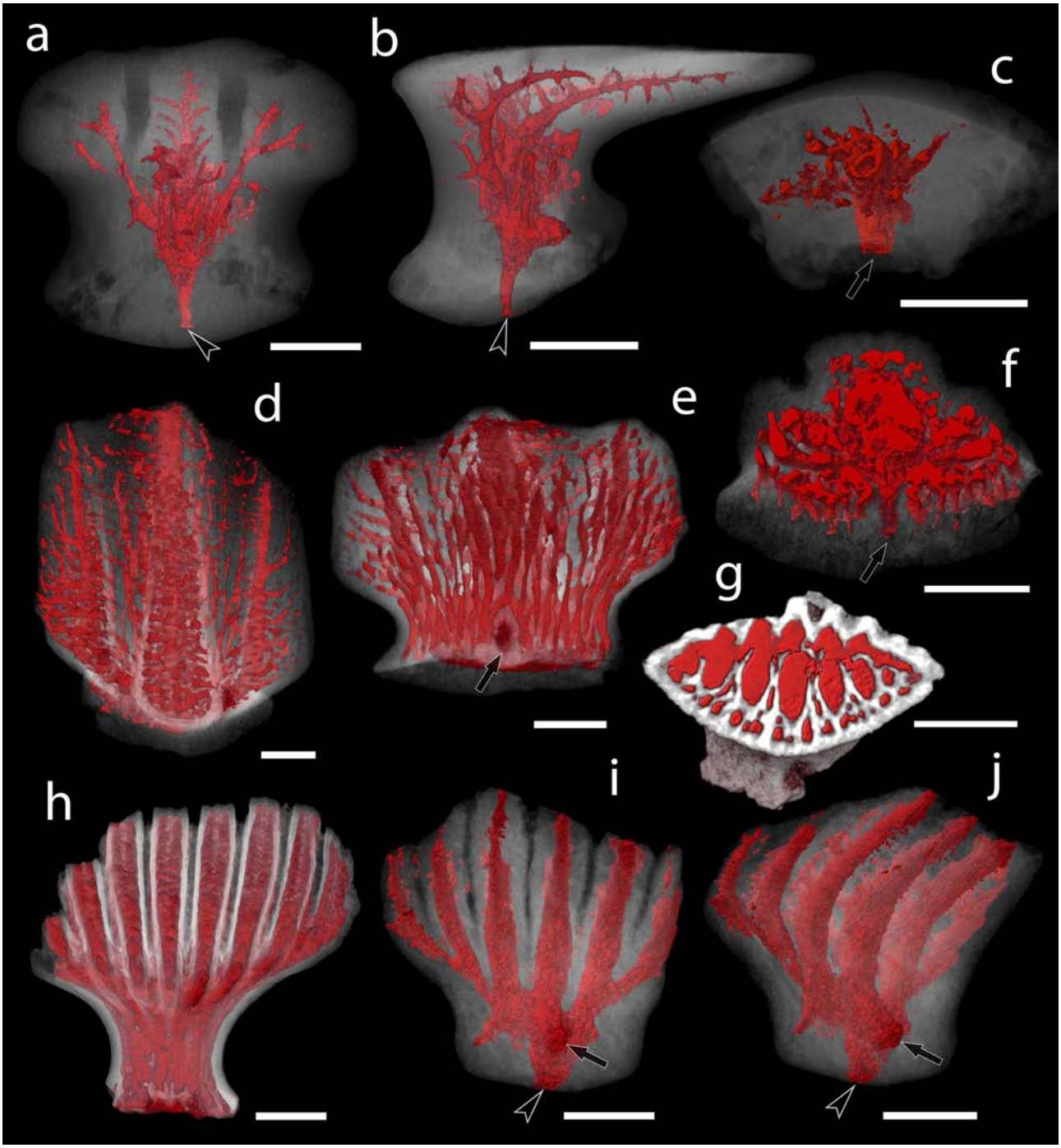
a
b
c
d
e
f
g
h
i
j

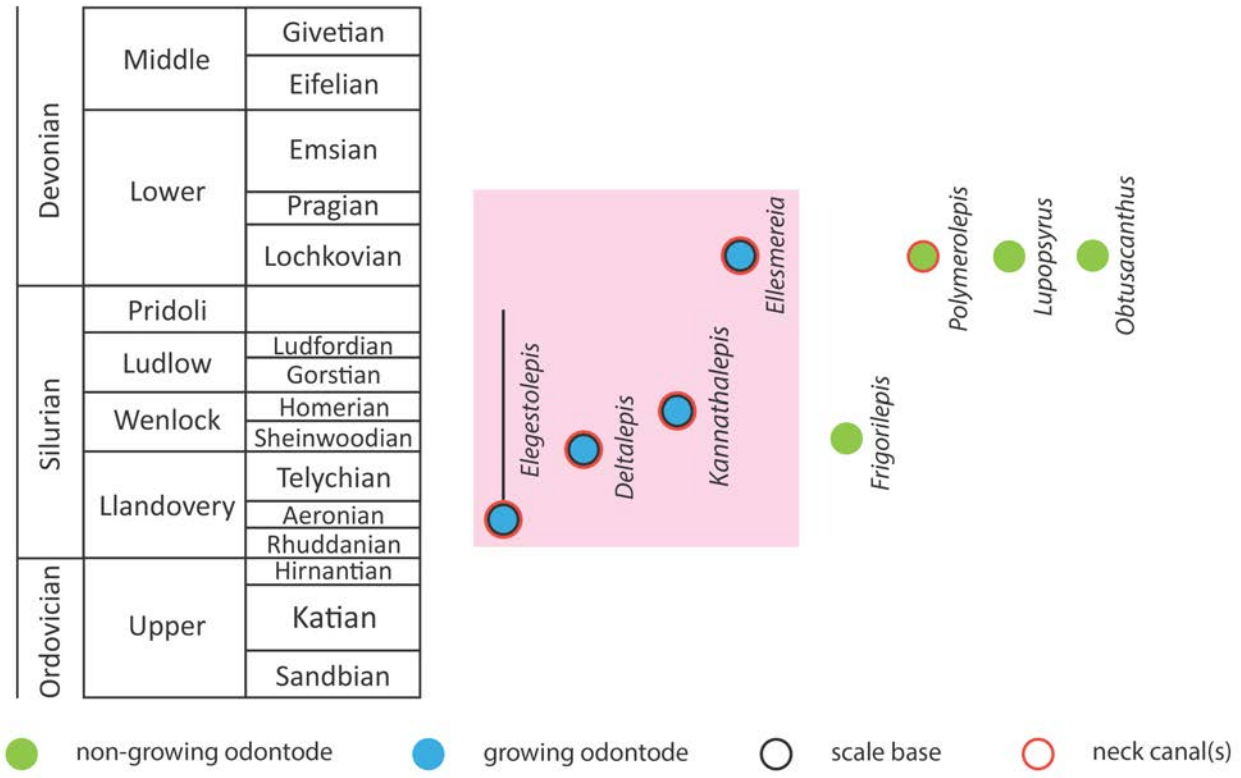

Figure 22. Characteristics of mono-odontode scales of recognised Lower Palaeozoic chondrichthyans and their stratigraphic range. Pink rectangle designates elegestolepid taxa. *Elegestolepis* (Karatajūtė-Talimaa 1973 and data from this study), *Deltalepis* gen. nov. (data from this study), *Kannathalepis* (Märss and Gagnier 2001), *Ellesmereia* (Vieth 1980); *Frigorilepis* (Märss et al. 2002, 2006), *Polymerolepis* (Karatajūtė-Talimaa 1998, Hanke et al. 2013), *Lupopsyrus* and *Obtusacanthus* (Hanke and Wilson 2004; Hanke and Davis 2012).

Chapter 6: Scale-based phylogeny of Palaeozoic chondrichthyans

6.1. INTRODUCTION

Disarticulated remains of chondrichthyan fish are ubiquitous in the fossil record, with dermal scales providing almost exclusive evidence for the first 50 Myr of their known evolutionary history (Sansom et al. 2001; Turner 2004; Turner et al. 2004). Although most of these presumed stem chondrichthyan scale taxa from the Middle Ordovician–Upper Silurian interval have been described (e.g. *Tantalepis* Sansom et al. 2012, *Canonlepis* Sansom et al. 2001; Chapter 3, *Tezakia* Sansom et al. 1996; Chapter 3, *Solinalepis* Sansom et al. 2001; Chapter 4, *Elegestolepis* Karatajūtė-Talimaa 1973, *Mongolepis* Karatajūtė-Talimaa et al. 1990, *Tuvalepis* Žigaitė and Karatajūtė-Talimaa 2008, and *Kannathalepis* Märss and Gagnier 2001), their inter-relationships and affiliations to higher-ranked clades are largely unknown. The primary obstacle that hampers progress is the lack of phylogenetic classification schemes for Palaeozoic chondrichthyans that incorporate or are entirely founded on scale characters. Instead, the existing systematic framework of fossil chondrichthyan taxa is built upon studies of relationships of crown (*sensu* Brazeau and Friedman 2014 following Grogan et al. 2012) and total group chondrichthyans (Zangerl 1981; Stahl 1999; Ginter et al. 2010) that primarily employ tooth and/or endoskeletal characters as means to diagnose taxonomic units.

Apart from a limited number of dermal scale features used in phylogenetic investigations of chondrichthyans (Grogan and Lund 2008; Grogan et al. 2012), the only other research that integrates scale-ba116sed data are phenetic classifications that produce taxon hierarchies determined entirely by morphological parameters (Tway and

Zidek 1982, 1983; Johns et al. 1997) and the categorization of scale morphogenetic patterns performed by Reif (1978) and Karatajūtė-Talimaa (1992).

The present work addresses the problem of the still insufficiently studied systematics of early Chondrichthyes by conducting a scale-based phylogenetic analysis that incorporates the majority of the putative Lower Palaeozoic stem chondrichthyans recognised in the literature and representatives of major crown chondrichthyan clades from the Upper Palaeozoic. A reevaluation of scale morphogenetic categories in chondrichthyans, last revised by Karatajūtė-Talimaa (1998), was also performed in the light of newly described taxa, and allowed the determination of scale morphogenetic patterns inside the high-ranked clades identified by the analysis. The inclusion of osteichthyan, acanthodian-grade and placoderm-grade taxa into the data matrix for the phylogenetic investigation provided the basis for correlation between resultant tree topologies and those produced by recent studies on the relationships of derived gnathostomes (Brazeau 2009; Davis et al. 2012; Zhu et al. 2013; Dupret et al. 2014).

6.2. RESULTS

6.2.1 Classification schemes of scale morphogenesis in chondrichthyans

Previous studies that attempted to identify patterns of morphogenesis in fossil chondrichthyan scales diagnose these patterns by a combination of features related to crown and base histology/development and mechanism of scale-cover ontogenesis (Reif 1978; Karatajūtė-Talimaa 1992, 1998).

The present investigation determined that the attachment portion of the scales of Palaeozoic chondrichthyans can have a separate developmental origin (odontogenic/

osteogenic) in taxa possessing similar crown architecture, or to be composed of the same tissue type in scales with distinct crown odontode patterning (Figs. 23–26; for details refer to Chapters 3–5). The former condition is documented in the polyodontode genera *Tezakia* (Upper Ordovician) and *Altholepis* (Lower Devonian), which have scale crown supports formed of dentine and basal bone (Karatajūtė-Talimaa 1997) respectively and, likewise, in the mono-odontode scales of the Silurian genus *Elegestolepis* (basal bone support) and those e.g. of the Lower Devonian taxa *Polymerolepis*, *Lupopsyrus* and *Obtusacanthus* (Hanke and Wilson 2004; Hanke and Davis 2012) that develop a dentine attachment. An example of one tissue type (acellular basal bone) forming the support of crowns with contrasting patterns of odontode arrangement are the mono-odontocomplex scales of *Seretolepis* (Lower Devonian) and *Wodnika* (Upper Permian) and the polyodontocomplex of Lower Silurian Mongolian mongolepids (*Mongolepis*, *Teslepis* and *Sodolepis*). Scale base/pedicle characteristics are therefore considered not to carry a phylogenetic signal at higher systematic levels and are excluded from use in conjunction with those of the crown in the descriptions of scale morphogenetic types (defined as categories consistent within Orders or higher ranked taxa).

The pattern of ontogenetic development of the squamation (defined as either microsquamose, mesosquamose and macrosquamose by Reif 1982) could not be ascertained in pre-Devonian chondrichthyan scale taxa because of the lack of data from articulated specimens that preserve a ‘snapshot’ of the scale cover at a particular stage of ontogenesis. This approach is contrary to interpretations (Karatajūtė-Talimaa 1992, 1998) of integumentary skeleton growth/replacement mechanisms founded solely on isolated scale elements, as scales lack recognizable specimen-specific features. In order to provide a consistent characterization of all morphogenetic types, ontogenetic features of the scale cover discernable in body fossils of stratigraphically younger chondrichthyan species are not included in their definitions.

The interpretation of scale crown developmental processes in this study departs from the views of Reif (1978) and Karatajūtė-Talimaa (1992, 1998) on the presumed formation of polyodontode scales and accounts for the difference between the main morphogenetic categories recognised here (based on odontode number and patterning) and those proposed (growing and non-growing scales) by Karatajūtė-Talimaa (1992). It is presently argued that polyodontode crowns invariably form through sequential addition of odontodes, identifying them as growing structures, as opposed to being able to develop either synchronomorially or cyclomorially (Reif 1978; Karatajūtė-Talimaa 1992, 1998). The synchronous generation of non-growing linear odontocomplexes in mongolepid chondrichthyans, suggested by Karatajūtė-Talimaa et al. (1990) and Karatajūtė-Talimaa (1998), is refuted by the identification of 'juvenile' scales with rudimentary crowns in the mongolepid genus *Shiqianolepis* (see also Sansom et al. 2000; Chapter 4). The odontocomplex structure of *Shiqianolepis* is typical for the Mongolepidida (underlining a common mechanism of development) and is similarly present in taxa with *Ctenacanthus*-type of morphogenesis, considered here to possess growing crowns (also acknowledged by Karatajūtė-Talimaa 1992). Furthermore, developing dentitions of elasmobranch embryos have shown that the patterning of vertical tooth rows, which exhibit the linear architecture of scale odontocomplexes, proceeds in a stepwise manner and is dependent on spatial information from an initially formed horizontal tooth row (Smith 2003; Smith et al. 2013). As hypothesised for odontocomplexes, unidirectional addition of odontodes accounts for the elongation of vertical tooth rows, whose constituent elements (teeth) are continuously produced by localised populations of progenitor cells (Smith et al. 2009; Tucker and Fraser 2014).

Karatajūtė-Talimaa (1992) considered scale morphogenetic types to be linked in a evolutionary transformational series, where simple mono-odontode scales (composed of either tubular or atubular dentine) give rise to all other scale types documented in

Palaeozoic chondrichthyans. This model has not been supported by more recent data from fossil taxa. The new evidence suggests that chondrichthyans with mineralised integumentary skeleton appeared in the Ordovician and these are known to possess compound scale crowns with an ordered arrangement of crown odontodes (identified in the genera *Tantalepis*, *Tezakia*, *Canonlepis* and *Solinalepis*). The early occurrence of the latter in the stratigraphic record correlates with the identification by the present phylogenetic analysis of polyodontode scales as plesiomorphic for chondrichthyans. Hence, instead of a progression from simple crowns to ones with complex developmental patterns, the early evolution of dermal scales within the Chondrichthyes does not appear to follow a linear path towards increasingly elaborate mechanisms of morphogenesis.

6.2.2. Scale morphogenetic types in chondrichthyans

Based on the number and arrangement of primary odontodes it is possible to distinguish four categories of morphogenetic types: mono-odontode, polyodontode non-odontocomplex, mono-odontocomplex and polyodontocomplex.

Mono-odontode scales. These are present in putative stem and crown chondrichthyans and can be differentiated into separate morphogenetic types on the basis of developmental, histological and canal system features.

Elegestolepis-type (originally defined by Karatajūtė-Talimaa 1992). Identified in the stratigraphically oldest single-odontode scale taxa attributed to the Chondrichthyes. These are represented by the recently united in the order Elegestolepida (Chapter 5) genera *Elegestolepis* (Llandovery–Pridoli, Karatajūtė-Talimaa 1973; Karatajūtė-Talimaa and Predtechenskyj 1995), *Deltalepis* (Upper Llandovery–Lower Wenlock, Chapter 5), *Kannathalepis* (Wenlock, Märss and Gagnier 2001) and *Ellesmereia* (Lochkovian, Vieth 1980). Scale odontode development proceeds in discrete growth phases that result in the

stepwise elongation of the lower crown region and the formation of a pedicle and neck canal openings in mature scales (Fig. 23a–c).

All other recognised modes of mono-odontode scale development (*Polymerolepis*, *Lupopsyrus* and *Heterodontus* types) in chondrichthyans produce non-growing crowns.

Polymerolepis-type (originally defined by Karatajūtė-Talimaa 1992). Exemplified by the Lower Devonian putative chondrichthyan genus *Polymerolepis* and characteristic for non-growing scales that consist of a single odontode formed exclusively of dentine and possessing a system of neck canals (Fig. 23d, e).

Lupopsyrus-type. Exhibited by the scales of *Frigorilepis* (Sheinwoodian, Märss et al. 2006), *Lupopsyrus* (Lochkovian, Hanke and Wilson 2004) and *Obtusacanthus* (Lochkovian, Hanke and Davis 2012), regarded to be among the stratigraphically oldest taxa of chondrichthyan affinities known from articulated specimens. This type of morphogenesis produces non-growing, single odontode scales devoid of neck canal openings.

Heterodontus-type (originally defined as placoid-type by Reif 1978 and subsequently revised under the name *Heterodontus*-type morphogenesis in Karatajūtė-Talimaa 1992). This developmental pattern is recorded in the crown-group chondrichthyan clades Petalodontiformes (in *Janassa* Ørvig 1966; Malzahn 1968), Hybodontiformes and Neoselachii (Johns et al. 1997; Thies and Leidner 2011). The scales of these taxa develop as non-growing, single odontode elements that possess neck canal openings and are formed of dentine and capping enameloid tissue (Fig. 23f, g).

Polyodontode scales. Within the Chondrichthyes, compound scale crowns are a feature of putative stem-group taxa and stem euchondrichthyans (*sensu* Grogan et al. 2012), exhibiting a wide range of odontode patterning styles on the basis of which there can be distinguished separate morphogenetic categories.

Eugeneodus-type. Recognised in the scales of the earliest known chondrichthyan taxon, the Middle Ordovician species *Tantalepis gatehousei* (Sansom et al. 2012), the supposed basal chondrichthyan *Tuvalepis* (Pridoli–Lochkovian, Žigaitė and Karatajūtė-Talimaa 2008) and the eugeneodontiform species *Eugeneodus richardsoni* (Zangerl 1966, 1981). The polyodontode growing crowns of their scales constitute of a single medio-lateral (non-odontocomplex) odontode row (Fig. 24), deposited through areal bidirectional addition of odontodes lateral to the crown primordium.

Seretolepis-type (originally defined by Karatajūtė-Talimaa 1992). Exemplified by the Lower Devonian ‘acanthodians’ *Parexus* (Burrow et al. 2013) and *Brochoadmones* (Hanke and Wilson 2006), the putative stem chondrichthyan *Seretolepis* (Lower Devonian, Karatajūtė-Talimaa 1997; Hanke and Wilson 2010) and the Permian ‘sphenacanthid’ shark *Wodnika* (Schaumberg 1999). This type of morphogenesis produces areally growing scale crowns with mono-odonocomplex architecture of linearly (antero-posteriorly) arranged odontodes characterised by incremental increase in size in posterior direction (Fig. 25 a–d).

Protacrodus-type (originally defined by Karatajūtė-Talimaa 1992). A second kind of single odontocomplex crown occurs in the scales of the poracanthodid ‘acanthodian’ *Poracanthodes* (Upper Silurian–Lower Devonian; Gross 1956; Märss 1986; Valiukevičius 1992, 2003a), the euselachians *Protacrodus* (Devonian–Carboniferous; Gross 1938, 1973) and *Holmesella* (Upper Carboniferous Ørvig 1966; Cicimurri and Fahrenbach 2002). It consists of a series of nested scale odontodes added areally in a concentric pattern (Fig. 25e–i).

Chondrichthyan scales with polyodontocomplex structure possess odontocomplexes of exclusively linear composition. Patterns of odontode size-change

within the primary odontocomplexes of these scales and their crown histology are used to distinguish separate modes of morphogenesis within this category.

Mongolepis-type (originally defined by Karatajūtė-Talimaa 1992). Identified in members of the chondrichthyan Order Mongolepidida (the Upper Ordovician genus *Solinalepis* and the Lower/Middle Silurian genera *Mongolepis*, *Teslepis*, *Sodolepis*, *Xinjiangichthys*, *Shiqianolepis* and *Rongolepis*, Sansom et al. 2000). Scale morphogenesis is characterised by the development of a polyodontocomplex crown (Fig. 26a, b) composed solely of atubular dentine (lamelline) that grows areally through posteriorly directed deposition of progressively larger odontodes.

Ctenacanthus-type (originally defined by Karatajūtė-Talimaa 1992). Recognised in the scales of the cladodont taxa *Cladolepis* (Lower Devonian, Burrow et al. 2000), *Cladoselache* (Upper Devonian, Dean 1909), *Goodrichthys* (Mississippian, Ginter 2009), the Middle–Upper Devonian antarctilamniform *Antarctilamna* (Young 1982) and the Mississippian xenacanthiform *Diplodoselache* (Dick 1981). This type of development produces scale crowns with a mongolepid architecture and growth pattern, composed exclusively of tubular dentine (Fig. 26c, d).

Two more developmental types (the *Altholepis* and *Ohiolepis* types) are described for polyodontocomplex scales with irregular pattern of odontode size change within odontocomplex rows.

Altholepis-type (originally defined by Karatajūtė-Talimaa 1992). In the putative chondrichthyans *Tezakia* (Upper Ordovician, Sansom et al. 1996; Chapter 3) and *Altholepis* (Lower Devonian, Karatajūtė-Talimaa 1997). The primordial odontode consistently develops as the largest crown element of growing polyodontocomplex crowns (Fig. 26g, h).

Ohiolepis-type. Present in the Upper Ordovician scale genus *Canonlepis* (Sansom et al. 2001; Chapter 3) and the Middle Devonian putative cladodontomorph *Ohiolepis* (Wells 1944; Gross 1973). The crowns of scales with this type of morphogenesis are growing polyodontocomplex structures with primordial odontodes that do not exceed the size of the other primary odontodes (Fig. 26e, f).

6.2.3. Chondrichthyes-specific developmental pattern of the integumentary skeleton

The defined here types of scale morphogenesis allow to differentiate patterns of ontogenesis of integumentary skeletal elements within the Chondrichthyes. The majority of these types represent specific modes of development for single odontode (the *Elegestolepis*-, *Polymerolepis*-, *Lupopsyrus*- and *Heterodontus*- types) and polyodontode (the *Eugeneodus*-, *Seretolepis*-, *Protacrodus*-, *Mongolepis*-, *Altholepis*- types) crowns not recognised in taxa placed stem-ward of the chondrichthyan node (as resolved herein), whereas the rest can be identified in other crown gnathostomes (e.g. the *Ctenacanthus*- and *Ohiolepis*- types are also present in the crown osteichthyans *Ligulalepis* and *Dialipina* respectively). Despite shared crown-development patterns with osteichthyans, the taxa possessing *Ctenacanthus* and *Ohiolepis* types of morphogenesis can be united by a combination of attributes (similarly recognised in the rest of the taxa included in the description section) that are considered unique to the chondrichthyan integumentary skeleton; lack of enamel, lack of dermal bone osteons, lack of hard tissue resorption and non-superpositional addition of odontodes.

Enamel is widely accepted to be among the earliest to emerge mineralised-tissue components of the vertebrate skeleton (but see Murdock et al. 2013), as it is documented in the crowns of euconodont oropharyngeal elements (Donoghue 1998; Donoghue and Sansom 2002; Donoghue et al. 2006), whereas dermatoskeletal enamel only makes an

appearance at the terminal branches of the vertebrate phylogenetic tree, in the Osteichthyes (Donoghue and Sansom 2002; Donoghue et al. 2006; Sire et al. 2009; this study). By contrast, osteon formation is common in the scales of stem (in anaspids Blom et al. 2002, pteraspidomorphs Denison 1967; Donoghue and Sansom 2002; Donoghue et al. 2006 and ‘placoderms’ Giles et al. 2013) and crown gnathostomes (in osteichthyans), along with resorption and/or remodeling of mineralised tissues (in pteraspidomorphs Denison 1967; Donoghue et al. 2006, osteostracans Denison 1952; Donoghue et al. 2006, ‘placoderms’ and osteichthyans). Crown growth that involves superpositional addition of odontodes (newly deposited odontodes covering the free surfaces of previously deposited ones) is identified in some of the phylogenetically most basal vertebrate taxa known to possess polyodontode scale crowns (pteraspidomorphs Denison 1967), and it is also a prevalent feature of jawed gnanthostomes, found in ‘placoderms’, ‘acanthodians’ and osteichthyans (Gross 1968; Denison 1979; Burrow and Turner 1998; Qu et al. 2013a).

The chondrichthyan dermal skeleton is thus suggested to have evolved a distinct developmental signature by means of elimination of a number of gnathostome plesiomorphies and not through acquisition of novel characteristics. As the number of phylogenetically primitive characters retained in other major jawed gnathostome groups is greater than that documented in chondrichthyans, the latter are considered to exhibit the most derived dermatoskeletal features among vertebrates.

6.2.4. Remarks on the phylogenetic analyses

The calculated four strict consensus trees (SCTs; Figs. 28, 29b, 30b, 31b), one for each of the performed analyses (I–IV), are partially resolved, with the highest number of polytomies (24 unresolved nodes) occurring on the branch carrying putative and established chondrichthyan taxa in SCT I and SCT III, compared to only six unresolved

nodes in SCT II and SCT IV. The SCT II polytomies are near the stem of the tree (affecting the thelodont branch, and those supporting the ‘placoderms’ *Connemaraspis* and *Gladbachus* and the osteichthyans *Ligulalepis* and *Cheirolepis*), whereas in SCT IV they appear more crown-wards (polytomies on the branches bearing *Ligulalepis*/*Cheirolepis*, *Poracanthodes*/*Polymerolepis* and *Altholepis*/*Orodus* respectively). The generated 50 percent majority-rule trees (MRTs; Figs. 27, 29a, 30a, 31a) similarly have unresolved regions but possess fewer polytomies above node of the lowest placed chondrichthyan taxon (7 in MRT I, 4 in MRT III and 1 in MRT IV) than produced by the strict consensus analyses. The SCT and MRT polytomies are regarded to be soft, as both types of trees were calculated from sets of fully resolved most parsimonious trees (MPTs).

Those taxa that exhibit chondrichthyan-type scale morphogenesis form a monophyletic group in MRTs, when the full character-taxon dataset is used in analyses with either no preferential weighting of characters (analysis I) or with higher weight values assigned to a subset of characters deemed diagnostic to the chondrichthyan dermal skeleton (analysis III). The consistent taxon composition and similar branch topology of the chondrichthyan clade resolved in both of these analyses indicates that a strong phylogenetical signal is carried by the scale characters defined as Chondrichthyes-specific. This interpretation is further substantiated by the difference between MRT I, III (Figs. 27, 30a) and the MRT produced by analysis II (higher weight values given to a subset of developmental characters; Fig. 29a) where all ‘acanthodian’ genera with non-chondrichthyan, superpositional, crown growth pattern are placed on the chondrichthyan branch. The exclusion of anaspid and thelodont taxa from the outgroup (analysis IV) similarly resolves a MRT that contains a monophyletic group comprised of taxa with chondrichthyan and ‘acanthodian’ (superpositionally growing mono-odontocomplex crown) type of scale morphogenesis, but the inter-relationships of the latter differ from those established in analysis II.

The synapomorphies of the Chondrichthyes identified from analyses I and III (all scale odontodes exposed on the crown surface; areal addition of odontodes) are considered to give the latter more relevance in comparison to analyses II and IV, where the loss of certain features (absence of scale peg-and-socket articulation; absence of enamel) is recognised instead as synapomorphic. Moreover, MRT I and MRT III are regarded to provide the most congruent taxon composition of the chondrichthyan clade based upon the absence of what are believed to be more basal acanthodian-grade taxa (see above), and on the account of the fully resolved stem of MRT I, the latter is given preference over MRT III to be representative of the conducted phylogenetic study.

6.2.5. Populating the stem of the chondrichthyan tree

The largest clade to exclusively consist of taxa sharing a common pattern of scale morphogenesis of a chondrichthyan type is the one uniting the six mongolepid genera included in the present study (*Mongolepis*, *Teslepis*, *Sodolepis*, *Xinjiangichthys*, *Shiqianolepis* and *Solinalepis*; Fig. 32), and this is consistently resolved in all generated trees. These results are in accordance with previous work that supports the validity of the Mongolepidida (Karatajūtė-Talimaa et al. 1990; Sansom et al. 2000; Sansom et al. 2001), and re-affirm its status as a chondrichthyan Order by grouping the mongolepids with putative and established chondrichthyan genera in the produced MRTs.

A large monophyletic group of Middle Ordovician to Lower Devonian chondrichthyans (*Tantalepis*, *Canonlepis*, *Tezakia*, *Elegestolepis*, *Frigorilepis*, *Kannathalepis*, *Tuvalepis*, *Lupopsyrus* and *Obtusacanthus*; Fig. 32) is also recognised to be a feature of most MRTs (I, III, IV), but, in contrast to the Mongolepidida, the former is heterogeneous with regard to the scale developmental types recognised in its component taxa. Crown characteristics exhibit polarisation within the clade, with the

polyodontocomplex genera *Canonlepis* and *Tezakia* being its basal-most members and the mono-odontode condition predominating among more derived taxa (*Elegestolepis*, *Frigorilepis*, *Kannathalepis*, *Lupopsyrus* and *Obtusacanthus*). The only part of this clade's tree structure not collapsed in SCTs I and III is that above the node bearing the branches for *Tuvalepis, Elegestolepis* and *Kannathalepis*, the latter two of which are resolved as sister taxa in conjunction with their recent inclusion into the Order Elegestolepida (Chapter 5). The derived position within the Chondrichthyes of the elegestolepids and other lower–mid Palaeozoic taxa with single odontode scales, e.g. *Lupopsyrus* and *Obtusacanthus*, in all MRTs is at odds with the placement of the latter as stem chondrichthyans by Davis et al. (2012) and Zhu et al. (2013). This discrepancy could possibly be due to the composition of the character set used in the present analyses, 20 percent of which consists of characters not applicable to scales with mono-odontode crowns, that might cause a crown ward displacement of Elegestolepida+*Lupopsyrus* and *Obtusacanthus* as a consequence of missing data.

A grouping of all taxa with *Seretolepis*-type of scale morphogenesis (*Parexus*, *Brochoadmones*, *Seretolepis* and *Wodnika*) included in the present investigation is weakly supported (only resolved by analysis II), whereas the *Parexus*/*Seretolepis* pairing remains stable under the variable parameters of the performed analyses. When resolved in comparison to other internal nodes (in MRTs I, III, IV), the *Parexus*/*Seretolepis* clade is identified as a sister taxon to genera with *Ctenacanthus*-type of scale development (*Antarctilamna* and *Goodrichthys*), which on their own form a natural group in all of the calculated trees.

Gladbachus is the sole taxon identified previously as a chondrichthyan (Heidtke and Krätschmer 2001) to fall outside the chondrichthyan branch in the resultant phylogenies. Its repeated placement as either basal to or nested among 'placoderm'-grade genera

implies a more stem-ward position, nearer the root node of jawed gnathostomes. It is considered that the unordered patterning of crown odontodes of *Gladbachus* scales (a condition yet to be documented in chondrichthyans) influences its grouping with ‘placoderms’ despite sharing a set of character states (areal odontode addition, absence of enamel, bone osteons and mineralised-tissue resorption) with the polyodontode scales of chondrichthyans that are derived for jawed gnathostomes.

Summarising the above observations, two main configurations of the chondrichthyan branch in terms of topology and taxon composition can be recognised in MRTs. The fully resolved chondrichthyan node in MRTs II and IV supports a larger number of taxa as a result of the inclusion within the clade of ‘acanthodians’ (*Tchunacanthus*, *Machaeracanthus*, *Ptomacanthus*, *Uranicanthus*, *Diplacanthus* and *Acanthodes*) with box-in-box (superpositional) pattern of scale odontocomplex formation. This type of crown development is not considered (Reif 1978; Karatajūtė-Talimaa 1992, 1998 and herein) to have evolved in the dermal skeleton of the Chondrichthyes and consequently it weakens the support for the phylogenetic placement of these taxa, determined from analyses II and IV. MRTs II and IV nevertheless show certain congruency with recent phylogenetic schemes of the total-group Chondrichthyes (Grogan and Lund 2008, 2009; Grogan et al. 2012) with regard to the inter-relationships of genera belonging to the Antarctilamniformes (*Antarctilamna*), the Ctenacanthiformes (*Goodrichthys*), the Euselachii (*Protacrodus* and *Wodnika*), the Orodontiformes (*Orodus*) and the Petalodontiformes (*Janassa*). The grouping of *Orodus* with *Janassa* on the same branch in MRT II (similarly in SCT II) is in agreement with the position of orodontiforms and petalodontiforms inside Paraselachii, one of the high ranked clades of the Chondrichthyes (Grogan et al. 2012). The Subclass Elasmobranchii, the sister taxon to Paraselachii (Grogan et al. 2012), can similarly be identified by the association of *Protacrodus* and *Wodnika* into a single clade in MRT II and MRT IV. The elasmobranchs *Antarctilamna* and *Goodrichthys* however are

phylogenetically unstable due to being resolved as basal chondrichthyans (in SCT II and MRT II) or by falling inside the clade containing *Protacrodus* and *Wodnika* in SCT IV and MRT IV (uniting all elasmobranch taxa included in this study on the same branch). Analysis IV also shifts the position of *Janassa* from the presumed paraselachian clade (analysis III) to the sister group containing all elasmobranch taxa.

In the partially resolved chondrichthyan node recovered in MRTs I and III (missing acanthodian-grade taxa, identified by superpositional crown growth), the tree topology crown-wards of the node supporting *Orodus* (and putative Middle Ordovician to Lower Devonian chondrichthyans) is largely consistent with that of MRTs II and IV, and represents the most stable region of the chondrichthyan branch. Due to the polytomy at the chondrichthyan root node in analyses I and III, *Protacrodus* is the sole elasmobranch genus to be resolved (as a sister taxon) relative to *Orodus* in both MRT I and MRT III, in conjunction with its placement in analysis II and IV trees.

6.2.6. Degree of correlation with existing gnathostome phylogenies

Recent phylogenetic investigations of gnathostome relationships (Brazeau 2009; Davis et al. 2012; Zhu et al. 2013; Dupret et al. 2014) use a relatively consistent set of characters, largely based on the work of Brazeau (2009), that codes for features of all skeletal systems (dermal, endoskeletal and splanchnocranial), of which only approximately one-tenth are related to dermal scales. The Galeaspida and the Osteostraci have repeatedly been selected in these analyses as an outgroup, in contrast to the trend towards increasing the size of the ingroup in newer studies. The cited above studies recover placoderms as a paraphyletic assemblage of basal jawed gnathostomes and monophyletic Chondrichthyes and Osteichthyes in a sister-group relationship. The position of taxa traditionally allied within the Acanthodii (Denison 1979; Gagnier and Wilson 1996) is in a

state of flux as they are recognised as either a natural group of crown gnathostomes (Dupret et al. 2014), stem chondrichthyans and/or osteichthyans (Brazeau 2009; Zhu et al. 2013) or are split into derived stem gnathostomes and crown gnathostomes (Davis et al. 2012). Tree topology (MRT I) is thus in conflict with the established position of osteichthyans and ‘placoderms’ by recovering the Osteichthyes as a paraphyletic group basal to a clade uniting acanthothoracid and arthrodire ‘placoderms’. It is plausible to assume that the inclusion of Anaspida and Thelodonti in analysis I affects the stem branches of the ingroup, since the use of a simple outgroup (Galeaspida+Osteostraci; analysis IV) reverses the positions of osteichthyan and ‘placoderm’ genera. Alternatively, the recently described Upper Silurian crown osteichthyan *Guiyu* (Zhu et al. 2009) and the ‘placoderm’ *Entelognathus* (Zhu et al. 2013) demonstrate a combination of what are traditionally considered osteichthyan and placoderm specific characteristics of the dermal skeleton (median dorsal plates in *Guiyu* and marginal jaw bones in *Entelognathus*), lending support to the placement by this study of at least some placoderm-grade taxa inside the gnathostome crown group.

Another outcome of this analysis is the recognition of a paraphyletic Acanthodii as a result of the placement of ‘acanthodians’ with mono-odontode or polyodontode areally growing scale crowns (*Poracanthodes*, *Lupopsyrus, Obtusacanthus, Brochoadmones* and *Parexus*) inside the Chondrichthyes. This is the first study to provide unequivocal support for the chondrichthyan affinities of *Poracanthodes*, contradicting the earlier proposed alternative position of the genus among stem osteichthyans (Brazeau 2009; Davis et al. 2012). The recovery of taxa with acanthodian-grade scale structure (*Machearacanthus*, *Acanthodes*, *Diplacanthus* and *Uraniacanthus*) as stem chondrichthyans in MRT I (Fig. 27) clashes with the identified here patterns of morphogenesis of the chondrichthyan dermal skeleton and is not supported by any of the recent gnathostome phylogenies (Brazeau 2009; Davis et al. 2012; Zhu et al. 2013; Dupret et al. 2014). Considering the latter,

‘acanthodians’ possessing superpositional arrangement of scale odontodes are tentatively proposed to fall outside the total-group Chondrichthyes as sister taxa to the chondrichthyan clade, in agreement with Zhu et al. (2013) and Dupret et al. (2014).

The results of the conducted investigation also imply a pattern of phylogenetic development of the gnathostome dermal skeleton concordant with recent work on the subject by Zhu et al. (2013), suggesting that the macromeric skeletons of osteichthyans and placoderms are homologous (plesiomorphic for jawed gnathostomes), and macromery represents the derived condition for the common ancestor of ‘acanthodians’ and chondrichthyans.

6.3. CONCLUSIONS

On the basis of dermal-scale characteristics this study resolves a monophyletic Chondrichthyes that unites Palaeozoic taxa traditionally identified as ‘acanthodian’, stem and crown chondrichthyans. A consistent feature of the calculated trees is the placement of genera (*Antarctilamna*, *Protacrodus*, *Goodrichthys*, *Orodus*, *Janassa* and *Wodnika*) belonging to high-ranked crown chondrichthyan taxa (Grogan and Lund 2008, 2009; Grogan et al. 2012) closest to the chondrichthyan node, and therefore no stem group members of the clade are resolved. The Ordovician–Silurian record of mongolepids and that of *Tantalepis*, *Tezakia*, *Canonlepis*, *Elegestolepis* and *Kannathalepis* however is not concordant with their derived position in the produced phylogenies, and given the dearth of previous cladistic investigations of Lower Palaeozoic chondrichthyans, the relationships of the former in regard to the chondrichthyan crown group are still considered uncertain.

Several of the well-supported by the present analysis Order-level monophyletic groups (Mongolepidida, Elegestolepida, an unnamed clade uniting *Lupopsyrus* and *Obtusacanthus* and an unnamed clade uniting *Parexus* and *Seretolepis*) have been recognised in earlier work (Karatajùtè-Talimaa et al. 1990; Sansom et al. 2000; Dupret et al. 2014; Chapters 4, 5), and, as each can be differentiated by a particular chondrichthyan scale morphogenetic pattern, it is suggested that the crown characteristics of scales are diagnostic for Order ranked taxa inside the Chondrichthyes.

Despite deviating from traditional (Janvier 1996) and recent (Brazeau 2009; Davis et al. 2012; Zhu et al. 2013; Dupret et al. 2014) classification schemes of jawed gnathostomes by recovering a paraphyletic Osteichthyes basal to placoderm-grade gnathostomes, the present investigation is in agreement with the schemes of Zhu et al. (2013) and Dupret et al. (2014) on the derived position of the Chondrichthyes as the most closely related clade to acanthodian-grade taxa. The resultant topology of the tree stem will need to be corroborated by future studies, as scale characters of ‘placoderms’ and early osteichthyans have been documented only in a rather small body of published accounts on the micromeric skeleton of these taxa. One way to test the robustness of this and subsequent scale-based phylogenies would be to perform analyses that use an expanded dataset that integrates their character matrices with those of existing phylogenies of Palaeozoic gnathostomes. Nevertheless, a downside of this approach is that it causes taxa known exclusively from scale remains to be under-represented in terms of number of applicable characters.

Figure 23 (on the following page). Types of morphogenetic patterns of chondrichthyan mono-odontode scales. (**a**–**c**) *Elegestolepis*-type of development exhibited by *Elegestolepis grossi* scales from the Upper Ludlow–Pridoli (Upper Silurian) Baital Formation of Tuva, Russian Federation. Ontogenetically (**a**) young (BU5343) and (**b**) mature (BU5284) scales in posterior view and a longitudinally sectioned mature scale (BU5283). (**d**, **e**) *Polymerolepis*-type of development in *Polymerolepis whitei* scales from the Lochkovian (Lower Devonian) of Dobrivlyany (Dniester section), Podolia, Ukraine. K-T1998Fig6f depicted in (**d**) baso-posterior view and in (**e**) antero-posterior section. (**f**–**g**) *Heterodontus*-type of development exemplified by a (**f**) hybodont scale (transversely sliced specimen, BU5295) from the Tournaisian (Mississippian) Muhua Formation of Muhua (south China) and a scale (upper crown portion of specimen BU5301) from the extant neoselachian *Raja montagui*. SEM micrograph (a), volume renderings (b, d–f), Nomarski differential interference contrast micrographs (c, g). Enameloid layer marked by an asterisk. Neck canal openings indicated by arrows. Anterior to the left in (e, g) and to the right in (c). Scale bar equals 100 µm in (a–c) and 200 µm in (d–g).

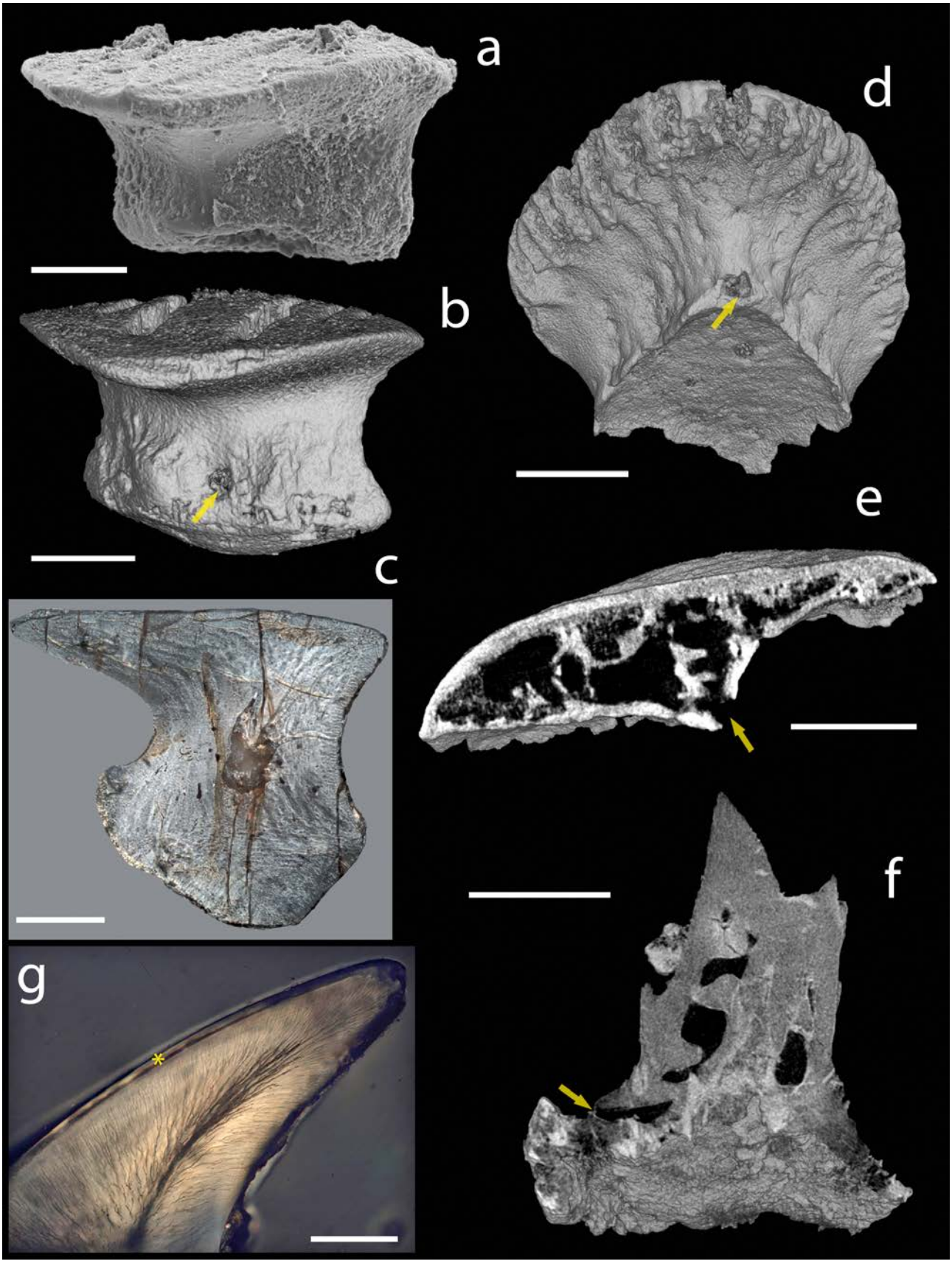
a
b
c
d
e
f
g

Figure 24. Morphogenetic pattern of chondrichthyan polyodontode non-odontocomplex scales. *Eugeneodus*-type development in (**a**, **b**) *Tuvalepis schulzei* scale (BU5342) from Pridoli–Lochkovian (Upper Silurian–Lower Devonian) strata of the Khondergei Formation of Tuva (Russian Federation) and in the (**c**, **d**) scales of *Tantalepis gatehousei* from the Darriwilian (Middle Ordovician) Stairway Sandstone (Northern Territory, Australia). BU5342 in (**a**) crown view and (**b**) sliced transversely in posterior-crown view; (**c**) BU5319 in antero-lateral view and (**d**) transversely sectioned BU5320. Volume renderings (a–c), Nomarski differential interference contrast micrograph (d). Anterior towards the top in (d). Scale bar equals 200 µm in (a) and 100 µm in (b–d).

Figure 25 (on the following page). Types of morphogenetic patterns of chondrichthyan mono-odontocomplex scales. (**a**–**d**) *Seretolepis*-type of development in a (**a**, **b**) *Seretolepis* scale from the Lochkovian (Lower Devonian) Ivane Formation of Podolia (Ukraine) and (**c**, **d**) *Wodnika* scales from the (**c**) Wuchiapingian (Lopingian, Upper Permian) Werra Formation of central Germany and (**d**) the Marl Slate of Durham (UK). (**a**) 5-461 in anterior view and (**b**) longitudinally sliced; (**c**) NHM 36059 in lateral crown view and a (**d**) longitudinally sectioned specimen (NHMUK PV P. 66677). (**e**–**i**) *Protacrodus*-type of development in a (**e**–**g**) *Poracanthodes punctatus* scale from the Pridoli of the USA and a (**h**, **i**) protacrodont scale from the Tournaisian (Mississippian) Muhua Formation of Muhua, south China. (**e**) BU5300 in crown view, (**f**) transversely and (**g**) longitudinally sliced BU5300; (**h**) transversely and (**i**) longitudinally sliced PKUM02–0178. Volume renderings (a–c, e–i), Nomarski differential interference contrast micrograph (d). Crosses mark primordial odontodes. Anterior to the left in (a, g), to the right in (b, d, i) and towards the bottom in (e, f, h). Scale bar equals 200 µm in (a, b, d, i) and 100 µm in (c, e, f–h).

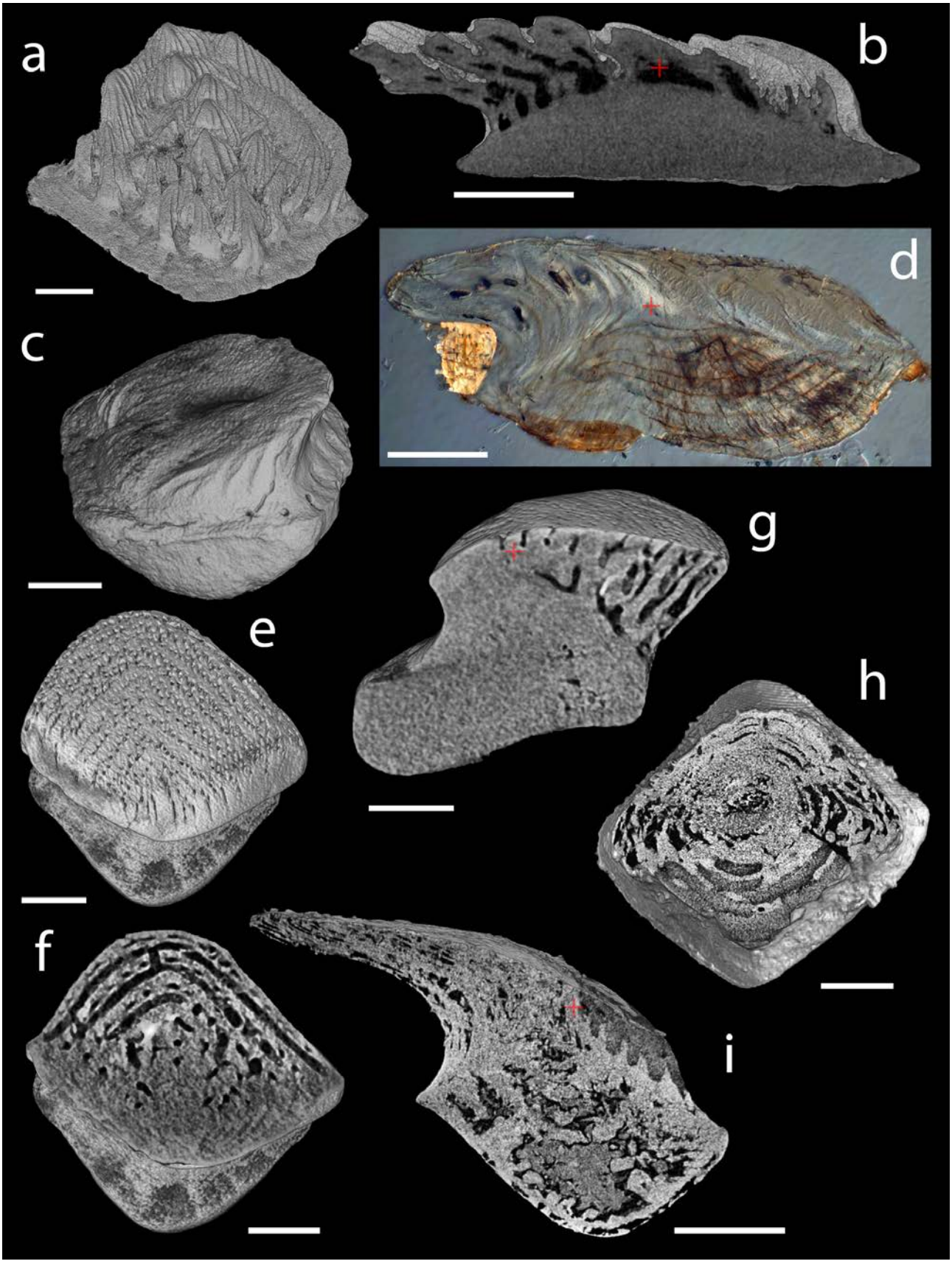
a
b
c
d
e
f
g
h
i

Figure 26 (on the following page). Types of morphogenetic patters of chondrichthyan polyodontocomplex scales. (**a**, **b**) *Mongolepis*-type of development in (**a**) *Mongolepis rozmanae* and (**b**) *Shiqianolepis hollandi* scales from the Upper Llandovery–Lower Wenlock (Silurian) Chargat Formation of north-western Mongolia and the Xiushan Formation of Guizhou Province (south China), respectively. (**a**) BU5299 in crown view and (**b**) NIGP 130311 in longitudinal section. (**c**, **d**) *Ctenacanthus*-type of development in *Goodrichthys* scale from the Visean (Mississippian) of Scotland. (**c**) BMNH P.20142a in anterior view and (**d**) longitudinally sliced. (**e**, **f**) *Ohiolepis*-type of development in *Canonlepis* scales from the Sandbian (Upper Ordovician) Harding Sandstone of Colorado, USA. (**e**) BU5265 in crown view and (**f**) longitudinally sectioned BU5267. (**g**, **h**) *Altholepis*-type of development in *Tezakia* scales from the Sandbian (Upper Ordovician) Winnipeg Formation (Shell Pine Unit No. 1) of Montana, USA and the Harding Sandstone of Colorado, USA. (**g**) BU5338 in crown view and (**h**) longitudinally sliced BU5327. SEM micrographs (a, e, g), Nomarski differential interference contrast micrographs (b, f), Volume renderings (c, d, h). Crosses mark primordial odontodes. Anterior to the left in (d, f, h), to the right in (b) and towards the bottom in (a, e, g). Scale bar equals 500 µm in (a) 200 µm in (b, g) and 100 µm in (c– f, h).

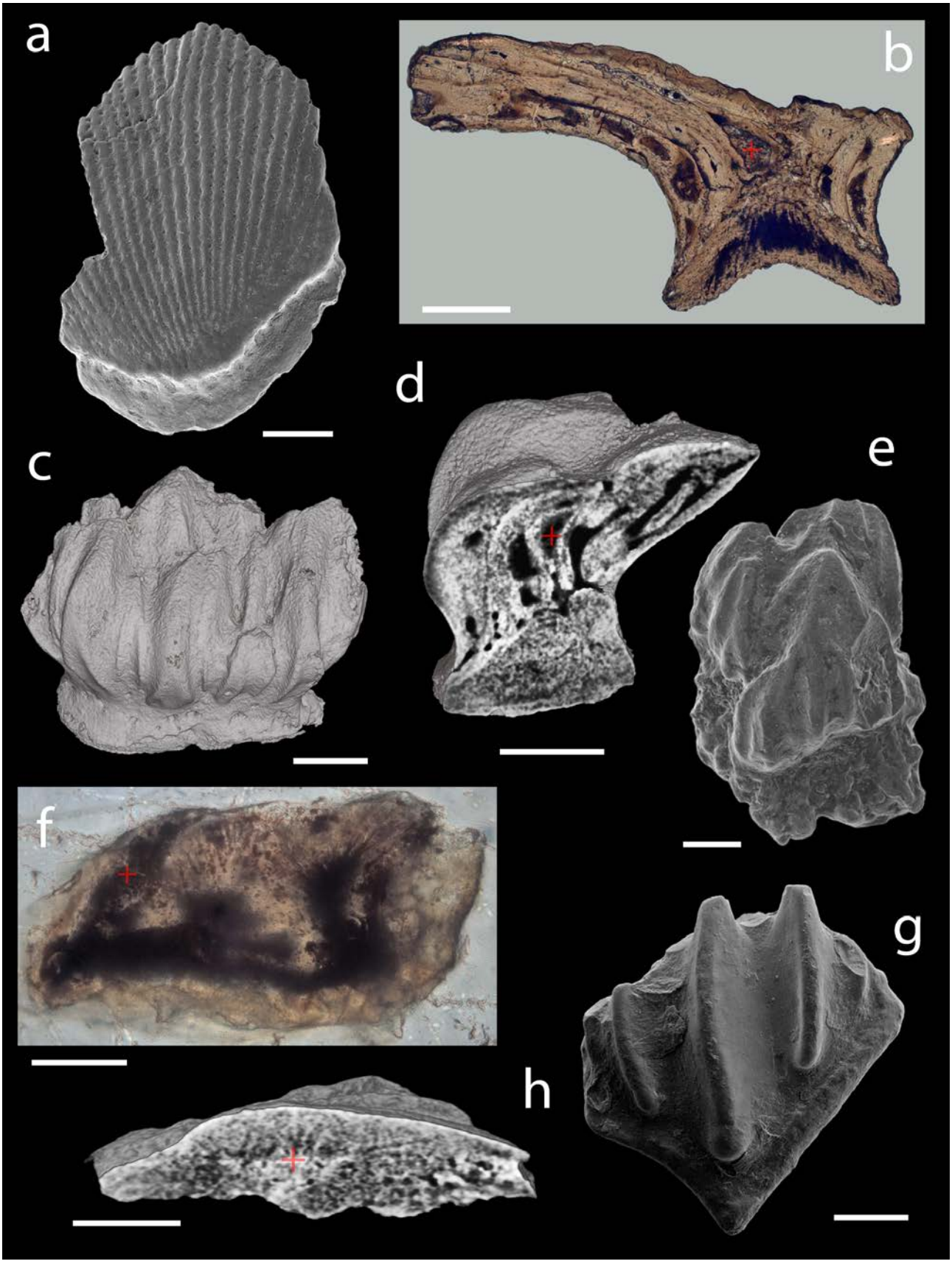
a
b
c
d
e
f
g
h

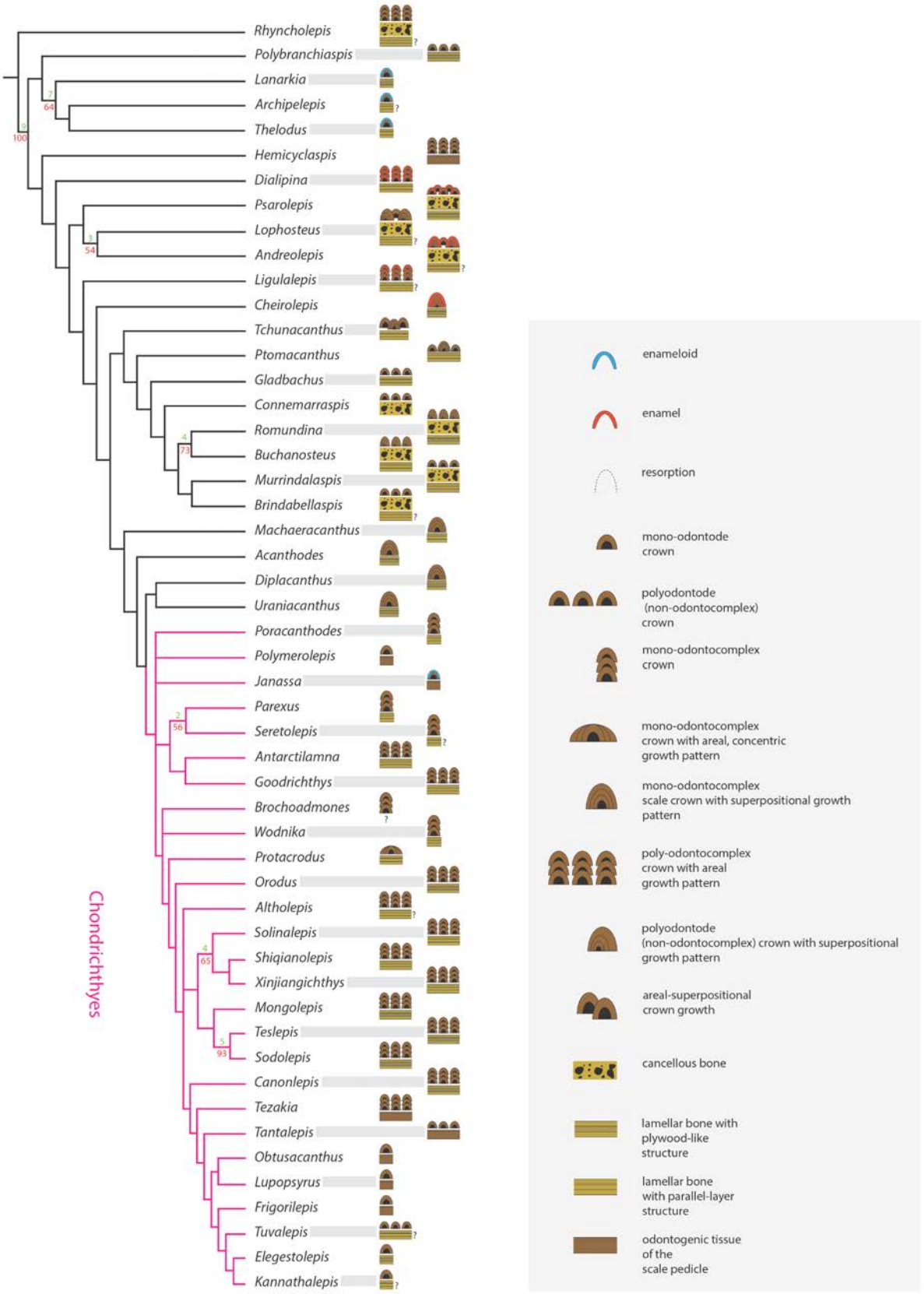

Figure 27. Majority-rule consensus (tree length 597 steps) of 51 most parsimonious trees from phylogenetic analysis I and diagrammatic representation of scale characteristics of Palaeozoic gnathostomes. Green and red numbers indicate Bremer support and bootstrap values, respectively.

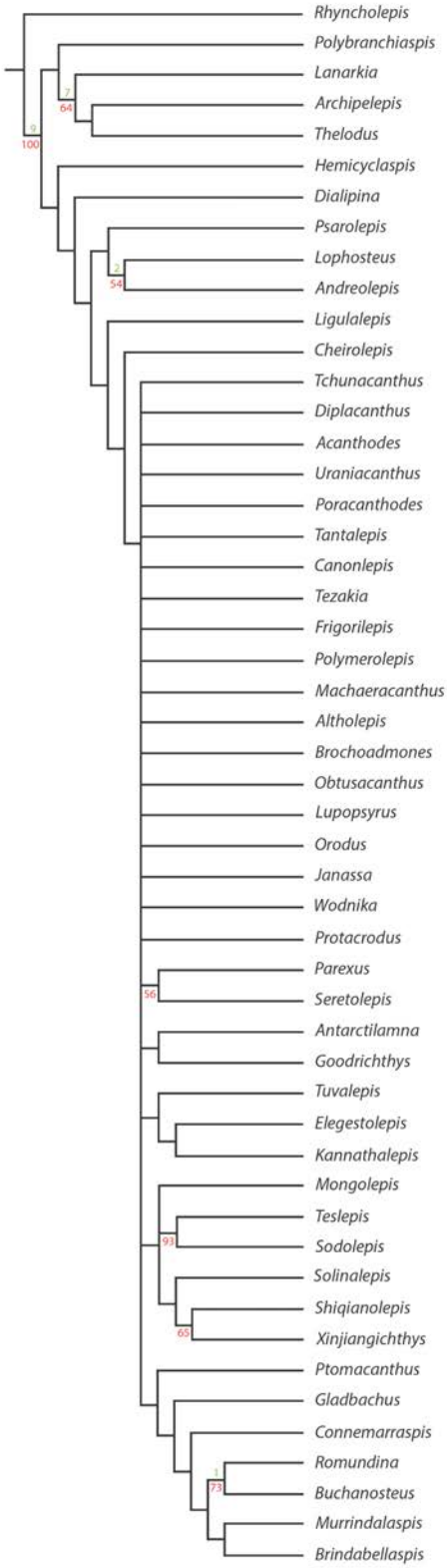

Figure 28. Strict consensus (tree length 735 steps) of 51 most parsimonious trees fro m phylogenetic analysis I. Green and red numbers represent Bremer support and bootstrap values, respectively.

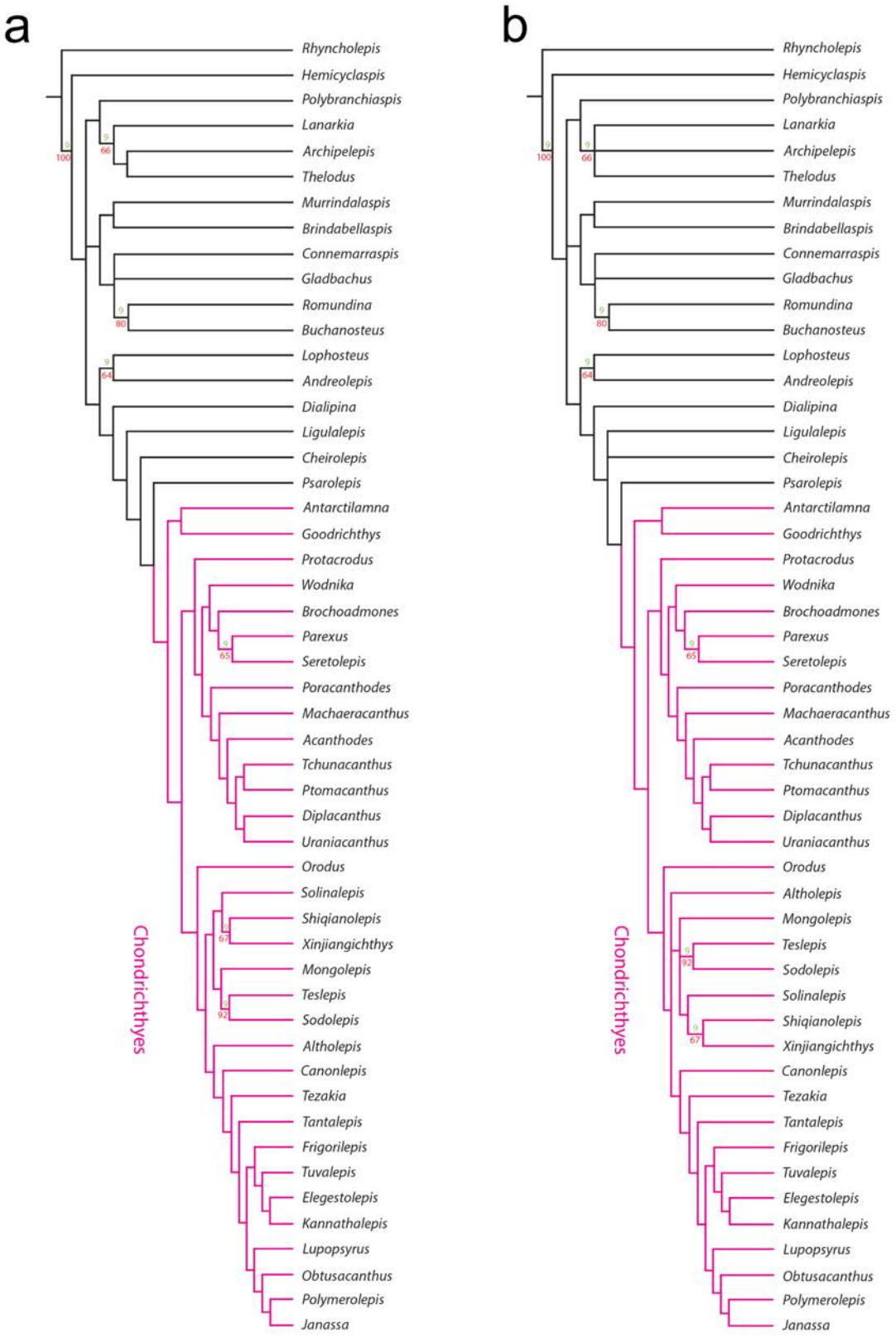

Figure 29. Results of phylogenetic analysis II. (**a**) Majority-rule consensus (tree length 654 steps) of 22 most parsimonious trees. (**b**) Strict consensus (tree length 661 steps) of 22 most parsimonious trees. Green and red numbers represent Bremer support and bootstrap values, respectively.

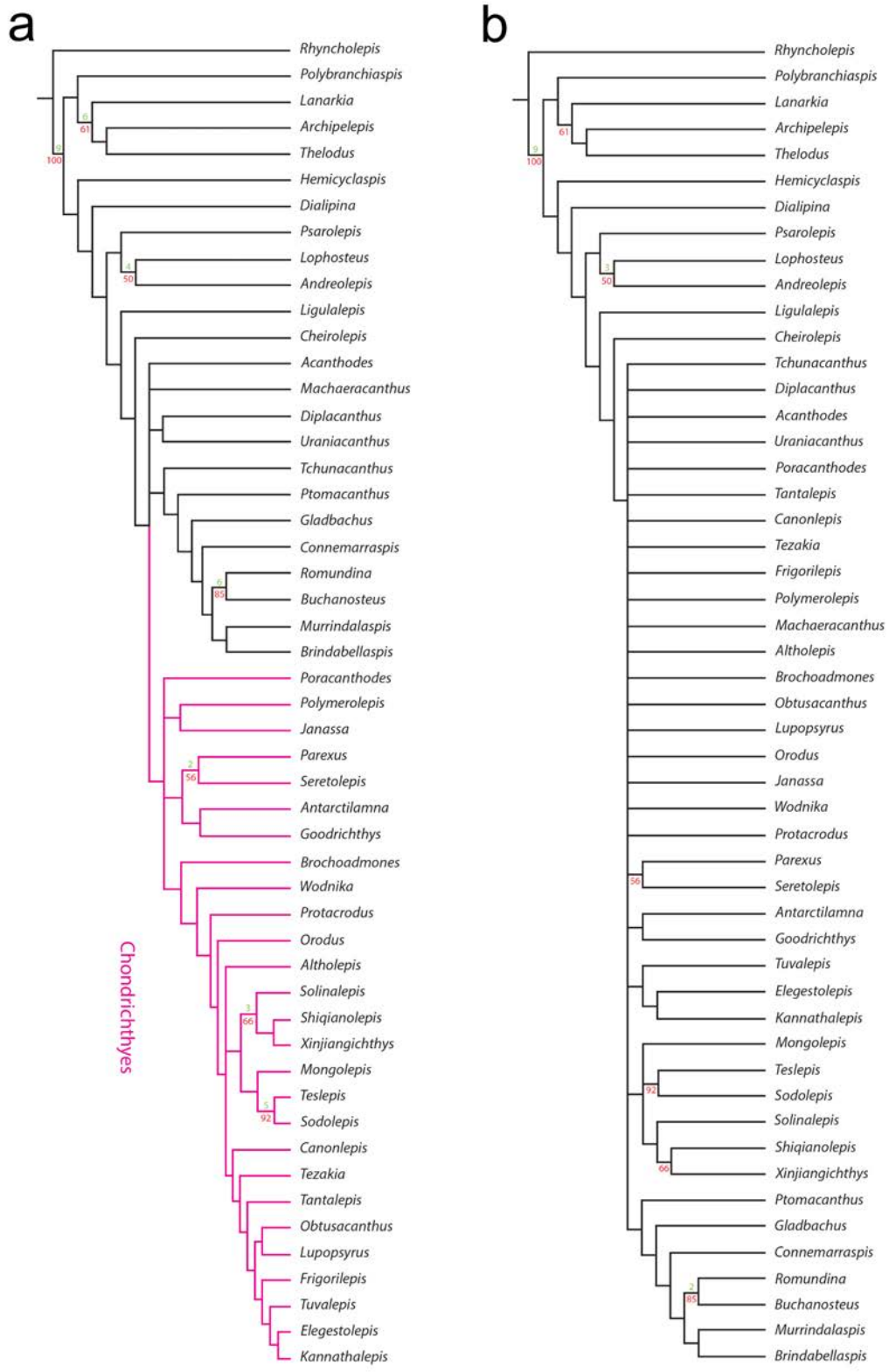

Figure 30. Results of phylogenetic analysis III. (**a**) Majority-rule consensus (tree length 622 steps) of 112 most parsimonious trees. (**b**) Strict consensus (tree length 757 steps) of 112 most parsimonious trees. Green and red numbers represent Bremer support and bootstrap values, respectively.

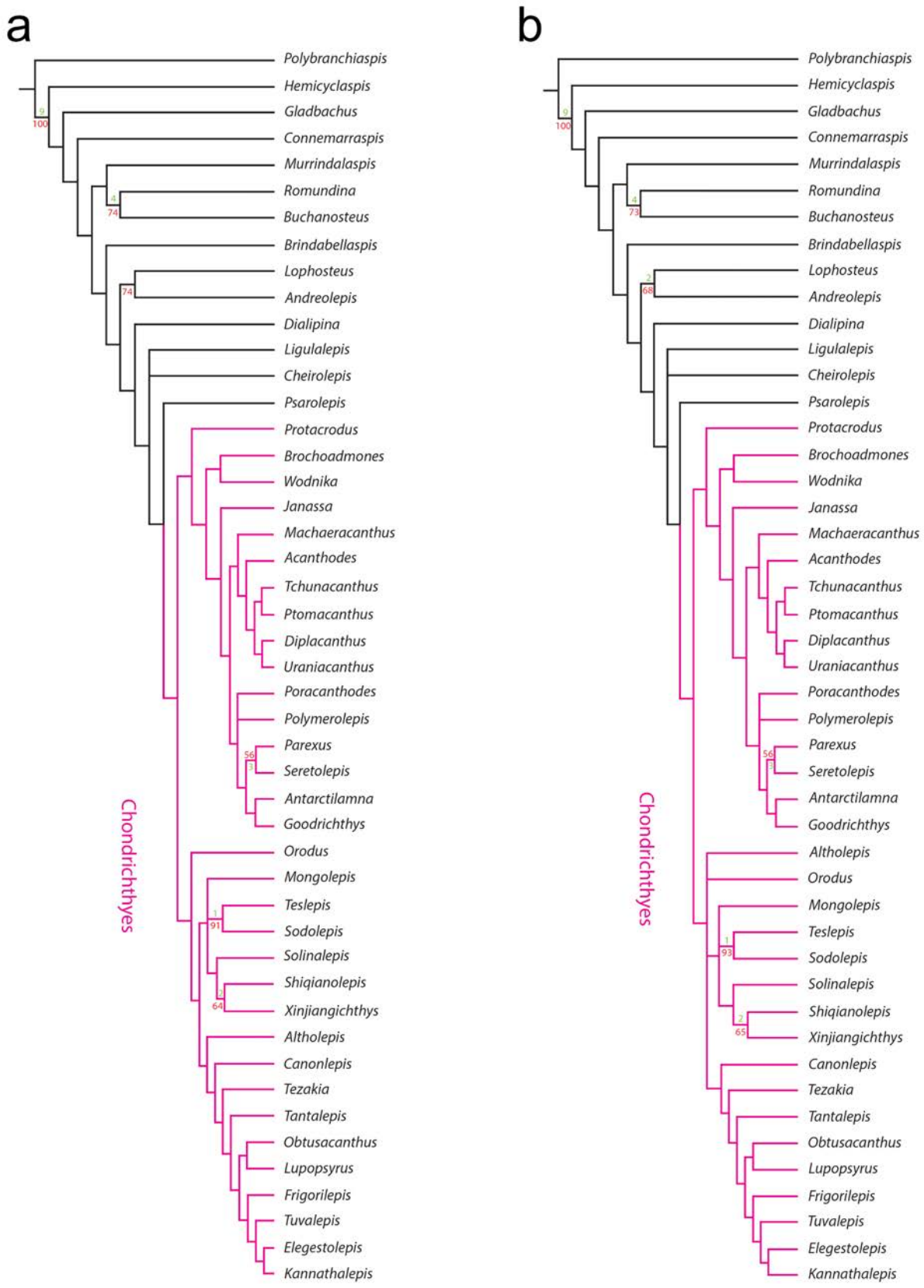

Figure 31. Results of phylogenetic analysis IV. (**a**) Majority-rule consensus (tree length 533 steps) of 16 most parsimonious trees. (**b**) Strict consensus (tree length 537 steps) of 16 most parsimonious trees. Green and red numbers represent Bremer support and bootstrap values, respectively.

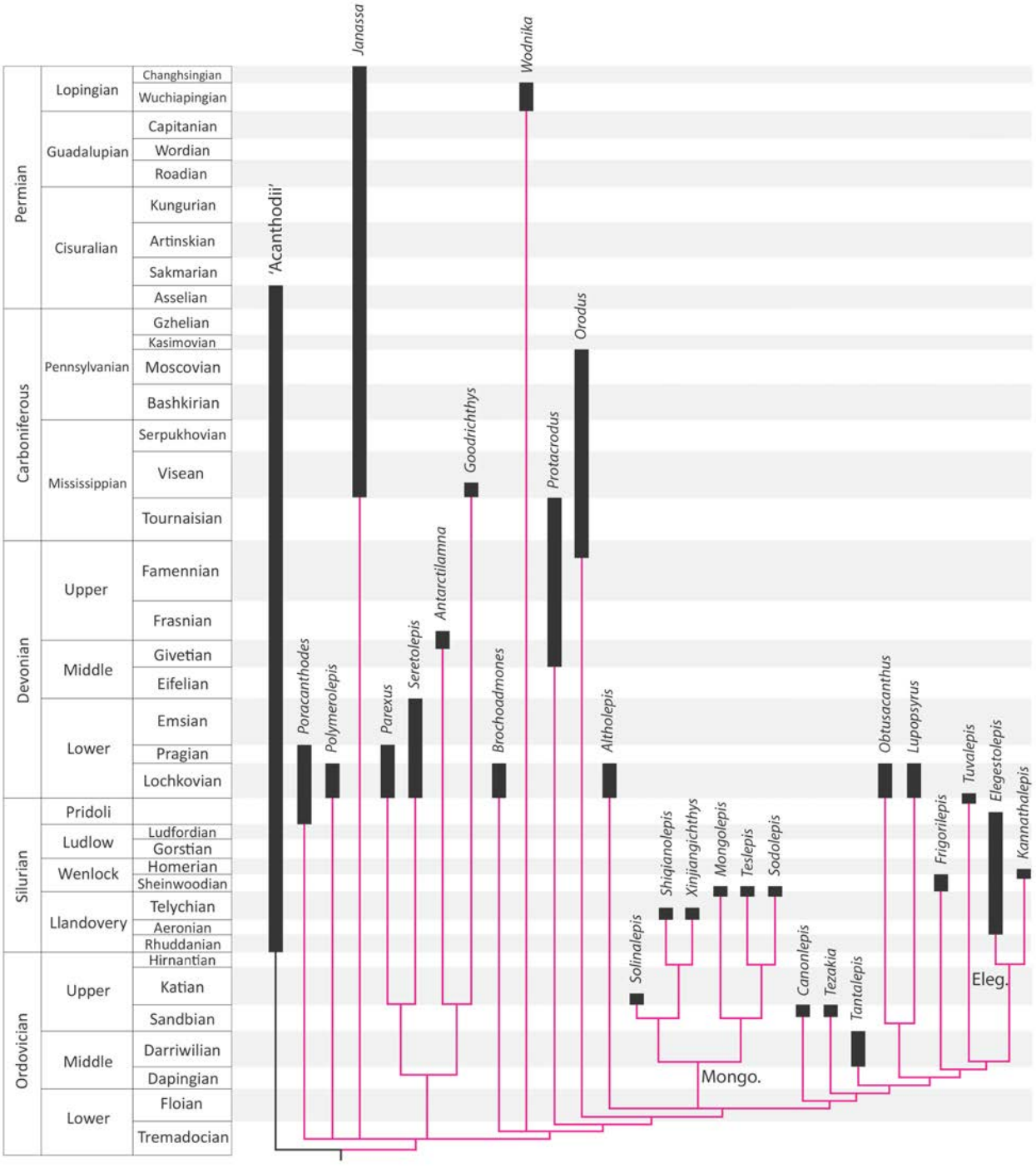

Figure 32. Stratigraphic ranges and inter-relationships of chondrichthyan taxa (in pink) recovered in MPT of phylogenetic analysis I.

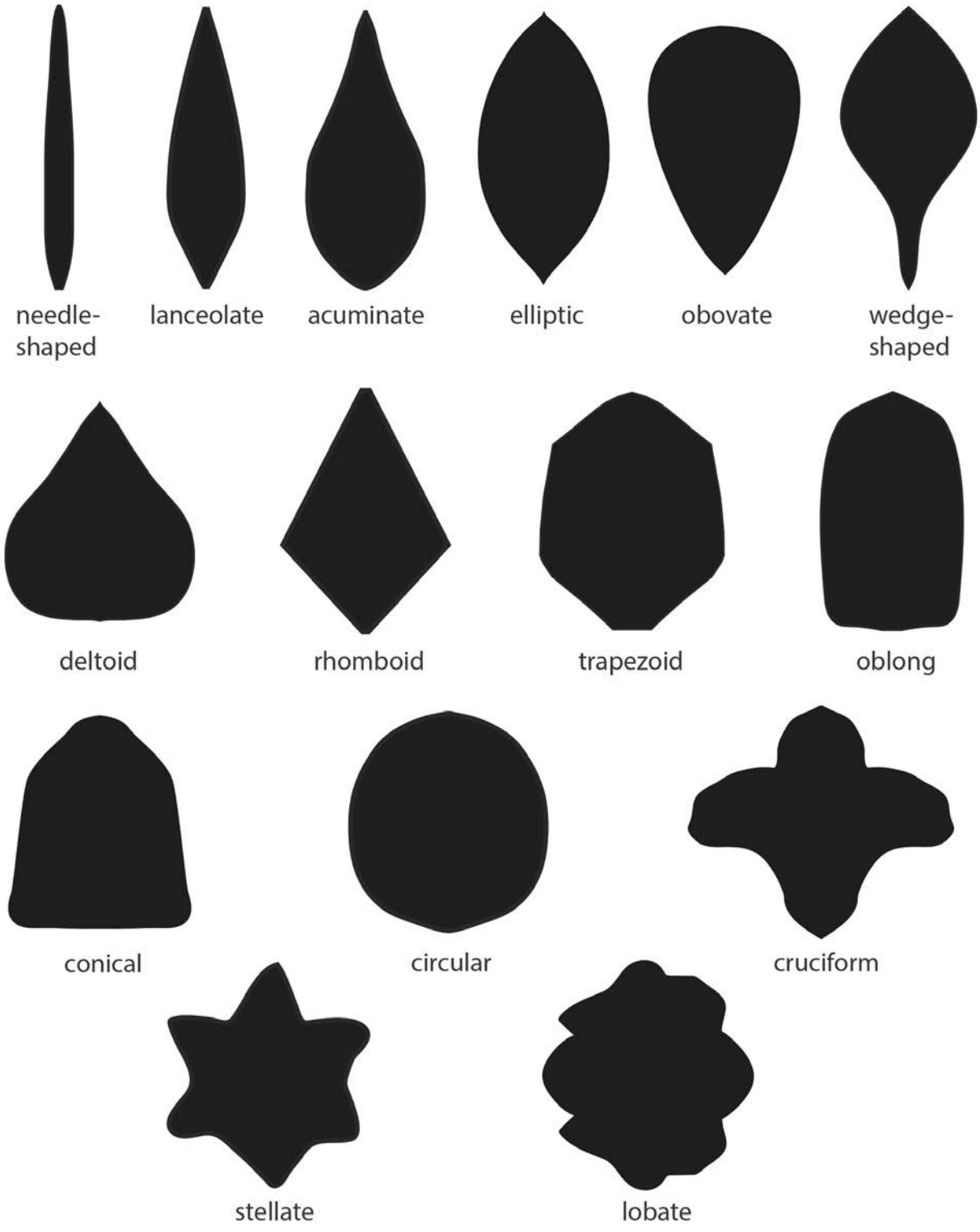

Figure 33. Diagrammatic representation of odontode, crown and base shapes of the taxa included in the phylogenetic analyses.

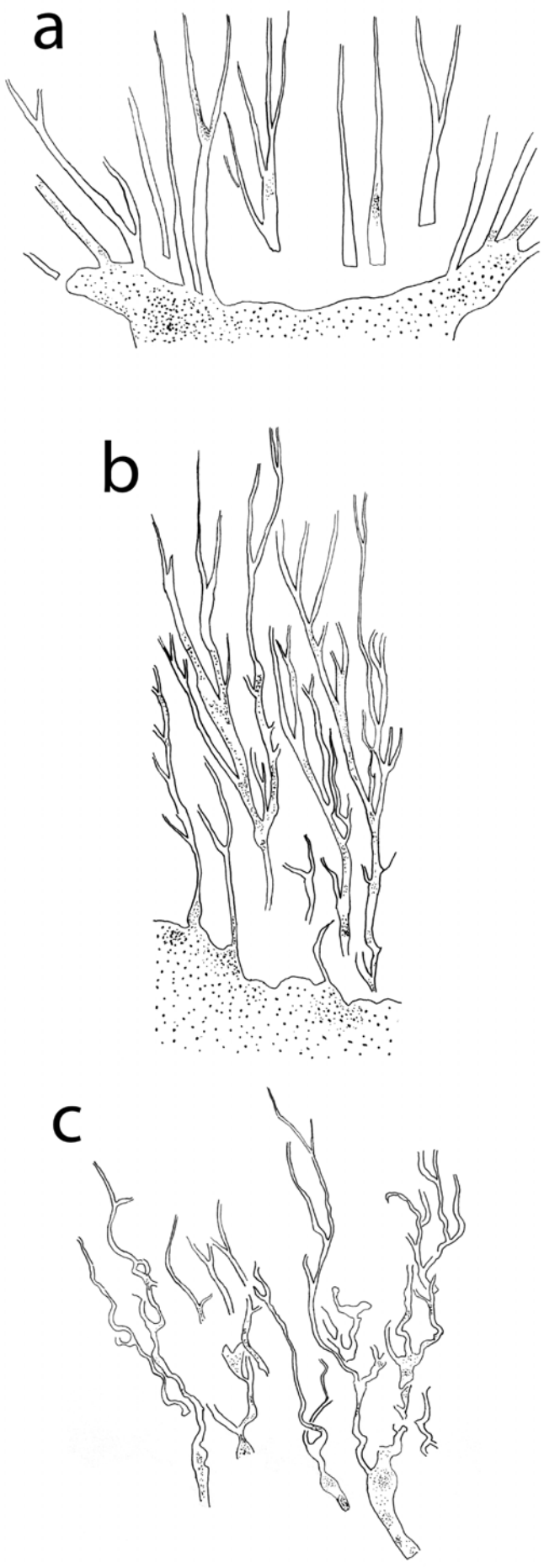

Figure 34. Types of dentine tubules in respect to their appearance proximally. Line drawings. (**a**) straight tubules (dermoskeletal dentine of the pteraspidomorph genus *Eriptychius* BU5294 from the Upper Llandovery–Lower Wenlock Chargat Formation of north-western Mongolia), (**b**) sinuous tubules (scale dentine of the extant neoselachian species *Raja montagui* BU5302) and (**c**) coiled tubules (scale dentine of the chondrichthyan genus *Tezakia* BU5340 from the Sandbian (Upper Ordovician) Winnipeg Formation (Shell Pine Unit No. 1) of Montana, USA.

Chapter 7: Conclusions

A comparison of scale characteristics of lower Palaeozoic taxa (*Tantalepis*, altholepids, *Canonlepis*, elegestolepids, mongolepids, *Tuvalepis*, *Polymerolepis* and *Seretolepis*) to those of established chondrichthyans and other total group gnathostomes (anaspids, thelodonts, pteraspidomorphs, osteostracans, ‘placoderms’, ‘acanthodians’ and osteichthyans) has demonstrated their chondrichthyan affinities, which are supported by the performed phylogenetic analysis. Although this interpretation is in broad agreement with previous work (e.g. Karatajūtė-Talimaa et al. 1990; Karatajūtė-Talimaa and Novitskaya 1992, 1997; Sansom et al. 1996, 2000, 2001, 2012), the present investigation allows for the first time the identification of characters common to the diverse scale types documented within the Chondrichthyes. These constitute synapomorphies of the chondrichthyan dermal skeleton (lack of superpositional scale-crown growth, cancellous bone, enamel and mineralized-tissue resorption) that in conjunction with other characters (scale morphology, odontode patterning and vascularisation) serve to differentiate the Class among gnathostomes. The additional features specify an orderly arrangement of odontodes in compound (polyodontode) crowns of trunk scales, which in chondrichthyans can be linear or concentric, symmetrical body scales and presence of neck canal openings in mono-odontode scales with growing crowns.

Contrary to previous work (Karatajūtė-Talimaa 1995; Hanke and Wilson 2010; Davis et al. 2012), the chondrichthyan taxa from the l149ower Palaeozoic are recovered as derived members of the crown group. This implies the presence of significant ghost lineages within the Chondrichthyes, and their

systematic position relative to other taxa within the clade needs further corroboration with additional data from as yet unrecovered articulated specimens.

Genera historically placed inside the ‘Acanthodii’ whose polyodontode scales exhibit characters apomorphic for jawed gnathostomes (*Parexus*, *Lupopsyrus*, *Poracanthodes* and *Brochoadmones*) are recognised here to be chondrichthyan and were recovered as such in all calculated trees. The favoured interpretation of the phylogenetic data places acanthodian-grade taxa (*Machaeracanthus, Diplacanthus*, *Uraniacanthus* and *Acanthodes*) with exclusively superpositional pattern of scale crown growth in a sister group subtending the chondrichthyan node, in conflict with some recent classification schemes of lower vertebrates (Johanson 2002; Janvier 2007; Davis et al. 2012), but supported by the phylogenies of Zhu et al. (2013) and Dupret et al. (2014).

Contra Karatajūtė-Talimaa (1992) and Reif (1978), only the crown characteristics of chondrichthyan scales were found to be phylogenetically informative at high taxonomic levels (above Family) and these define the morphogenetic scale types established here. In a conceptual shift from Karatajūtė-Talimaa (1992), growth is a feature of all polyodontode scale crowns (through addition of odontodes) and is also seen to occur in single odontode scales (through odontode elongation). A greater number than previously acknowledged (Karatajūtė-Talimaa 1992; Reif 1978) types of mono-odontode scale morphogenesis (the *Elegestolepis*, *Polymerolepis*, *Lupopsyrus* and *Heterodontus* types) were differentiated on the basis of developmental, histological or canal system criteria, whereas odontode pattering was found to be the primary discriminator between the morphogenetic types recognised in polyodontode scales (with the exception of the *Mongelepis*-type). The

phylogenetic data show that monophyletic chondrichthyan groups can possess a consistent scale morphogenetic signature (e.g. in Mongolepidida, Elegestolepida and a clade uniting *Lupopsyrus* and *Obtusacanthus*), with a tendency of wider systematic distribution of scale developmental patterns among geologically younger taxa (e.g. the *Ctenacanthus*-type in Antarctilamniformes and Cladoselachiformes and the *Heterodontus*-type in Hybodontiformes and Neoselachii).

These observations suggest rapid rates of evolution of the chondrichthyan integumentary skeleton during the Upper Ordovician–Lower Devonian interval (equated with major episodes of phylogenetic radiation), which generated diverse patterns of scale morphogenesis. This mid-Palaeozoic diversification episode is succeeded by progressive loss of scale-type diversity through the upper Palaeozoic and the lower Mesozoic.

References

ALLARD, B., MAGLOIRE, H., COUBLE, M. L., MAURIN, J. C. and BLEICHER, F. 2006. Voltage-gated sodium channels confer excitability to human odontoblasts. *Journal of Biological Chemistry*, **281**, 29002-29010.

ANDREEV, P. S. and CUNY, G. 2012. New Triassic stem selachimorphs (Chondrichthyes, Elasmobranchii) and their bearing on the evolution of dental enameloid in Neoselachii. *Journal of Vertebrate Paleontology*, **32**, 255-266.

ARRATIA, G. 2009. Identifying patterns of diversity of the actinopterygian fulcra. *Acta Zoologica*, **90**, 220-235.

ARRATIA, G. and CLOUTIER, R. 1996. Reassessment of the morphology of *Cheirolepis canadensis* (Actinopterygii). 165-197. *In* SCHULTZE, H.-P. and CLOUTIER, R. (eds). *Devonian Fishes and Plants of Miguasha, Quebec, Canada*. Verlag Dr. Friedrich Pfeil, Munich.

BASDEN, A. M, BURROW, C., HOCKING, M., PARKES, R. and YOUNG, G. 2000. Siluro-Devonian microvertebrates from south-eastern Australia. 201-222. *In* BLIECK, A. and TURNER, S. (eds). Courier Forschungsinstitut Senckenberg, *Palaeozoic Vertebrate Biochronology and Global Marine/Non-marine Correlation: Final Report of IGCP 328 (1991-1996)*. Senckenbergische Naturforschende Gesellschaft, Frankfurt a. M., pp. 575.

BASDEN, A. M. and YOUNG, G. C. 2001. A primitive actinopterygian neurocranium from the Early Devonian of southeastern Australia. *Journal of Vertebrate Paleontology*, **21**, 754-766.

BERNACSEK, G. M. and DINELEY, D. L. 1977. New acanthodians from the Delorme Formation (Lower Devonian) of NWT Canada. *Palaeontographica Abteilung A*, **158**, 1-25.

BEZNOSOV, P. 2009. A redescription of the Early Carboniferous acanthodian *Acanthodes lopatini* Rohon, 1889. *Acta Zoologica*, **90**, 183-193.

BLIECK, A. and TURNER, S. 2003. Global Ordovician vertebrate biogeography. *Palaeogeography, Palaeoclimatology, Palaeoecology*, **195**, 37-54.

BLOM, H., MÄRSS, T. and MILLER, C. G. 2002. Silurian and earliest Devonian birkeniid anaspids from the Northern Hemisphere. *Transactions of the Royal Society of Edinburgh-Earth Sciences*, **92**, 263-323.

BOTELLA, H., DONOGHUE, P. and MARTÍNEZ-PÉREZ, C. 2009. Enameloid microstructure in the oldest known chondrichthyan teeth. *Acta Zoologica*, **90**, 103-108.

BOTELLA, H., MARTÍNEZ-PÉREZ, C. and SOLER-GIJÓN, R. 2012. *Machaeracanthus goujeti* n. sp.(Acanthodii) from the Lower Devonian of Spain and northwest France, with special reference to spine histology. *Geodiversitas*, **34**, 761-783.

BRANDT, S. 1996. *Janassa korni* (Weigelt)—Neubeschreibung eines petalodonten Elasmobranchiers aus dem Kupferschiefer und Zechsteinkalk (Perm) von Eisleben (Sachsen-Anhalt). *Paläontologische Zeitschrift*, **70**, 505-520.

BRAZEAU, M. D. 2009. The braincase and jaws of a Devonian 'acanthodian' and modern gnathostome origins. *Nature*, **457**, 305-308.

BRAZEAU, M. D. 2011. Problematic character coding methods in morphology and their effects. *Biological Journal of the Linnean Society*, **104**, 489-498.

BRAZEAU, M. D. 2012. A revision of the anatomy of the Early Devonian jawed vertebrate *Ptomacanthus anglicus* Miles. *Palaeontology*, **55**, 355-367.

BRAZEAU, M. D. and FRIEDMAN, M. 2014. The characters of Palaeozoic jawed vertebrates. *Zoological Journal of the Linnean Society*, **170**, 779-821.

BURROW, C. J. 1994. Form and function in scales of *Ligulalepis toombsi* Schultze, a palaeoniscoid from the Early Devonian of Australia. *Records of the South Australian Museum*, **27**, 175-185.

BURROW, C. J. 1996. Placoderm scales from the Lower Devonian of New South Wales, Australia. *Modern Geology*, **20**, 351-370.

BURROW, C. J. and TURNER, S. 1998. Devonian placoderm scales from Australia. *Journal of Vertebrate Paleontology*, **18**, 677-695.

BURROW, C. J. and TURNER, S. 1999. A review of placoderm scales, and their significance in placoderm phylogeny. *Journal of Vertebrate Paleontology*, **19**, 204-219.

BURROW, C. J., TURNER, S. and WANG, S. 2000. Devonian microvertebrates from Longmenshan, China: Taxonomic assessment. 391-451. *In* BLIECK, A. and TURNER, S. (eds). *Palaeozoic Vertebrate Biochronology and Global Marine/ Non-marine Correlation: Final Report of IGCP 328 (1991-1996)*. Courier Forschungsinstitut Senckenberg **223**, Frankfurt a. M.

BURROW, C. J. 2003a. Earliest Devonian gnathostome microremains from central New South Wales (Australia). *Geodiversitas*, **25**, 273-288.

BURROW, C. J. 2003b. Poracanthodid acanthodian from the Upper Silurian (Pridoli) of Nevada. *Journal of Vertebrate Paleontology*, **23**, 489-493.

BURROW, C. J. 2003c. Redescription of the gnathostome fish fauna from the mid-Palaeozoic Silverband Formation, the Grampians, Victoria. *Alcheringa*, **27**, 37-49.

BURROW, C. J. 2006. Placoderm fauna from the Connemarra Formation (?late Lochkovian, Early Devonian), central New South Wales, Australia. *Alcheringa Special Issue*, **1**, 59-88.

BURROW, C. J., LONG, J. A. and TRINAJSTIC, K. 2009. Disarticulated acanthodian and chondrichthyan remains from the upper Middle Devonian Aztec Siltstone, southern Victoria Land, Antarctica. *Antarctic Science*, **21**, 71-88.

BURROW, C. J., DESBIENS, S., EKRT, B., SÜDKAMP, W., ELLIOTT, D., MAISEY, J., XIAOBO, Y. and DESUI, M. 2010a. A new look at *Machaeracanthus*. 59-84. *In* ELLIOTT, D. K., MAISEY, J. G., YU, X. and MIAO, D. (eds). *Morphology,*

Phylogeny and Paleobiogeography of Fossil Fishes. Verlag Dr. Friedrich Pfeil, Munich.

BURROW, C. J., TURNER, S. and YOUNG, G. C. 2010b. Middle Palaeozoic microvertebrate assemblages and biogeography of East Gondwana (Australasia, Antarctica). *Palaeoworld*, **19**, 37-54.

BURROW, C. J. and TURNER, S. 2012. Fossil fish taphonomy and the contribution of microfossils in documenting Devonian vertebrate history. 189-223. *In* A., T. J. (ed.) *Earth and Life*. Springer.

BURROW, C. J. and TURNER, S. 2013. Scale structure of putative chondrichthyan *Gladbachus adentatus* Heidtke & Krätschmer, 2001 from the Middle Devonian Rheinisches Schiefergebirge, Germany. *Historical Biology*, **25**, 385-390.

BURROW, C. J., NEWMAN, M. J., DAVIDSON, R. G. and DEN BLAAUWEN, J. L. 2013. Redescription of *Parexus recurvus*, an Early Devonian acanthodian from the Midland Valley of Scotland. *Alcheringa: An Australasian Journal of Palaeontology*, **37**, 392-414.

CAPPETTA, H. 1987. Handbook of Paleoichthyology, Volume 3B. *Chondrichthyes II: Mesozoic and Cenozoic Elasmobranchii*. Verlag Dr. Friedrich Pfeil, Munich, 193 pp.

CAPPETTA, H. 2012. Handbook of Paleoichthyology, Volume 3E. *Chondrichthyes. Mesozoic and Cenozoic Elasmobranchii: Teeth*. Verlag Dr. Friedrich Pfeil, Munich, 512 pp.

CHEN, D., JANVIER, P., AHLBERG, P. E. and BLOM, H. 2012. Scale morphology and squamation of the Late Silurian osteichthyan *Andreolepis* from Gotland, Sweden. *Historical Biology*, **24**, 411-423.

CICIMURRI, D. and FAHRENBACH, M. 2002. Chondrichthyes from the upper part of the Minnelusa Formation (Middle Pennsylvanian: Desmoinesian), Meade

County, South Dakota. *Proceedings of the South Dakota Academy of Science*, **81**, 81-92.

COATES, M. and SEQUEIRA, S. 2001. A new stethacanthid chondrichthyan from the Lower Carboniferous of Bearsden, Scotland. *Journal of Vertebrate Paleontology*, **21**, 438-459.

COMPAGNO, L. J. 1988. *Sharks of the order Carcharhiniformes*. Princeton University Press Princeton, New Jersey, 486 pp.

DAVIS, S. P., FINARELLI, J. A. and COATES, M. I. 2012. *Acanthodes* and shark-like conditions in the last common ancestor of modern gnathostomes. *Nature*, **486**, 247-250.

DEAN, B. 1909. Studies on fossil fishes (sharks, chimaeroids and arthrodires). *Memoirs of the American Museum of Natural History*, **9**, 211-248.

DENISON, R. H. 1952. Early Devonian fishes from Utah. I. Osteostraci. *Fieldiana: Geology*, **11**, 265-287.

DENISON, R. H. 1953. Early Devonian fishes from Utah: part II - Heterostraci. *Fieldiana: Geology*, **11**, 291–355.

DENISON, R. H. 1967. Ordovician vertebrates from western United States. *Fieldiana: Geology*, **16**, 131-192.

DENISON, R. H. 1978. *Placodermi*. Gustav Fischer Verlag, Stuttgart, New York, 128 pp.

DENISON, R. H. 1979. Handbook of Paleoichthyology. *Acanthodii*. Gustav Fischer Verlag, Stuttgart, New York, 62 pp.

DERYCKE, C., BLIECK. A. and TURNER, S. 1995 Vertebrate microfauna from the Devonian/Carboniferous boundary stratotype at La Serre, Montagne Noire (Hérault, France). *Bulletin du Museum national d'Histoire naturelle, Serie*, **4**, 461-85.

DERYCKE, C. and CHANCOGNE-WEBER, C. 1995. Histological discovery on acanthodian scales from the Famennian of Belgium. *Geobios*, **28**, 31-34.

DICK, J. R. 1978. On the Carboniferous shark *Tristychius arcuatus* Agassiz from Scotland. *Transactions of the Royal Society of Edinburgh*, **70**, 63-108.

DICK, J. R. 1981. *Diplodoselache woodi* gen. et sp. nov., an early Carboniferous shark from the Midland Valley of Scotland. *Transactions of the Royal Society of Edinburgh: Earth Sciences*, **72**, 99-113.

DICK, J. R. and MAISEY, J. 1980. The Scottish Lower Carboniferous shark *Onychoselache traquairi*. *Palaeontology*, **23**, 363-374.

DONG, X. P., DONOGHUE, P. C. and REPETSKI, J. E. 2005. Basal tissue structure in the earliest euconodonts: Testing hypotheses of developmental plasticity in euconodont phylogeny. *Palaeontology*, **48**, 411-421.

DONOGHUE, P. C. J. 1998. Growth and patterning in the conodont skeleton. *Philosophical Transactions of the Royal Society B: Biological Sciences*, **353**, 633–666.

DONOGHUE, P. C. J. 2002. Evolution of development of the vertebrate dermal and oral skeletons: unraveling concepts, regulatory theories, and homologies. *Paleobiology*, **28**, 474-507.

DONOGHUE, P. C. J. and SANSOM, I. J. 2002. Origin and early evolution of vertebrate skeletonization. *Microscopy Research and Technique*, **59**, 352-372.

DONOGHUE, P. C. J., SANSOM, I. J. and DOWNS, J. P. 2006. Early evolution of vertebrate skeletal tissues and cellular interactions, and the canalization of skeletal development. *Journal of Experimental Zoology Part B: Molecular and Developmental Evolution*, **306**, 278-294.

DOWNS, J. P. and DONOGHUE, P. C. 2009. Skeletal histology of *Bothriolepis canadensis* (Placodermi, Antiarchi) and evolution of the skeleton at the origin of jawed vertebrates. *Journal of Morphology*, **270**, 1364-1380.

DUFFIN, C. and WARD, D. 1993. The Early Jurassic Palaeospinacid sharks of Lyme Regis, southern England. *Professional Paper of the Belgian Geological Survey, Elasmobranches et stratigraphie*, **264**, 53-102.

DUPRET, V., SANCHEZ, S., GOUJET, D., TAFFOREAU, P. and AHLBERG, P. E. 2014. A primitive placoderm sheds light on the origin of the jawed vertebrate face. *Nature*, **507**, 500-503.

EAMES, B. F., ALLEN, N., YOUNG, J., KAPLAN, A., HELMS, J. A. and SCHNEIDER, R. A. 2007. Skeletogenesis in the swell shark *Cephaloscyllium ventriosum*. *Journal of Anatomy*, **210**, 542-554.

FISCHER, J., SCHNEIDER, J. W. and RONCHI, A. 2010. New hybondontoid shark from the Permocarboniferous (Gzhelian-Asselian) of Guardia Pisano (Sardinia, Italy). *Acta Palaeontologica Polonica*, **55**, 241-264.

FOREY, P. L., YOUNG, V. and MCCLURE, H. 1992. Lower Devonian fishes from Saudi Arabia. *Bulletin of the British Museum, Natural History. Geology*, **48**, 25-43.

FOREY, P. L. and KITCHING, I. 2000. Experiments in coding multistate characters. 54-80. *In* SCOTLAND, R. and PENNINGTON, R. T. (eds). Systematics Association Special Volume, *Homology and Systematics: Coding Characters for Phylogenetic Analysis*. CRC Press.

FRASER, G. J., CERNY, R., SOUKUP, V., BRONNER-FRASER, M. and STREELMAN, J. T. 2010. The odontode explosion: The origin of tooth-like structures in vertebrates. *Bioessays*, **32**, 808-817.

FRIEDMAN, M. and BRAZEAU, M. D. 2010. A reappraisal of the origin and basal radiation of the Osteichthyes. *Journal of Vertebrate Paleontology*, **30**, 36-56.

GAGNIER, P.-Y. 1996. Acanthodii. 149-164. *In* SCHULTZE, H.-P. and CLOUTIER, R. (eds). *Devonian Fishes and Plants of Miguasha, Quebec, Canada*. Verlag Dr. Freidrich Pfeil, Munich

GAGNIER, P.-Y. and WILSON, M. V. 1996. Early Devonian acanthodians from northern Canada. *Palaeontology*, **39**, 241-258.

GEMBALLA, S. and BARTSCH, P. 2002. Architecture of the integument in lower teleostomes: Functional morphology and evolutionary implications. *Journal of Morphology*, **253**, 290-309.

GILES, S., RÜCKLIN, M. and DONOGHUE, P. C. 2013. Histology of "placoderm" dermal skeletons: Implications for the nature of the ancestral gnathostome. *Journal of Morphology*, **274**, 627-644.

GILLIS, J. A. and DONOGHUE, P. C. 2007. The homology and phylogeny of chondrichthyan tooth enameloid. *Journal of Morphology*, **268**, 33-49.

GINTER, M. 2004. Devonian sharks and the origin of Xenacanthiformes. 473-486. *In* ARRATIA, G., WILSON, M. V. H. and CLOUTIER, R. (eds). *Recent Advances in the Origin and Early Radiation of Vertebrates*. Verlag Friedrich Pfeil, Munich.
GINTER, M. 2009. The dentition of *Goodrichthys*, a Carboniferous ctenacanthiform shark from Scotland. *Acta Zoologica*, **90**, 152-158.

GINTER, M. 2009. The dentition of *Goodrichthys*, a Carboniferous ctenacanthiform shark from Scotland. *Acta Zoologica*, **90**, 152-158.

GINTER, M. and SUN, Y. 2007. Chondrichthyan remains from the Lower Carboniferous of Muhua, southern China. *Acta Palaeontologica Polonica*, **52**, 705-727.

GINTER, M., HAMPE, O. and DUFFIN, C. J. 2010. Handbook of Paleoichthyology. *Chondrichthyes: Paleozoic Elasmobranchii: Teeth*. Verlag Dr. Friendrich Pfeil, Munich, 168 pp.

GOLOBOFF, P. A., FARRIS, J. S. and NIXON, K. C. 2008. TNT, a free program for phylogenetic analysis. *Cladistics*, **24**, 774-786.

GOUJET, D. and YOUNG, G. C. 2004. Placoderm anatomy and phylogeny: new insights. 109-126. *In* ARRATIA, G., WILSON, M. V. H. and CLOUTIER, R. (eds). *Recent Advances in the Origin and Early Radiation of Vertebrates*. Verlag Dr. Friedrich Pfeil, Munich.

GROGAN, E. D. and LUND, R. 2008. A basal elasmobranch, *Thrinacoselache gracia* n. gen and sp., (Thrinacodontidae, new family) from the Bear Gulch Limestone, Serpukhovian of Montana, USA. *Journal of Vertebrate Paleontology*, **28**, 970-988.

GROGAN, E. D. and LUND, R. 2009. Two new iniopterygians (Chondrichthyes) from the Mississippian (Serpukhovian) Bear Gulch Limestone of Montana with evidence of a new form of chondrichthyan neurocranium. *Acta Zoologica*, **90**, 134-151.

GROGAN, E. D., LUND, R. and GREENFEST-ALLEN, E. 2012. The Origin and Relationships of Early Chondrichthyans. 3-29. *In* CARRIER, J. C., MUSICK J. A., HEITHAUS M. R. (ed.) *Biology of Sharks and Their Relatives*. Taylor & Francis, New York.

GROSS, W. 1938. Das kopfskelett von *Cladodus wildungensis* Jaekel. 2. teil: der kieferbogen. anhang: *Protacrodus vetustus* Jaekel. *Senckenbergiana*, **20**, 123-145.

GROSS, W. 1947. Die Agnathen und Acanthodier des obersilurische Beyrichienkalks. *Palaeontographica A*, **96**, 91–158.

GROSS, W. 1953. Devonische Palaeonisciden-Reste in Mittel-und Osteuropa. *Paläontologische Zeitschrift*, **27**, 85-112.

GROSS, W. 1956. Über Crossopterygier und Dipnoer aus dem baltischen Oberdevon im Zusammenhang einer vergleichenden Untersuchung des Porenkanalsystems paläozoischer Agnathen und Fische. *Kungliga Svenska vetenskapsakademiens handlingar*, **5**, 1–140.

GROSS, W. 1961. Aufbau des Panzers obersilurischer Heterostraci und Osteostraci Norddeutschlands (Geschiebe) und Oesels. *Acta Zoologica*, **42**, 73-150.

GROSS, W. 1962. Neuuntersuchung der Stensioellida (Arthrodira, Unter- devon). *Notizblatt des Hessischen Landesamtes für Bodenforschung zu Wiesbaden*, **90**, 48–86.

GROSS, W. 1967. Über Thelodontier-Schuppen. *Palaeontographica Abteilung A*, **127**, 1-67.

GROSS, W. 1968. Fragliche Actinopterygier-Schuppen aus dem Silur Gotlands. *Lethaia*, **1**, 184-218.

GROSS, W. 1969. *Lophosteus superbus* Pander, ein Teleostome aus dem Silur Oesels. *Lethaia*, **2**, 15-47.

GROSS, W. 1971. *Lophosteus superbus* Pander: Zähne, Zahnknochen und besondere schuppenformen. *Lethaia*, **4**, 131-152.

GROSS, W. 1973. Kleinschuppen, Flossenstacheln und Zähne von Fischen aus europäischen und nordamerikanischen Bonebeds des Devons. *Palaeontographica Abteilung A*, **142**, 51-155.

GUINOT, G. and CAPPETTA, H. 2011. Enameloid microstructure of some Cretaceous Hexanchiformes and Synechodontiformes (Chondrichthyes, Neoselachii): new structures and systematic implications. *Microscopy Research and Technique*, **74**, 196-205.

HAMPE, O. 1997. Zur funktionellen Deutung des Dorsalstachels und der Placoidschuppen der Xenacanthida (Chondrichthyes: Elasmobranchii;

Unterperm). *Neues Jahrbuch für Geologie und Paläontologie, Abhandlungen*, **206**, 29-51.

HANKE, G. F. and WILSON, M. V. H. 2004. New teleostome fishes and acanthodian systematics. 189-216. *In* ARRATIA, G., WILSON, M. V. H. & R. CLOUTIER (ed.) *Recent Advances in the Origin and Early Radiation of Vertebrates*. Verlag Dr. Friedrich Pfeil, Munich.

HANKE, G. F. and WILSON, M. V. H. 2006. Anatomy of the Early Devonian acanthodian *Brochoadmones milesi* based on nearly complete body fossils, with comments on the evolution and development of paired fins. *Journal of Vertebrate Paleontology*, **26**, 526-537.

HANKE, G. F. and DAVIS, S. P. 2008. Redescription of the acanthodian *Gladiobranchus probaton* Bernacsek & Dineley, 1977, and comments on diplacanthid relationships. *Geodiversitas*, **30**, 303-330.

HANKE, G. F. and WILSON, M. V. H. 2010. The putative stem-group chondrichthyans *Kathemacanthus* and *Seretolepis* from the Lower Devonian MOTH locality, Mackenzie Mountains, Canada. 159-182. *In* D. K. ELLIOTT, J. G. M., X. YU & D. MIAO (ed.) *Morphology, Phylogeny and Paleobiogeography of Fossil Fishes.* Verlag Dr. Friedrich Pfiel, Munich.

HANKE, G. F. and DAVIS, S. P. 2012. A re-examination of *Lupopsyrus pygmaeus* Bernacsek & Dineley, 1977 (Pisces, Acanthodii). *Geodiversitas*, **34**, 469-487.

HANKE, G. F., WILSON, M. V. H. and SAURETTE, F. J. 2013. Partial articulated specimen of the Early Devonian putative chondrichthyan *Polymerolepis whitei* Karatajute-Talimaa, 1968, with an anal fin spine. *Geodiversitas*, **35**, 529-543.

HEIDTKE, U. H. 1993. Studien über *Acanthodes*. 4. *Acanthodes boyi* n. sp., die dritte Art der Acanthodier (Acanthodii: Pisces) aus dem Rotliegend (Unterperm) des

Saar-Nahe-Beckens (SW-Deutschland). *Paläontologische Zeitschrift*, **67**, 331-341.

HEIDTKE, U. H. 1996. *Acanthodes bourbonensis* n. sp., ein neuer Acanthodier (Acanthodii: Pisces) aus dem Autunium (Unterperm) von Bourbon l'Archambault (Allier, Frankreich). *Paläontologische Zeitschrift*, **70**, 497-504.

HEIDTKE, U. H. and KRÄTSCHMER, K. 2001. *Gladbachus adentatus* nov. gen. et sp., ein primitiver Hai aus dem Oberen Givetium (Oberes Mitteldevon) der Bergisch Gladbach-Paffrath-Mulde (Rheinisches Schiefergebirge). *Mainzer Geowissenschaftliche Mitteilungen*, **30**, 105-122.

HEMMINGS, S. K. 1978. Palaeontographical Society Monographs. *The old red sandstone antiarchs of Scotland: Pterichthyodes and Microbrachius*. Palaeontographical Society, 64 pp.

HUXLEY, T. H. 1880. On the application of the laws of evolution to the arrangement of the Vertebrata, and more particularly of the Mammalia. *Proceedings of the Zoological Society of London*, **43**, 649-662.

IVANOV, A. 1996. The Early Carboniferous chondrichthyans of the South Urals, Russia. *Geological Society, London, Special Publications*, **107**, 417-425.

IVANOV, A. 2005. Early Permian chondrichthyans of the middle and south Urals. *Revista Brasileira de Paleontologia*, **8**, 127-138.

IVANOV, A., CHEREPANOV, G. and LUSKEVICS, E. 1995. Ontogenetic development of antiarch dermal ossifications. *Geobios*, **28**, 97-102.

IVANOV, A., NESTELL, G. P. and NESTELL, M. K. 2013. Fish assemblage from the Capitanian (Middle Permian) of the Apache Mountains, West Texas, USA. *New Mexico Museum of Natural History and Science, Bulletin*, **60**, 152-160.

JANVIER, P. 2007. Living primitive fishes and fishes from deep time. 1-51. In MCKENZIE, D., FARRELL, A. and BRAUNER, C. (eds). *Fish Physiology*, *Volume 26*. Elsevier, New York.

JEPPSSON, L., FREDHOLM, D. and MATTIASSON, B. 1985. Acetic acid and phosphatic fossils—a warning. *Journal of Paleontology*, **59**, 952-956.

JEPPSSON, L. and ANEHUS, R. 1995. A buffered formic acid technique for conodont extraction. *Journal of Paleontology*, 790-794.

JOHANSON, Z. 2002. Vascularization of the osteostracan and antiarch (Placodermi) pectoral fin: similarities, and implications for placoderm relationships. *Lethaia*, **35**, 169-186.

JOHANSON, Z. and SMITH, M. M. 2003. Placoderm fishes, pharyngeal denticles, and the vertebrate dentition. *Journal of Morphology*, **257**, 289-307.

JOHANSON, Z., SMITH, M. M. and JOSS, J. M. P. 2007. Early scale development in *Heterodontus* (Heterodontiformes; Chondrichthyes): a novel chondrichthyan scale pattern. *Acta Zoologica*, **88**, 249-256.

JOHANSON, Z., TANAKA, M., CHAPLIN, N. and SMITH, M. 2008. Early Palaeozoic dentine and patterned scales in the embryonic catshark tail. *Biology Letters*, **4**, 87-90.

JOHNS, M. J., BARNES, C. R. and ORCHARD, M. J. 1997. Geological Survey of Canada Bulletin. *Taxonomy and Biostratigraphy of Middle and Late Triassic Elasmobranch Ichthyoliths from Northeastern British Columbia*. Geological Survey of Canada, 235 pp.

KARATAJŪTĖ-TALIMAA, V. 1968. New thelodonts, heterostracans and arthrodires from the Chortkov Stage of Podolia. 33–42. *In* OBRUCHEV, D. V. (ed.) *Sketches in Phylogenesis and Taxonomy of Fossil Fishes and Agnatha*. Nauka, Moscow (in Russian).

KARATAJŪTĖ-TALIMAA, V. 1973. *Elegestolepis grossi* gen. et sp. nov., ein neuer Typ der Placoidschuppe aus dem Oberen Silur der Tuwa. *Palaeontographica Abt. A*, **143**, 35–50.

KARATAJŪTĖ-TALIMAA, V. 1978. *Silurian and Devonian Thelodonts of the U.S.S.R. and Spitsbergen*. Mokslas, Vilnius, 334 pp. (in Russian).

KARATAJŪTĖ-TALIMAA, V. 1992. The early stages of the dermal skeleton formation in chondrichthyans. 223-231. *In* MARK-KURIK, E. (ed.) *Fossil Fishes as Living Animals*. Institute of Geology, Tallinn.

KARATAJŪTĖ-TALIMAA, V. 1995. The Mongolepidida: scale structure and systematic position. *Geobios*, **19**, 35-37.

KARATAJŪTĖ-TALIMAA, V. 1997. Chondrichthyan scales from Lochkovian (Lower Devonian) of Podolia (Ukraine). *Geologija*, **22**, 5-17.

KARATAJŪTĖ-TALIMAA, V. 1998. Determination methods for the exoskeletal remains of early vertebrates. *Mitteilungen ausdem Museum für Naturkunde in Berlin, Geowissenschaftliche Reihe*, **1**, 21-51.

KARATAJŪTĖ-TALIMAA, V., NOVITSKAYA, L., ROZMAN, K. S. and SODOV, Z. 1990. *Mongolepis*—a new lower Silurian genus of elasmobranchs from Mongolia. *Paleontologicheskii Zhurnal*, **1990**, 76-86 (in Russian).

KARATAJŪTĖ-TALIMAA, V. and NOVITSKAYA, L. 1992. *Teslepis*—a new representative of mongolepid elasmobranchs from the Lower Silurian of Mongolia. *Paleontologicheskii Zhurnal*, **4**, 36-46 (in Russian).

KARATAJŪTĖ-TALIMAA, V. and PREDTECHENSKYJ, N. 1995. The distribution of the vertebrates in the Late Ordovician and Early Silurian palaeobasins of the Siberian Platform. *Bulletin du Muséum National d'Histoire Naturelle*, **17**, 39-55.

KARATAJŪTĖ-TALIMAA, V. and NOVITSKAYA, L. 1997. *Sodolepis*—a new representative of Mongolepidida (Chondrichthyes?) from the Lower Silurian of Mongolia. *Paleontologicheskii Zhurnal*, **1997**, 96-103 (in Russian).

KARATAJŪTĖ-TALIMAA, V. and SMITH, M. M. 2003. Early acanthodians from the Lower Silurian of Asia. *Transactions of the Royal Society of Edinburgh: Earth Sciences*, **93**, 277-299.

KARATAJUTE-TALIMAA, V. and SMITH, M. M. 2004. *Tesakoviaspis concentrica*: microskeletal remains of a new order of vertebrate from the Upper Ordovician and Lower Silurian of Siberia. 53-64. *In* G. ARRATIA, M. V. H. W. R. C. (ed.) *Recent Advances in the Origin and Early Radiation of Vertebrates.* Verlag Dr. Friedrich Pfeil, Munich.

KARATAJŪTĖ-TALIMAA, V., SANSOM, I. J., ŽIGAITĖ, Z. and ANDREEV, P. S. in prep. An eriptychiid (Agnatha, Pteraspidomorpha) from the Silurian of Mongolia.

KERR, T. 1952. The scales of primitive living actinopterygians. *Proceedings of the Zoological Society of London*, **122**, 55-78.

KERR, T. 1955. The scales of modern lungfish. *Proceedings of the Zoological Society of London*, **125**, 335-345.

LELIÈVRE, H. and DERYCKE, C. 1998. Microremains of vertebrate near the devonian-carboniferous boundary of Southern China (Hunan province) and their biostratigraphical significance. *Revue de Micropaléontologie*, **41**, 297-320.

LINDE, A. 1989. Dentin matrix proteins: composition and possible functions in calcification. *The Anatomical Record*, **224**, 154-166.

LINDE, A. and LUNDGREN, T. 1995. From serum to the mineral phase. The role of the odontoblast in calcium transport and mineral formation. *International Journal of Developmental Biology*, **39**, 213-213.

LONG, J. A. 1984. New placoderm fishes from the Early Devonian Buchan Group, eastern Victoria. *Proceedings of the Royal Society of Victoria*, **96**, 173-186.

LUND, R. 1982. *Harpagofututor volsellorhinus* new genus and species (Chondrichthyes, Chondrenchelyiformes) from the Namurian Bear Gulch Limestone, *Chondrenchelys problematica* Traquair (Visean), and their sexual dimorphism. *Journal of Paleontology*, 938-958.

LUND, R. 1985. The morphology of *Falcatus falcatus* (St. John and Worthen), a Mississippian stethacanthid chondrichthyan from the Bear Gulch Limestone of Montana. *Journal of Vertebrate Paleontology*, **5**, 1-19.

LUND, R. 1986. On *Damocles serratus*, nov. gen. et sp.(Elasmobranchii: Cladodontida) from the Upper Mississippian Bear Gulch Limestone of Montana. *Journal of Vertebrate Paleontology*, **6**, 12-19.

LUND, R. and GROGAN, E. D. 1997. Relationships of the Chimaeriformes and the basal radiation of the Chondrichthyes. *Reviews in Fish Biology and Fisheries*, **7**, 65-123.

MADDISON, W. P. and MADDISON, D. R. 2011. Mesquite: a modular system for evolutionary analysis. Version 2.75 http://mesquiteproject.org.

MADER, H. 1986. Göttinger Arbeiten zur Geologie und Paläontogie. *Schuppen und Zähne von Acanthodiern und Elasmobranchiern aus dem Unter-Devon Spaniens (Pisces)*. Geologischen Institute der Georg-August-Universität Göttingen, Göttingen, 59 pp.

MAGLOIRE, H., COUBLE, M. L., ROMEAS, A. and BLEICHER, F. 2004. Odontoblast primary cilia: facts and hypotheses. *Cell Biology International*, **28**, 93-99.

MAGLOIRE, H., COUBLE, M. L., THIVICHON-PRINCE, B., MAURIN, J. C. and BLEICHER, F. 2009. Odontoblast: a mechano-sensory cell. *Journal of Experimental Zoology Part B: Molecular and Developmental Evolution*, **312**, 416-424.

MAISEY, J. G. 1984. Chondrichthyan phylogeny: a look at the evidence. *Journal of Vertebrate Paleontology*, **4**, 359-371.

MAISEY, J. G. 1986. Heads and tails: a chordate phylogeny. *Cladistics*, **2**, 201-256.

MAISEY, J. G. 1988. Phylogeny of early vertebrate skeletal induction and ossification patterns. 1-36. *In* MACINTYRE, R. and CLEGG, M. (eds). *Evolutionary Biology, Volume 22*. Springer,

MAISEY, J. G. 1989. *Hamiltonichthys mapesi,* g. & sp. nov.(Chondrichthyes, Elasmobranchii), from the Upper Pennsylvanian of Kansas. *American Museum Novitates*, **2931**, 1–42.

MAISEY, J., MILLER, R. and TURNER, S. 2009. The braincase of the chondrichthyan *Doliodus* from the Lower Devonian Campbellton formation of New Brunswick, Canada. *Acta Zoologica*, **90**, 109-122.

MALZAHN, E. 1968. Über neue Funde von *Janassa bituminosa* (Schloth.) im niederrheinischen Zechstein. *Geologisches Jahrbuch*, **85**, 67-96.

MANZANARES, E., PLA, C., MARTÍNEZ-PÉREZ, C., RASSKIN, D. and BOTELLA, H. in prep. The enameloid microstructure of Euselachian (Chondrichthyes) scales. *Paleontological Journal*.

MÄRSS, T. 1986. *Silurian vertebrates of Estonia and west Latvia*. Valgus, Tallinn, 104 pp. (in Russian).

MÄRSS, T. 2002. Silurian and Lower Devonian anaspids (Agnatha) from Severnaya Zemlya (Russia). *Geodiversitas*, **24**, 123-137.

MÄRSS, T. 2006. Exoskeletal ultrasculpture of early vertebrates. *Journal of Vertebrate Paleontology*, **26**, 235-252.

MÄRSS, T. 2011. A unique Late Silurian *Thelodus* squamation from Saaremaa (Estonia) and its ontogenetic development. *Estonian Journal of Earth Sciences*, **60**, 137–146.

MÄRSS, T. and RITCHIE, A. 1998. Articulated thelodonts (Agnatha) of Scotland. *Transactions of the Royal Society of Edinburgh: Earth Sciences*, **88**, 143-195.

MÄRSS, T. and GAGNIER, P. Y. 2001. A new chondrichthyan from the Wenlock, Lower Silurian, of Baillie-Hamilton Island, the Canadian Arctic. *Journal of Vertebrate Paleontology*, **21**, 693-701.

MÄRSS, T. and KARATAJŪTĖ-TALIMAA, V. 2002. Ordovician and Lower Silurian thelodonts from Severnaya Zemlya Archipelago (Russia). *Geodiversitas*, **24**, 381-404.

MÄRSS, T., WILSON, M. V. and THORSTEINSSON, R. 2002. New thelodont (Agnatha) and possible chondrichthyan (Gnathostomata) taxa established in the Silurian and Lower Devonian of the Canadian Arctic Archipelago. *Proceedings of the Estonian Academy of Sciences, Geology*, **51**, 88–120.

MÄRSS, T., WILSON, M. V. and THORSTEINSSON, R. 2006. Special Papers in Palaeontology, No 75. *Silurian and Lower Devonian thelodonts and putative chondrichthyans from the Canadian Arctic archipelago*. The Palaeontological Association 144 pp.

MÄRSS, T., KARATAJŪTĖ-TALIMAA, V. and TURNER, S. 2007. Handbook of Paleoichthyology. *Agnatha II. Thelodonti*. Verlag Dr. Friendrich Pfeil, Munich, 143 pp.

MARTÍNEZ-PÈREZ, C., DUPRET, V., MANZANARES, E. and BOTELLA, H. 2010. New data on the Lower Devonian chondrichthyan fauna from Celtiberia (Spain). *Journal of Vertebrate Paleontology*, **30**, 1622-1627.

MILES, R. S. 1968. Jaw articulation and suspension in *Acanthodes* and their significance. 109-127. *In* ØRVIG, T. (ed.) *Current Problems of Lower Vertebrate Phylogeny: Proceedings of the fourth Nobel Symposium. Academic Press,* Stockholm.

MILES, R. S. 1973. Articulated acanthodian fishes from the Old Red Sandstone of England, with a review of the structure and evolution of the acanthodian shoulder-girdle. *Bulletin of the British Museum (Natural History)*, **24**, 111-213.

MILLER, R. F., CLOUTIER, R. and TURNER, S. 2003. The oldest articulated chondrichthyan from the Early Devonian period. *Nature*, **425**, 501-504.

MIN, Z. and SCHULTZE, H.-P. 2001. Interrelationships of basal osteichthyans. 289–314. *In* AHLBERG, E. (ed.) *Major Events in Early Vertebrate Evolution*.

MIYAKE, T., VAGLIA, J. L., TAYLOR, L. H. and HALL, B. K. 1999. Development of dermal denticles in skates (Chondrichthyes, Batoidea): patterning and cellular differentiation. *Journal of Morphology*, **241**, 61-81.

MOTTA, P. 1977. Anatomy and functional morphology of dermal collagen fibers in sharks. *Copeia*, 454-464.

MOY-THOMAS, J. 1936. The structure and affinities of the fossil elasmobranch fishes from the Lower Carboniferous rocks of Glencartholm, Eskdale. *Proceedings of the Zoological Society of London*, **106**, 761-788.

MURDOCK, D. J., DONG, X.-P., REPETSKI, J. E., MARONE, F., STAMPANONI, M. and DONOGHUE, P. C. 2013. The origin of conodonts and of vertebrate mineralized skeletons. *Nature*, **502**, 546-549.

NEWMAN, M. J., DAVIDSON, R. G., BLAAUWEN, J. L. D. and BURROW, C. J. 2012. The Early Devonian Acanthodian *Uraniacanthus curtus* (Powrie, 1870) n. comb. from the Midland Valley of Scotland. *Geodiversitas*, **34**, 739-759.

NOVITSKAYA, L. I. and KARATAJŪTĖ-TALIMAA, V. 1986. Remarks about the cladistic analysis in connection with myopterygian hypothesis and the problem of the origin of gnathostomes. 102–125. *In* VOROBYEVA, E. and LEBEDKINA, N. (eds). *Morphology and Evolution of Animals*. Nauka, Moscow (in Russian).170

OBRUCHEV, D. and KARATAJŪTĖ-TALIMAA, V. 1967. Vertebrate faunas and correlation of the Ludlovian-Lower Devonian in eastern Europe. *Journal of the Linnean Society of London, Zoology*, **47**, 5-14.

OKUMURA, R., SHIMA, K., MURAMATSU, T., NAKAGAWA, K., SHIMONO, M., SUZUKI, T., MAGLOIRE, H. and SHIBUKAWA, Y. 2005. The odontoblast as a sensory receptor cell? The expression of TRPV1 (VR-1) channels. *Archives of Histology and Cytology*, **68**, 251-257.

ØRVIG, T. 1966. Histologic studies of Ostracoderms. Placoderms and fossil Elasmobranchs. 2. On the dermal skeleton of two late Palaeozoic Elasmobranchs. *Arkiv för Zoologi*, **19**, 1-39.

ØRVIG, T. 1967. Phylogeny of tooth tissues: evolution of some calcified tissues in early vertebrates. 45-110. *In* MILES, A. E. W. (ed.) *Structural and Chemical Organization of Teeth, Volume 1*. Academic Press, New York.

ØRVIG, T. 1968. The dermal skeleton: general considerations. 374-397. *In* ØRVIG, T. (ed.) *Current problems of lower vertebrate phylogeny.* Almquist and Wiksell, Stockholm.

ØRVIG, T. 1977. A survey of odontodes ('dermal teeth') from developmental, structural, functional, and phyletic points of view. 53-75. *In* ANDREWS, M., R. S. & WALKER, A. D. (ed.) *Problems in Vertebrate Evolution*. Academic Press, London, New York.

ØRVIG, T. 1989. Histologic studies of ostracoderms, placoderms and fossil elasmobranchs. 6. Hard tissues of Ordovician vertebrates. *Zoologica Scripta*, **18**, 427-446.

PEARSON, D. 1982. Primitive bony fishes, with especial reference to *Cheirolepis* and palaeonisciform actinopterygians. *Zoological Journal of the Linnean Society*, **74**, 35-67.

QU, Q., SANCHEZ, S., BLOM, H., TAFFOREAU, P. and AHLBERG, P. E. 2013a. Scales and tooth whorls of ancient fishes challenge distinction between external and oral ‘teeth’. *PloS One*, **8**, e71890.

QU, Q., ZHU, M. and WANG, W. 2013b. Scales and dermal skeletal histology of an early bony fish *Psarolepis romeri* and their bearing on the evolution of rhombic scales and hard tissues. *PloS One*, **8**, e61485.

REIF, W.-E. 1978. Types of morphogenesis of the dermal skeleton in fossil sharks. *Paläontologische Zeitschrift*, **52**, 110-128.

REIF, W.-E. 1979. Morphogenesis and histology of large scales of batoids (Elasmobranchii). *Paläontologische Zeitschrift*, **53**, 26-37.

REIF, W.-E. 1980a. A model of morphogenetic processes in the dermal skeleton of elasmobranchs. *Neues Jahrbuch für Geologie und Paläontologie, Abhandlungen*, **159**, 339-359.

REIF, W.-E. 1980b. Development of dentition and dermal skeleton in embryonic *Scyliorhinus canicula*. *Journal of morphology*, **166**, 275-288.

REIF, W.-E. 1982. Evolution of Dermal Skeleton and Dentition in Vertebrates - the Odontode Regulation Theory. *Evolutionary Biology*, **15**, 287-368.

REIF, W.-E. 1985. Courier Forschungsinstitut Senckenberg. *Squamation and Ecology of Sharks*. Senckenbergische Naturforschende Gesellschaft, Frankfurt am Main, 255 pp.

RICHTER, M. and SMITH, M. 1995. A microstructural study of the ganoine tissue of selected lower vertebrates. *Zoological Journal of the Linnean Society*, **114**, 173-212.

RITCHIE, A. 1980. The late Silurian anaspid genus *Rhyncholepis* from Oesel, Estonia, and Ringerike, Norway. *American Museum Novitates*; no. 2699.

ROSS, R. J. 1957. Ordovician Fossils from Wells in the Williston Basin, Eastern Montana. *United States Geological Survey Bulletin*, **1021-M**, 439-510.

SANSOM, I. J. 1996. *Pseudooneotodus*: a histological study of an Ordovician to Devonian vertebrate lineage. *Zoological Journal of the Linnean Society*, **118**, 47-57.

SANSOM, I. J., SMITH, M. M. and SMITH, M. P. 1996. Scales of thelodont and shark-like fishes from the Ordovician of Colorado. *Nature*, **379**, 628-630.

SANSOM, I. J., ALDRIDGE, R. and SMITH, M. 2000. A microvertebrate fauna from the Llandovery of South China. *Transactions of the Royal Society of Edinburgh: Earth Sciences*, **90**, 255-272.

SANSOM, I. J., SMITH, M. M. and SMITH, M. P. 2001. The Ordovician radiation of vertebrates. 156-171. *In* AHLBERG, E. (ed.) *Major Events in Early Vertebrate Evolution, Systematics Association Special Volume*. Taylor & Francis, London and New York.

SANSOM, I. J., DONOGHUE, P. C. and ALBANESI, G. 2005a. Histology and affinity of the earliest armoured vertebrate. *Biology Letters*, **1**, 446-449.

SANSOM, I. J., WANG, N. Z. and SMITH, M. 2005b. The histology and affinities of sinacanthid fishes: primitive gnathostomes from the Silurian of China. *Zoological Journal of the Linnean Society*, **144**, 379-386.

SANSOM, I. J., MILLER, C. G., HEWARD, A., DAVIES, N. S., BOOTH, G. A., FORTEY, R. A. and PARIS, F. 2009. Ordovician fish from the Arabian Peninsula. *Palaeontology*, **52**, 337-342.

SANSOM, I. J., DAVIES, N. S., COATES, M. I., NICOLL, R. S. and RITCHIE, A. 2012. Chondrichthyan-like scales from the Middle Ordovician of Australia. *Palaeontology*, **55**, 243-247.

SASAGAWA, I. 1995. Evidence of two types of odontoblasts during dentinogenesis in Elasmobranchs. *Connective Tissue Research*, **33**, 223-229.

SCHAUMBERG, G. 1982. *Hopleacanthus richelsdorfensis* n. g. n. sp., ein Euselachier aus dem permischen Kupferschiefer von Hessen (W-Deutschland). *Paläontologische Zeitschrift*, **56**, 235-257.

SCHAUMBERG, G. 1999. Ergänzungen zur Revision des Euselachiers *Wodnika striatula* Muenster, 1843 aus dem oberpermischen Kupferschiefer und Marl-Slate. *Geologica et Palaeontologica*, **33**, 203-217.

SCHMIDT, W. J. and KEIL, A. 1971. *Polarizing Microscopy of Dental Tissues*. Pergamon Press, 584 pp.

SCHULTZE, H.-P. 1968. Palaeoniscoidea-Schuppen aus dem Unterdevon Australiens und Kanadas und aus dem Mitteldevon Spitzbergens. *Bulletin of the British Museum (Natural History)*, **16**, 343-368.

SCHULTZE, H.-P. 1977. Ausgangsform und Entwicklung der rhombischen Schuppen der Osteichthyes (Pisces). *Paläontologische Zeitschrift*, **51**, 152-168.

SCHULTZE, H.-P. and CUMBAA, S. L. 2001. *Dialipina* and the characters of basal actinopterygians. 315-332. *In* AHLBERG, E. (ed.) *Major Events in Early Vertebrate Evolution, Systematics Association Special Volume*. Taylor & Francis, London and New York.

SCHULTZE, H.-P. and MÄRSS, T. 2004. Revisiting *Lophosteus*, a primitive osteichthyan. *Acta Universitatis Latviensis. Earth and Environment Sciences*, **679**, 57–78.

SERVAIS, T., OWEN, A. W., HARPER, D. A., KRÖGER, B. and MUNNECKE, A. 2010. The great ordovician biodiversification event (GOBE): the palaeoecological dimension. *Palaeogeography, Palaeoclimatology, Palaeoecology*, **294**, 99-119.

SIRE, J. Y. 1994. Light and TEM study of nonregenerated and experimentally regenerated scales of *Lepisosteus oculatus* (Holostei) with particular attention to ganoine formation. *The Anatomical Record*, **240**, 189-207.

SIRE, J. Y. 1993. Development and fine structure of the bony scutes in *Corydoras arcuatus* (Siluriformes, Callichthyidae). *Journal of Morphology*, **215**, 225-244.

SIRE, J. Y. and HUYSSEUNE, A. 1996. Structure and development of the odontodes in an armoured catfish, *Corydoras aeneus* (Siluriformes, Callichthyidae). *Acta Zoologica*, **77**, 51-72.

SIRE, J. Y. and HUYSSEUNE, A. 2003. Formation of dermal skeletal and dental tissues in fish: a comparative and evolutionary approach. *Biological Reviews*, **78**, 219-249.

SIRE, J. Y., DONOGHUE, P. C. J. and VICKARYOUS, M. K. 2009. Origin and evolution of the integumentary skeleton in non-tetrapod vertebrates. *Journal of anatomy*, **214**, 409-440.

SMITH, M. M. 1979. Scanning electron microscopy of odontodes in the scales of a coelacanth embryo, *Latimeria chalumnae* Smith. *Archives of oral biology*, **24**, 179-183.

SMITH, M. M. 2003. Vertebrate dentitions at the origin of jaws: when and how pattern evolved. *Evolution & Development*, **5**, 394-413.

SMITH, M. M. and MILES, A. 1971. The ultrastructure of odontogenesis in larval and adult urodeles; differentiation of the dental epithelial cells. *Zeitschrift für Zellforschung und mikroskopische Anatomie*, **121**, 470-498.

SMITH, M. M., HOBDELL, M. H. and MILLER, W. 1972. The structure of the scales of *Latimeria chalumnae*. *Journal of Zoology*, **167**, 501-509.

SMITH, M. M. and HALL, B. K. 1990. Development and evolutionary origins of vertebrate skeletogenic and odontogenic tissues. *Biological Reviews*, **65**, 277-373.

SMITH, M. M. and HALL, B. K. 1993. A developmental model for evolution of the vertebrate exoskeleton and teeth. The role of cranial and trunk neural crest. 387-448. *In* HECHT, M. K., MACINTYRE, R. J. and CLEGG, M. (eds). *Evolutionary biology*. Plenum Press, New York.

SMITH, M. M., SANSOM, I. J., AND SMITH, M. P. 1996. 'Teeth' before armour: The earliest vertebrate mineralized issues. *Modern Geology*, **20**, 303-319.

SMITH, M. M. and COATES, M. 1998. Evolutionary origins of the vertebrate dentition: phylogenetic patterns and developmental evolution. *European journal of oral sciences*, **106**, 482-500.

SMITH, M. M., FRASER, G. J. and MITSIADIS, T. A. 2009. Dental lamina as source of odontogenic stem cells: evolutionary origins and developmental control of tooth generation in gnathostomes. *Journal of Experimental Zoology Part B: Molecular and Developmental Evolution*, **312**, 260-280.

SMITH, M. M., JOHANSON, Z., UNDERWOOD, C. and DIEKWISCH, T. G. 2013. Pattern formation in development of chondrichthyan dentitions: a review of an evolutionary model. *Historical Biology*, **25**, 127-142.

SOEHN, K. L., MÄRSS, T., CALDWELL, M. W. and WILSON, M. V. 2001. New and biostratigraphically useful thelodonts from the Silurian of the Mackenzie Mountains, Northwest Territories, Canada. *Journal of Vertebrate Paleontology*, **21**, 651-659.

SOLER-GIJÓN, R. 1997. New discoveries of xenacanth sharks from the Late Carboniferous of Spain (Puertollano Basin) and Early Permian of Germany (Saar-Nahe-Basin): Implications for the phylogeny of xenacanthiform and. *Neues Jahrbuch fur Geologie und Palaontologie-Abhandlungen*, **205**, 1-32.

STAHL, B. J. 1999. Handbook of Paleoichthyology. *Chondrichthyes III: Holocephali*. Verlag Dr. Friedrich Pfeil, Munich, 164 pp.

STENSIÖ, E. A. 1932. *The Cephalaspids of Great Britain*. The British Museum (Natural History), London, 220 pp.

STENSIÖ, E. A. 1961. Permian vertebrates. *In* G. Raasch (ed). *Geology of the Arctic*. *Volume 1.* University of Toronto, Toronto.

STENSIÖ, E. and ØRVIG, T. 1951–1957. On the scales of Edestids. Unpublished manuscript, Stensiö archives, Swedish Museum of Natural History, Stockholm.

SYKES, J. 1974. On elasmobranch dermal denticles from the Rhaetic bone bed at Barnstone, Nottinghamshire. *Mercian Geologist*, **5**, 49-64.

THANH, T.-D., JANVIER, P., PHUNONG, T. H. and NHAT TRUONG, D. 1995. Lower Devonian biostratigraphy and vertebrates of the Tong Vai valley, Vietnam. *Palaeontology*, **38**, 169-186.

THIES, D. 1995. Placoid Scales (Chondrichthyes: Elasmobranchii) from the late Jurassic (Kimmeridgian) of northern Germany. *Journal of Vertebrate Paleontology*, **15**, 463-481.

THIES, D. and LEIDNER, A. 2011. Sharks and guitarfishes (Elasmobranchii) from the Late Jurassic of Europe. *Palaeodiversity*, **4**, 63-184.

THORSTEINSSON, R. 1973. Dermal elements of a new lower vertebrate from Middle Silurian (Upper Wenlockian) Rocks of the Canadian Arctic Archipelago. *Palaeontographica Abteilung A*, **143**, 51-57.

TUCKER, A. S. and FRASER, G. J. 2014. Evolution and developmental diversity of tooth regeneration. *Seminars in cell & developmental biology*, **25–26**, 71–80.

TURNER, S. 2004. Early vertebrates: analysis from microfossil evidence. 67-94. *In* ARRATIA, G., WILSON, M. V. H. and CLOUTIER, R. (eds). *Recent Advances in the Origin and Early Radiation of Vertebrates*. Verlag Dr. Friedrich Pfeil, Munich.

TURNER, S. and MURPHY, M. A. 1988. Early Devonian vertebrate microfossils from the Simpson Park Range, Eureka County, Nevada. *Journal of Paleontology*, **62**, 959-964.

TURNER, S., BLIECK, A. and NOWLAN, G. 2004. Vertebrates (agnathans and gnathostomes). 327-335. *In* WEBBY, B. D., PARIS, F., DROSER, M. L. and PERCIVAL, I. (eds). *The Great Ordovician Biodiversification Event*. Columbia University Press.

TWAY, L. E. and ZIDEK, J. 1982. Catalog of Late Pennsylvanian ichthyoliths, part I. *Journal of Vertebrate Paleontology*, **2**, 328-361.

TWAY, L. E. and ZIDEK, J. 1983. Catalog of late Pennsylvanian ichthyoliths, Part II. *Journal of Vertebrate Paleontology*, **2**, 414-438.

UPENIECE, I. 2011. Palaeoecology and juvenile individuals of the Devonian placoderm and acanthodian fishes from Lode site, Latvia. University of Latvia, doctoral thesis.

VALIUKEVIČIUS, J. 1992. First articulated *Poracanthodes* from the Lower Devonian of Severnaya Zemlya. 193-214. *In* MARK-KURIK, E. (ed.) *Fossil Fishes as Living Animals*. Academy of Sciences of Estonia, Tallinn.

VALIUKEVIČIUS, J. 1995. Acanthodian histology: Some significantaspects in taxonomical and phylogenetical research. *Geobios*, **28**, 157–159.

VALIUKEVIČIUS, J. 2003a. Devonian acanthodians from Severnaya Zemlya Archipelago (Russia). *Geodiversitas*, **25**, 131-204.

VALIUKEVIČIUS, J. 2003b. New late Silurian to Middle Devonian acanthodians of the Timan-Pechora region. *Acta Geologica Polonica*, **53**, 209-245.

VALIUKEVIČIUS, J. 2004. Silurian acanthodian succession of the Luzni-4 borehole (Latvia). *Acta Universitatis Latviensis*, **679**, 120–147.

VALIUKEVIČIUS, J. and BURROW, C. J. 2005. Diversity of tissues in acanthodians with Nostolepis-type histological structure. *Acta Palaeontologica Polonica*, **50**, 635-649.

VERGOOSSEN, J. M. 1999. Late Silurian fish microfossils from an East Baltic-derived erratic from Oosterhaule, with a description of new acanthodian taxa. *Geologie en Mijnbouw*, **78**, 231-251.

VERGOOSSEN, J. M. 2000. Acanthodian and chondrichthyan microremains in the Siluro-Devonian of the Welsh Borderland, Great Britain, and their biostratigraphical potential. 175-200. *In* BLIECK, A. and TURNER, S. (eds). *Palaeozoic vertebrate biochronology and global marine/non-marine correlation: final report of IGCP 328 (1991-1996)*. Courier Forschungsinstitut Senckenberg **223**, Frankfurt a. M.

VERGOOSSEN, J. M. 2003. Fish microfossils from the Upper Silurian Öved Sandstone Formation, Skåne, southern Sweden. PhD Thesis. University of Groningen, Netherlands, 328 pp.

VIETH, J. 1980. Goettinger Arbeiten zur Geologie und Paläeontologie. *Thelodontier-, Acanthodier-und Elasmobranchier-Schuppen aus dem Unter-Devon der Kanadischen Arktis (Agnatha, Pisces)*. In Selbstverlag des Geologisch-Paläontologischen Institut der Georg-August-Universität Göttingen, Göttingen, 69 pp.

VLADIMIRSKAYA, E. V. 1978. Brachiopods of the Silurian in Tuva. *Ezhegodnik Vsesoyuznogo Paleontologicheskogo Obshchestva*, **21**, 148-167 (in Russian).

VOIGT, M. and WEBER, D. 2011. Field Guide for Sharks of the Genus Carcharhinus. Verlag Dr. Friedrich Pfeil, Munich, 151 pp.

WANG, N.-Z., ZHANG, S.-B., WANG, J.-Q. and ZHU, M. 1998. Early Silurian chondrichthyan microfossils from Bachu County, Xinjiang, China. *Vertebrata PalAsiatica*, **36**, 257-267.

WANG, N.-Z., DONOGHUE, P. C., SMITH, M. M. and SANSOM, I. J. 2005. Histology of the galeaspid dermoskeleton and endoskeleton, and the origin and early evolution of the vertebrate cranial endoskeleton. *Journal of Vertebrate Paleontology*, **25**, 745-756.

WANG, N.-Z., ZHANG, X., ZHU, M. and ZHAO, W. J. 2009. A new articulated hybodontoid from Late Permian of northwestern China. *Acta Zoologica*, **90**, 159-170.

WANG, N.-Z., SANSOM, I. J., SMITH, M. M., WANG, J. Q., ZHU, M., ZHAO, W. J. and ANDREEV, P. S. in prep. Early Silurian Chondrichthyan microfossils from Tarim Basin, Xinjiang, China and its chronological and paleobiogeographic significance.

WANG, R. 1993. Courier Forschungsinstitut Senckenberg. *Taxonomie, Palökologie und Biostratigraphie der Mikroichthyolithen aus dem Unterdevon Keltiberiens, Spanien*. Senckenbergische Naturforschende Gesellschaft, Frankfurt a. M., 205 pp.

WEBBY, B. D., PARIS, F. and DROSER, M. L. 2004. *The Great Ordovician Biodiversification Event*. Columbia University Press, New York, 408 pp.

WELLS, J. W. 1944. Fish remains from the Middle Devonian bone beds of the Cincinnati Arch region. *Palaeontographica Americana*, **3**, 103-158.

WILLIAMS, M. E. 1998. A new specimen of *Tamiobatis vetustus* (Chondrichthyes, Ctenacanthoidea) from the late Devonian Cleveland Shale of Ohio. *Journal of Vertebrate Paleontology*, **18**, 251-260.

WILSON, M. V. and MÄRSS, T. 2009. Thelodont phylogeny revisited, with inclusion of key scale-based taxa. *Estonian Journal of Earth Sciences*, **58**.

YOSHIBA, K., YOSHIBA, N., EJIRI, S., IWAKU, M. and OZAWA, H. 2002. Odontoblast processes in human dentin revealed by fluorescence labeling and transmission electron microscopy. *Histochemistry and Cell Biology*, **118**, 205-212.

YOUNG, G. 1979. New information on the structure and relationships of *Buchanosteus* (Placodermi: Euarthrodira) from the Early Devonian of New South Wales. *Zoological Journal of the Linnean Society*, **66**, 309-352.

YOUNG, G. 1980. A new Early Devonian placoderm from New South Wales, Australia, with a discussion of placoderm phylogeny. *Palaeontographica Abteilung A*, 10-76.

YOUNG, G. 1982. Devonian sharks from south-eastern Australia and Antarctica. *Palaeontology*, **25**, 817-843.

YOUNG, G. 1997. Ordovician microvertebrate remains from the Amadeus Basin, central Australia. *Journal of Vertebrate Paleontology*, **17**, 1-25.

YU, X. 1998. A new porolepiform-like fish, *Psarolepis romeri*, gen. et sp. nov.(Sarcopterygii, Osteichthyes) from the Lower Devonian of Yunnan, China. *Journal of Vertebrate Paleontology*, **18**, 261-274.

ZANGERL, R. 1966. A new shark of the family Edestidae, *Ornithoprion hertwigi*, from the Pennslyvanian Mecca and Logan quarry shales of Indiana. *Fieldiana: Geology*, **16**, 1-43.

ZANGERL, R. 1968. The morphology and the developmental history of the scales of the Paleozoic sharks *Holmesella*? sp. and *Orodus*. 399-412. *In* ØRVIG, T. (ed.) *Current Problems of Lower Vertebrate Phylogeny*. Almqvist & Wiksell, Stockholm.

ZANGERL, R. 1979. New chondrichthyes from the Mazon Creek fauna (Pennsylvanian) of Illinois. *Mazon Creek Fossils. Academic Press, New York*, 449-500.

ZANGERL, R. 1981. Handbook of Paleoichthyology. *Chondrichthyes I: Paleozoic Elasmobranchii*. Gustav Fischer, Stuttgart and New York, 113 pp.

ZANGERL, R. and RICHARDSON, E. 1963. The paleoecological history of two Pennsylvanian black shales. *Fieldiana: Geology Memoirs*, **4**, 1-352.

ZANGERL, R. and CASE, G. R. 1973. Fieldiana: Geology Memoirs, vol. 6. *Iniopterygia: A New Order of Chondrichthyan Fishes from the Pennsylvanian of North America*. Field Museum of Natural History, Chicago, 67 pp.

ZHU, M. 1998. Early Silurian sinacanths (Chondrichthyes) from China. *Palaeontology*, **41**, 157-172.

ZHU, M., YU, X. and JANVIER, P. 1999. A primitive fossil fish sheds light on the origin of bony fishes. *Nature*, **397**, 607-610.

ZHU, M., YU, X., WANG, W., ZHAO, W. and JIA, L. 2006. A primitive fish provides key characters bearing on deep osteichthyan phylogeny. *Nature*, **441**, 77-80.

ZHU, M., ZHAO, W., JIA, L., LU, J., QIAO, T. and QU, Q. 2009. The oldest articulated osteichthyan reveals mosaic gnathostome characters. *Nature*, **458**, 469-474.

ZHU, M., YU, X., CHOO, B., WANG, J. and JIA, L. 2012. An antiarch placoderm shows that pelvic girdles arose at the root of jawed vertebrates. *Biology Letters*, **8**, 453-456.

ZHU, M., YU, X., AHLBERG, P. E., CHOO, B., LU, J., QIAO, T., QU, Q., ZHAO, W., JIA, L. and BLOM, H. 2013. A Silurian placoderm with osteichthyan-like marginal jaw bones. *Nature*, **502**, 188-193.

ZIDEK, J. 1976. Kansas Hamilton Quarry (Upper Pennsylvanian) *Acanthodes*, with remarks on the previously reported North American occurrences of the genus. *University of Kansas Paleontological Contributions*, **83**, 1–41.

ZIDEK, J. 1985. Growth inacanthodes (acanthodii: pisces) data and implications. *Paläontologische Zeitschrift*, **59**, 147-166.

ŽIGAITĖ, Ž. and KARATAJŪTĖ-TALIMAA, V. 2008. New genus of chondrichthyans from the Silurian–Devonian boundary deposits of Tuva (Russia). *Evolution and diversity of chondrichthyans. Acta Geologica Polonica*, **58**, 127-131.

ŽIGAITĖ, Ž., KARATAJŪTĖ-TALIMAA, V. and BLIECK, A. 2011. Vertebrate microremains from the Lower Silurian of Siberia and Central Asia: palaeobiodiversity and palaeobiogeography. *Journal of Micropalaeontology*, **30**, 97-106.

ŽIGAITĖ, Ž., RICHTER, M., KARATAJŪTĖ-TALIMAA , V. and SMITH, M. M. 2013. Tissue diversity and evolutionary trends of the dermal skeleton of Silurian thelodonts. *Historical Biology*, **25**, 143-154.

Appendix

Matrix of character states assigned to the 51 taxa included in the phylogenetic analyses

Acanthodes	--?3-1001-111211030210-00-01000100010001--11001-000--0000000-00110000010-010010110?06010-0
Altholepis	1-?6-0111-223611322200-00-011110100??01--11000-0?1?0?000000-10010000?10-0100100111123010-0
Andreolepis	1-24-0001-21423003220101?-031122301?10??--00001-001111001000-11010010111112001010-?33010-0
Antarctilamna	11?5210?10101112020211001141101120???1?--1110110?100?000000-??110000110-0?0010011?23110-0
Archipelepis	---3---1-----201222111010-0111003001?002111000--001001-10000-1?00000??10-0?0001------011?1
Brindabellaspis	40-44001002242?0031200-0010111200002??0?—1000??001??00001000?12?010?1001?001000-123110-0
Brochoadmones	0?01?101??11-0110?2?00-?????1?210?030011--1??0????0-?00000???0?1?000??11?010010110?201?0-?
Buchanosteus	4--8-1101-2249103?1201010-6111210102??0?--1000?-0?1?1?000010010000110111112101010-?48010-0

Canonlepis 1-?0-1011-222211221101010-011001010?????--10000-00100?000000-01000000010-000010011123010-0

Cheirolepis ---4-1001-111211031100000-031121301210?1--01001-000-01001000-000100000111010010110?06010-0

Connemarraspis 4-28-0010-224210311101010-01112?3104????--11000-001?0100001000112100 01?1111001020-025010-0

Dialipina 1-04-0010-204231031201010-03112130141011--01001-00110?001000-?0010010?10-000010011123010-0

Diplacanthus --20-1001-111311020011001-01000100010001--11001-110--1000000-001110000100010010110?06010-0

Elegestolepis ---0---1-----302030110-00-410001000?????101100--11100?-00110000000000010-000001------01111

Frigorilepis ---0---1-----312221-01000---------000012101000--01---?-00000-010000---------000------001?-

Gladbachus 4-28-0010-2249103??201010-0111210001??01--1100?-0?0--000001000012000011110000101 0-?25010-0

Goodrichthys 11262100111141110121110001410011100?????--1110111?100?000?00-?????00???0-010010111?23110-0

Hemicyclaspis 1-26-1011-000830032-00-10————1510103101001-10---1100000-001210---------110011?23001?-

Janassa ---3---1-----210022-110?1---------03000?111100--10---?-10000-00111
0---------010------0010-

Kannathalepis ---3---1-----212001?11000-21000?2?0??????01100--00100?0?0000-
01000000?10-0?0001------01111

Lanarkia ---5---1-----502221101010-721100300010121010 00--001001-10000-
11010000010-000001------01111

Ligulalepis 11-4010110114231032201000103112030 12????--010111100-
01001000-00010100?1110?0010111?23110-0

Lophosteus 2-24-1001-114230222201010-031122311?????--00000-01111000
0000-11010010??1112001010-137010-0

Lupopsyrus ---4---1-----400221-11010---------000102201000--00---00000101??1?
00---------000------0010-

Machaeracanthus --?3-1001-111211010211001-011021000?????--11011-000-0?
000000-001100000111010010110?06010-0

Mongolepis 11?411011-110721010200-010011021000?????--11000000110?
100102-----0000010-010010011123110-0

Murrindalaspis 40-400110022430131020101016111210102??1?--1000??00111?
00001001012001?11??1??01000-?23110-0

Obtusacanthus ---7---1-----610222-00-??---------030002201000--0?---0000000-??00?
0---------000------0010-

Orodus 11?611011110021232220100010111010 00?0001--1??0???00-0?000
000-10010000010-010010111123110-0

Parexus 001011010011-31?3201010??1??101?2?010011--11?01???0--000

00101????00001?0-010010010?20110-0

Polybranchiaspis 4--8-0110-224-10310200-00-0111210002????--100000000-0?000?

02-????0000010-00001010-?25010-1

Polymerolepis ---3---1-----211220-11011--------10?0111201110--11--0?-00000-010110-

-------0000------001--

Poracanthodes 3-03-1010-111211010210-01-0210000100??01--11111-111--0100000-

00120000110-0100100101260l0-0

Protacrodus 30?2010111111211121200-001011100000???01--11001??00--?0000

00-1001?000110-010010110?20110-0

Psarolepis 11-4?10011111231022210-0000311213012????--0100110010011

01000-10011010211011001010-?13110-0

Ptomacanthus 2-14-1001-113610320101010-01003120010001--11?0?-000--00000

101??120000111101001011014701O-0

Rhyncholepis 11-5000100204830322200-00033114230121010--00001100111?0?

?000-??0?1010110-12?011011?23110-0

Romundina 4--8-0?01-224??03??201210-???12?1?02??0?--??00?-001??

0000010000121112011012101O?0-?4801--?

Seretolepis 00?011010011-3110201010011011111210??011--1110111

0100000001010?1?0000?10?010010010020110-0

Shiqianolepis 10241101111102120211111011510011210?????--111000000--?0001

02-----00001110010010011123110-0

Sodolepis 1-?4-1011-100111001200-01-621100000?????--10000-00100?000102-----0000010-0100100110230l0-0

Solinalepis 1-16-1011-100711322100-01-110001010?????--10000-00111?000102-----00001100000010011123010-0

Tantalepis 2-?4-1111---2822221-01001--1------0?????2110000-00---?0????????????--------??10-0-0210011-

Tchunacanthus 3-10-1001-111311031211200-01002100010???--10000-000--00000100101100001110010010010?36010-0

Teslepis 1-?4-1011-100111021200-01-621100000?????--11000-00100?000102-----0000010-0100100110230l0-0

Tezakia 1-?6-1111-202212211-00-00--1------0?????0110000-00---?000000-010200---------0100110230011-

Thelodus ---4---1-----401031111010-0110000003000210l000--001000-10000-11000000110-020001------01111

Tuvalepis 2-?4-1111---2112031100-00-11103?210?????--11001-01100?000000-01120000?1??000010-0-021010-0

Uraniacanthus --20-1000-111301022011000-01000101050001--11011-100--0000000-01120000010-0100101100060l0-0

Wodnika 01-0010111111311122200-01101110100060001--110010100--00000101011100001l0-0100101l0?20110-0

Xinjiangichthys 11?6310111100722002110-010510011210?????--11100000000?
000102-----00001110010010011123110-0

Character list

Scale morphology

1. Arrangement of primary odontodes on the crown surface of trunk scales: (0) in a single antero-posterior row, (1) in two or more antero-posterior rows, (2) in a single transverse (medio-lateral) row, (3) concentric, (4) unordered, (-) not applicable (mono-odontode scale or polyodontode scale with only a single odontode exposed on the crown surface).

2. Arrangement of secondary scale odontodes on the crown surface of trunk scales: (0) unordered, (1) ordered, (-) not applicable (mono-odontode scales or polyodontode scales without developed secondary odontodes).

3. Arrangement of odontodes on the crown surface of head scales (term restricted to the scales covering the pre-branchial segment of the head): (0) in rows, (1) radial, (2) unordered, (-) not applicable (mono-odontode scales or lack of head scale cover).

4. Predominant morphology of trunk-scale primary odontodes (Fig. 33): (0) deltoid, (1) circular, (2) elliptical, (3) rhomboid, (4) acuminate, (5) lanceolate, (6) needle-shaped, (7) cruciform, (8) stellate.

5. Predominant morphology of trunk-scale secondary odontodes (Fig. 33): (0) deltoid, (1) acuminate, (2) lanceolate, (3) conical, (4) stellate, (-) not applicable (scales without developed secondary odontodes).

6. Morphologically similar primary scale odontodes: (0) absent, (1) present, (-) not applicable (mono-odontode scale crowns).

7. Crown primordium of polyodontode trunk scales the largest odontode element: (0) absent, (1) present, (-) not applicable (mono-odontode scale).

8. All primary crown odontodes of trunk scales exposed on the crown surface: (0) absent, (1) present.

9. Suturing of primary trunk-scale odontodes: (0) absent, (1) present, (-) not applicable (mono-odontode scale).

10. Suturing of secondary trunk-scale odontodes: (0) absent, (1) present, (-) not applicable (mono-odontode scale or polyodontode scale lacking secondary crown odontodes).

11. In posterior direction, the length of trunk scale primary odontodes: (0) remains consistent, (1) increases, (2) changes randomly, (-) not applicable (mono-odontode scales or poly-odontode scales with odontodes arranged in a single transverse row).

12. In posterior direction, the width of trunk-scale primary odontodes: (0) remains constant, (1) increases, (2) changes in a random manner, (-) not applicable (mono-odontode scales or polyodontode scales organised in a single transverse row).

13. In direction of the lateral crown margins, primary-odontode size of trunk scales: (0) remains constant, (1) increases, (2) decreases, (3) increases and then decreases, (4) changes randomly, (-) not applicable (mono-odontode scales or scales with primary odontodes organised in a single antero-posterior row).

14. Crown shape of trunk scales (Fig. 33): (0) circular, (1) elliptic, (2) rhomboid, (3) deltoid, (4) acuminate, (5) lanceolate, (6) cruciform, (7) trapezoid, (8) oblong, (9) irregular.

Revised character 10 of Wilson and Märss (2009).

15. The width of trunk-scale crowns greatest: (0) at their anterior third, (1) at their mid third, (2) at their posterior third, (3) crown width constant.

16. Degree of extension of the posterior portion of the crown in trunk scales: (0) not protruded beyond the base/pedicle margin, (1) extended by less than half of its length beyond the base/pedicle margin, (2) extended by more than half of its length beyond the base/pedicle margin.

Adapted character 16 of Wilson and Märss (2009).

17. Crown surface profile of trunk scales: (0) planar, (1) concave, (2) convex, (3) irregular.

Revised character 11 of Wilson and Märss (2009).

18. Maximal scale crown height reached: (0) at the anterior third of the scale, (1) at the mid third of the scale, (2) at the posterior third of the scale, (3) crown surface of uniform height.

19. Crown length to crown width ratio of trunk scales: (0) 1, (1) >1, (2) <1.

20. Crown thickness to base thickness ratio of trunk scales: (0) 1, (1) >1, (2) <1, (-) not applicable (scales not developing bases).

21. Constricted lower portion of trunk-scale crowns: (0) absent, (1) present.

22. Ornamented crown surface (anterior crown surface of scales with erect crown odontodes) of primary trunk-scale odontodes: (0) absent, (1) present.

23. Crown-surface of trunk-scale primary odontodes ornamented by: (0) ridges, (1) tubercles, (2) tubercles and ridges, (-) not applicable (no ornament developed).

Revised character 17 of Wilson and Märss (2009).

24. Ornamented lower crown surface (posterior crown surface of scales with erect crown odontodes) of primary trunk-scale odontodes: (0) absent, (1) present.

Adapted character 18 of Wilson and Märss (2009).

25. Grooved lower crown surface of primary trunk scale odontodes: (0) absent, (1) present.

26. Secondary trunk-scale odontodes with ornamented crown surface: (0) absent, (1) present, (-) not applicable (scales without developed secondary odontodes).

27. Outline of trunk scale bases (Fig. 33): (0) rhomboid, (1) trapezoid, (2) deltoid, (3) oblong, (4) elliptic, (5) lobate, (6) obovate (egg-shaped), (7) wedge-shaped, (-) not applicable (scales not developing bases).

Revised character 21 of Wilson and Märss (2009).

28. Bases of trunk scales widest: (0) at their anterior third, (1) at their middle third, (2) at their posterior third, (3) base width constant, (-) not applicable (scales not developing bases).

29. Trunk-scale base extended beyond the anterior crown margin: (0) absent, (1) present, (-) not applicable (scales not developing bases).

30. Lateral sides of trunk-scale bases extended beyond the crown margins: (0) absent, (1) present, (-) not applicable (scales not developing bases).

31. Away from the peripheral contact with the crown, the perimeter of the scale base: (0) decreases, (1) increases, (2) increases and then decreases, (3) remains constant, (4) changes randomly, (-) not applicable (scales not developing bases).

32. Scale base thickest: (0) at its anterior third, (1) at its medial third, (2) at its posterior third, (3) of uniform thickness, (-) not applicable (scales not developing bases).

33. Lower-base surface of ontogenetically mature trunk scales: (0) convex, (1) flat, (2) concave, (3) irregular, (-) not applicable (scales not developing bases).

Revised and united characters 12 and 13 of Brazeau (2009), Davis et al. (2012) and Zhu et al. (2013).

34. Basal surface of trunk scales: (0) smooth, (1) grooved, (-) not applicable (scales not developing bases).

35. Trunk scales with peg-and-socket articulation: (0) absent, (1) present.

Character 10 of Brazeau (2009), character 138 of Zhu et al. (2009), character 24 of Friedman and Brazeau (2010), character 10 of Davis et al. (2012) and Zhu et al. (2013).

36. Dermocranial skeleton represented by: (0) trunk-type scales (scales with identifiable anterior and posterior sides), (1) tessera-like scales (scales with no discernible anterior and posterior sides), (2) dermal bones, (3) trunk-type scales and tessera-like scales, (4) trunk-type scales and dermal bones, (5) tessera-like scales and dermal bones, (6) dermatocranial skeleton not developed.

37. Distinct from the squamation scale-like dermoskeletal elements (scutes and/or basal fulcra *sensu* Arratia 2009) developed along the dorsal margin of the caudal fin: (0) absent, (1) present.

Combined characters 187 and 188 of Min and Schultze (2001).

38. Enlarged caudal keel scales (enlarged keeled scutes of Hanke and Davis 2012): (0) absent, (1) present.

39. Overlapping margins of trunk-scale crowns: (0) absent, (1) present.

Revised character 10 of Burrow and Turner (1999).

40. Arrangement of flank scales: (0) in vertical rows, (1) in serial (oblique) rows (*sensu* Gemballa and Bartsch, 2002), (2) unordered.

Character 15 of Brazeau (2009), character 14 of Davis et al. (2012) and Zhu et al. (2013).

41. Lower pedicle surface of trunk scales: (0) convex, (1) flat, (2) concave, (3) irregular, (-) not applicable (scales not developing pedicles).

42. The pedicle of trunk scales protruded beyond the anterior crown margin: (0) absent, (1) present, (-) not applicable (scales not developing pedicles).

43. Bilaterally symmetrical trunk scales: (0) absent, (1) present.

Revised character 15 of Brazeau (2009), character 12 of Davis et al. (2012) and character 14 of Zhu et al. (2013).

Scale canal system

44. Canal opening(s) formed at the lower surface of trunk-scale odontodes; equivalent to neck-canal openings *sensu* Reif (1978): (0) absent, (1) present.

45. Vertical rows of foramina formed at the lower crown face: (0) absent, (1) present.

46. Odontode pulp-canals opening on the crown surface of trunk scales: (0) absent, (1) present.

47. Canal connections between the pulp cavity spaces of primary trunk-scale odontodes: (0) absent, (1) present, (-) not applicable (mono-odontode scales).

48. Canal connections between the pulp cavity spaces of primary and secondary odontodes: (0) absent, (1) present, (-) not applicable (mono-odontode scales or scales not forming secondary odontodes).

49. Vertically branched pulp cavity space of primary scale odontodes: (0) absent, (1) present.

50. Scale crown dentine canals: (0) absent, (1) present.

Revised character 30 of Wilson and Märss (2009).

51. Scale base canal system: (0) absent, (1) present, (-) not applicable (scales not developing a base).

52. Ramification of scale-base canals: (0) absent, (1) present, (-) not applicable (avascular scale base tissue or scales not developing bases).

53. Canal openings formed at the basal surface of trunk-scales: (0) absent, (1) present, (-) not applicable (avascular scale base tissue or scales not developing bases).

54. Trunk scales penetrated by the canals of the lateral line system: (0) absent, (1) present.

Revised character 16 of Brazeau (2009), character 36 of Friedman and Brazeau (2010) and character 15 of Davis et al. (2012) and Zhu et al (2013).

55. Pore-canal system housed inside the crowns of trunk scales: (0) absent, (1) present, (-) not applicable (scales with mono-odontode crowns).

A pore-canal system is defined as a network of inter-odontode cavity-spaces opened on the crown surface.

Histology

56. Scale crown enameloid: (0) absent, (1) present.

Revised character 151 of Zhu et al. (2009), character 46 of Friedman and Brazeau (2010) and character 140 of Zhu et al. (2013).

57. Scale crown enamel: (0) absent, (1) present.

Character 5 of Schultze and Märss (2004).

58. Type of scale crown dentine: (0) tubular, (1) atubular.

59. Cellular scale crown dentine: (0) absent, (1) present.

60. Type of scale dentine mineralisation: (0) inotropic, (1) spheritic, (2) inotropic and spheritic.

61. Shape of scale-crown odontocyte lacunae: (0) rounded, (1) elongate (Stranglakune in Gross 1973), (2) rounded and elongate, (-) not applicable (acellular dentine).

62. The stem of scale-dentine tubules branching: (0) along its length, (1) terminally, (-) not applicable (atubular scale crown dentine).

63. Branches longer than the stem of the dentine tubules: (0) absent, (1) present, (-) not applicable (atubular crown dentine).

64. Organisation of the proximal end of scale-dentine tubules: (0) polarised, (1) tangled, (-) not applicable (atubular scale crown dentine).

65. Appearance of the proximal end of scale dentine tubules (Fig. 34): (0) straight, (1) sinuous, (2) coiled, (-) not applicable (atubular scale dentine).

Revised character 31 of Wilson and Märss (2009).

66. Scale-crown denteons: (0) absent, (1) present.

67. Resorption of scale dentine: (0) absent, (1) present.

68. Basal bone of trunk scales composed of two or more histologically distinct layers: (0) absent, (1) present, (-) not applicable (scales not developing bases).

69. Type of mineralisation of the scale base: (0) inotropic, (1) spheritic, (2) inotropic and spheritic, (-) not applicable (scales not developing a base).

70. Structure of the mineralised basal bone matrix: (0) lamellar, with plywood-like fibre organisation, (1) lamellar, with parallel alignment of mineralised fibres, (2) lamellar, with plywood-like and parallel fibre organisation, (-) not applicable (scales not developing a base).

71. Basal bone mineralised matrix containing vertically oriented attachment (extraneous) fibres: (0) absent, (1) present, (-) not applicable (scales not developing bases).

72. Cellular scale-base bone tissue: (0) absent, (1) present, (-) not applicable (scales not developing a base).

73. Scale base osteocyte canaliculi: (0) absent, (1) present, (-) not applicable (scales lacking a base or possessing acellular basal bone tissue).

74. Osteon formation in scale basal bone: (0) absent, (1) present, (-) not applicable (scales not developing a base).

75. Outline of the scale crown/scale base contact surface: (0) planar, (1) chevron-shaped, (2) irregular, (-) not applicable (scales not developing a base).

76. Resorption of scale dermal bone: (0) absent, (1) present, (-) not applicable (scales lacking basal bone).

77. Elasmodine (lamellar dentine *sensu* Sire et al. 2009) formation in scales: (0) absent, (1) present.

Scale morphogenesis

78. Type of trunk scale crown according to primary odontode number: (0) mono-odontode (Fig. 2), (1) polyodontode (Fig. 3).

Revised character 8 of Brazeau (2009), Davis et al. (2012) and Zhu et al. (2013) and character 2 of Wilson and Märss (2009).

79. Growing trunk-scale odontodes: (0) absent, (1) present.

80. Position of the crown primordium in polyodontode trunk scales: (0) at the anterior third of the scale, (1) at the mid third of the scale, (2) at the posterior third of the scale, (-) not

applicable (mono-odontode scales or polyodontode scales with odontodes organised into a single transverse row).

81. Primary odontocomplex formation in trunk scales (Fig. 3): (0) absent, (1) present, (-) not applicable (mono-odontode scale).

82. Number of primary trunk-scale odontocomplexes: (0) one, (1) more than one, (-) not applicable (scales not developing odontocomplexes).

83. Number of crown odontodes increasing with the increase in the size of ontogenetically mature trunk scales: (0) absent, (1) present, (-) not applicable (mono-odontode scales).

84. Type of primary odontode addition in polyodontode scales: (0) superpositional, (1) areal-superpositional, (2) areal, (3) superpositional and areal-superpositional, (4) superpositional and areal, (-) not applicable (mono-odontode scales).

85. Direction of primary odontode addition in scales with polyodontode crowns: (0) posterior, (1) lateral bidirectional, (2) lateral unidirectional, (3) posterior and lateral bidirectional, (4) posterior and lateral unidirectional, (5) anterior, posterior and lateral bidirectional, (6) concentric, (7) concentric and lateral bidirectional, (8) concentric, anterior, posterior and lateral bidirectional, (-) not applicable (scales with mono-odontode crowns).

Character state 5: circumferential type of deposition resulting in the formation of a nested set of odontodes.

86. Secondary scale odontodes: (0) absent, (1) present.

87. Scale base (Figs. 1, 2**)**: (0) absent, (1) present.

88. Scale pedicle **(**Fig. 2**)**: (0) absent, (1) present.

89. Relative timing of pedicle and crown development in trunk scales: (0) synchronous, (1) asynchronous, (-) not applicable (scales not developing pedicles).

90. Relative timing of scale crown and scale base development: (0) synchronous (1) asynchronous, (-) not applicable (scales not developing bases).

Taxa included in the analyses, studied material, literature used in the coding the character-taxon matrix

Acanthodes: **Gross (1947, 1973); Miles (1968); Zidek (1976, 1985); Denison (1979); Heidtke (1993, 1996); Derycke and Chancogne-Weber (1995); Valiukevičius (1995); Lelièvre and Derycke (1998); Beznosov (2009).**

Altholepis: unpublished macrographs of a partial body fossil (UALVP 41483) with articulated squamation from the Man on the hill locality (Mackenzie Mountains, Northwest Territories, Canada) and c. 100 isolated scales from the Ivane Formation of Podolia,

Ukraine (Ivane-Zolotoye outcrop, sample 76-16). **Karatajùtè-Talimaa (1997); Martínez-Pèrez et al. (2010).**

Andreolepis: **Gross (1968); Richter and Smith (1995); Märss (1986, 2001); Chen et al. (2012); Qu et al. (2013a).**

Antarctilamna: **Young (1982); Forey et al. (1992); Burrow et al. (2009).**

Archipelepis: **Soehn et al. (2001); Märss et al. (2002, 2006, 2007).**

Brindabellaspis: **Young (1980); Burrow and Turner (1998, 1999).**

Brochoadmones: unpublished macrographs of two articulated specimens—UALVP 41494 and UALVP 41495. **Hanke and Wilson (2006).**

Buchanosteus: **Young (1979); Burrow and Turner (1998, 1999).**

Canonlepis: 5 isolated scales (BU5265–BU5268, BU5346) from the Harding Sandstone Formation (Harding Quarry, ~1 km W of Cañon City, Fremont County, Colorado, USA; sample number H94-7). Two thin-sectioned specimens (BU5267, BU5268) was investigated with Nomarski DIC optics and one specimen was examined by X-ray microtomography. **Sansom et al. (2001).**

Cheirolepis: **Gross (1947, 1953, 1973); Schultze (1968); Pearson (1982); Richter and Smith (1995); Arratia and Cloutier (1996).**

Connemarraspis: **Burrow (1996, 2003a, 2006); Burrow and Turner (1998, 1999).**

Dialipina: **Schultze (1968, 1977); Burrow et al. (2000); Schultze and Cumbaa (2001).**

Diplacanthus: articulated body fossil of *D*. *longispinus* (BIRUG 4099) and thin-sectioned scales (BIRUG 4040) embedded in matrix investigated by Nomarski DIC optics. **Gross (1947, 1973); Gagnier (1996); Valiukevičius (1995, 2003a, 2003b).**

Elegestolepis: more than 200 isolated scales from the Baital Formation (beds 236, 291, 293 and 295 of the Elegest River outcrop, Tuva, Russian Federation). **Karatajùtè-Talimaa (1973, 1992, 1998).**

Frigorilepis: **Märss (2006); Märss et al. (2002, 2006).**

Gladbachus: articulated partial body fossil (holotype UCMZ2000.32) and eleven scales extracted from the same specimen examined in section by Nomarski DIC optics. **Heidtke and Krätschmer (2001); Burrow and Turner (2013).**

Goodrichthys: isolated scales from specimen BMNH P.20142a. **Moy-Thomas (1936); Ginter (2009).**

Hemicyclaspis: **Stensiö (1932); Ørvig (1968); Vergoossen (2003); Sire et al. (2009).**

Janassa: **Ørvig (1966); Malzahn (1968); Brandt (1996).**

Kannathalepis: **Märss and Gagnier (2001); Märss (2006).**

Lanarkia: **Gross (1967); Märss and Ritchie (1998); Märss et al. (2007); Wilson and Märss (2009).**

Ligulalepis: **Schultze (1968); Burrow (1994); Basden and Young (2001).**

Lophosteus: **Gross (1969, 1971); Schultze and Märss (2004).**

Lupopsyrus: unpublished macrographs of specimens UALVP 41493 and UALVP 42208. **Bernacsek and Dineley (1977); Hanke and Wilson (2004); Hanke and Davis (2012).**

Machaeracanthus: 4 isolated scales from the Chester Bjerg Formation of North Greenland (Halls Grav locality, sample GGU 82738,). 1 specimen was examined by X-ray microtomography. **Gross (1973), Mader (1986); Burrow et al. (2010a); Botella et al. (2012).**

Mongolepis: hundreds of isolated scales from Chargat Formation (type locality, 80 km north of the Khar-Us Lake, Mongolia). Specimens extracted from samples 16/3 and ЦГЭ N 1009. Four thin-sectioned specimens (BU5297, BU5298, BU5354, 41706) were investigated with Nomarski DIC optics and scanning electron microscopy, with one other specimen (BU5296) examined by X-ray microtomography. **Karatajùtè-Talimaa et al., (1990); Karatajùtè-Talimaa (1995, 1998).**

Murrindalaspis: **Long (1984); Burrow and Turner (1998, 1999, 2012); Burrow et al. (2010b).**

Obtusacanthus: unpublished macrographs of specimen UALVP 41488. **Hanke and Wilson (2004).**

Orodus: articulated partial body fossil (FMNH PF 2201) and patches of articulated scales from the same specimen (Logan Quarry shale, Stauton Formation, Indiana, USA). **Zangerl and Richardson (1963); Zangerl (1968, 1981).**

Parexus: Articulated specimen NMS G.1956.14.14. **Denison (1979); Burrow et al. (2013).**

Polybranchiaspis: **Thanh et al. (1995); Wang et al. (2005)**.

Polymerolepis: c. 30 isolated *P. whitei* scales (443-447, 473) from the Ivane Formation of Podolia, Ukraine (outcrops Bedrikovtsy, Dobrovliany, Gorodok and Ivane-Zolotoye). One specimen (K-T1998Fig6f) was investigated by X-ray microtomography. **Obruchev and Karatajùtè-Talimaa (1967); Turner and Murphy (1988); Karatajùtè-Talimaa (1992, 1998); Hanke et al. (2013).**

Poracanthodes: two isolated scales from the Downtonian of the USA. One scale (BU5300) was examined by X-ray microtomography. **Gross (1956); Märss (1986); Vergoossen (1999, 2000); Burrow (2003b); Valiukevičius (1992, 2003a, 2004).** Contra Vergoossen (1999), the diagnosis of *Porcanthodes* is amended to include inside the genus only

poracanthodid species with trunk scales that possess a pore-canal system and demonstrate areal crown-growth pattern; identified in *P. punctatus* (Gross 1956; Märss 1986; Valiukevičius 2003a) and *P. menneri* (Valiukevičius 1992).

Protacrodus: 3 isolated scales from the Muhua Formation (Muhua village, Guizhou province, south China). Material extracted from sample MH-1 (Ginter and Sun 2007). One specimen (PKUM02–0178) examined by X-ray microtomography. **Gross (1938, 1973); Ginter and Sun (2007).**

Psarolepis: **Yu (1998)**; **Zhu et al. (1999)**; **Qu et al. (2013b).**

Ptomacanthus: embedded in siltstone matrix scales from specimen NHM P 53880 examined in section by Nomarski DIC optics and by means of X-ray microtomography. **Miles (1973); Brazeau (2009, 2012).**

Rhyncholepis: **Märss (1986); Ritchie (1980); Blom et al. (2002).**

Romundina: **Denison (1978); Burrow and Turner (1999); Johanson and Smith (2003); Goujet and Young (2004); Giles et al. (2013).**

Seretolepis: 14 isolated scales from the Ivane Formation of Podolia, Ukraine. Material from the Bedrikovtsy (sample 148-0), Dobrovliany (samples 74-2, 76-5), Gorodok, Ivane-Zolotoye, Kostelniki and Zaleshchiki outcrops. 5-461 examined by X-ray microtomography. **Karatajùtè-Talimaa (1997); Hanke and Wilson (2010); Martínez-Pérez et al. (2010).**

Shiqianolepis: hundreds of isolated scales from sample Shiqian 14B (Lower Member of the Xiushan Formation, Shiqian County, China), including type specimens (NIGP 130293–NIGP 130317). Complete and thin-sectioned scales were investigated with Nomarski DIC optics and SEM. One of the specimens (NIGP 130307) was examined by X-ray microtomography. **Sansom et al. (2000); Wang et al. (in prep).**

Sodolepis: hundreds of isolated scales from the Chargat Formation (type locality, 80 km north of the Khar-Us Lake, Mongolia). Two thin-sectioned specimens (BU5306 and BU5344) were investigated with Nomarski DIC optics and scanning electron microscopy; two other specimens (BU5305 and BU5347) were examined by X-ray microtomography. **Karatajùtè-Talimaa (1992, 1998); Karatajùtè-Talimaa and Novitskaya (1997).**

Solinalepis: over 200 isolated scales from the Harding Sandstone Formation (Harding Quarry, ~1 km W of Cañon City (Fremont County, Colorado, USA). Specimens extracted from sediment samples from horizons H94-20, 26 and H96-20. Thin-sectioned specimens (BU5316, BU5317, BU5355–BU5358, BU4440) were investigated with Nomarski DIC optics with two other specimens (BU5318, BU5359) being examined by X-ray microtomography. **Sansom et al. (2001); Donoghue and Sansom (2002); Sire et al. (2009).**

Tantalepis: approximately 200 isolated scales from the Stairway Sandstone Formation (Maloney Creek, Northern Territory, Australia), including six thin sectioned specimens (BU5320, BU5360–BU5364) and one (BU5319) examined by X-ray microtomography. All specimens extracted from rock sample SS06 – 10H. **Sansom et al. (2012).**

Teslepis: hundreds of isolated scales from Chargat Formation (type locality, 80 km north of the Khar-Us Lake, Mongolia). Specimens extracted from samples 16/3 and ЦГЭ N 1009. Two thin-sectioned specimens (BU5324 and BU5348) were investigated with Nomarski DIC optics and scanning electron microscopy and one other specimen (BU5325) was examined by X-ray microtomography. **Karatajùtè-Talimaa and Novitskaya (1992); Karatajùtè-Talimaa (1992, 1998).**

Tezakia: a total of over 300 isolated scales from the Harding Sandstone Formation (samples from horizons H94-16, 26 and H96-20 of the Harding Quarry, ~1 km W of Cañon City, Fremont County, Colorado, USA) and the Winnipeg Formation (Shell Pine Unit No. 1)

of Montana, USA. Ten thin-sectioned scales (BU2582, NRM-PZ X5, NRM-PZ X6 and seven non-figured specimens from the Shell Pine Unit No. 1) were investigated with Nomarski DIC optics and other two specimens (BU5327 and an non-figured scale from the Shell Pine Unit No. 1) were examined by X-ray microtomography. **Sansom et al. (1996, 2001); Donoghue and Sansom (2002); Johanson et al. (2008).**

Tchunacanthus: **Karatajùtè-Talimaa and Smith (2003); Valiukevičius and Burrow (2005).**

Thelodus: **Gross (1967); Karatajùtè-Talimaa (1978); Märss and Karatajùtè-Talimaa (2002); Märss et al. (2007); Märss (2011).**

Tuvalepis: 5 isolated scales from the Khondergei Formation (Bazhyn-Alaak locality, River Tchadan, Tuva (Russian Federation). One thin-sectioned scale (BU5350) was investigated with Nomarski DIC optics and one other specimen (BU5342) was examined by X-ray microtomography. **Žigaitė and Karatajùtè-Talimaa (2008).**

Uraniacanthus: **Hanke and Davis (2008); Newman et al. (2012).**

Wodnika: isolated scales and patches of articulated scales from specimen NHM 36059 (Kupferschiefer Member of the Werra Formation at the Hasbergen outcrop, central Germany) and a complete body fossil (NHMUK PV P. 66677) with preserved squamation from the Marl Slate of Durham (Quarrington Quarry, Old Quarrington, Durham County, England). One scale from NHM 36059 was examined by X-ray microtomography and three of the scales (two from NHM 36059 and one from NHMUK PV P. 66677) were thin-sectioned for light microscopy investigation.

Xinjiangichthys: five isolated scales from the Yimugantawu Formation (Bachu County, Xinjiang, China) and two scales (NIGP 130291 and NIGP 130292) from the Lower Member of the Xiushan Formation (Shiqian County, China). IVPP V X1 was thin sectioned and

investigated with Nomarski DIC optics and three further specimens (IVPP V X2 and two non-figured specimens from the Xiushan Formation) were examined by X-ray microtomography. **Wang et al. (1998); Sansom et al. (2000); Wang et al. (in prep).**

Examined taxa not included in the phylogenetic analysis.

Ctenacanthus-type scales: ten isolated scales from Upper Visean (Carboniferous) of the Czech Republic (Czerna 1 locality, 25 km north west of Cracow). One specimen (BU5353) thin sectioned and examined with Nomarski DIC optics.

Cladoselache: approximately 30 disarticulated scales (NHM P9266) from the Cleveland Shale (Ohio) of USA.

Deltalepis: 12 isolated scales from the Chargat Formation of north west Mongolia. One thin sectioned scale (BU5273) was examined with Nomarski DIC optics and further two specimens (BU5273, BU5280, BU5281) were investigated by X-ray microtomography.

Raja montagui (extant neoselachian): head scale cover of a single specimen. Skin samples with articulated squamation thin sectioned (BU5301, BU5302) and examined by Nomarski DIC optics.